Immunity to Chlamydia trachomatis and Host-Pathogen Interactions During Infection

Immunity to *Chlamydia trachomatis* and Host-Pathogen Interactions During Infection

A dissertation presented

by

Andrew James Olive

To

The Division of Medical Sciences

in partial fulfillment of the requirements

for the degree of

Doctor of Philosophy

in the subject of

Microbiology and Molecular Genetics

Harvard University

Cambridge, Massachusetts

October 2013

Professor Michael Starnbach Andrew James Olive

Immunity to *Chlamydia trachomatis* and Host-Pathogen Interactions During Infection

Abstract

Infections with the bacterial pathogen *Chlamydia trachomatis* are a critical public health problem. *Chlamydia* remains the number one cause of preventable blindness worldwide and the leading cause of bacterial sexually transmitted infections in the United States. In humans, repeat and persistent infections with *Chlamydia* result in severe inflammation. Inflammation in the conjunctiva can result in blindness, while inflammation in the genital tract can result in pelvic inflammatory disease, ectopic pregnancy or infertility. In order to curb the increasing incidence of *Chlamydia* infections worldwide it will be necessary to develop a protective vaccine that affords long-term protection and prevents pathologies. To better inform vaccine development we must understand the mechanisms that drive long-term immunity in the genital tract and elucidate critical interactions between *Chlamydia* and host cells to uncover potential mechanisms of immune evasion.

This dissertation is focused on understanding interactions between *Chlamydia trachomatis* and its host while leveraging those finding for future therapeutic intervention. First, using a novel infection model I characterized mechanisms that afford long-lived protection in the genital mucosa following *C. trachomatis* infection. These studies identified that $CD4^+$ T cells are necessary and sufficient to protect mice from *C. trachomatis* infection. I further examined the migration of $CD4^+$ T cells to the genital mucosa and discovered that the integrin $\alpha4\beta1$ and the chemokine receptors CXCR3 and CCR5 are all required for the efficient recruitment of *Chlamydia*-specific T cells to the genital mucosa to mediate protection. Because immunity to *Chlamydia* in humans has been shown to be short-lived I next characterized how *Chlamydia*

may actively evade the host immune response. Using both proteomic and genomic approaches I identified hundreds of human proteins that are altered during *Chlamydia* infection. Using gain-of-function and loss-of-function approaches I next identified host pathways and proteins that are also required for efficient intracellular *Chlamydia* development and can be targeted by small molecules. Together the approaches described here characterize mechanisms that drive long-lived protective immunity in the genital mucosa, and elucidate virulence strategies employed by the *Chlamydia* to avoid clearance. These findings can now be used to better inform vaccine development and eradicate this costly disease.

Table of Contents

I dedicate this dissertation to my parents, Mike and Sandy Olive, who for as long as I can remember have taught me, believed in me, pushed me, and always loved me no matter what. Thanks for inspiring me to pursue Science.

Acknowledgments

It is hard to believe the journey of Graduate school is coming to an end. As I reflect back on my time, I'm amazed at the things I've learned, the friends I've made, and the experiences I've had. Graduate school would have been an even more difficult road if I didn't enjoy coming in to lab every day. A work environment where students and post-docs alike feel comfortable and have the freedom to examine questions that interest them is only possible because of a PI like Michael Starnbach. I wanted to join Michael's lab very quickly after joining the BBS program. Over the years Michael has taught me many things that go beyond bench science and scotch. His emphasis on personal interactions, developing writing skills, and giving a quality seminar are skills that will continue to serve me well in the future. Above all Michael is the biggest fan of all people in his lab. He will go to bat for any issues we have and never seems bothered when you talked to him about science or life problems. I have immensely enjoyed my time in his lab and look forward to interacting with him in science for years to come.

Of course Michael has hired a supremely talented and fun group of scientists to work with that have greatly influenced my graduate experience. In particular, when I joined the lab in 2008 there were 3 post-doctoral fellows that all played a huge role in my training. Dr. Esi Lamouse-Smith has been a great confidant and friend throughout the years. Teaching me the ins and outs of professional situations and acting as my every day physician. Dr. David Gondek taught me almost everything I know about T cell biology, in vivo experiments and how to harness the power of FACS. Finally, Dr. Jorn Coers who I consider my scientific mentor. He taught me to critically think about science and to think mechanistically in a way I never appreciated before. I wouldn't be the scientist I am today without the immense influence these three had on my professional development.

I have made many other lifelong friends in the Starnbach Lab. While I want to thank the new crop of graduate students and post-docs who arrived over the last couple years I need to thank Stephanie Jehl, Sarah Fankhauser, and Catarina Nouigiera in particular. These three

have become some of my best friends and are the most encouraging people in my life, yet are sassy to the core. I will greatly miss working with each of you on a daily basis and procrastinating for hours in the break room. Know you have made my graduate experience memorable. I also must thank Maddy Haff who is the worlds greatest technician and someone that was critical to so many experiments presented in this dissertation.

Since moving to Boston I have also made many lifelong friends outside of lab. I want to thank all of you for playing a role in some part of my graduate career. Included in this group are the wonderful individuals that staff the BBS office. They made graduate school straightforward and are always amazing to each of us in the program. Thanks!

I want to thank both my Dissertation Advisory Committee and my Defense Committee for agreeing to guide me through the graduate school process. My DAC meetings were always engaging and helpful in deciding new avenues of science to pursue. Without these committed scientists my graduate education would not have been the same.

Finally my time in Graduate school helped me appreciate all things that I have been blessed with. While in graduate school my brother-in-law Matt died from metastasized cancer. While his death was a struggle for me, his strength and determination until the end inspire me to do research every day. Matt didn't care if he understood everything but he always was one of the few non-scientists who wanted to *really* know what I do in lab. He was the bravest individual I have had the honor to know and I hope that one day the research I do can better help those with devastating diseases like Matt had.

I would also not have been able to complete this journey without the constant support and patience of Jessica. She put up with me for days at a time while hunkered down writing last minute grants. She always was willing to edit manuscripts and thesis chapters. And most of all she always encouraged me even in times of self-doubt. Thanks for all that you have been to me and done for me these last three years. I love you.

Finally I must thank the amazing Olive Family. Easily the hardest part about graduate school for me was being thousands of miles away from them. While we have had ups and downs the last 7 years, and I haven't been present for everything, you all continued to encourage me. I am so proud to call all of you my family. I love you all!

List of Figures

Chapter 2

Chapter 3

Chapter 4

Appendix B

List of Supplementary Tables

Chapter 1: Introduction

The balance of host-pathogen interactions

Interactions with the world around us have strongly influenced human evolution (1). Nowhere is this more apparent than in studies examining the influence of bacteria on fundamental human processes (2). Bacteria outnumber cells in the human body by ten-fold, which alone highlights the constant interactions between people and microbes (3). Recent studies suggest that the proper balance of commensal bacteria is critical for the acquisition of nutrients, immune development, and more (4, 5). Unfortunately, while the majority of bacteria are relatively harmless to humans, history has shown that pathogenic bacteria, which disrupt the normal balance of host interactions, can lead to devastating diseases (6).

When humans encounter bacterial pathogens, it is the job of the immune system to sense these dangers, to activate the proper defenses, and to clear the infections with the least harm to the host. This results in the development of memory, which protects against future infections. Our standard view of infections and immunity usually is associated with acute pathogens (7). Infection with acute pathogens normally results in one of two outcomes. Either the pathogen is cleared completely, and the host develops long-lived immunity or the pathogen wins evades the immune system and the host succumbs to the infection.

Unlike acute infections, several bacterial pathogens cause persistent infections that infect a single host and can survive for extended periods of time without clearance (8). From an immunological standpoint, persistent infections by definition are the result of failures in the immune response (9, 10). These failures ultimately lead the host to be unable to cope with the bacterial pathogen. What drives this failure of immunity is a central question we must answer in order to develop protective vaccines or antibiotics that help the host detect, and destroy these pathogens, even when bacteria are in a quiescent state. Many chronic pathogens have tropism for a narrow host range allowing them to evolve directly in response to those particular hosts immune mechanisms over time (8, 11). The success of these diseases is startling. For example, over one-third of the world's population is infected with the bacterial pathogen *Mycobacterium*

tuberculosis, with many unaware that they are infected (12, 13). These types of pathogens put a massive burden on public health and drive up healthcare costs (14, 15). In order to address this unmet clinical need and identify methods that skew hosts towards long-lived protective immunity that prevents future infections successfully, we must better understand the interactions between these chronic pathogens and their hosts to elucidate mechanisms of immune evasion. This dissertation is focused on understanding interactions between the chronic pathogen *Chlamydia trachomatis* and its mammalian host. Through the characterization of mechanisms that drive long-lived protective immunity, in conjunction with understanding virulence strategies employed by the pathogen to support growth and avoid clearance, we will be better equipped to prevent these infections in the future.

Chlamydia trachomatis epidemiology

Chlamydia trachomatis is a gram-negative obligate intracellular pathogen that infects the mucosal epithelium (16). While several species of *Chlamydia* exist, each has very limited host tropism and has evolved closely within their host environment (17). Therefore *Chlamydia* species are superbly adapted to survive within their specific host niche, but are rapidly cleared from host species of a broader range (11).

Chlamydia trachomatis is a growing public health concern in humans, which costs millions of dollars in treatment each year (18, 19). In developing countries, *C. trachomatis* is the causative agent of blinding trachoma and is the leading cause of preventable blindness worldwide (20). Furthermore, *C. trachomatis* is the number one cause of bacterial sexually transmitted disease in the United States, with infection rates continuing to rise (16). Infections with *Chlamydia* can lead to the development of immune sequelae at the infection site (21). Infections of the conjunctiva lead to the development of inflammation in the eye leading to corneal damage. In the genital tract, *C. trachomatis* infections can lead to pelvic inflammatory disease, and result in complications such as ectopic pregnancy and infertility. Infections with

Chlamydia are rapidly cleared with antibiotics such as azithromycin, however, the majority of infections are asymptomatic, complicating diagnosis and treatment. Ultimately, a protective vaccine that prevents both infection and immunopathologies will be required to curb the impact of *Chlamydia* burden worldwide.

Chlamydia trachomatis serovars are sub-divided into three major groups defined by their infection route and disease course (22). Serovars A-C infect the conjunctiva of the ocular tract and are highly prevalent in developing countries, particularly in the region of sub-Saharan Africa (22). Serovars D-K infect the columnar epithelial cells of the cervix (16). These infections are known to ascend to the upper genital mucosa, where they can persist over time. The third serovar group, L1-L3, infect through the genital mucosa and tend to cause systemic infections following spread to the draining lymphnodes, causing a condition known as lymphogranuloma venereum (17, 20, 23). These infections are more aggressive than those caused by other *C. trachomatis* serovars (17, 23). The focus of this dissertation will be on the genital serovars of *Chlamydia trachomatis* and their influence on immunity and pathology within the upper genital mucosa.

Chlamydia **intracellular development**

Chlamydia trachomatis is an obligate intracellular pathogen that must complete a unique bi-phasic developmental cycle in order to infect, replicate, and productively infect new cells. *C. trachomatis* enters host epithelial cells as a metabolically inactive elementary body (EB) (24). Once EBs enter host cells they are maintained in a membrane bound vacuole known as an inclusion. In the inclusion, EBs differentiate into reticulate bodies (RBs) that are the more metabolically active, replicative form of *C. trachomatis*. RBs divide by binary fission and replicate 100-1000 fold inside a single human cell. RBs are non-infectious, and lysing cells that contain solely RBs will halt infection completely (24). Once replication is complete, due to signals that are entirely undescribed, RBs then re-differentiate into EBs in order to prepare for

further infection of new host cells. *Chlamydia* is then released from infected host cells via one of two mechanisms, lysis or extrusion, and infectious EBs then contact new host cells to begin the developmental cycle anew (24, 25). Because *C. trachomatis* is closely associated with host cells, infection triggers a wide-ranging immune response that is designed to sense, activate and protect against *Chlamydia* infections in the genital mucosa (16).

Innate immunity and *C. trachomatis*

Upon exposure to *C. trachomatis*, the mucosal barrier is the first line of defense to prevent against infection. The endometrial epithelium in the upper genital tract is unique in that turns over rapidly in line with the estrous cycle, which directly influences *C. trachomatis* infectious capacity (26, 27). Furthermore, mucin, defensins, and antimicrobial peptides are likely to be secreted into the lumen of the genital mucosa and are predicted to play a protective role (28-30). However, detailed mechanistic insight into the importance of these proteins remains limited.

Once *Chlamydia* invades the epithelial layer in the genital mucosa, infected cells initiate early immune responses (31, 32). Studies have shown that epithelial cells can sense microbial products through the action of toll-like receptors (TLRs) and nod-like receptors (NLRs) and produce cytokines that recruit innate cells such as neutrophils, macrophages and NK cells (31, 32). While *Chlamydia* contains several pathogen associate molecular patterns (PAMPs), studies have shown that the activation of TLR2 drives several aspects of the host immune response (33-36). Infection of epithelial cells with *Chlamydia* leads to the secretion of specific pro-inflammatory cytokines such as interleukin 8 (IL-8), IL-1, and GM-CSF (37, 38). These cytokines initiate the immune response and attract adaptive immune cells to the site of infection. Ultimately, responding immune cells secrete interferon-γ (IFNγ), an essential cytokine that can directly restrict *Chlamydia* replication (39, 40). Mice deficient in IFNγ are unable to efficiently

clear *Chlamydia* infections in the genital mucosa, suggesting a critical role for this cytokine in limiting infection (40-42).

IFNγ restricts bacterial growth through several mechanisms that together lead to clearance. In general, IFNγ increases phagocytosis, upregulates important immunity genes such as MHC Class II, and activates other immune functions (39, 43-45). In human cells, IFNγ can also directly restrict bacterial growth through the induction of nitric oxide produced by upregulated inducible nitric oxide synthase (iNOS) (43, 44). Furthermore, IFNγ induces the enzyme indolamine 2-3-dioxygenase (IDO) which in turn depletes intracellular stores of tryptophan and increases the concentration of immunoregulatory metabolites known as kynurenines (46-48). Unlike humans, murine epithelial cells do not robustly initiate IDO dependent restriction. Instead of IDO, mice possess a family of p47 IFNγ -inducible GTPases (IRGs) that restrict bacterial growth both *in vivo* and in primary cells (49-51). Recent studies suggest that direct localization of these GTPases at the inclusion membrane disrupts the intracellular niche required for *Chlamydia* replication (52).

Interestingly, while the murine IRG system efficiently restricts human serovars of *C. trachomatis*, *Chlamydia* strains originally isolated from mice (such as *Chlamydia muridarum*) are largely resistant to this response (50, 51). Because of this resistance, infections of the murine genital mucosa with *C. muridarum* have increased duration and magnitude when compared directly to human strains (26, 31, 42, 53, 54). *C. muridarum* recapitulates many aspects of acute *Chlamydia* infection seen in humans and is used as an alternative tool to examine immunity development in the genital mucosa. However, because *C. muridarum* is not a human pathogen and uses different virulence mechanisms than *C. trachomatis*, its use is ultimately limited (41, 50, 51). Even so, understanding mechanistic differences between human and mouse IFNγ responses will allow the development of infection models that more closely recapitulate the human disease course (11).

Adaptive immunity and *C. trachomatis*

The initiation of the innate immune response during *C. trachomatis* infection leads to the activation, expansion and development of long-term immunity afforded by the adaptive immune compartment. While all major branches of the adaptive immune response are activated during *Chlamydia* infection, their importance in long-lived immunity differs dramatically. Through human clinical studies and mechanistic experiments in mice, we are beginning to understand what drives protective immunity in the genital mucosa to *C. trachomatis*.

B cell responses to *C. trachomatis* infection

B cells are adaptive immune cells that detect soluble extracellular antigens in an antigen specific manner (55). Even though *Chlamydia* is predominantly found inside host cells during infection, EBs are exposed to the extracellular environment between rounds of replication. This affords an opportunity for B cells and the antibodies they produce to target exposed bacteria. Antibody binding to extracellular *Chlamydia* can directly inhibit invasion of host cells as well as opsonize *Chlamydia* particles for uptake by professional antigen presenting cells (APCs). This enhances the presentation of *Chlamydia* antigens to activate a robust T cell response, which will be discussed later.

In human patients, antibodies can be detected against several *Chlamydia* antigens, but predominantly against the Major Outer Membrane protein (MOMP) (56). Early studies showed that protection correlated with the presence of *Chlamydia* antibodies, and that antibodies could inhibit infection *in vitro* (57, 58). Unfortunately, later studies showed that *Chlamydia* antibodies are strain specific, which is caused by high variability of the MOMP proteins between strains (59). Because of this variability, antibodies are not anticipated to be broadly protective against further *Chlamydia* infections in humans.

The importance of B cells *in vivo* has been confirmed using murine models of genital *Chlamydia* infection. Experimentally, mice deficient in B cells cleared primary *Chlamydia* infections similar to wild type mice (60). Further studies also showed B cells are not required for the recall response in the genital tract, although clearance was slightly delayed (61). Another study has shown that transfer of protective antibodies *in vivo* can partially protect mice from infection, but they do so rather weakly (62). Together, these data suggest that B cells are not the main drivers of protective immunity against *C. trachomatis*, and that antibodies play a limited role in *Chlamydia* clearance. Therefore, vaccine strategies that promote high antibody titers against *Chlamydia* may not provide true protection. Rather, vaccine strategies should be focused on developing robust cell mediated immunity.

T cell mediated Immunity

While it is clear that antibodies specific for *Chlamydia* are produced during infections, they do not appear to be necessary or sufficient for protection. Furthermore, mice infected previously with *Chlamydia* show strong resistance to re-infection, suggesting that the T cell compartment mediates protection against infection since B cells are not important for this resistance (26, 40).

T cells are characterized by the expression of protein heterodimers known as the T cell receptor (TCR), which defines T cell antigen specificity (55). There are two main classes of T cells that differ in their function and protective capacity, $\alpha\beta$ T cells, which are the main focus of this dissertation, and $\gamma\delta$ T cells which remain relatively uncharacterized during *Chlamydia* infections (63). During T cell development specific rearrangement events in the TCR, known as VDJ recombination, give rise to a broad range of antigen specificities. Specific steps during thymic selection ensure that T cells that enter the periphery can detect MHC molecules (positive selection) and do not cross-react with self-antigens (negative selection) (55, 64). This gives rise to a pool of naïve T cells that each detect unique foreign antigens such as invading pathogens.

In order for T cells to become activated and respond to infection, they must be able to find foreign antigens through a process known as antigen presentation. Distinct pathways of antigen presentation lead to the activation of distinct T cell populations.

$CD8^+$ T cell Responses during *C. trachomatis* Infection

The TCR does not recognize full-length proteins, but rather binds to short peptides that are produced through proteolytic cleavage. How peptides are processed and presented to T cells is dependent upon the MHC molecule. There are two major classes of MHC molecules, Class I and Class II (55). MHC class I molecules bind to peptides that are typically 8-10 amino acids in length, which are produced in the cytosol of host cells (65). These cytosolic peptides can be produced through proteasomal degradation as well as by other proteases in the cytosol. Peptides are then transported into the endoplasmic reticulum via Transporter associated with antigen processing (TAP) where they are then loaded into MHC class I molecules (65). Pre-loaded class I molecules are trafficked to the surface of the host cell, where they can stimulate $CD8^+$ T cell immunity. Upon detecting an antigen via TCR signaling, $CD8^+$ T cells become activated and secrete a range of important cytokines, including IFNγ that can mediate protection (66). Furthermore, activated $CD8^+$ T cells upregulate bioactive molecules such as perforin, FasL, or granzyme B, which can directly lyse or induce death of cells presenting the particular peptide (55). In this way $CD8^+$ T cells can directly detect and destroy cells that are infected with intracellular pathogens such as *C. trachomatis*, removing the intracellular niche entirely (67, 68). Importantly, MHC class I expression occurs in almost all cell types, giving $CD8^+$ T cells a broad capacity to protect regardless of cell type.

During infections of the genital mucosa with *C. trachomatis*, antigen specific $CD8^+$ T cells are activated and recruited to the site of infection (68). In infected human patients, cervical samples show the presence of *Chlamydia* specific $CD8^+$ T cells that secrete IFNγ (68, 69). In

mice, the presence of antigen specific T cells can also be found in the upper genital tract following *Chlamydia* infection. $CD8^+$ T cells mostly recognize cytosolic proteins and *C. trachomatis* is maintained in a membrane vacuole intracellularly protecting most *Chlamydia* antigens from the MHC Class I pathway (70-72). However *Chlamydia* is known to secrete bacterial virulence proteins directly into the cytosol that can be processed and presented in MHC class I molecules to stimulate $CD8^+$ T cell responses. Several *Chlamydia* proteins have been identified as $CD8^+$ T cell antigens, however, their role in the cytosol generally remains unknown (70-72).

Since $CD8^+$ T cells are stimulated and recruited to the genital tract investigators tested whether they are necessary and sufficient for protection. Transfer of *Chlamydia* specific $CD8^+$ T cells cultured *in vitro* robustly protected mice from *Chlamydia* infection (73, 74). However, using depletion studies or genetic knockout-mice, investigators see a limited role for $CD8^+$ T cells during primary infection or in response to secondary infection (75). In fact, it has been suggested that the $CD8^+$ T cell memory response is blunted following *Chlamydia* infection. Inhibition of T cell memory prevents a robust recall response from the $CD8^+$ T cell compartment and may influence the progression of disease and the development of immunopathologies (74). This suggests perhaps that *Chlamydia* has developed virulence mechanisms to directly influence the development of $CD8^+$ T cell immunity during infection, preventing robust memory development and long-lived protective immunity.

$CD4^+$ T cell responses during *Chlamydia* infection

Unlike MHC class I that normally binds peptides processed in the host cytosol, MHC class II molecules bind peptides derived from antigens initially found outside of host cells (55). Professional APCs, such as dendritic cells, phagocytose foreign antigens into an endosomal compartment that matures, accumulates proteases, and processes the antigens into peptides that are 12-15 amino acids in length. Eventually these intracellular compartments fuse with

vesicles where the cleaved peptides are loaded onto MHC class II and trafficked to the surface of the host cell (76). Once on the surface, loaded class II molecules can stimulate antigen-specific CD4 $^{+}$ T cell responses that promote pathogen clearance. The exact cytokines and activation profile of CD4^{+} T cells is variable and depends on the APC presenting the antigen, the cytokine milieu and other signals that are not entirely characterized. There are three main sub-types of activated CD4^{+} T helper (Th) cells, Th1, Th2, and Th17 that secrete distinct cytokines and serve different purposes during immunity (55, 77). Th1 responses, characterized by the secretion of cytokines like IFNγ and TNFα, are activated during infections with intracellular pathogens while Th2 responses are characterized by the production of IL-4 and are associated with resolving helminth infections efficiently (78). Finally, Th17 immunity develops to control extracellular bacteria and fungal infections, and also is implicated in many autoimmune diseases, such as rheumatoid arthritis (78). Together these CD4^{+} subsets can tune immune responses to effectively clear pathogens with broad tropism or multi-cellularity. CD4^{+} T cells are initially activated by professional APCs that constitutively express MHC class II molecules on their surface (79). However, the induction of MHC Class II molecules on other cells types, such as epithelial cells, is known to occur, but the understanding of the functional implications of CD4^{+} T cell interactions with these cell types remains limited (79).

In the context of *C. trachomatis* infection, CD4^{+} T cells are proposed to play the largest role in providing long lasting protective immunity. *Chlamydia* specific CD4^{+} T cells are activated through APCs that have engulfed free extracellular EBs or infected cells (80). In human patients, cervical samples from infected individuals showed the presence of *Chlamydia* specific CD4^{+} T cells (81). The activation of these T cells is predominantly skewed towards a Th1 response, which is not surprising given the restrictive effects of IFNγ on *C. trachomatis* growth. However even though robust CD4^{+} responses are activated and limit pathogen growth, one recent study suggested these CD4^{+} T cells wane over time and do not develop into long-lasting

memory cells (81). This may be one mechanism responsible for the high rates of re-infection with *C. trachomatis*.

In murine models of *Chlamydia* infection $CD4^+$ T cells are considered the primary indicators of effective immunity. During infection in the murine genital mucosa $CD4^+$ T cells are recruited and secrete high levels of IFNγ (80, 82, 83). Studies using TCR transgenic mice to track *Chlamydia*-specific $CD4^+$ T cells during infection showed that $CD4^+$ T cells are initially primed in the iliac lymph node that drains the genital mucosa (84). These T cells proliferate in the lymph node and then traffic to the genital tract to mediate protection. Mice depleted of $CD4^+$ T cells are unable to efficiently control primary or secondary infections with the mouse adapted species *C. muridarum* (82). Mice previously infected with *C. muridarum* show strong resistance to re-infection in a CD4 dependent manner beyond six months, suggesting the development of long-lived protective immunity. Furthermore, transfer of *Chlamydia*-specific $CD4^+$ T cells limited bacterial growth during systemic routes of *C. trachomatis* infection (85). However, one recent study suggested that immunity to infections of the murine genital tract with the human strains of *C. trachomatis* were not driven by $CD4^+$ T cells (54). This result was confounding based on the literature, and warranted further investigation to understand the mechanisms responsible for these conclusions. Chapter 2 in this dissertation will examine this discrepancy in the literature to determine the role of $CD4^+$ T cells in providing protective immunity in the genital mucosa during infections with *C. trachomatis*.

T cell Trafficking to the Genital Mucosa

In order for T cells to impart their protective capacity at the genital mucosa during *Chlamydia* infection, they must first traffic to the mucosal tissue. As described above, *Chlamydia* specific $CD4^+$ T cells initially become activated in the iliac lymph node that drains from the genital tissue (84). Following activation, these T cells must exit the lymphatic system and traffic directly into the genital mucosa, where the protective cytokines produced by $CD4^+$ T cells can mediate

clearance. $CD4^+$ T cells home to the genital mucosa through the coordinated action of chemokine receptors, integrins, and selectins. It is known that different combinations of homing molecules promote trafficking to specific tissues. For example, a combination of the integrin $\alpha4\beta7$ and the chemokine receptor CCR9 direct T cells to the intestines (86). There is great interest in characterizing the trafficking "area-code" for pathogen-specific T cells in the genital mucosa following infection with *Chlamydia*, yet few studies have pursued these experiments and no (86)studies have used antigen specific methods for characterization. In the limited published reports, investigators suggest that the chemokine receptor CCR5 may be required for efficient lymphocyte recruitment to the genital mucosa since $CCR5^{-/-}$ mice are unable to efficiently clear infections with C. *muridarum* (87). In separate studies examining integrin expression, one group describes the enrichment of T cells expressing $\alpha4\beta1$ in the genital mucosa while a second group suggests $\alpha4\beta7$ is the critical mediator of T cell trafficking (88, 89). However, all these studies examined the expression of receptors on bulk pools of T cells, and did not examine the influence of receptor expression on the protective capacity of the T cells. Because of the lack of strong evidence supporting the mechanisms of T cell recruitment to the genital tract, this dissertation will begin to characterize these processes in mice in chapters 3 and 4.

Failures of adaptive immunity to *Chlamydia*

Although murine models of *Chlamydia* infection recapitulate several aspects of human disease, there are limitations to their use in the context of persistent infections. It is clear that *C. trachomatis* infections of the murine genital tract stimulate a robust protective T cell response that results in sterile immunity that is long lasting (42). However, in humans immunity appears short-lived and non-protective, resulting in multiple infections in a single patient (81). Clinical data also shows that some patients who are culture negative still shed *Chlamydia* DNA and

RNA, suggesting persistent infections with *Chlamydia* occur in vivo (90, 91). The discrepancies in the outcome of infection and immunity between mice and humans with *Chlamydia* are likely due to distinct differences in the disease course and the subsequent immune response between hosts. As described previously, *C. trachomatis* has a host tropism limited to humans and therefore has developed specific mechanisms that subvert human immune processes. By introducing *C. trachomatis* into a host environment that contains different immune effectors relative to humans and within which the pathogen is not evolved to survive, we may activate alternative immune processes that are not relevant in humans or prevent virulence mechanisms that are relevant in humans (11). Therefore, it is critical that we not only understand mechanisms that drive long lasting protective immunity, but also that we characterize virulence strategies used by *C. trachomatis* in human cells to promote growth, replication, evade the immune response and persist in the human genital mucosa. The following sections will detail known virulence mechanisms used by *C. trachomatis* to support growth and alter host immunity.

Bacterial mechanisms used to subvert host cells and support intracellular growth.

Chlamydia trachomatis has a relatively small genome that contains roughly 1MB of DNA and 1000 open-reading frames (ORFs) (92). Based on bioinformatics studies this small genome size suggests that *Chlamydia* species have undergone reductive evolution that limits the host range of *C. trachomatis* infections (23). Transcriptional analysis of *Chlamydia* genes during infection has shown that there is tight regulation of bacterial genes that are broken down into three groups, the early, middle and late genes (93). Early genes are transcribed quickly following inclusion formation and primary differentiation into RBs. Middle genes begin to be transcribed 12-18 hours following infection, and late genes are activated after 20 hours post-infection. It is hypothesized that the timing of the distinct gene clusters in *Chlamydia* is initiated by unknown signals, and prepares *Chlamydia* for all stages of growth, including the final re-differentiation into EBs that is required for productive infection. Recent proteomic studies that examined the

Chlamydia proteome in purified EBs or RBs showed that EBs, although metabolically limited, are pre-loaded with a variety of virulence proteins that drive invasion and promote infection (94). Unfortunately, due to the obligate intracellular nature of *C. trachomatis*, it has remained difficult to use standard genetic techniques to knockout bacterial genes and to elucidate the function of individual virulence determinants. This has led investigators to develop different tools to understand the role of specific gene products (95, 96). The following sections will examine how these studies have informed our understanding of the virulence mechanisms used by *Chlamydia* to invade cells, acquire nutrients and subvert immunity.

The *Chlamydia* type III secretion system

Like many gram-negative pathogens, *Chlamydia* uses a specialized type III secretion system to translocate effector proteins directly into the host cell cytoplasm (97). Bioinformatic studies predict that *Chlamydia* secretes over 100 unique virulence factors into the host cell where they manipulate host cell processes to the benefit of the pathogen, yet the function of most effectors remains entirely unknown (98). Type III secretion systems are essentially a needle-and-syringe-like structure, which protrudes from the bacterial surface and makes contact directly with host membranes. This creates a conduit for proteins within *Chlamydia* to translocate directly into host cells. Studies using yeast-two hybrid assays have begun to tease apart the important structural components of the *Chlamydia* type III secretion apparatus (99). These have defined the proteins that make up the basal body, or the base, of the secretion apparatus that spans both the inner and outer membrane of Chlamydia. Again, due to a lack of tractable genetics it has remained difficult to directly test the role of each protein in the overall structure and function of the type III secretion system. However, using chemical inhibitors that prevent type III secretion in other gram-negative pathogens, it is clear that a functional type III secretion system is required for productive bacterial growth and survival (100, 101).

Host cell adhesion and invasion

C. trachomatis is able to invade and infect most cultured cells, suggesting that the mechanisms of invasion are not cell type specific. Therefore, individual receptors that influence invasion are most likely ubiquitously expressed on many different cell types. It is hypothesized that initial binding and invasion occurs in a two-step process (102). First, there is a reversible binding that is mediated primarily by charge interactions. This is followed by a second irreversible step that is mediated by the binding of *Chlamydia* to secondary receptors. RNAi studies in drosophila cells that examined host factors required for initial entry of *Chlamydia* showed an unexpected role of growth factors and their receptors in initial *Chlamydia* binding and invasion (103, 104). These studies identified the PDGF receptors and FGFR as critical to initial invasion and to promote further rounds of *Chlamydia* replication. One recent study using a haploid cell line trap screen identified that the overall sulfation of cells, is an essential factor that influences the infectivity of host cells (105). Several bacterial factors including MOMP, OmcB, and PMPs have been suggested to influence these initial binding interactions, but it has remained difficult to understand the influence and mechanisms of each interaction in the absence of targetable genetic techniques (102).

Chlamydia enters non-phagocytic cells through a process mediated by both host and bacterial products. The invasion of *C. trachomatis* is driven by a rearrangement of actin through the action of host small GTPases (102, 106). *C. trachomatis* EBs are preloaded with specific effector proteins that are poised to be secreted into host cells upon contact. The best characterized of these factors is the *Chlamydia* protein TARP. TARP is a multifunctional virulence determinant that can directly polymerize actin to promote uptake of Chlamydia, and is phosphorylated by host tyrosine kinases such as ABL to influence invasion (107, 108). One study showed microinjection of TARP antibodies directly into host cells prior to infection could inhibit efficient invasion, giving direct evidence that TARP mediates infection (109). These data

suggest that *Chlamydia* uses a subset of secreted effectors to directly mediate uptake into host cells to initiate the infectious cycle.

Inclusion development and localization

Upon entering host cells, EBs maintained in the inclusion are diverted from the endolysosomal pathway, preventing lysosomal fusion (110). In a microtubule dependent fashion, inclusions are trafficked from the cellular periphery to the Peri-Golgi region, where both host and bacterial proteins are recruited to the inclusion membrane (110, 111). While the mechanistic details remain unknown, it is hypothesized that several *Chlamydia* proteins actively promote this transport in a dynein dependent fashion. *Chlamydia* is known to secrete several effector proteins known as Incs that possess a bi-lobed hydrophobic domain, allowing their insertion directly into the inclusion membrane (112). These Inc proteins have been shown to recruit and interact with several host trafficking proteins, such as Rabs and SNAREs that may promote acquisition of nutrients from the host through vesicle fusion with the inclusion (113-115). In support of this concept, several Inc proteins such as IncA contain similarities to eukaryotic SNARE proteins that may drive these processes in host cells. Together these previous findings suggest that active reorganization of the inclusion membrane is an essential step in the *Chlamydia* developmental cycle and is driven primarily by secreted effector proteins.

Nutrient acquisition by *Chlamydia* in the host cell

One of the primary goals of *Chlamydia* is to acquire the necessary nutrients to replicate robustly and survive in the intracellular niche. It has become clear that lipid acquisition is a critical component of *Chlamydia* virulence strategies. Lipid acquisition is required for efficient replication and for successful completion of the entire developmental cycle of *Chlamydia*. Early work by Hackstadt and colleagues suggested that *Chlamydia* is able to intercept host sphingomyelin and cholesterol for growth (116). More recent studies suggest that *Chlamydia*

also recruits lipids through non-vesicular trafficking mechanisms. For example two reports have shown a requirement for the host Ceramide transfer protein (CERT) to be recruited to the inclusion, and it is hypothesized that Ceramide may be directly converted to sphingomyelin at the inclusion (117, 118). CERT was shown to interact directly with the *Chlamydia* effector IncD, suggesting lipid acquisition is actively promoted by *Chlamydia* for survival.

Studies have also shown that infection with *Chlamydia* leads to Golgi fragmentation, which is predicted to enhance nutrient acquisition in the inclusion (119). Initial studies suggested this process was mediated by the *Chlamydia* protease CPAF, however subsequent investigations showed this might be an artifact of post-lysis activity of the protease (120). Therefore, our understanding of which *Chlamydia* effectors mediate this host alteration remains unclear. Beyond these mechanisms, *Chlamydia* has also been shown to actively recruit lipid droplets to the inclusion as an alternative source of nutrients. One report showed that lipid droplets co-fractionate with the secreted effector IncA, suggesting that this process is actively mediated by *Chlamydia* (121). Finally, close association of inclusions with mitochondria and lysosomes suggests a potential resource for essential amino acids that are required for efficient *Chlamydia* replication (122, 123). However, the mechanisms responsible or the importance of these pathways remains to be elucidated.

Beyond nutrient acquisition, *Chlamydia* infection directly interferes with normal host cell processes such as cell cycle progression. Work has shown that infection with *Chlamydia* directly leads to the cleavage of CyclinB1 halting cell cycle progression (124). Further work showed that infection with *Chlamydia* leads to abnormal spindle formation, centrosome amplification, and segregation defects (125-127). In combination with a recent study that showed that infection with *Chlamydia* leads to massive rearrangement of chromatin and DNA damage in host cells, it is tempting to speculate that infection with *Chlamydia* may also lead to a cancerous state (128). Future studies will need to better elucidate the long-term implications of *Chlamydia* infection on cancer development.

Inhibition of innate immune responses during *Chlamydia* infection.

Because *Chlamydia* is entirely dependent on host cells for replication and survival, *Chlamydia* has evolved specific mechanisms that alter the initial innate immune response to promote infection. Our lab identified that *Chlamydia* encodes two specific deubiquitinating/deneddylating enzymes, ChlaDub1 and ChlaDub2, that can directly remove ubiquitin chains from proteins targeted for proteasomal degradation (129). One report has suggested that ChlaDub1 can prevent the activation of the NF-κB pathway by preventing the proteasomal degradation of the IκBα (130). This would prevent robust activation of the NF-κB cascade, which in turn would inhibit the secretion of proinflammatory cytokines that initiate an immune response to *C. trachomatis*. Other studies have shown that *Chlamydia* infection leads to the destruction of RelA, a subunit of the NF-κB complex (131). It is hypothesized that this inactivation plays a similar role to ChlaDub1 by preventing strong activation of the pathways needed to initiate host responses to infection. However, the exact bacterial factors that are responsible for this phenotype remain controversial. Future studies are needed to clarify the role of NF-κB inhibition during *Chlamydia* infection, particularly *in vivo*.

When cells are infected with pathogens, one way in which the host can activate the immune response is through the induction of apoptosis, thereby removing the intracellular niche required by *Chlamydia* for survival. Apoptotic cells can then be phagocytosed by professional APCs, resulting in the activation of a robust immune response (55). Because of this, *Chlamydia* has developed mechanisms that prevent premature apoptosis or cell death to ensure the developmental cycle can be completed without interruption. One mechanism by which this can occur is through the degradation of proapoptotic proteins such as the BH3-only proteins Bad, Bim and Puma (131-133). A separate mechanism by which this can occur is through the stabilization of inhibitors of apoptosis such as IAP2 and Mcl-1, which promotes cell survival

during *Chlamydia* infection (134-136). By directly manipulating innate immune signaling pathways and host survival pathways, *Chlamydia* ensures the intracellular replicative niche remains intact for the duration of infection, allowing it to complete the entire developmental cycle and to infect new cells.

***Chlamydia trachomatis* subverts the IFNγ response in epithelial cells.**

As discussed earlier, *Chlamydia* clearance is dependent on IFNγ, as mice deficient in IFNγ are unable to efficiently clear infections (40). However, epithelial cells in mice and humans differ in their response to IFNγ (11). In mice, IFNγ induces the IRG response, which is almost entirely absent in humans. In human cells, IFNγ leads to the robust upregulation of IDO, which in turn depletes intracellular stores of tryptophan (137). Upon the depletion of tryptophan, *C. trachomatis* transitions from actively replicating RBs into a quiescent noninfectious "persistent" form (138). These aberrant or persistent forms can remain in cells undetected for extended periods of time. This is possible because human strains of *C. trachomatis* contain a partial Tryptophan operon that can use exogenously found indole, most likely produced by commensals in the lower genital mucosa, to produce tryptophan and survive in cells even under high expression of IDO (139). This is the major mechanism that is hypothesized to promote chronic infections with *C. trachomatis* in humans.

Unfortunately, modeling of this persistent response to IFNγ has remained difficult in vivo due to distinct differences between mice and men, as addressed previously. One recent study examined whether loss of the IRG regulators would lead to the induction of persistent *Chlamydia* infection in the murine genital mucosa (41). Interestingly, this study found that loss of the IRG system resulted in robust growth of *Chlamydia* similar to IFNγ knockout mice early during infection, but it was later resolved through a compensatory $CD4^+$ T cell response that was sufficient to mediate protection. Therefore, it seems that some level of restriction is

necessary for *Chlamydia* to persist. Because IDO is not induced robustly in murine epithelial cells, it is hypothesized that humanizing mice to allow robust IDO expression in murine epithelial cells in the absence of IRGs may lead to a model of *Chlamydia* persistence. However, this remains to be tested and will be a major focus of in vivo *Chlamydia* research in the future.

Chlamydia infection directly alters antigen presentation in infected cells

Another mechanism by which *C. trachomatis* has been shown to actively alter immune responses is by inhibiting antigen presentation. Studies by Zhong and colleagues suggest that during infection *Chlamydia* downregulates the surface expression of MHC molecules. One mechanism by which this occurs is through the degradation of host transcription factors RFX5 and USF-1, which are responsible for MHC induction (140, 141). Through this process, *Chlamydia* is hypothesized to prevent efficient presentation of bacterial peptides to the immune system, thereby inhibiting robust activation. Initially, these phenotypes were associated with the *Chlamydia* protease CPAF, but recently these findings have been questioned (120). Therefore, it will be important to understand bacterial factors outside of CPAF that may be responsible for altering the expression of MHC molecules and to determine how this impacts subsequent immunity and memory development.

Chlamydia infection leads to a blunted $CD8^+$ T cell response limiting memory potential

As discussed previously, the fact that *Chlamydia trachomatis* can cause persistent infections suggests there is a failure of the adaptive immune response to efficiently detect and eradicate infection. One area that has puzzled investigators is that $CD8^+$ T cells do not appear to be important for mediating *Chlamydia* clearance. *Chlamydia* is an infection of epithelial cells, similar to many viruses in which $CD8^+$ T cells are absolutely required for clearance. Furthermore, $CD8^+$ T cells have the capacity to directly lyse *Chlamydia* infected cells, removing the intracellular niche and halting infection prior to re-differentiation into EBs (67, 71). It seems

that although $CD8^+$ T cells can be protective when activated and supplied independently of *Chlamydia* infection, those $CD8^+$ T cells produced during natural infection are deficient in some way. Several studies have shown repeatedly that $CD8^+$ T cells do not play a major role during primary or secondary challenge in the genital mucosa (82, 142). Recent studies have begun to examine factors that may prevent a robust $CD8^+$ T cell response during *Chlamydia* infection. Work in our lab has shown that following initial infection with *Chlamydia*, the $CD8^+$ T cell memory response to *Chlamydia* infections is blunted (74). Normally, a recall T cell response should be faster and amplified in comparison to primary infection. However, in mice infected with *Chlamydia*, pathogen specific $CD8^+$ T cells do not expand robustly, and appear to have exhausted T cell phenotypes. Furthermore, co-infection of *Chlamydia* with Listeria, which normally induces a robust secondary response, prevents efficient recall responses to both pathogens, suggesting that *Chlamydia* uses active mechanisms to alter immunity. However, the mechanistic details responsible for these observations remain to be elucidated and will be the focus of future work.

Summary

In this thesis I describe interdisciplinary approaches that I used to characterize immunity and host-pathogen interactions of the intracellular bacterium *C. trachomatis*. The first part of this dissertation presents findings that elucidate mechanisms of host immunity that drive protection in the murine genital mucosa. These studies identified that $CD4^+$ T cells are necessary and sufficient for protection from *C. trachomatis* infection. Furthermore, I identified mechanisms that promoted the recruitment of *Chlamydia*-specific $CD4^+$ T cells to the genital mucosa, where they were required for protection. In the second part of this dissertation I investigated how infection of human cells with *C. trachomatis* directly alters the host proteome. By using layered proteomic and genomic approaches, I uncovered broad host protein networks that were altered in their stability independently of changes in host transcription. In addition, I demonstrated that several

of these host-pathogen interactions are required for the intracellular development of *C. trachomatis*. Leveraging these findings, I showed that therapeutic approaches that use small molecules to alter the host pathways that are required for the survival of *C. trachomatis* have great potential. By characterizing mechanisms of host immunity that promote protection, as well as identifying critical host-pathogen interactions needed for Chlamydia propagation, we are better equipped to develop a protective vaccine that promotes long-term protective immunity without inducing immune pathologies.

1. Hooper LV, Midtvedt T, Gordon JI. How host-microbial interactions shape the nutrient environment of the mammalian intestine. Annual review of nutrition. 2002;22:283-307. Epub 2002/06/11. doi: 10.1146/annurev.nutr.22.011602.092259. PubMed PMID: 12055347.

2. Zaneveld J, Turnbaugh PJ, Lozupone C, Ley RE, Hamady M, Gordon JI, et al. Host-bacterial coevolution and the search for new drug targets. Current opinion in chemical biology. 2008;12(1):109-14. Epub 2008/02/19. doi: 10.1016/j.cbpa.2008.01.015. PubMed PMID: 18280814; PubMed Central PMCID: PMC2348432.

3. Hooper LV, Gordon JI. Commensal host-bacterial relationships in the gut. Science. 2001;292(5519):1115-8. Epub 2001/05/16. PubMed PMID: 11352068.

4. Garrett WS, Gordon JI, Glimcher LH. Homeostasis and inflammation in the intestine. Cell. 2010;140(6):859-70. Epub 2010/03/23. doi: 10.1016/j.cell.2010.01.023. PubMed PMID: 20303876; PubMed Central PMCID: PMC2845719.

5. Kau AL, Ahern PP, Griffin NW, Goodman AL, Gordon JI. Human nutrition, the gut microbiome and the immune system. Nature. 2011;474(7351):327-36. Epub 2011/06/17. doi: 10.1038/nature10213. PubMed PMID: 21677749; PubMed Central PMCID: PMC3298082.

6. Vance RE, Isberg RR, Portnoy DA. Patterns of pathogenesis: discrimination of pathogenic and nonpathogenic microbes by the innate immune system. Cell host & microbe. 2009;6(1):10-21. Epub 2009/07/21. doi: 10.1016/j.chom.2009.06.007. PubMed PMID: 19616762; PubMed Central PMCID: PMC2777727.

7. Lara-Tejero M, Pamer EG. T cell responses to Listeria monocytogenes. Current opinion in microbiology. 2004;7(1):45-50. Epub 2004/03/24. doi: 10.1016/j.mib.2003.12.002. PubMed PMID: 15036139.

8. Rittershaus ES, Baek SH, Sassetti CM. The normalcy of dormancy: common themes in microbial quiescence. Cell host & microbe. 2013;13(6):643-51. Epub 2013/06/19. doi: 10.1016/j.chom.2013.05.012. PubMed PMID: 23768489; PubMed Central PMCID: PMC3743100.

9. Miyairi I, Ramsey KH, Patton DL. Duration of untreated chlamydial genital infection and factors associated with clearance: review of animal studies. The Journal of infectious diseases. 2010;201 Suppl 2:S96-103. Epub 2010/05/28. doi: 10.1086/652393. PubMed PMID: 20470047.

10. Torti N, Oxenius A. T cell memory in the context of persistent herpes viral infections. Viruses. 2012;4(7):1116-43. Epub 2012/08/02. doi: 10.3390/v4071116. PubMed PMID: 22852044; PubMed Central PMCID: PMC3407898.

11. Coers J, Starnbach MN, Howard JC. Modeling infectious disease in mice: co-adaptation and the role of host-specific IFNgamma responses. PLoS pathogens. 2009;5(5):e1000333. Epub 2009/05/30. doi: 10.1371/journal.ppat.1000333. PubMed PMID: 19478881; PubMed Central PMCID: PMC2682201.

12. Behr MA. Evolution of Mycobacterium tuberculosis. Advances in experimental medicine and biology. 2013;783:81-91. Epub 2013/03/08. doi: 10.1007/978-1-4614-6111-1_4. PubMed PMID: 23468104.

13. Brites D, Gagneux S. Old and new selective pressures on Mycobacterium tuberculosis. Infection, genetics and evolution : journal of molecular epidemiology and evolutionary genetics in infectious diseases. 2012;12(4):678-85. Epub 2011/08/27. doi: 10.1016/j.meegid.2011.08.010. PubMed PMID: 21867778; PubMed Central PMCID: PMC3253320.

14. Goldberg DE, Siliciano RF, Jacobs WR, Jr. Outwitting evolution: fighting drug-resistant TB, malaria, and HIV. Cell. 2012;148(6):1271-83. Epub 2012/03/20. doi: 10.1016/j.cell.2012.02.021. PubMed PMID: 22424234; PubMed Central PMCID: PMC3322542.

15. Workowski K. In the clinic. Chlamydia and gonorrhea. Annals of internal medicine. 2013;158(3):ITC2-1. Epub 2013/02/06. doi: 10.7326/0003-4819-158-3-20130205-01002. PubMed PMID: 23381058.

16. Roan NR, Starnbach MN. Immune-mediated control of Chlamydia infection. Cellular microbiology. 2008;10(1):9-19. Epub 2007/11/06. doi: 10.1111/j.1462-5822.2007.01069.x. PubMed PMID: 17979983.

17. Gomes JP, Bruno WJ, Nunes A, Santos N, Florindo C, Borrego MJ, et al. Evolution of Chlamydia trachomatis diversity occurs by widespread interstrain recombination involving hotspots. Genome research. 2007;17(1):50-60. Epub 2006/11/09. doi: 10.1101/gr.5674706. PubMed PMID: 17090662; PubMed Central PMCID: PMC1716266.

18. Burton MJ, Mabey DC. The global burden of trachoma: a review. PLoS neglected tropical diseases. 2009;3(10):e460. Epub 2009/10/28. doi: 10.1371/journal.pntd.0000460. PubMed PMID: 19859534; PubMed Central PMCID: PMC2761540.

19. Aronson SM. The global burden of trachoma. Medicine and health, Rhode Island. 2004;87(4):91. Epub 2004/06/01. PubMed PMID: 15168629.

20. Paavonen J. Chlamydia trachomatis infections of the female genital tract: state of the art. Annals of medicine. 2012;44(1):18-28. Epub 2011/02/03. doi: 10.3109/07853890.2010.546365. PubMed PMID: 21284529.

21. Geisler WM. Duration of untreated, uncomplicated Chlamydia trachomatis genital infection and factors associated with chlamydia resolution: a review of human studies. The Journal of infectious diseases. 2010;201 Suppl 2:S104-13. Epub 2010/05/28. doi: 10.1086/652402. PubMed PMID: 20470048.

22. Wang SP, Grayston JT, Gale JL. Three new immunologic types of trachoma-inclusion conjunctivitis organisms. J Immunol. 1973;110(3):873-9. Epub 1973/03/01. PubMed PMID: 4631875.

23. Borges V, Nunes A, Ferreira R, Borrego MJ, Gomes JP. Directional evolution of Chlamydia trachomatis towards niche-specific adaptation. Journal of bacteriology. 2012;194(22):6143-53. Epub 2012/09/11. doi: 10.1128/JB.01291-12. PubMed PMID: 22961851; PubMed Central PMCID: PMC3486361.

24. Moulder JW. Interaction of chlamydiae and host cells in vitro. Microbiological reviews. 1991;55(1):143-90. Epub 1991/03/01. PubMed PMID: 2030670; PubMed Central PMCID: PMC372804.

25. Hybiske K, Stephens RS. Mechanisms of host cell exit by the intracellular bacterium Chlamydia. Proceedings of the National Academy of Sciences of the United States of America. 2007;104(27):11430-5. Epub 2007/06/27. doi: 10.1073/pnas.0703218104. PubMed PMID: 17592133; PubMed Central PMCID: PMC2040915.

26. Ramsey KH, Rank RG. Resolution of chlamydial genital infection with antigen-specific T-lymphocyte lines. Infection and immunity. 1991;59(3):925-31. Epub 1991/03/01. PubMed PMID: 1705244; PubMed Central PMCID: PMC258348.

27. Tuffrey M, Falder P, Gale J, Taylor-Robinson D. Salpingitis in mice induced by human strains of Chlamydia trachomatis. British journal of experimental pathology. 1986;67(4):605-16. Epub 1986/08/01. PubMed PMID: 3741777; PubMed Central PMCID: PMC2013048.

28. Wiesenfeld HC, Heine RP, Krohn MA, Hillier SL, Amortegui AA, Nicolazzo M, et al. Association between elevated neutrophil defensin levels and endometritis. The Journal of infectious diseases. 2002;186(6):792-7. Epub 2002/08/29. doi: 10.1086/342417. PubMed PMID: 12198613.

29. Chong-Cerrillo C, Selsted ME, Peterson EM, de la Maza LM. Susceptibility of human and murine Chlamydia trachomatis serovars to granulocyte- and epithelium-derived antimicrobial peptides. The journal of peptide research : official journal of the American Peptide Society. 2003;61(5):237-42. Epub 2003/03/29. PubMed PMID: 12662357.

30. Radtke AL, Quayle AJ, Herbst-Kralovetz MM. Microbial products alter the expression of membrane-associated mucin and antimicrobial peptides in a three-dimensional human endocervical epithelial cell model. Biology of reproduction. 2012;87(6):132. Epub 2012/10/12. doi: 10.1095/biolreprod.112.103366. PubMed PMID: 23053434.

31. Darville T, Hiltke TJ. Pathogenesis of genital tract disease due to Chlamydia trachomatis. The Journal of infectious diseases. 2010;201 Suppl 2:S114-25. Epub 2010/06/05. PubMed PMID: 20524234; PubMed Central PMCID: PMC3150527.

32. Joyee AG, Yang X. Role of toll-like receptors in immune responses to chlamydial infections. Current pharmaceutical design. 2008;14(6):593-600. Epub 2008/03/14. PubMed PMID: 18336303.

33. Massari P, Toussi DN, Tifrea DF, de la Maza LM. Toll-like receptor 2-dependent activity of native major outer membrane protein proteosomes of Chlamydia trachomatis. Infection and immunity. 2013;81(1):303-10. Epub 2012/11/08. doi: 10.1128/IAI.01062-12. PubMed PMID: 23132491; PubMed Central PMCID: PMC3536141.

34. Agrawal T, Bhengraj AR, Vats V, Salhan S, Mittal A. Expression of TLR 2, TLR 4 and iNOS in cervical monocytes of Chlamydia trachomatis-infected women and their role in host immune response. Am J Reprod Immunol. 2011;66(6):534-43. Epub 2011/09/03. doi: 10.1111/j.1600-0897.2011.01064.x. PubMed PMID: 21883620.

35. Darville T, O'Neill JM, Andrews CW, Jr., Nagarajan UM, Stahl L, Ojcius DM. Toll-like receptor-2, but not Toll-like receptor-4, is essential for development of oviduct pathology in chlamydial genital tract infection. J Immunol. 2003;171(11):6187-97. Epub 2003/11/25. PubMed PMID: 14634135.

36. O'Connell CM, Ionova IA, Quayle AJ, Visintin A, Ingalls RR. Localization of TLR2 and MyD88 to Chlamydia trachomatis inclusions. Evidence for signaling by intracellular TLR2 during infection with an obligate intracellular pathogen. The Journal of biological chemistry. 2006;281(3):1652-9. Epub 2005/11/19. doi: 10.1074/jbc.M510182200. PubMed PMID: 16293622.

37. Quayle AJ. The innate and early immune response to pathogen challenge in the female genital tract and the pivotal role of epithelial cells. Journal of reproductive immunology. 2002;57(1-2):61-79. Epub 2002/10/19. PubMed PMID: 12385834.

38. Rank RG, Lacy HM, Goodwin A, Sikes J, Whittimore J, Wyrick PB, et al. Host chemokine and cytokine response in the endocervix within the first developmental cycle of Chlamydia muridarum. Infection and immunity. 2010;78(1):536-44. Epub 2009/10/21. doi: 10.1128/IAI.00772-09. PubMed PMID: 19841073; PubMed Central PMCID: PMC2798225.

39. Zhong GM, de la Maza LM. Activation of mouse peritoneal macrophages in vitro or in vivo by recombinant murine gamma interferon inhibits the growth of Chlamydia trachomatis serovar L1. Infection and immunity. 1988;56(12):3322-5. Epub 1988/12/01. PubMed PMID: 3141289; PubMed Central PMCID: PMC259745.

40. Perry LL, Feilzer K, Caldwell HD. Immunity to Chlamydia trachomatis is mediated by T helper 1 cells through IFN-gamma-dependent and -independent pathways. J Immunol. 1997;158(7):3344-52. Epub 1997/04/01. PubMed PMID: 9120292.

41. Coers J, Gondek DC, Olive AJ, Rohlfing A, Taylor GA, Starnbach MN. Compensatory T cell responses in IRG-deficient mice prevent sustained Chlamydia trachomatis infections. PLoS pathogens. 2011;7(6):e1001346. Epub 2011/07/07. doi: 10.1371/journal.ppat.1001346. PubMed PMID: 21731484; PubMed Central PMCID: PMC3121881.

42. Gondek DC, Olive AJ, Stary G, Starnbach MN. CD4+ T cells are necessary and sufficient to confer protection against Chlamydia trachomatis infection in the murine upper genital tract. J Immunol. 2012;189(5):2441-9. Epub 2012/08/03. doi: 10.4049/jimmunol.1103032. PubMed PMID: 22855710.

43. Chen B, Stout R, Campbell WF. Nitric oxide production: a mechanism of Chlamydia trachomatis inhibition in interferon-gamma-treated RAW264.7 cells. FEMS immunology and medical microbiology. 1996;14(2-3):109-20. Epub 1996/06/01. PubMed PMID: 8809546.

44. Igietseme JU, Uriri IM, Chow M, Abe E, Rank RG. Inhibition of intracellular multiplication of human strains of Chlamydia trachomatis by nitric oxide. Biochemical and biophysical research communications. 1997;232(3):595-601. Epub 1997/03/27. doi: 10.1006/bbrc.1997.6335. PubMed PMID: 9126319.

45. van den Broek MF, Muller U, Huang S, Zinkernagel RM, Aguet M. Immune defence in mice lacking type I and/or type II interferon receptors. Immunological reviews. 1995;148:5-18. Epub 1995/12/01. PubMed PMID: 8825279.

46. Taylor MW, Feng GS. Relationship between interferon-gamma, indoleamine 2,3-dioxygenase, and tryptophan catabolism. FASEB journal : official publication of the Federation of American Societies for Experimental Biology. 1991;5(11):2516-22. Epub 1991/08/01. PubMed PMID: 1907934.

47. Daubener W, MacKenzie CR. IFN-gamma activated indoleamine 2,3-dioxygenase activity in human cells is an antiparasitic and an antibacterial effector mechanism. Advances in experimental medicine and biology. 1999;467:517-24. Epub 2000/03/18. PubMed PMID: 10721095.

48. Desvignes L, Ernst JD. Interferon-gamma-responsive nonhematopoietic cells regulate the immune response to Mycobacterium tuberculosis. Immunity. 2009;31(6):974-85. Epub 2010/01/13. doi: 10.1016/j.immuni.2009.10.007. PubMed PMID: 20064452; PubMed Central PMCID: PMC2807991.

49. Bernstein-Hanley I, Coers J, Balsara ZR, Taylor GA, Starnbach MN, Dietrich WF. The p47 GTPases Igtp and Irgb10 map to the Chlamydia trachomatis susceptibility locus Ctrq-3 and mediate cellular resistance in mice. Proceedings of the National Academy of Sciences of the United States of America. 2006;103(38):14092-7. Epub 2006/09/09. doi: 10.1073/pnas.0603338103. PubMed PMID: 16959883; PubMed Central PMCID: PMC1599917.

50. Coers J, Bernstein-Hanley I, Grotsky D, Parvanova I, Howard JC, Taylor GA, et al. Chlamydia muridarum evades growth restriction by the IFN-gamma-inducible host resistance factor Irgb10. J Immunol. 2008;180(9):6237-45. Epub 2008/04/22. PubMed PMID: 18424746.

51. Nelson DE, Virok DP, Wood H, Roshick C, Johnson RM, Whitmire WM, et al. Chlamydial IFN-gamma immune evasion is linked to host infection tropism. Proceedings of the National Academy of Sciences of the United States of America. 2005;102(30):10658-63. Epub 2005/07/16. doi: 10.1073/pnas.0504198102. PubMed PMID: 16020528; PubMed Central PMCID: PMC1180788.

52. Haldar AK, Saka HA, Piro AS, Dunn JD, Henry SC, Taylor GA, et al. IRG and GBP host resistance factors target aberrant, "non-self" vacuoles characterized by the missing of "self" IRGM proteins. PLoS pathogens. 2013;9(6):e1003414. Epub 2013/06/21. doi: 10.1371/journal.ppat.1003414. PubMed PMID: 23785284; PubMed Central PMCID: PMC3681737.

53. Morrison SG, Morrison RP. In situ analysis of the evolution of the primary immune response in murine Chlamydia trachomatis genital tract infection. Infection and immunity. 2000;68(5):2870-9. Epub 2000/04/18. PubMed PMID: 10768984; PubMed Central PMCID: PMC97499.

54. Morrison SG, Farris CM, Sturdevant GL, Whitmire WM, Morrison RP. Murine Chlamydia trachomatis genital infection is unaltered by depletion of CD4+ T cells and diminished adaptive immunity. The Journal of infectious diseases. 2011;203(8):1120-8. Epub 2011/02/16. doi: 10.1093/infdis/jiq176. PubMed PMID: 21321103; PubMed Central PMCID: PMC3068022.

55. Murphy K, Travers P, Walport M, Janeway C. Janeway's immunobiology. 8th ed. New York: Garland Science; 2012. xix, 868 p. p.

56. Jawetz E, Rose L, Hanna L, Thygeson P. Experimental inclusion conjunctivitis in man: measurements of infectivity and resistance. JAMA : the journal of the American Medical Association. 1965;194(6):620-32. Epub 1965/11/08. PubMed PMID: 5319187.

57. Barenfanger J, MacDonald AB. The role of immunoglobulin in the neutralization of trachoma infectivity. J Immunol. 1974;113(5):1607-17. Epub 1974/11/01. PubMed PMID: 4214333.

58. Peeling R, Maclean IW, Brunham RC. In vitro neutralization of Chlamydia trachomatis with monoclonal antibody to an epitope on the major outer membrane protein. Infection and immunity. 1984;46(2):484-8. Epub 1984/11/01. PubMed PMID: 6209221; PubMed Central PMCID: PMC261559.

59. Schnorr KL. Chlamydial vaccines. Journal of the American Veterinary Medical Association. 1989;195(11):1548-61. Epub 1989/12/01. PubMed PMID: 2689409.

60. Su H, Feilzer K, Caldwell HD, Morrison RP. Chlamydia trachomatis genital tract infection of antibody-deficient gene knockout mice. Infection and immunity. 1997;65(6):1993-9. Epub 1997/06/01. PubMed PMID: 9169723; PubMed Central PMCID: PMC175275.

61. Williams DM, Grubbs BG, Pack E, Kelly K, Rank RG. Humoral and cellular immunity in secondary infection due to murine Chlamydia trachomatis. Infection and immunity. 1997;65(7):2876-82. Epub 1997/07/01. PubMed PMID: 9199462; PubMed Central PMCID: PMC175404.

62. Cotter TW, Meng Q, Shen ZL, Zhang YX, Su H, Caldwell HD. Protective efficacy of major outer membrane protein-specific immunoglobulin A (IgA) and IgG monoclonal antibodies in a murine model of Chlamydia trachomatis genital tract infection. Infection and immunity. 1995;63(12):4704-14. Epub 1995/12/01. PubMed PMID: 7591126; PubMed Central PMCID: PMC173675.

63. Konigshofer Y, Chien YH. Gammadelta T cells - innate immune lymphocytes? Current opinion in immunology. 2006;18(5):527-33. Epub 2006/08/02. doi: 10.1016/j.coi.2006.07.008. PubMed PMID: 16879956.

64. Krangel MS. Gene segment selection in V(D)J recombination: accessibility and beyond. Nature immunology. 2003;4(7):624-30. Epub 2003/06/28. doi: 10.1038/ni0703-624. PubMed PMID: 12830137.

65. Flutter B, Gao B. MHC class I antigen presentation--recently trimmed and well presented. Cellular & molecular immunology. 2004;1(1):22-30. Epub 2005/10/11. PubMed PMID: 16212917.

66. Drake DR, 3rd, Braciale TJ. Not all effector CD8+ T cells are alike. Microbes and infection / Institut Pasteur. 2003;5(3):199-204. Epub 2003/04/12. PubMed PMID: 12681408.

67. Starnbach MN, Bevan MJ, Lampe MF. Protective cytotoxic T lymphocytes are induced during murine infection with Chlamydia trachomatis. J Immunol. 1994;153(11):5183-9. Epub 1994/12/01. PubMed PMID: 7525725.

68. Ibana JA, Myers L, Porretta C, Lewis M, Taylor SN, Martin DH, et al. The major CD8 T cell effector memory subset in the normal and Chlamydia trachomatis-infected human endocervix is low in perforin. BMC immunology. 2012;13:66. Epub 2012/12/12. doi: 10.1186/1471-2172-13-66. PubMed PMID: 23216954; PubMed Central PMCID: PMC3538661.

69. Matyszak MK, Gaston JS. Chlamydia trachomatis-specific human CD8+ T cells show two patterns of antigen recognition. Infection and immunity. 2004;72(8):4357-67. Epub 2004/07/24. doi: 10.1128/IAI.72.8.4357-4367.2004. PubMed PMID: 15271891; PubMed Central PMCID: PMC470615.

70. Grotenbreg GM, Roan NR, Guillen E, Meijers R, Wang JH, Bell GW, et al. Discovery of CD8+ T cell epitopes in Chlamydia trachomatis infection through use of caged class I MHC tetramers. Proceedings of the National Academy of Sciences of the United States of America. 2008;105(10):3831-6. Epub 2008/02/05. doi: 10.1073/pnas.0711504105. PubMed PMID: 18245382; PubMed Central PMCID: PMC2268777.

71. Starnbach MN, Loomis WP, Ovendale P, Regan D, Hess B, Alderson MR, et al. An inclusion membrane protein from Chlamydia trachomatis enters the MHC class I pathway and stimulates a CD8+ T cell response. J Immunol. 2003;171(9):4742-9. Epub 2003/10/22. PubMed PMID: 14568950.

72. Fling SP, Sutherland RA, Steele LN, Hess B, D'Orazio SE, Maisonneuve J, et al. CD8+ T cells recognize an inclusion membrane-associated protein from the vacuolar pathogen Chlamydia trachomatis. Proceedings of the National Academy of Sciences of the United States of America. 2001;98(3):1160-5. Epub 2001/02/07. doi: 10.1073/pnas.98.3.1160. PubMed PMID: 11158611; PubMed Central PMCID: PMC14725.

73. Roan NR, Starnbach MN. Antigen-specific CD8+ T cells respond to Chlamydia trachomatis in the genital mucosa. J Immunol. 2006;177(11):7974-9. Epub 2006/11/23. PubMed PMID: 17114470.

74. Loomis WP, Starnbach MN. Chlamydia trachomatis infection alters the development of memory CD8+ T cells. J Immunol. 2006;177(6):4021-7. Epub 2006/09/05. PubMed PMID: 16951365.

75. Magee DM, Williams DM, Smith JG, Bleicker CA, Grubbs BG, Schachter J, et al. Role of CD8 T cells in primary Chlamydia infection. Infection and immunity. 1995;63(2):516-21. Epub 1995/02/01. PubMed PMID: 7822016; PubMed Central PMCID: PMC173025.

76. Karlsson L. DM and DO shape the repertoire of peptide-MHC-class-II complexes. Current opinion in immunology. 2005;17(1):65-70. Epub 2005/01/18. doi: 10.1016/j.coi.2004.11.003. PubMed PMID: 15653313.

77. Kolls JK. CD4(+) T-cell subsets and host defense in the lung. Immunological reviews. 2013;252(1):156-63. Epub 2013/02/15. doi: 10.1111/imr.12030. PubMed PMID: 23405903; PubMed Central PMCID: PMC3576701.

78. Jager A, Kuchroo VK. Effector and regulatory T-cell subsets in autoimmunity and tissue inflammation. Scandinavian journal of immunology. 2010;72(3):173-84. Epub 2010/08/11. doi: 10.1111/j.1365-3083.2010.02432.x. PubMed PMID: 20696013; PubMed Central PMCID: PMC3129000.

79. Giacomini P, Fisher PB, Duigou GJ, Gambari R, Natali PG. Regulation of class II MHC gene expression by interferons: insights into the mechanism of action of interferon (review). Anticancer research. 1988;8(6):1153-61. Epub 1988/11/01. PubMed PMID: 2464333.

80. Su H, Caldwell HD. CD4+ T cells play a significant role in adoptive immunity to Chlamydia trachomatis infection of the mouse genital tract. Infection and immunity. 1995;63(9):3302-8. Epub 1995/09/01. PubMed PMID: 7642259; PubMed Central PMCID: PMC173455.

81. Vicetti Miguel RD, Reighard SD, Chavez JM, Rabe LK, Maryak SA, Wiesenfeld HC, et al. Transient detection of Chlamydial-specific Th1 memory cells in the peripheral circulation of women with history of Chlamydia trachomatis genital tract infection. Am J Reprod Immunol. 2012;68(6):499-506. Epub 2012/09/01. doi: 10.1111/aji.12008. PubMed PMID: 22934581; PubMed Central PMCID: PMC3493686.

82. Morrison SG, Morrison RP. Resolution of secondary Chlamydia trachomatis genital tract infection in immune mice with depletion of both CD4+ and CD8+ T cells. Infection and immunity. 2001;69(4):2643-9. Epub 2001/03/20. doi: 10.1128/IAI.69.4.2643-2649.2001. PubMed PMID: 11254630; PubMed Central PMCID: PMC98202.

83. Morrison SG, Su H, Caldwell HD, Morrison RP. Immunity to murine Chlamydia trachomatis genital tract reinfection involves B cells and CD4(+) T cells but not CD8(+) T cells. Infection and immunity. 2000;68(12):6979-87. Epub 2000/11/18. PubMed PMID: 11083822; PubMed Central PMCID: PMC97807.

84. Roan NR, Gierahn TM, Higgins DE, Starnbach MN. Monitoring the T cell response to genital tract infection. Proceedings of the National Academy of Sciences of the United States of America. 2006;103(32):12069-74. Epub 2006/08/02. doi: 10.1073/pnas.0603866103. PubMed PMID: 16880389; PubMed Central PMCID: PMC1567698.

85. Gondek DC, Roan NR, Starnbach MN. T cell responses in the absence of IFN-gamma exacerbate uterine infection with Chlamydia trachomatis. J Immunol. 2009;183(2):1313-9. Epub 2009/06/30. doi: 10.4049/jimmunol.0900295. PubMed PMID: 19561106; PubMed Central PMCID: PMC2723820.

86. Stenstad H, Ericsson A, Johansson-Lindbom B, Svensson M, Marsal J, Mack M, et al. Gut-associated lymphoid tissue-primed CD4+ T cells display CCR9-dependent and -independent homing to the small intestine. Blood. 2006;107(9):3447-54. Epub 2006/01/05. doi: 10.1182/blood-2005-07-2860. PubMed PMID: 16391017.

87. Barr EL, Ouburg S, Igietseme JU, Morre SA, Okwandu E, Eko FO, et al. Host inflammatory response and development of complications of Chlamydia trachomatis genital infection in CCR5-deficient mice and subfertile women with the CCR5delta32 gene deletion. Journal of microbiology, immunology, and infection = Wei mian yu gan ran za zhi. 2005;38(4):244-54. Epub 2005/08/25. PubMed PMID: 16118671.

88. Kelly KA, Rank RG. Identification of homing receptors that mediate the recruitment of CD4 T cells to the genital tract following intravaginal infection with Chlamydia trachomatis. Infection and immunity. 1997;65(12):5198-208. Epub 1997/12/11. PubMed PMID: 9393816; PubMed Central PMCID: PMC175749.

89. Perry LL, Feilzer K, Portis JL, Caldwell HD. Distinct homing pathways direct T lymphocytes to the genital and intestinal mucosae in Chlamydia-infected mice. J Immunol. 1998;160(6):2905-14. Epub 1998/03/24. PubMed PMID: 9510194.

90. Rahman MU, Cheema MA, Schumacher HR, Hudson AP. Molecular evidence for the presence of chlamydia in the synovium of patients with Reiter's syndrome. Arthritis and rheumatism. 1992;35(5):521-9. Epub 1992/05/01. PubMed PMID: 1374250.

91. Patton DL, Askienazy-Elbhar M, Henry-Suchet J, Campbell LA, Cappuccio A, Tannous W, et al. Detection of Chlamydia trachomatis in fallopian tube tissue in women with postinfectious tubal infertility. American journal of obstetrics and gynecology. 1994;171(1):95-101. Epub 1994/07/01. PubMed PMID: 8030740.

92. Stephens RS, Kalman S, Lammel C, Fan J, Marathe R, Aravind L, et al. Genome sequence of an obligate intracellular pathogen of humans: Chlamydia trachomatis. Science. 1998;282(5389):754-9. Epub 1998/10/23. PubMed PMID: 9784136.

93. Belland RJ, Zhong G, Crane DD, Hogan D, Sturdevant D, Sharma J, et al. Genomic transcriptional profiling of the developmental cycle of Chlamydia trachomatis. Proceedings of the National Academy of Sciences of the United States of America. 2003;100(14):8478-83. Epub 2003/06/20. doi: 10.1073/pnas.1331135100. PubMed PMID: 12815105; PubMed Central PMCID: PMC166254.

94. Saka HA, Thompson JW, Chen YS, Kumar Y, Dubois LG, Moseley MA, et al. Quantitative proteomics reveals metabolic and pathogenic properties of Chlamydia trachomatis developmental forms. Molecular microbiology. 2011;82(5):1185-203. Epub 2011/10/22. doi: 10.1111/j.1365-2958.2011.07877.x. PubMed PMID: 22014092; PubMed Central PMCID: PMC3225693.

95. Nguyen BD, Valdivia RH. Virulence determinants in the obligate intracellular pathogen Chlamydia trachomatis revealed by forward genetic approaches. Proceedings of the National Academy of Sciences of the United States of America. 2012;109(4):1263-8. Epub 2012/01/11. doi: 10.1073/pnas.1117884109. PubMed PMID: 22232666; PubMed Central PMCID: PMC3268281.

96. Kari L, Goheen MM, Randall LB, Taylor LD, Carlson JH, Whitmire WM, et al. Generation of targeted Chlamydia trachomatis null mutants. Proceedings of the National Academy of Sciences of the United States of America. 2011;108(17):7189-93. Epub 2011/04/13. doi: 10.1073/pnas.1102229108. PubMed PMID: 21482792; PubMed Central PMCID: PMC3084044.

97. Samudrala R, Heffron F, McDermott JE. Accurate prediction of secreted substrates and identification of a conserved putative secretion signal for type III secretion systems. PLoS pathogens. 2009;5(4):e1000375. Epub 2009/04/25. doi: 10.1371/journal.ppat.1000375. PubMed PMID: 19390620; PubMed Central PMCID: PMC2668754.

98. Saka HA, Valdivia RH. Acquisition of nutrients by Chlamydiae: unique challenges of living in an intracellular compartment. Current opinion in microbiology. 2010;13(1):4-10. Epub 2009/12/17. doi: 10.1016/j.mib.2009.11.002. PubMed PMID: 20006538; PubMed Central PMCID: PMC3202608.

99. Spaeth KE, Chen YS, Valdivia RH. The Chlamydia type III secretion system C-ring engages a chaperone-effector protein complex. PLoS pathogens. 2009;5(9):e1000579. Epub 2009/09/15. doi: 10.1371/journal.ppat.1000579. PubMed PMID: 19750218; PubMed Central PMCID: PMC2734247.

100. Muschiol S, Bailey L, Gylfe A, Sundin C, Hultenby K, Bergstrom S, et al. A small-molecule inhibitor of type III secretion inhibits different stages of the infectious cycle of Chlamydia trachomatis. Proceedings of the National Academy of Sciences of the United States of America. 2006;103(39):14566-71. Epub 2006/09/16. doi: 10.1073/pnas.0606412103. PubMed PMID: 16973741; PubMed Central PMCID: PMC1566191.

101. Wolf K, Betts HJ, Chellas-Gery B, Hower S, Linton CN, Fields KA. Treatment of Chlamydia trachomatis with a small molecule inhibitor of the Yersinia type III secretion system disrupts progression of the chlamydial developmental cycle. Molecular microbiology. 2006;61(6):1543-55. Epub 2006/09/14. doi: 10.1111/j.1365-2958.2006.05347.x. PubMed PMID: 16968227; PubMed Central PMCID: PMC1615999.

102. Dautry-Varsat A, Subtil A, Hackstadt T. Recent insights into the mechanisms of Chlamydia entry. Cellular microbiology. 2005;7(12):1714-22. Epub 2005/11/29. doi: 10.1111/j.1462-5822.2005.00627.x. PubMed PMID: 16309458.

103. Kim JH, Jiang S, Elwell CA, Engel JN. Chlamydia trachomatis co-opts the FGF2 signaling pathway to enhance infection. PLoS pathogens. 2011;7(10):e1002285. Epub 2011/10/15. doi: 10.1371/journal.ppat.1002285. PubMed PMID: 21998584; PubMed Central PMCID: PMC3188521.

104. Elwell CA, Ceesay A, Kim JH, Kalman D, Engel JN. RNA interference screen identifies Abl kinase and PDGFR signaling in Chlamydia trachomatis entry. PLoS pathogens. 2008;4(3):e1000021. Epub 2008/03/29. doi: 10.1371/journal.ppat.1000021. PubMed PMID: 18369471; PubMed Central PMCID: PMC2267011.

105. Rosmarin DM, Carette JE, Olive AJ, Starnbach MN, Brummelkamp TR, Ploegh HL. Attachment of Chlamydia trachomatis L2 to host cells requires sulfation. Proceedings of the National Academy of Sciences of the United States of America. 2012;109(25):10059-64. Epub 2012/06/08. doi: 10.1073/pnas.1120244109. PubMed PMID: 22675117; PubMed Central PMCID: PMC3382535.

106. Carabeo RA, Dooley CA, Grieshaber SS, Hackstadt T. Rac interacts with Abi-1 and WAVE2 to promote an Arp2/3-dependent actin recruitment during chlamydial invasion. Cellular microbiology. 2007;9(9):2278-88. Epub 2007/05/16. doi: 10.1111/j.1462-5822.2007.00958.x. PubMed PMID: 17501982.

107. Jewett TJ, Dooley CA, Mead DJ, Hackstadt T. Chlamydia trachomatis tarp is phosphorylated by src family tyrosine kinases. Biochemical and biophysical research communications. 2008;371(2):339-44. Epub 2008/04/30. doi: 10.1016/j.bbrc.2008.04.089. PubMed PMID: 18442471; PubMed Central PMCID: PMC2394672.

108. Jewett TJ, Fischer ER, Mead DJ, Hackstadt T. Chlamydial TARP is a bacterial nucleator of actin. Proceedings of the National Academy of Sciences of the United States of America. 2006;103(42):15599-604. Epub 2006/10/10. doi: 10.1073/pnas.0603044103. PubMed PMID: 17028176; PubMed Central PMCID: PMC1622868.

109. Jewett TJ, Miller NJ, Dooley CA, Hackstadt T. The conserved Tarp actin binding domain is important for chlamydial invasion. PLoS pathogens. 2010;6(7):e1000997. Epub 2010/07/27. doi: 10.1371/journal.ppat.1000997. PubMed PMID: 20657821; PubMed Central PMCID: PMC2904776.

110. Fields KA, Hackstadt T. The chlamydial inclusion: escape from the endocytic pathway. Annual review of cell and developmental biology. 2002;18:221-45. Epub 2002/07/27. doi: 10.1146/annurev.cellbio.18.012502.105845. PubMed PMID: 12142274.

111. Grieshaber SS, Grieshaber NA, Hackstadt T. Chlamydia trachomatis uses host cell dynein to traffic to the microtubule-organizing center in a p50 dynamitin-independent process. Journal of cell science. 2003;116(Pt 18):3793-802. Epub 2003/08/07. doi: 10.1242/jcs.00695. PubMed PMID: 12902405.

112. Betts HJ, Wolf K, Fields KA. Effector protein modulation of host cells: examples in the Chlamydia spp. arsenal. Current opinion in microbiology. 2009;12(1):81-7. Epub 2009/01/14. doi: 10.1016/j.mib.2008.11.009. PubMed PMID: 19138553.

113. Brumell JH, Scidmore MA. Manipulation of rab GTPase function by intracellular bacterial pathogens. Microbiology and molecular biology reviews : MMBR. 2007;71(4):636-52. Epub 2007/12/08. doi: 10.1128/MMBR.00023-07. PubMed PMID: 18063721; PubMed Central PMCID: PMC2168649.

114. Rejman Lipinski A, Heymann J, Meissner C, Karlas A, Brinkmann V, Meyer TF, et al. Rab6 and Rab11 regulate Chlamydia trachomatis development and golgin-84-dependent Golgi fragmentation. PLoS pathogens. 2009;5(10):e1000615. Epub 2009/10/10. doi: 10.1371/journal.ppat.1000615. PubMed PMID: 19816566; PubMed Central PMCID: PMC2752117.

115. Paumet F, Wesolowski J, Garcia-Diaz A, Delevoye C, Aulner N, Shuman HA, et al. Intracellular bacteria encode inhibitory SNARE-like proteins. PloS one. 2009;4(10):e7375. Epub 2009/10/14. doi: 10.1371/journal.pone.0007375. PubMed PMID: 19823575; PubMed Central PMCID: PMC2756591.

116. Hackstadt T, Rockey DD, Heinzen RA, Scidmore MA. Chlamydia trachomatis interrupts an exocytic pathway to acquire endogenously synthesized sphingomyelin in transit from the Golgi apparatus to the plasma membrane. The EMBO journal. 1996;15(5):964-77. Epub 1996/03/01. PubMed PMID: 8605892; PubMed Central PMCID: PMC449991.

117. Derre I, Swiss R, Agaisse H. The lipid transfer protein CERT interacts with the Chlamydia inclusion protein IncD and participates to ER-Chlamydia inclusion membrane contact sites. PLoS pathogens. 2011;7(6):e1002092. Epub 2011/07/07. doi: 10.1371/journal.ppat.1002092. PubMed PMID: 21731489; PubMed Central PMCID: PMC3121800.

118. Elwell CA, Jiang S, Kim JH, Lee A, Wittmann T, Hanada K, et al. Chlamydia trachomatis co-opts GBF1 and CERT to acquire host sphingomyelin for distinct roles during intracellular development. PLoS pathogens. 2011;7(9):e1002198. Epub 2011/09/13. doi: 10.1371/journal.ppat.1002198. PubMed PMID: 21909260; PubMed Central PMCID: PMC3164637.

119. Heuer D, Rejman Lipinski A, Machuy N, Karlas A, Wehrens A, Siedler F, et al. Chlamydia causes fragmentation of the Golgi compartment to ensure reproduction. Nature. 2009;457(7230):731-5. Epub 2008/12/09. doi: 10.1038/nature07578. PubMed PMID: 19060882.

120. Chen AL, Johnson KA, Lee JK, Sutterlin C, Tan M. CPAF: a Chlamydial protease in search of an authentic substrate. PLoS pathogens. 2012;8(8):e1002842. Epub 2012/08/10. doi: 10.1371/journal.ppat.1002842. PubMed PMID: 22876181; PubMed Central PMCID: PMC3410858.

121. Cocchiaro JL, Kumar Y, Fischer ER, Hackstadt T, Valdivia RH. Cytoplasmic lipid droplets are translocated into the lumen of the Chlamydia trachomatis parasitophorous vacuole. Proceedings of the National Academy of Sciences of the United States of America. 2008;105(27):9379-84. Epub 2008/07/02. doi: 10.1073/pnas.0712241105. PubMed PMID: 18591669; PubMed Central PMCID: PMC2453745.

122. Ouellette SP, Dorsey FC, Moshiach S, Cleveland JL, Carabeo RA. Chlamydia species-dependent differences in the growth requirement for lysosomes. PloS one. 2011;6(3):e16783. Epub 2011/03/17. doi: 10.1371/journal.pone.0016783. PubMed PMID: 21408144; PubMed Central PMCID: PMC3050816.

123. Derre I, Pypaert M, Dautry-Varsat A, Agaisse H. RNAi screen in Drosophila cells reveals the involvement of the Tom complex in Chlamydia infection. PLoS pathogens. 2007;3(10):1446-58. Epub 2007/10/31. doi: 10.1371/journal.ppat.0030155. PubMed PMID: 17967059; PubMed Central PMCID: PMC2042019.

124. Balsara ZR, Misaghi S, Lafave JN, Starnbach MN. Chlamydia trachomatis infection induces cleavage of the mitotic cyclin B1. Infection and immunity. 2006;74(10):5602-8. Epub 2006/09/22. doi: 10.1128/IAI.00266-06. PubMed PMID: 16988235; PubMed Central PMCID: PMC1594933.

125. Grieshaber SS, Grieshaber NA, Miller N, Hackstadt T. Chlamydia trachomatis causes centrosomal defects resulting in chromosomal segregation abnormalities. Traffic. 2006;7(8):940-9. Epub 2006/08/03. doi: 10.1111/j.1600-0854.2006.00439.x. PubMed PMID: 16882039.

126. Johnson KA, Tan M, Sutterlin C. Centrosome abnormalities during a Chlamydia trachomatis infection are caused by dysregulation of the normal duplication pathway. Cellular microbiology. 2009;11(7):1064-73. Epub 2009/03/18. doi: 10.1111/j.1462-5822.2009.01307.x. PubMed PMID: 19290915; PubMed Central PMCID: PMC3308718.

127. Alzhanov DT, Weeks SK, Burnett JR, Rockey DD. Cytokinesis is blocked in mammalian cells transfected with Chlamydia trachomatis gene CT223. BMC microbiology. 2009;9:2. Epub 2009/01/07. doi: 10.1186/1471-2180-9-2. PubMed PMID: 19123944; PubMed Central PMCID: PMC2657910.

128. Chumduri C, Gurumurthy RK, Zadora PK, Mi Y, Meyer TF. Chlamydia infection promotes host DNA damage and proliferation but impairs the DNA damage response. Cell host & microbe. 2013;13(6):746-58. Epub 2013/06/19. doi: 10.1016/j.chom.2013.05.010. PubMed PMID: 23768498.

129. Misaghi S, Balsara ZR, Catic A, Spooner E, Ploegh HL, Starnbach MN. Chlamydia trachomatis-derived deubiquitinating enzymes in mammalian cells during infection. Molecular microbiology. 2006;61(1):142-50. Epub 2006/07/11. doi: 10.1111/j.1365-2958.2006.05199.x. PubMed PMID: 16824101.

130. Le Negrate G, Krieg A, Faustin B, Loeffler M, Godzik A, Krajewski S, et al. ChlaDub1 of Chlamydia trachomatis suppresses NF-kappaB activation and inhibits IkappaBalpha ubiquitination and degradation. Cellular microbiology. 2008;10(9):1879-92. Epub 2008/05/28. doi: 10.1111/j.1462-5822.2008.01178.x. PubMed PMID: 18503636.

131. Lad SP, Li J, da Silva Correia J, Pan Q, Gadwal S, Ulevitch RJ, et al. Cleavage of p65/RelA of the NF-kappaB pathway by Chlamydia. Proceedings of the National Academy of Sciences of the United States of America. 2007;104(8):2933-8. Epub 2007/02/16. doi: 10.1073/pnas.0608393104. PubMed PMID: 17301240; PubMed Central PMCID: PMC1815284.

132. Dong F, Pirbhai M, Xiao Y, Zhong Y, Wu Y, Zhong G. Degradation of the proapoptotic proteins Bik, Puma, and Bim with Bcl-2 domain 3 homology in Chlamydia trachomatis-infected cells. Infection and immunity. 2005;73(3):1861-4. Epub 2005/02/26. doi: 10.1128/IAI.73.3.1861-1864.2005. PubMed PMID: 15731089; PubMed Central PMCID: PMC1064967.

133. Ying S, Fischer SF, Pettengill M, Conte D, Paschen SA, Ojcius DM, et al. Characterization of host cell death induced by Chlamydia trachomatis. Infection and immunity. 2006;74(11):6057-66. Epub 2006/08/31. doi: 10.1128/IAI.00760-06. PubMed PMID: 16940144; PubMed Central PMCID: PMC1695498.

134. Rajalingam K, Sharma M, Paland N, Hurwitz R, Thieck O, Oswald M, et al. IAP-IAP complexes required for apoptosis resistance of C. trachomatis-infected cells. PLoS pathogens. 2006;2(10):e114. Epub 2006/10/31. doi: 10.1371/journal.ppat.0020114. PubMed PMID: 17069460; PubMed Central PMCID: PMC1626104.

135. Sharma M, Machuy N, Bohme L, Karunakaran K, Maurer AP, Meyer TF, et al. HIF-1alpha is involved in mediating apoptosis resistance to Chlamydia trachomatis-infected cells. Cellular microbiology. 2011;13(10):1573-85. Epub 2011/08/10. doi: 10.1111/j.1462-5822.2011.01642.x. PubMed PMID: 21824245.

136. Rajalingam K, Sharma M, Lohmann C, Oswald M, Thieck O, Froelich CJ, et al. Mcl-1 is a key regulator of apoptosis resistance in Chlamydia trachomatis-infected cells. PloS one. 2008;3(9):e3102. Epub 2008/09/05. doi: 10.1371/journal.pone.0003102. PubMed PMID: 18769617; PubMed Central PMCID: PMC2518856.

137. Thomas SM, Garrity LF, Brandt CR, Schobert CS, Feng GS, Taylor MW, et al. IFN-gamma-mediated antimicrobial response. Indoleamine 2,3-dioxygenase-deficient mutant host cells no longer inhibit intracellular Chlamydia spp. or Toxoplasma growth. J Immunol. 1993;150(12):5529-34. Epub 1993/06/15. PubMed PMID: 8515074.

138. Beatty WL, Byrne GI, Morrison RP. Morphologic and antigenic characterization of interferon gamma-mediated persistent Chlamydia trachomatis infection in vitro. Proceedings of the National Academy of Sciences of the United States of America. 1993;90(9):3998-4002. Epub 1993/05/01. PubMed PMID: 8387206; PubMed Central PMCID: PMC46433.

139. Beatty WL, Belanger TA, Desai AA, Morrison RP, Byrne GI. Role of tryptophan in gamma interferon-mediated chlamydial persistence. Annals of the New York Academy of Sciences. 1994;730:304-6. Epub 1994/08/15. PubMed PMID: 8080194.

140. Zhong G, Fan T, Liu L. Chlamydia inhibits interferon gamma-inducible major histocompatibility complex class II expression by degradation of upstream stimulatory factor 1.

The Journal of experimental medicine. 1999;189(12):1931-8. Epub 1999/06/22. PubMed PMID: 10377188; PubMed Central PMCID: PMC2192973.

141. Zhong G, Liu L, Fan T, Fan P, Ji H. Degradation of transcription factor RFX5 during the inhibition of both constitutive and interferon gamma-inducible major histocompatibility complex class I expression in chlamydia-infected cells. The Journal of experimental medicine. 2000;191(9):1525-34. Epub 2000/05/03. PubMed PMID: 10790427; PubMed Central PMCID: PMC2213440.

142. Starnbach MN, Roan NR. Conquering sexually transmitted diseases. Nature reviews Immunology. 2008;8(4):313-7. Epub 2008/03/01. doi: 10.1038/nri2272. PubMed PMID: 18309315.

Chapter 2: $CD4^+$ T cells are necessary and sufficient to confer protection against *C. trachomatis* infection in the murine upper genital tract.

Contribution:

The experiments presented in this chapter were done in collaboration with Dr. David Gondek.

This chapter has been published in the Journal of Immunology

Introduction

The obligate intracellular bacterial pathogen *Chlamydia trachomatis* causes significant morbidity throughout the world (1). The major complications of *C. trachomatis* genital tract infections arise primarily in women, and include pelvic inflammatory disease (PID), which can result in fallopian tube scarring, infertility, and ectopic pregnancy(2, 3). Better understanding of the interaction of *C. trachomatis* and the mammalian host is critical for the development of a vaccine to combat the prevalent human diseases caused by this pathogen.

Human infection with *C. trachomatis* stimulates multiple elements of the immune system, but these responses often fail to clear the organism or prevent subsequent re-infection (4-6). The inability to clear chronic *C. trachomatis* infections suggests a failure in adaptive immunity – specifically the memory responses that should provide long-lasting protection. Studies have shown that mice intravaginally infected with human strains of *C. trachomatis* clear infection quickly and without the inflammation and pathology associated with human disease (7-9). Following genital infection with human *C. trachomatis*, $CD4^+$ T cells become activated, proliferate, and are recruited to the genital mucosa (9-15). These $CD4^+$ T cells exhibit a characteristic Th1 response, secreting the high amounts of IFNγ required for bacterial clearance. (9, 16). Infection of CD4-/- mice with *C. trachomatis* leads to higher pathogen load during primary infection, and a diminished ability to be protected from secondary infection (9). However, studies examining the protective quality of the $CD4^+$ T cell memory cells induced following *C. trachomatis* infection have been contradictory (8, 9). One investigation examined *C. trachomatis* infection of wild type and μMT mice demonstrating a requirement for $CD4^+$ T cells in protective immunity to secondary infection (17). In contrast, a recent study where antibody was used to deplete $CD4^+$ cells suggested that prior infection of mice with *C. trachomatis* does not yield strong protective immunity, and that $CD4^+$ T cells are not critical for the clearance of human strains (8). These contradictory reports highlight the limited understanding of the dynamics of the $CD4^+$ memory T cell response to *C. trachomatis*, particularly in tracking antigen

specific T cell responses over time. One possible reason for the limited data examining $CD4^+$ T cell memory responses is that current small animal models do not accurately recapitulate human infections.

In pursuing mouse models of host defense against *Chlamydia*, investigators have had to choose between infecting mice with *C. trachomatis*, the human pathogen, or *Chlamydia muridarum*, a pathogen isolated from a natural mouse infection. *C. muridarum* has been an attractive option in that infections with this organism persist several days longer than infections with *C. trachomatis*, and are characterized by higher bacterial loads, ascending infections into the upper genital tract, and the development of pathologies such as hydrosalpinx and infertility (18-21). The use of the *C. muridarum* model has increased our knowledge about *Chlamydia* pathogenesis and immunity however, there are limitations to its use, specifically in the identification of antigens for use in a vaccine to protect against *C. trachomatis* (22-26). To date, there have been no published T cell epitopes shared between *C. trachomatis* and *C. muridarum*(6, 27, 28). Furthermore, *C. muridarum* only models acute phases of human *C. trachomatis* infection and not the chronic phases that are responsible for pathology in humans (5, 6). By identifying new protective T cell antigens and tracking *C. trachomatis*-specific responses to those antigens we may be able to differentiate responses that lead to protective immunity versus those that cause deleterious pathologies (6).

We hypothesized that in the standard vaginal inoculation method of *C. trachomatis* infection, the organism does not reach the upper genital tract and therefore is unable to stimulate robust adaptive immunity, similar to human infections. Here, we describe a model of mouse infection with *C. trachomatis* where the cervical barrier is bypassed. Using this transcervical infection model we are able to directly infect the upper genital tract of mice with *C. trachomatis*, colonizing the clinically relevant site. Compared to vaginal inoculation with *C. trachomatis*, transcervical inoculation allowed for more efficient colonization and stimulated a more robust and inflammatory antigen specific T cell response in the upper genital tract while

also allowing for the consistent development of pathology. Using this model, we characterized the induction of antigen specific memory $CD4^+$ T cells and show that they are necessary and sufficient for protection against re-infection of the murine genital mucosa. This study demonstrates a novel inoculation method that will allow investigators to build on each other's research results by using *C. muridarum* or *C. trachomatis* interchangeably. These data move the field significantly forward with a model system that stimulates immunity, is highly reproducible, and causes disease at the site biologically relevant for human *C. trachomatis* (29). This model system will accelerate our understanding of *Chlamydia* pathogenesis in vivo, help to uniformly define the immune components needed for protection, and enhance the ability to test the capacity of vaccines to protect against infection in the genital mucosa using *C. trachomatis*.

Results

Transcervical inoculation of *C. trachomatis* allows robust and consistent murine upper genital tract infection.

Our primary objective in this study was to compare murine models of *Chlamydia* genital infection on the induction of $CD4^+$ T cell responses. More specifically, we examined the differences between the intravaginal inoculation method and a newly-developed transcervical (intrauterine) inoculation method using both *C. trachomatis* and *C. muridarum*. The transcervical infection model uses a thin flexible probe (NSET device) to bypass the cervix and inject the bacteria directly into the lumen of the uterus. To understand how the bacterial burden in the upper genital tract changes with infection route or *Chlamydia* species, mice were given 10^6, $4.5x10^5$, or 10^3 IFU of *C. trachomatis* or *C. muridarum* by either the intravaginal or transcervical method. Three days after infection with 10^6 IFU of *C. trachomatis* transcervically (gray bars) or *C. muridarum* intravaginally (white bars), the murine uteri harbored similar levels of bacteria, (Figure 2-1). In stark contrast, vaginal inoculation with 10^6 IFU of *C*. *trachomatis* resulted in two logs less bacterial burden in the upper genital tract (black bars). These results suggest that when the physical barrier of the cervix is bypassed, the human-adapted *C. trachomatis* can colonize the murine upper genital tract as efficiently as the murine-adapted *C. muridarum*.

We next examined changes in *Chlamydia* burden over the course of primary infection. For *C. trachomatis* given via the transcervical route, bacterial load remained constant from 3 to 6 days after infection, followed by a precipitous decrease on day 9 and 15 (Figure 2-1). Infection with *C. muridarum* intravaginally resulted in infection levels at day 3 comparable to that observed with *C. trachomatis* transcervical infection. By day 6 the *C. muridarum* level had increased 10-fold and then decreased somewhat at days 9 and 15. Infection with either pathogen or route becomes undetectable 21-28 days following infection (data not shown). We also examined bacterial load in mice infected with *C. muridarum* by transcervical inoculation.

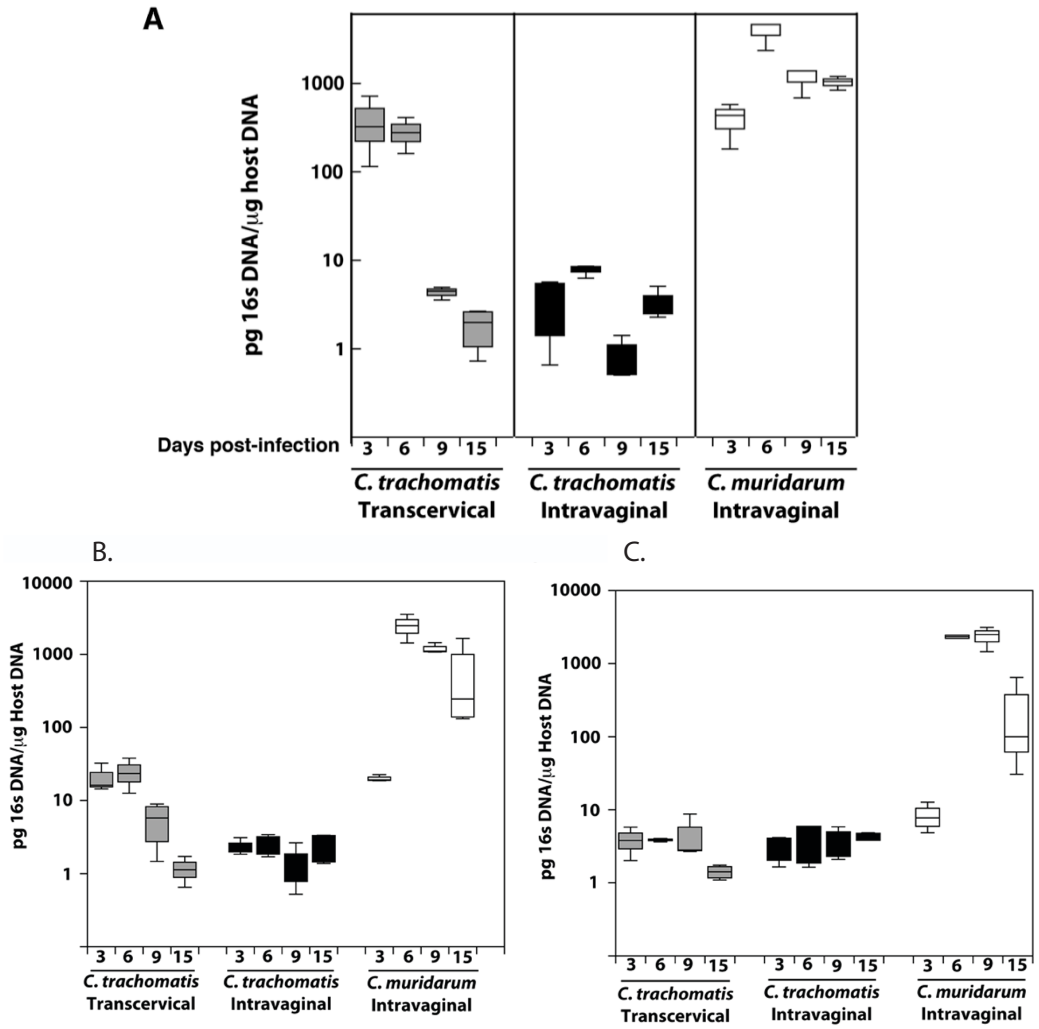

Figure 2-1. Transcervical infection of the genital mucosa with *C. trachomatis* leads to efficient colonization and pathology in the upper genital tract. Wildtype mice were infected by either intravaginal or trancervical inoculation with (A) 10^6 (B) $5x10^4$ or (C) 10^3 IFU of *C. trachomatis* or *C. muridarum*. At the indicated time points following infection, genomic DNA was isolated from the upper genital tract. Quantitative PCR was used to calculate the levels of *Chlamydia* 16s DNA relative to levels of host GAPDH. Shown is a box-and-whisker plot from one of two independent experiments.

Although there is an even higher load 3 days post-infection (3000 pg/ng), the bacterial burden was similar to intravaginal inoculation for the remainder of the time-course (data not shown). Therefore, we only used intravaginal inoculation of *C. muridarum* for the remainder of the study. When *C. trachomatis* was inoculated via the vaginal route, there was no consistent infection of the upper genital tract. These results show that both *C. trachomatis* and *C. muridarum* are capable of colonizing the upper genital tract, but that *C. trachomatis* must be inoculated across the cervix for colonization to occur.

We also examined the impact of infectious dose on the course of infection (Figure 2-1). Lowering the initial dose led to a corresponding decrease in bacterial burden on day three for both transcervical infections with *C. trachomatis* and vaginal inoculation with *C. muridarum.* As was seen with the higher dose (10^6 IFU), each of the lower doses ($5x10^4$ IFU, 10^3 IFU) resulted in similar burdens of organisms at day 3 using the two models. Regardless of the initial dose of *C. muridarum*, the amount of this organism rises to a similar high level by day six after infection, and the resolution of infection then follows a similar course, again regardless of inoculation dose. Therefore, transcervical delivery of *C. trachomatis* allows more robust initial infection compared to *C. trachomatis* intravaginal delivery but it never rises to the level seen following infection with *C. muridarum*.

We next examined whether transcervical infection leads to pathology in the upper genital mucosa. Mice were infected intravaginally with *C. trachomatis* or *C. muridarum* or infected transcervically with *C. trachomatis*. Twenty-five days after infection, the genital tract was removed and examined for gross pathology. Overall, pathology was seen in mice infected both intravaginally with *C. muridarum* and transcervically with *C. trachomatis* but never in mice infected intravaginally with *C. trachomatis*. Mice infected with *C. muridarum* showed severe oviduct hydrosalpinx similar to what has been described previously (Figure 2-2) (30). Mice infected transcervically with *C. trachomatis* showed major nodes of inflammation ascending the length of the upper genital tract (Figure 2-2). These data indicate that the transcervical model of

infection allows the formation of gross pathologies similar to what has been observed with *C. muridarum*. While there have been reports of pathology following *C. trachomatis* infection of innate immune-deficient mice strains, consistent pathology has never been described in wildtype C57Bl/6 mice – a strain restrictive for *C. trachomatis* growth. Furthermore, the pathology in *C. trachomatis* infected mice extends the length of the uterine horn, similar to rare cases described recently following *C. muridarum* infection (31).

Because there was no gross pathology observed on the ovary's following transcervical infection, we subjected several mice infected with *C. trachomatis* transcervically to histopathology in order to determine whether inflammation ascends the entire length of the upper genital tract as previously described for *C. trachomatis* infections in humans. The majority of mice examined following transcervical infection with *C. trachomatis* had severe oophoritis (inflammation of the uterine horn, oviduct, and ovary), examples of which can be seen in Figure 2-2. Evidence of large neutrophil and macrophage recruitment to the upper genital tract can be seen, as well as fibrin/mucus suggesting fluid buildup in these tissues. Importantly, we observed massive inflammation of the oviduct, a hallmark of murine infections with *C. muridarum*. Taken together, our transcervical model of *C. trachomatis* infection occurs throughout the upper genital tract and yields pathology similar to *C. muridarum* as well as human infection with *C. trachomatis*.

IFNγ restricts the initial growth of *C. trachomatis* in the murine upper genital tract following transcervical infection.

It is well accepted that the IFNγ response between mice and humans is quite different and that *C. muridarum* has adapted to evade this response in its murine host (22, 25). In contrast, the human pathogen *C. trachomatis* is highly susceptible to the murine IFNγ response (22, 25). We therefore tested whether the differential effect of IFNγ could explain why the level of *C. muridarum* increased 10-fold from day three to day six, whereas the level of *C. trachomatis* observed following transcervical inoculation did not increase over the same time period. As

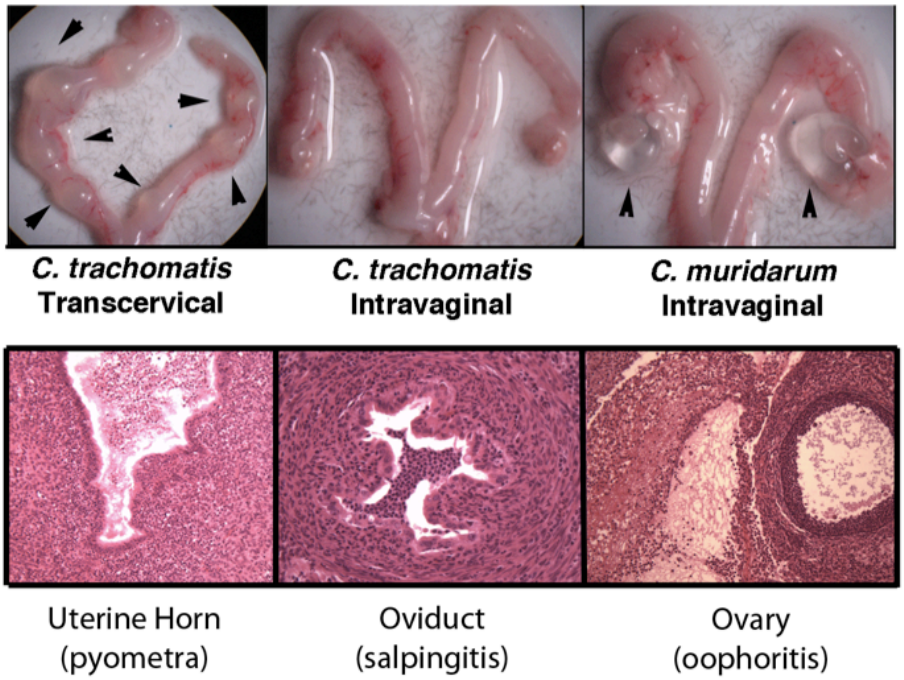

Figure 2-2. Transcervical infection leads to the development of immunopathologies in the upper genital tract. (Top) 25 days following infection the upper genital tract was isolated, photographed, and scored for pathology. Arrow heads indicate nodes of inflammation. Shown are representative images from 25 experimental mice per group from two independent experiments. (Bottom) Histological sections of the upper genital tract from mice infected transcervically with *C. trachomatis* were stained with hematoxylin and eosin. Shown are representative images of the inflammation seen in the uterine horn, oviduct, and ovary following transcervical infection.

shown in figure 2, we challenged wild type or IFNγ-/- mice transcervically with *C. trachomatis* and compared the bacterial burden to that obtained through vaginal inoculation with *C. muridarum*. In the mice lacking IFNγ, transcervical infection with *C. trachomatis* led to an expansion of organisms by day 6 that closely resembled the expansion of organisms observed in wild type mice infected with *C. muridarum*. These results suggest that IFNγ restricts the initial growth of *C. trachomatis* rapidly following infection of the upper genital tract. Since this rapid restriction is prior to the peak infiltration of T cells (10), it also leaves open the possibility of other sources of IFNγ capable of restricting *C. trachomatis* growth - such as NK cells resident in the cervical tissues (32). We suspected that the primary effectors of this IFNγ mediated restriction of *C. trachomatis* in mice were the immunity related GTPases (IRGs). When we examined the peak burden of *C. trachomatis* after transcervical infection of IRGm1/m3 deficient mice, we found a higher level of bacteria on day six compared to wild type mice, a level identical to what we observed using IFNγ-/- mice (Figure 2-3). These data indicate that even though the human adapted *C. trachomatis* is still constrained in its ability to grow due to innate responses mediated by a rapid induction of IFNγ and the murine IRG system, removal of Irgm1/m3 alone allows *C. trachomatis* to become resistant to the murine-specific IFNγ response and to grow similarly to *C. muridarum*.

Transcervical inoculation of *C. trachomatis* leads to a robust primary immune response

Previous reports have shown that $CD4^+$ T cells specific for *C. trachomatis* can protect against systemic infection (11, 16). However, a recent report by Morrison et al. suggests that $CD4^+$ T cells are dispensable for protection against genital infection with *C. trachomatis*. In their experiments, Morrison et al. inoculated mice in the vaginal vault, a method which we have now shown does not promote efficient infection of the upper genital tract by *C. trachomatis*. This led us to suspect that Morrison's finding resulted from a lack of colonization of the target tissue when comparing the two *Chlamydia* species. We hypothesized that if transcervical infection was

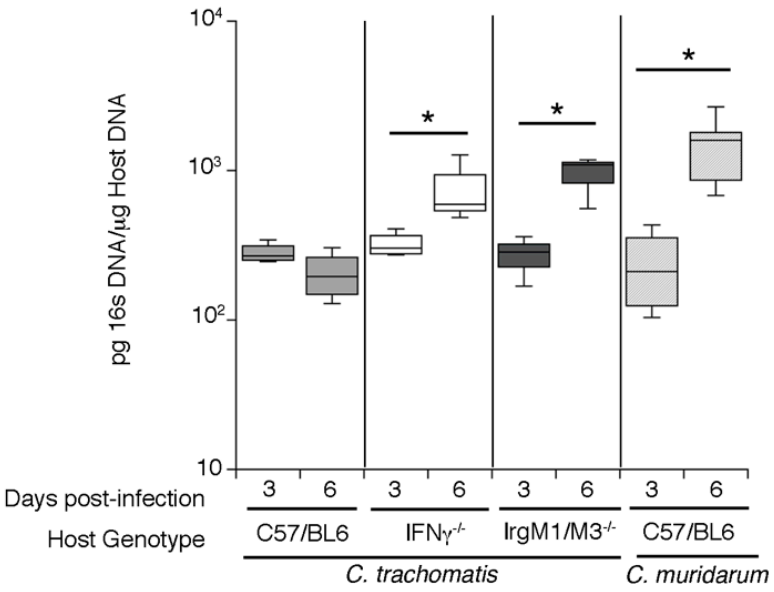

Figure 2-3. IFNγ restricts *C. trachomatis* rapidly following infection of the upper genital mucosa. Wild-type, IFNg$^{-/-}$ or Irgm1/m3$^{-/-}$ mice were infected transcervically with 10^6 IFU of *C. trachomatis.* A separate group of wild-type mice were infected with 10^6 IFU of *C. muridarum.* Three and six days following infection, genomic DNA was isolated from the upper genital tract. Quantitative PCR was used to calculate the levels of *Chlamydia* 16s DNA relative to levels of host GAPDH. Shown is a box-and-whisker plot from one of two independent experiments. *P<.05.

used to directly infect the upper genital tract with *C. trachomatis* we would observe a significant role for $CD4^+$ T cells in immunity to this organism. To test this we used antigen specific $CD4^+$ T cells to directly compare T cell proliferation, activation, cytokine secretion, and recruitment to the genital mucosa between mice infected with *C. trachomatis* intravaginally or transcervically.

We first wanted to determine whether antigen-specific $CD4^+$ T cells are activated following transcervical or intravaginal infection. We transferred CFSE-labeled *C. trachomatis*-specific $CD4^+$ TCR transgenic T cells into naïve mice, which were then challenged with *C. trachomatis* either by the transcervical or vaginal route of infection. As demonstrated in Figure 2-4, these *C. trachomatis*-specific T cells were capable of recognizing the infecting bacteria and proliferated to a similar degree regardless of the route of infection (93% vs. 89% becoming CFSE-low). However, the proliferation of *Chlamydia* specific T cells was more robust when infected transcervically than intravaginally, as seen by the marked difference in their accumulation following division. We also examined the phenotype of these pathogen specific T cells based on activation markers CD44 and CD62L, and found that there was no difference in the activation state of T cells stimulated by the two routes of infection (Figure 2-4).

Recent evidence from multiple studies using mice, non-human primates, and humans has shown convincingly that the quality of a T cell response is a critical factor in defining protective immunity (33). To examine if there is a difference in the quality of the T cell response following different routes of infection, we compared the ability of pathogen-specific T cells to produce multiple cytokines following either transcervical or intravaginal infection with *C. trachomatis*. We transferred *C. trachomatis*-specific $CD4^+$ TCR transgenic T cells into naïve mice, which were then challenged with *C. trachomatis* either by the transcervical or vaginal route of infection. Seven days after infection, we examined the ability of the pathogen specific cells to produce multiple cytokines by flow cytometry. Transcervical inoculation induced over 50% of antigen-specific $CD4^+$ T cells into a “triple producer” phenotype - capable of robustly producing TNFα, IFNγ, and IL-2 simultaneously (Figure 2-4). These “triple producer” populations have been

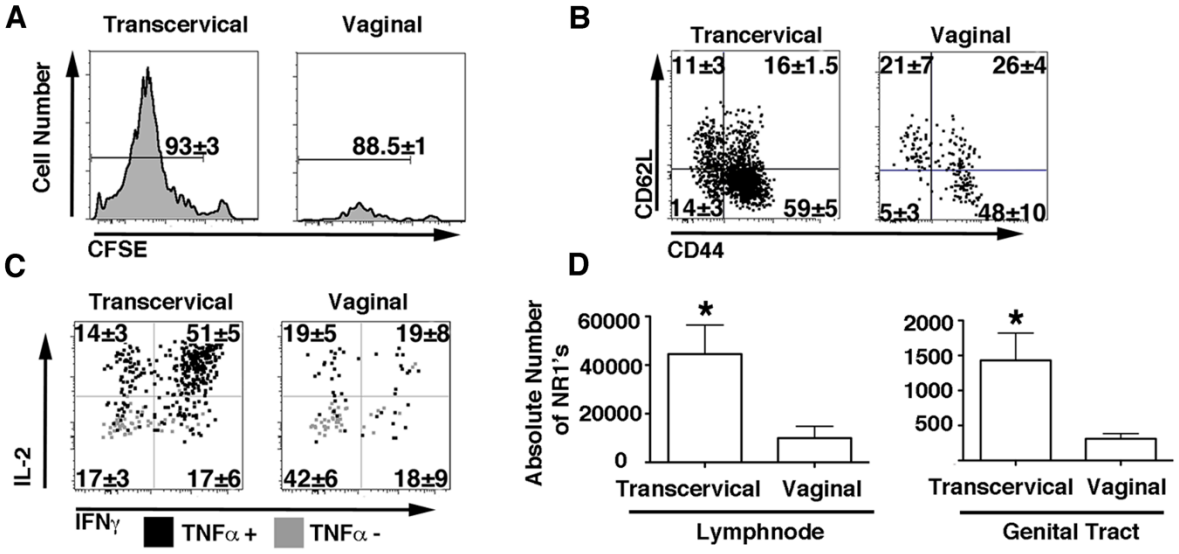

Figure 2-4. Transcervical infection with *C. trachomatis* leads to the accumulation of cytokine secreting pathogen specific CD4$^+$ T cells. Wildtype mice were infected by either intravaginal or trancervical inoculation with 10^6 IFU of *C. trachomatis* or *C. muridarum*. Wild-type CD90.1$^+$ transgenic CD4$^+$ T cells were CFSE labeled and transferred into CD90.2 hosts one day before they were inoculated transcervically or intravaginally with 10^6 IFU of *C. trachomatis*. Seven days following infection the draining lymph nodes were harvested and cells were prepared for flow cytometry. Antigen specific CD4$^+$ T cells (CD90.1$^+$ CD4$^+$) were analyzed for CFSE dilution (A) and the surface levels of the activation markers CD62L and CD44 (B). (C) Wild-type CD90.1$^+$ transgenic CD4$^+$ T cells were isolated seven days following infection, re-stimulated in vitro, and prepared for intracellular cytokine staining. Gray or Black dots indicate whether cells are positive or negative for TNFa repectively. (D) Wild-type CD90.1$^+$ transgenic CD4$^+$ T cells were transferred into CD90.2 hosts one day before they were inoculated transcervically or intravaginally with 10^6 IFU of *C. trachomatis.* Seven days following infection the draining lymph nodes and the genital tract were isolated and prepared for flow cytometry. The absolute number of *Chlamydia*-specific CD4$^+$ T cells in each tissue was enumerated. Shown are representative plots from three independent experiments.

associated with enhanced protection in other infection models (33). Interestingly, *Chlamydia*-specific T cells from mice infected intravaginally did not contain a high proportion of "triple producing" T cells (black dots vs. gray dots in Figure 2-4). This suggests that transcervical infection yields a higher quality immune response when compared directly to intravaginal infection.

Our CFSE proliferation data suggested that transcervical infection leads to more proliferation and accumulation of antigen specific T cells (Figure 2-4). We next wanted to directly quantify the accumulation of *Chlamydia*-specific T cells in the draining lymph node and genital mucosa. We transferred *C. trachomatis*-specific $CD4^+$ TCR transgenic T cells into naïve mice, and then challenged them with *C. trachomatis* either by the transcervical or vaginal route of infection. Seven days after infection, we measured the absolute number of pathogen-specific T cells in the draining lymph nodes and the genital mucosa. We identified five-fold more *Chlamydia*-specific $CD4^+$ T cells in the draining lymph node ($p<0.03$) and upper genital tract ($p<0.02$) when mice were infected transcervically compared to intravaginally (Figure 2-4). These data indicate that transcervical infection leads to enhanced recruitment of antigen specific cells to both the site of activation (the draining lymph node) and the target tissue (the genital mucosa) when compared directly to intravaginal inoculation. Together these data suggest that although vaginal infection of mice with *C. trachomatis* elicits a pathogen-specific immune response, the quality of the response is minimal and the pathogen-specific $CD4^+$ T cells are not robustly activated. Conversely, when the physical barrier of the cervix is bypassed using transcervical inoculation, *C. trachomatis*-specific $CD4^+$ T cells are stimulated, the response of those T cells is more potent, and the cells accumulate in the both the draining lymph node and genital mucosa to promote clearance.

$CD4^+$ T cells are necessary and sufficient to confer protection against *C. trachomatis* infection in mice

As shown above, transcervical inoculation of *C. trachomatis* leads to higher bacterial loads in the upper genital tract throughout infection, causes the development of gross pathology, and induces a higher quality *Chlamydia*-specific $CD4^+$ T cell response when compared to the vaginal route of inoculation. With these data we clearly show that intravaginal inoculation of mice with *C. trachomatis* is a poor model of human infection. Therefore, as we continued these studies we used only the transcervical infection model to directly examine the role of $CD4^+$ T cells in protection against *C. trachomatis*. Morrison et al. showed that following intravaginal inoculation the depletion of $CD4^+$ T cells during the primary immune response did not result in enhanced disease (8). This is in contrast to previous work from our lab showing that depletion of $CD4^+$ T cells during primary infection leads to increased bacterial loads (34). To rectify the disparity in these findings, we examined whether protection from a secondary challenge with *C. trachomatis* would require a competent $CD4^+$ T cell compartment. Mice were either infected with 10^6 IFU of *C. trachomatis* transcervically or C. *muridarum* intravaginally, rested for greater than 4 weeks to allow clearance of the initial infection, then re-challenged with the same pathogen. Before re-challenge, the mice were divided into groups treated with either antibody to deplete $CD4^+$ T cells or an isotype control IgG (Figure 2-5). After secondary challenge of the group infected with *C. trachomatis*, we examined the level of organisms present in the genital tract. The immune mice were protected 100-fold more than the naïve control group ($p<0.01$). Immune mice that were depleted of $CD4^+$ T cells did not exhibit any protection and the bacterial burden of *C. trachomatis* was similar to that of naïve mice. In comparison, the bacterial burden in immune mice challenged with *C. muridarum* exhibited a nearly 1000-fold level of protection as compared to the naïve control. This protection was completely eliminated if *C. muridarum* immune mice were depleted of $CD4^+$ T cells before secondary challenge. These results demonstrate that $CD4^+$ T cells are necessary for protection in the genital tract, whether mice are infected with *C. muridarum* or *C. trachomatis*.

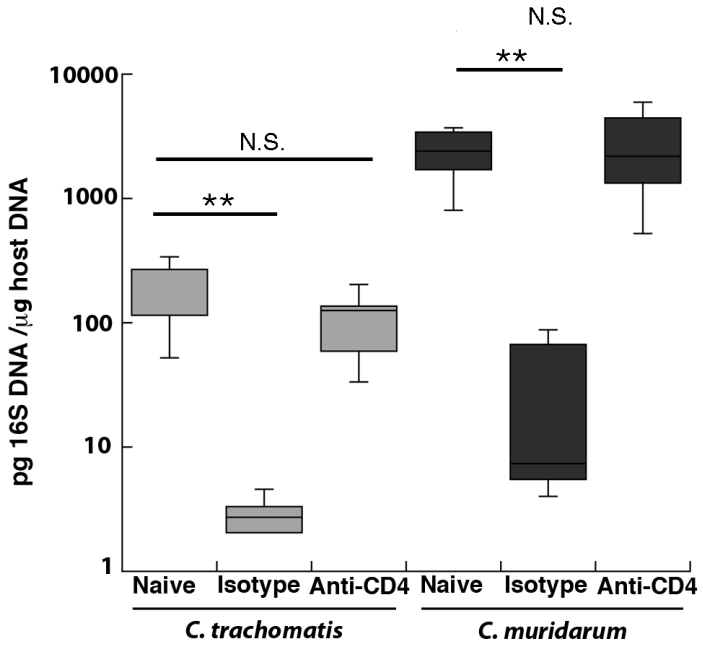

Figure 2-5. CD4$^+$ T cells protect the genital mucosa from re-infection with *C. trachomatis*. Wildtype mice were infected transcervically with 10^6 IFU of *C. trachomatis* or intravaginally with 10^6 IFU of *C. muridarum*. Five weeks after primary infection mice were injected with anti-CD4 or isotype control antibody. Naïve and immune mice were then infected with 10^6 IFU of *C. trachomatis* or *C. muridarum.* Six days after challenge genomic DNA was isolated from the upper genital tract. Quantitative PCR was used to calculate the levels of *Chlamydia* 16s DNA relative to levels of host GAPDH. Shown is a box-and-whisker plot from one of three independent experiments. **P<.01.

We next addressed if pathogen specific $CD4^+$ T cells are sufficient to confer protection. Our previous studies have indicated that transfer of 107 TH1-skewed antigen-specific cells could confer protection against *C. trachomatis* if the mice were challenged either intravenously (16) or transcervically (10, 34). However, these studies involved transfer of larger numbers of $CD4^+$ T cells, than we use here, and therefore might not have accurately reflected the behavior of endogenous antigen-specific cells (35). We wanted to determine the minimum number of transferred pathogen-specific $CD4^+$ T cells capable of conferring protection against *C. trachomatis*. *C. trachomatis*-specific T cells were first pre-activated and skewed towards the TH1 phenotype. Cells were then transferred into mice in numbers ranging from 10^4-10^7. One day after the transfer of T cells, the mice were infected transcervically with *C. trachomatis*. As demonstrated in Figure 2-6, all doses of TH1-skewed pathogen-specific T cells were capable of conferring protection. However, the level of protection provided by those cells was dose dependent, with any number greater than 10^5 transferred cells conferring similar protection typical of an immune mouse (Figure 2-5). It has been well-described that following transfer of transgenic T cells, only 10-15% of the transferred population takes hold in the new host (35). Therefore, these data suggest that only 104 pathogen-specific $CD4^+$ T cells are sufficient to confer protection against *C. trachomatis* in the genital mucosa. For the first time this allows us to estimate the lower limit of antigen specific $CD4^+$ T cells needed to protect the host from infection with *C. trachomatis*. By knowing this lower limit, future vaccines can be designed that offer protection, but where immunopathology can be limited.

C. trachomatis infection stimulates the activation and memory development of endogenous *C. trachomatis*-specific $CD4^+$ T cells

Many of the experiments described above depend on the response of TCR transgenic cells transferred into mice. As yet, there is no published report examining the endogenous *Chlamydia*-specific $CD4^+$ T cell population. Such data would be helpful in determining the

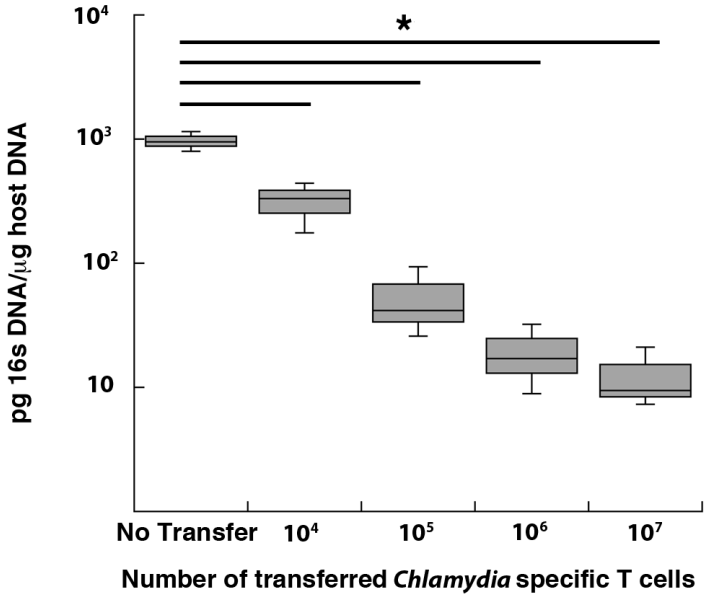

Figure 2-6. Antigen-specific TH1 cells are sufficient to protect the genital mucosa from infection with *C. trachomatis*. Wild type *Chlamydia* specific $CD4^+$ T cells were skewed *in vitro* to the TH1 phenotype for 5 days. These pre-activated T cells were then transferred into $IFNg^{-/-}$ host mice. The following day the mice were challenged transcervically with 10^6 IFU *C. trachomatis*. Six days after infection, the genital tract was harvested and genomic DNA was isolated. We used quantitative PCR to compare the levels of *Chlamydia* 16s DNA to host GAPDH. Shown is a box-and-whisker plot from one representative experiment of three independent experiments. *P<.05

biological relevance of the TCR transgenic transfer system. To address the capacity of *C. trachomatis* to elicit a response of endogenous pathogen specific $CD4^+$ T cells in mice, we used a MHC class-II tetramer, which recognizes T cells with the same epitope specificity as the T cells from the *C. trachomatis*-specific TCR transgenic mice. Using the MHC class-II tetramer, we isolated endogenous *C. trachomatis*-specific $CD4^+$ T cells from the peripheral lymphoid tissues of 1) naïve mice, 2) mice responding to a primary infection with *C. trachomatis*, and 3) mice that had recovered from infection and therefore harbored populations of memory T cells. For comparison, we also purified endogenous *C. trachomatis*-specific $CD8^+$ T cells from the same groups of mice using a tetramer that binds CrpA-specific T cells. As demonstrated in figure 6a, our tetramers were capable of identifying endogenous *C. trachomatis* specific $CD4^+$ and $CD8^+$ T cells. The number of antigen specific cells purified by the tetramer was enumerated in naïve mice, at the peak of primary infection, and during late memory development (Figure 2-7). The endogenous epitope- specific $CD8^+$ T cells vastly outnumbered the epitope-specific $CD4^+$ T cells at all time points. However, a similar trend was observed with both $CD4^+$ and $CD8^+$ $tetramer^+$ cells in which there was a 100-1000 fold expansion of the cell population during the primary immune response followed by a contraction, leaving a memory population which was 5-10 fold higher than the initial naïve population ($p < 0.05$). These experiments are the first to examine the expansion and contraction of endogenous pathogen-specific T cells following a genital infection. Interestingly, the absolute number of Class II tetramer-positive cells identified during the peak of infection is similar to the minimum number of transgenic T cells needed for protection (Figure 2-6). Therefore using two complimentary techniques we can show that between 5000 and 10000 antigen specific $CD4^+$ T cells are necessary for protection in the genital mucosa. Collectively, these data indicate that endogenous $CD4^+$ T cell immunity is primed following transcervical infection with *C. trachomatis* and a memory $CD4^+$ T cell pool develops to protect against re-infection.

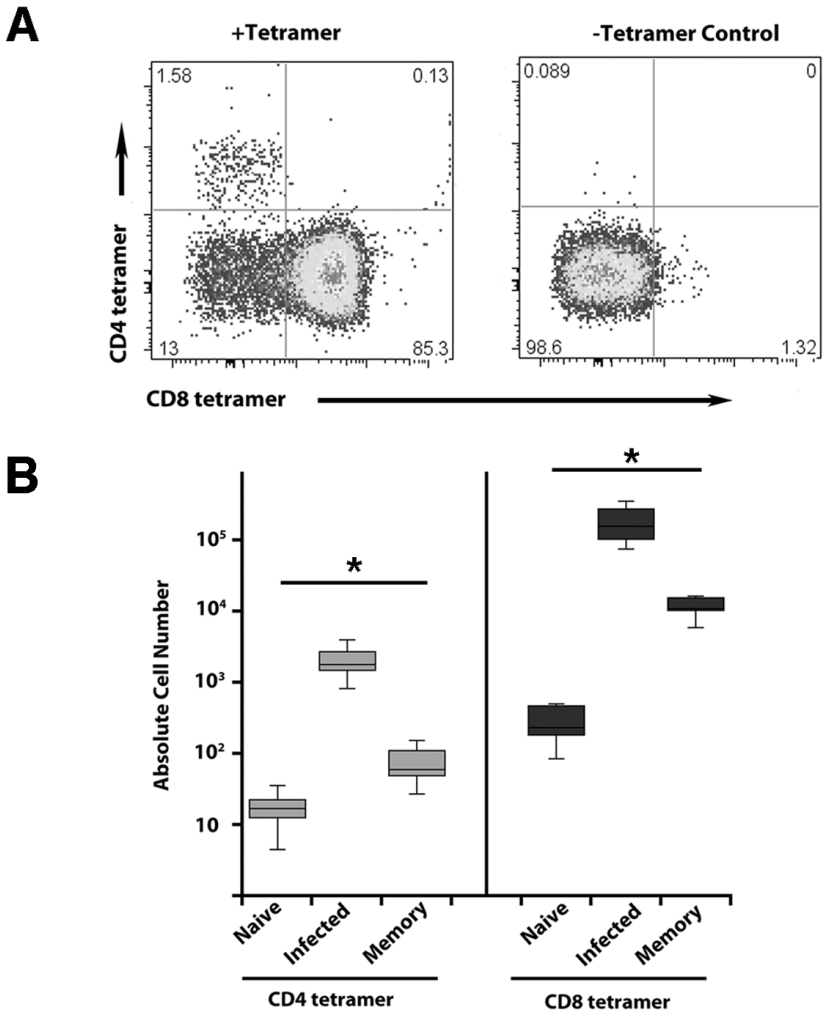

Figure 2-7. Endogenous T cell response to *C. trachomatis* infection. T cells specific for *C. trachomatis* were isolated from naïve, infected, or memory mice via magnetic isolation and tetramer pull down. A) Representative plot for isolation of tetramer specific and negative control at the peak of primary infection. The axis identifies $CD4^+$ and $CD8^+$ T cells specific for CTA-1 and CrpA, respectively. B) Absolute number of pathogen specific tetramer positive $CD4^+$ and $CD8^+$ T cells isolated from naïve, primary infected, and memory mice. *P<.05

Discussion

Understanding adaptive immunity to *C. trachomatis* is key to the development of an effective vaccine against this pathogen. Following vaginal infection in humans, the bacteria can ascend to the upper genital tract where persistent infection results in inflammation and tissue damage. In contrast to human infection, vaginal infection of mice with *C. trachomatis* does not result in significant upper genital tract infection or pathology (28). The mouse specific *Chlamydia* species, *C. muridarum*, is able to ascend from the vagina to the upper genital tract, causing robust inflammation but not persistent infection (36). Deciphering any differences in how the immune system responds to these organisms will allow both to be used in studies of disease pathogenesis and to develop vaccines.

Here we sought to compare the ability of the mouse to mount a $CD4^+$ T cell response against both *Chlamydia* species and measure the level of protection provided by that immunity. One of the most significant differences between the two species is the inability of *C. trachomatis* to ascend from the vagina/ectocervix to the upper genital tract in mice. This deficiency may prevent *C. trachomatis* from stimulating robust protective immunity in the vaginal vault as previous reports have suggested that the lower genital tract is an immune suppressive environment (37, 38). We hypothesized that the cervix is the primary physical barrier to upper genital tract infection with *C. trachomatis*, and that if we bypassed this restriction we might allow for an immune response to this human-adapted pathogen. We show there is a marked difference in the infection and the resulting immune response between transcervical and vaginal delivery of *C. trachomatis*. Transcervical infection also led to gross pathology in roughly 15% of animals while intravaginal inoculation of *C. trachomatis* led to no obvious pathology (Figure 2-2). This is the first fully immune competent mouse model to consistently demonstrate gross pathology after *C. trachomatis* infection (39). One important consideration with this study is the use of the LGV strain of *C. trachomatis*. Future studies will need to broadly examine the transcervical infection model with other genital strains of *C. trachomatis* that are of high public

health interest. These studies will allow us to begin examining the characteristics of both antigen specific cells and bystander cells that promote the induction of pathology across several clinically relevant strains of *C. trachomatis*; studies that have been difficult up to this point.

Our infection timecourse showed that bypassing the cervix alone does not lead to pathogen burden similar to the *C. muridarum*. The 10-fold increase in bacterial burden from day 3 to day 6 following *C. muridarum* infection was not seen with *C. trachomatis*. We next examined whether the lack of expansion was due to the suppression of *C. trachomatis* growth by the murine IFNγ response, as previous reports have shown that the absence of IFNγ leads to higher burden and longer duration of *C. trachomatis* infection (40, 41). IFNγ -mediated restriction of *C. trachomatis* is predominantly driven through the activity of the IRG family of GTPases (22, 25, 42). In contrast to *C. trachomatis*, *C. muridarum* is thought to evade IRG-mediated growth restriction due to the expression of a cytotoxin, which undermines this restriction mechanism (25). When mice deficient in either IFNγ or IRGs (Irgm1/m3) are infected with *C. trachomatis*, we observe a burst of bacterial growth from day 3 to day 6. These enhanced bacterial loads are identical, whether it is IFNγ -KO mice or IRGm1/m3-KO mice infected transcervically with *C. trachomatis*, or wildtype mice infected with *C. muridarum* (Figure 2-3). Thus, bypassing the physical restriction of the cervix, in combination with the lack of IRGs, leads to a *C. trachomatis* infection model system where loads and pathologies are comparable to that observed with *C. muridarum* vaginal infection. Both *C. trachomatis* transcervical infections and *C. muridarum* intravaginal infections are highly inflammatory as measured by the significant influx of neutrophils and the response of $CD4^+$ T cells that ultimately are able to clear infection with either species (data not shown and (34, 43)). Importantly, neither mouse model allows the development of the chronic infections observed in humans (34, 40). One explanation for the lack of persistent infection in mice is that mice and humans have different cell-autonomous mechanisms of responding to IFNγ. Humans lack an IFNγ-inducible IRG response, and instead respond to IFNγ by upregulating the expression of indolamine dioxygenase (IDO)

(7, 44). IDO induces tryptophan catabolism, resulting in a persistent form of *C. trachomatis* that does not grow rapidly and is not cleared. It is this critical difference in the response to IFNγ that may prevent *C. trachomatis* and *C. muridarum* from causing persistent infections in a murine model of genital infections. We are now examining whether transcervical infection of mice in which Irgm1 and Irgm3 are knocked out, and human IDO is knocked in might allow infection with *C. trachomatis* that more closely models the persistent infections seen in humans.

It is well accepted that the primary source of IFNγ seen during infection is the $CD4^+$ T helper cell. However, one recent report called into question the role, if any, $CD4^+$ T cells play in the resolution of, and protection against, *C. trachomatis* during murine infection. Morrison et al. showed that clearance of vaginal *C. trachomatis* genital infection is unaltered by depletion of $CD4^+$ T cells in mice deficient for innate immunity (8). The authors concluded that genital infection with *C. trachomatis* in mice does not stimulate an adaptive immune response and are not protected from subsequent infection. We hypothesized that the lack of adaptive immunity observed using their model was due to the inability of *C. trachomatis* to access the upper genital tract. Transcervical infection resulted in a significant enhancement in the ability of *C. trachomatis* to prime pathogen-specific T cells and recruit them to the upper genital mucosa (Figure 2-4). Transcervical infection with *C. trachomatis* also stimulated a robust $CD4^+$ memory response that was essential for protection following re-infection of the genital tract (Figure 2-5). We further characterized the protective capacity of $CD4^+$ T cells, showing that pathogen specific cells skewed towards TH1 are sufficient to protect naïve mice from *C. trachomatis* in a dose dependent manner (Figure 2-6). For the first time we were able to show that only 1000 *Chlamydia* specific T cells is the lower limit needed for significant protection (Fig 2-6). Finally, we tested whether transcervical inoculation was capable of stimulating endogenous *C. trachomatis*-specific T cells. Using a MHC-II tetramer for the first time to track T cells during a genital tract infection, we demonstrated clonal expansion and memory development of endogenous epitope-specific $CD4^+$ T cells (Figure 2-7). These results showed that during the

peak of infection, >1000 antigen specific T cells are induced, similar to the lowest transfer dose in our protection experiments (Figure 2-6). By quantifying the lower limit needed for protection we now have a baseline that allows us to tune the infiltration of different cell types to reduce pathology while still promoting protection. Together our studies illustrate our unique ability to examine physiological levels of *Chlamydia* specific T cell responses using a combination of TCR transgenic T cells and Class-I and Class-II tetramers. To date, there is lack of data using TCR transgenic T cells or MHC-II tetramers to determine the extent to which *Chlamydia*-specific $CD4^+$ T cells are recruited to the genital mucosa following *C. muridarum* infection. This shortcoming in the literature has made it impossible to know whether the T cells responding to *C. muridarum* infection are antigen-specific or whether many of them are bystander cells that merely follow the chemokine/cytokine gradients resulting from inflammation. Studying total $CD4^+$ T cell infiltration may not reflect the antigen-specific immune response generated by *C. trachomatis* and *C. muridarum* infections. Only by differentiating antigen specific and bystander immune responses can we determine the role of these populations in development of the immune pathologies seen clinically.

This study demonstrates that infection of the upper genital tract with either *C. trachomatis* or *C. muridarum* stimulates protective immune responses as well as gross pathology. Immunity to both species is dependent on $CD4^+$ T cells, and only 1000 *Chlamydia* specific $CD4^+$ T cells are sufficient to confer protection. Importantly, in the absence of the murine IRG or IFNγ response, *C. trachomatis* and *C. muridarum* colonize the murine upper genital tract at similar levels yet neither species causes persistent infections. The novel transcervical inoculation technique described here will provide a technically easy, non-invasive, highly reproducible, biologically relevant system for vaccine development (29). The model allows investigators to transcend discussions of relevant model system and focus on issues of pathology vs. protection following infection. These discussions are a critical step in defining the factors that drive *Chlamydia* specific pathogenesis and host defense.

Methods and Materials:

Mice

C57BL/6, B6.PL-Thy1a (CD90.1 congenic), and B6.129S7-IFNγtm1Agt (IFN-γ−/−) were purchased from The Jackson Laboratory. Irgm1/m3(-/-) and NR1 mice were described previously (11, 34) and are maintained and cared for within the Harvard Medical School Center for Animal Resources and Comparative Medicine (Boston, MA). All mice were treated with 2.5mg of medroxyprogetrone subcutaneously seven days prior to infection in order to normalize the murine estrous cycle. All experiments were approved by Institutional Animal Care and Use Committee. In all experiments four or five mice per group were used.

Growth, isolation and detection of bacteria.

C. trachomatis serovar L2 (434/Bu) or *C. muridarum* was propagated within McCoy cell monolayers grown in Eagle's MEM (Invitrogen, Grand Island NY) supplemented with 10% FCS, 1.5 g/L sodium bicarbonate, 0.1 M nonessential amino acids, and 1 mM sodium pyruvate. Infected monolayers were disassociated from plates using sterile glass beads and sonicated to disrupt the inclusion. EBs were purified by density gradient centrifugation as described previously (10). Aliquots were stored at -80°C in medium containing 250 mM sucrose, 10 mM sodium phosphate, and 5 mM L-glutamic acid and thawed immediately prior to use. To quantify the levels of *C. trachomatis* or *C. muridarum* we used quantitative PCR with 16s primers specific for *Chlamydia* as done previously (REF). For titering directly from the genital tract, at the given timepoints the upper genital tract was isolated, homogenized by mechanical disruption, and placed in six-well plates pre-seeded with 5x105 McCoy cells and incubated for 36 hours to allow the developmental cycle to finish. Cells were then lysed as described above and titered into 96-well plates containing 1x104 McCoy cells. Thirty hours post-infection the cells were fixed with methanol and stained using a *Chlamydia* culture diagnostic kit (Roche). Inclusions were then quantified by fluorescence microscopy.

Skewing of NR1 cells and protection assay.

$CD4^+$ T cells were purified from NR1 mice using a mouse CD4 negative isolation kit (Invitrogen) per the manufacturer's directions. The T cells were cultured in RPMI-1640 (Invitrogen) supplemented with 10% FCS, L-glutamine, HEPES, 50 μM 2-mercaptoethanol, 50 U/ml penicillin, and 50 ug/ml streptomycin. To stimulate the T cells, irradiated feeder splenocytes were pulsed with 5 μM of Cta1 133-152 peptide and cocultured with the CD4-enriched NR1 cells at a stimulator to T cell ratio of 4:1. To polarize T cells towards the Th1 phenotype cells were incubated with 10 ng/ml of IL-12 (Peprotech, Rocky Hill NJ) and 10 μg/ml of anti-IL4 (Biolegend). Cells were stimulated for five days then 106 cells were transfered into naïve $CD90.2^+$ IFNγ-/- host mice. Twenty-four hours following transfer, mice were challenged in the uterus with 106 IFU of *C. trachomatis* L2.

Flow cytometry

Tissues were mechanically disaggregated and immediately stained for activation markers or stimulated for 5 h with 50 ng/ml PMA (Alexis Biochemical) and 500 ng/ml ionomycin (Calbiochem) in the presence of brefeldin A (GolgiStop; BD Biosciences) for intracellular cytokine staining. Cells were preincubated with anti-FcRγ (Bio X-Cell) before staining with anti-CD4 Pacific Blue (Biolegend) and anti-CD90.1 peridinin chlorophyll-a protein (BD Bioscience). For activation marker analysis, we examined anti-CD44 PE-CyChrome 7 (Biolegend), anti-CD62L allophycocyanin-Alexa 750 (Ebioscience), and anti-CD25 allophycocyanin (BD Bioscience). For intracellular staining, the following antibodies were used: anti-IFN-γ PE, anti-IL2- allophycocyanin, anti-IL17 fitc, and anti-TNF-α PE-CyChrome 7 (BD Biosciences). Cells were permeabilized with the Cytofix/Cytoperm Plus kit according to the manufacturer's instructions (BD Bioscience). The absolute cell numbers in each sample was determined using accucheck counting beads (Invitrogen). Data were collected on a modified FACSCalibur (Cytek Development) or an LSRII (BD Bioscience) and analyzed using Flow Jo (Tree Star).

T cell depletion

For $CD4^+$ T cell depletion experiments, mice were infected with 106 IFU *C. trachomatis* or C. murdidarum then rested for greater than four weeks. Starting three days prior to secondary challenge, immune mice were intraperitoneally injected with 200µg/mouse anti-CD4 (clone GK1.5) or isotype control (clone LTF-2) everyday. Mice were sacrificed five days after challenge and their lymphocytes were assessed in the spleen, lymph nodes, and uterus. In addition, the bacterial load was determined by quantitative PCR.

Tetramer production, enrichment

Chlamydia trachomatis predicted periplasmic protein Cta1 133-152 (KGIDPQELWVWKKGMPNWEK) Biotin-labeled I-Ab molecules and the CrpA 63–71 (ASFVNPIYL) biotin labeled Db tetramer were produced by the NIH tetramer facility (Emory University), purified and tetramerized with streptavidin allophycocyanin or phycoerythrin, respectively. Spleen and lymph node cells were prepared, stained with CTA-1:I-Ab–SA-APC at 25°C for 1 h and then spiked with CrpA:Db-SA-PE at 4°C for 30min. Cells were then washed and incubated with anti-PE and anti-APC magnetic beads. Bead-bound cells were then enriched on magnetized columns and a sample was removed for counting. The enriched cells were surface stained with combinations of antibodies listed above.

Statistical analysis

All groups were evaluated for statistical significance through the use of unpaired two-tailed t tests. Where it appeared necessary to highlight significant differences between data points, the level of significance is depicted as: *, $p < 0.05$; **, $p < 0.01$; and ***, $p < 0.005$.

References

1. Belland R, Ojcius DM, Byrne GI. Chlamydia. Nat Rev Microbiol. 2004;2(7):530-1. Epub 2004/07/14. doi: 10.1038/nrmicro931. PubMed PMID: 15248311.

2. Beatty WL, Morrison RP, Byrne GI. Persistent chlamydiae: from cell culture to a paradigm for chlamydial pathogenesis. Microbiol Rev. 1994;58(4):686-99. Epub 1994/12/01. PubMed PMID: 7854252; PubMed Central PMCID: PMC372987.

3. Mpiga P, Ravaoarinoro M. Chlamydia trachomatis persistence: an update. Microbiol Res. 2006;161(1):9-19. Epub 2005/12/13. doi: 10.1016/j.micres.2005.04.004. PubMed PMID: 16338585.

4. Batteiger BE, Xu F, Johnson RE, Rekart ML. Protective immunity to Chlamydia trachomatis genital infection: evidence from human studies. J Infect Dis. 2010;201 Suppl 2:S178-89. Epub 2010/06/05. PubMed PMID: 20524235; PubMed Central PMCID: PMC2990949.

5. Brunham RC, Rey-Ladino J. Immunology of Chlamydia infection: implications for a Chlamydia trachomatis vaccine. Nat Rev Immunol. 2005;5(2):149-61. Epub 2005/02/03. doi: 10.1038/nri1551. PubMed PMID: 15688042.

6. Karunakaran KP, Yu H, Foster LJ, Brunham RC. Development of a Chlamydia trachomatis T cell Vaccine. Hum Vaccin. 2010;6(8):676-80. Epub 2010/06/05. PubMed PMID: 20523121; PubMed Central PMCID: PMC3056063.

7. Coers J, Starnbach MN, Howard JC. Modeling infectious disease in mice: co-adaptation and the role of host-specific IFNgamma responses. PLoS Pathog. 2009;5(5):e1000333. Epub 2009/05/30. doi: 10.1371/journal.ppat.1000333. PubMed PMID: 19478881; PubMed Central PMCID: PMC2682201.

8. Morrison SG, Farris CM, Sturdevant GL, Whitmire WM, Morrison RP. Murine Chlamydia trachomatis genital infection is unaltered by depletion of CD4+ T cells and diminished adaptive immunity. J Infect Dis. 2011;203(8):1120-8. Epub 2011/02/16. doi: 10.1093/infdis/jiq176. PubMed PMID: 21321103; PubMed Central PMCID: PMC3068022.

9. Johansson M, Schon K, Ward M, Lycke N. Studies in knockout mice reveal that anti-chlamydial protection requires TH1 cells producing IFN-gamma: is this true for humans? Scand J Immunol. 1997;46(6):546-52. Epub 1998/01/08. PubMed PMID: 9420616.

10. Olive AJ, Gondek DC, Starnbach MN. CXCR3 and CCR5 are both required for T cell-mediated protection against C. trachomatis infection in the murine genital mucosa. Mucosal Immunol. 2011;4(2):208-16. Epub 2010/09/17. doi: 10.1038/mi.2010.58. PubMed PMID: 20844481; PubMed Central PMCID: PMC3010299.

11. Roan NR, Gierahn TM, Higgins DE, Starnbach MN. Monitoring the T cell response to genital tract infection. Proc Natl Acad Sci U S A. 2006;103(32):12069-74. Epub 2006/08/02. doi: 10.1073/pnas.0603866103. PubMed PMID: 16880389; PubMed Central PMCID: PMC1567698.

12. Roan NR, Starnbach MN. Antigen-specific CD8+ T cells respond to Chlamydia trachomatis in the genital mucosa. J Immunol. 2006;177(11):7974-9. Epub 2006/11/23. PubMed PMID: 17114470.

13. Starnbach MN, Bevan MJ, Lampe MF. Protective cytotoxic T lymphocytes are induced during murine infection with Chlamydia trachomatis. J Immunol. 1994;153(11):5183-9. Epub 1994/12/01. PubMed PMID: 7525725.

14. Starnbach MN, Bevan MJ, Lampe MF. Murine cytotoxic T lymphocytes induced following Chlamydia trachomatis intraperitoneal or genital tract infection respond to cells infected with

multiple serovars. Infect Immun. 1995;63(9):3527-30. Epub 1995/09/01. PubMed PMID: 7642287; PubMed Central PMCID: PMC173488.

15. Marks E, Verolin M, Stensson A, Lycke N. Differential CD28 and inducible costimulatory molecule signaling requirements for protective CD4+ T-cell-mediated immunity against genital tract Chlamydia trachomatis infection. Infect Immun. 2007;75(9):4638-47. Epub 2007/07/20. doi: 10.1128/IAI.00465-07. PubMed PMID: 17635872; PubMed Central PMCID: PMC1951167.

16. Gondek DC, Roan NR, Starnbach MN. T cell responses in the absence of IFN-gamma exacerbate uterine infection with Chlamydia trachomatis. J Immunol. 2009;183(2):1313-9. Epub 2009/06/30. doi: 10.4049/jimmunol.0900295. PubMed PMID: 19561106; PubMed Central PMCID: PMC2723820.

17. Johansson M, Ward M, Lycke N. B-cell-deficient mice develop complete immune protection against genital tract infection with Chlamydia trachomatis. Immunology. 1997;92(4):422-8. Epub 1998/03/14. PubMed PMID: 9497482; PubMed Central PMCID: PMC1364146.

18. Barr EL, Ouburg S, Igietseme JU, Morre SA, Okwandu E, Eko FO, et al. Host inflammatory response and development of complications of Chlamydia trachomatis genital infection in CCR5-deficient mice and subfertile women with the CCR5delta32 gene deletion. J Microbiol Immunol Infect. 2005;38(4):244-54. Epub 2005/08/25. PubMed PMID: 16118671.

19. Igietseme JU, He Q, Joseph K, Eko FO, Lyn D, Ananaba G, et al. Role of T lymphocytes in the pathogenesis of Chlamydia disease. J Infect Dis. 2009;200(6):926-34. Epub 2009/08/07. doi: 10.1086/605411. PubMed PMID: 19656067; PubMed Central PMCID: PMC2847800.

20. Maxion HK, Liu W, Chang MH, Kelly KA. The infecting dose of Chlamydia muridarum modulates the innate immune response and ascending infection. Infect Immun. 2004;72(11):6330-40. Epub 2004/10/27. doi: 10.1128/IAI.72.11.6330-6340.2004. PubMed PMID: 15501762; PubMed Central PMCID: PMC523032.

21. Ramsey KH, Sigar IM, Schripsema JH, Denman CJ, Bowlin AK, Myers GA, et al. Strain and virulence diversity in the mouse pathogen Chlamydia muridarum. Infect Immun. 2009;77(8):3284-93. Epub 2009/05/28. doi: 10.1128/IAI.00147-09. PubMed PMID: 19470744; PubMed Central PMCID: PMC2715693.

22. Coers J, Bernstein-Hanley I, Grotsky D, Parvanova I, Howard JC, Taylor GA, et al. Chlamydia muridarum evades growth restriction by the IFN-gamma-inducible host resistance factor Irgb10. J Immunol. 2008;180(9):6237-45. Epub 2008/04/22. PubMed PMID: 18424746.

23. Eko FO, Okenu DN, Singh UP, He Q, Black C, Igietseme JU. Evaluation of a broadly protective Chlamydia-cholera combination vaccine candidate. Vaccine. 2011;29(21):3802-10. Epub 2011/03/23. doi: 10.1016/j.vaccine.2011.03.027. PubMed PMID: 21421002; PubMed Central PMCID: PMC3084325.

24. Kelly KA, Chan AM, Butch A, Darville T. Two different homing pathways involving integrin beta7 and E-selectin significantly influence trafficking of CD4 cells to the genital tract following Chlamydia muridarum infection. Am J Reprod Immunol. 2009;61(6):438-45. Epub 2009/04/28. doi: 10.1111/j.1600-0897.2009.00704.x. PubMed PMID: 19392981; PubMed Central PMCID: PMC2888875.

25. Nelson DE, Virok DP, Wood H, Roshick C, Johnson RM, Whitmire WM, et al. Chlamydial IFN-gamma immune evasion is linked to host infection tropism. Proc Natl Acad Sci U S A. 2005;102(30):10658-63. Epub 2005/07/16. doi: 10.1073/pnas.0504198102. PubMed PMID: 16020528; PubMed Central PMCID: PMC1180788.

26. Su H, Caldwell HD. CD4+ T cells play a significant role in adoptive immunity to Chlamydia trachomatis infection of the mouse genital tract. Infect Immun. 1995;63(9):3302-8. Epub 1995/09/01. PubMed PMID: 7642259; PubMed Central PMCID: PMC173455.

27. Olsen AW, Follmann F, Hojrup P, Leah R, Sand C, Andersen P, et al. Identification of human T cell targets recognized during Chlamydia trachomatis genital infection. J Infect Dis. 2007;196(10):1546-52. Epub 2007/11/17. doi: 10.1086/522524. PubMed PMID: 18008235.

28. Roan NR, Starnbach MN. Immune-mediated control of Chlamydia infection. Cell Microbiol. 2008;10(1):9-19. Epub 2007/11/06. doi: 10.1111/j.1462-5822.2007.01069.x. PubMed PMID: 17979983.

29. Finco O, Frigimelica E, Buricchi F, Petracca R, Galli G, Faenzi E, et al. Approach to discover T- and B-cell antigens of intracellular pathogens applied to the design of Chlamydia trachomatis vaccines. Proc Natl Acad Sci U S A. 2011;108(24):9969-74. Epub 2011/06/02. doi: 10.1073/pnas.1101756108. PubMed PMID: 21628568; PubMed Central PMCID: PMC3116399.

30. Farris CM, Morrison RP. Vaccination against Chlamydia genital infection utilizing the murine C. muridarum model. Infect Immun. 2011;79(3):986-96. Epub 2010/11/17. doi: 10.1128/IAI.00881-10. PubMed PMID: 21078844; PubMed Central PMCID: PMC3067520.

31. Zeng H, Gong S, Hou S, Zou Q, Zhong G. Identification of antigen-specific antibody responses associated with upper genital tract pathology in mice infected with Chlamydia muridarum. Infect Immun. 2011. Epub 2011/12/14. doi: 10.1128/IAI.05894-11. PubMed PMID: 22158739.

32. Tseng CT, Rank RG. Role of NK cells in early host response to chlamydial genital infection. Infect Immun. 1998;66(12):5867-75. Epub 1998/11/24. PubMed PMID: 9826367; PubMed Central PMCID: PMC108743.

33. Seder RA, Darrah PA, Roederer M. T-cell quality in memory and protection: implications for vaccine design. Nat Rev Immunol. 2008;8(4):247-58. Epub 2008/03/08. doi: 10.1038/nri2274. PubMed PMID: 18323851.

34. Coers J, Gondek DC, Olive AJ, Rohlfing A, Taylor GA, Starnbach MN. Compensatory T cell responses in IRG-deficient mice prevent sustained Chlamydia trachomatis infections. PLoS Pathog. 2011;7(6):e1001346. Epub 2011/07/07. doi: 10.1371/journal.ppat.1001346. PubMed PMID: 21731484; PubMed Central PMCID: PMC3121881.

35. Moon JJ, Chu HH, Hataye J, Pagan AJ, Pepper M, McLachlan JB, et al. Tracking epitope-specific T cells. Nat Protoc. 2009;4(4):565-81. Epub 2009/04/18. doi: 10.1038/nprot.2009.9. PubMed PMID: 19373228.

36. Rank RG, Whittum-Hudson JA. Protective immunity to chlamydial genital infection: evidence from animal studies. J Infect Dis. 2010;201 Suppl 2:S168-77. Epub 2010/05/28. doi: 10.1086/652399. PubMed PMID: 20470052.

37. Marks E, Tam MA, Lycke NY. The female lower genital tract is a privileged compartment with IL-10 producing dendritic cells and poor Th1 immunity following Chlamydia trachomatis infection. PLoS Pathog. 2010;6(11):e1001179. Epub 2010/11/17. doi: 10.1371/journal.ppat.1001179. PubMed PMID: 21079691; PubMed Central PMCID: PMC2973832.

38. Moniz RJ, Chan AM, Gordon LK, Braun J, Arditi M, Kelly KA. Plasmacytoid dendritic cells modulate nonprotective T-cell responses to genital infection by Chlamydia muridarum. FEMS Immunol Med Microbiol. 2010;58(3):397-404. Epub 2010/02/26. doi: 10.1111/j.1574-695X.2010.00653.x. PubMed PMID: 20180848; PubMed Central PMCID: PMC3153358.

39. Sturdevant GL, Kari L, Gardner DJ, Olivares-Zavaleta N, Randall LB, Whitmire WM, et al. Frameshift mutations in a single novel virulence factor alter the in vivo pathogenicity of Chlamydia trachomatis for the female murine genital tract. Infect Immun. 2010;78(9):3660-8. Epub 2010/06/16. doi: 10.1128/IAI.00386-10. PubMed PMID: 20547745; PubMed Central PMCID: PMC2937465.

40. Perry LL, Su H, Feilzer K, Messer R, Hughes S, Whitmire W, et al. Differential sensitivity of distinct Chlamydia trachomatis isolates to IFN-gamma-mediated inhibition. J Immunol. 1999;162(6):3541-8. Epub 1999/03/27. PubMed PMID: 10092812.

41. Perry LL, Feilzer K, Caldwell HD. Immunity to Chlamydia trachomatis is mediated by T helper 1 cells through IFN-gamma-dependent and -independent pathways. J Immunol. 1997;158(7):3344-52. Epub 1997/04/01. PubMed PMID: 9120292.

42. Bernstein-Hanley I, Coers J, Balsara ZR, Taylor GA, Starnbach MN, Dietrich WF. The p47 GTPases Igtp and Irgb10 map to the Chlamydia trachomatis susceptibility locus Ctrq-3 and mediate cellular resistance in mice. Proc Natl Acad Sci U S A. 2006;103(38):14092-7. Epub 2006/09/09. doi: 10.1073/pnas.0603338103. PubMed PMID: 16959883; PubMed Central PMCID: PMC1599917.

43. Frazer LC, O'Connell CM, Andrews CW, Jr., Zurenski MA, Darville T. Enhanced Neutrophil Longevity and Recruitment Contribute to the Severity of Oviduct Pathology during Chlamydia muridarum Infection. Infect Immun. 2011;79(10):4029-41. Epub 2011/08/10. doi: 10.1128/IAI.05535-11. PubMed PMID: 21825059.

44. Roshick C, Wood H, Caldwell HD, McClarty G. Comparison of gamma interferon-mediated antichlamydial defense mechanisms in human and mouse cells. Infect Immun. 2006;74(1):225-38. Epub 2005/12/22. doi: 10.1128/IAI.74.1.225-238.2006. PubMed PMID: 16368976; PubMed Central PMCID: PMC1346650.

Chapter 3: CXCR3 and CCR5 are both required for T cell mediated protection against *C. trachomatis* infection in the murine genital mucosa

Contributions

I conducted all of the experiments presented in this chapter with the exception of the competitive homing experiment, which was done in collaboration with Dr. David Gondek.

The results of this chapter are published in Mucosal Immunology

Introduction

The ability of a host to respond to and clear infections depends on coordinated communication between the innate and adaptive immune responses. Infection stimulates innate immune sensing mechanisms, such as Toll-like receptors that secrete specific chemokines into the tissues (1). Activated T cells follow these chemokine gradients by upregulating the expression of distinct chemokine receptors in order to exit the lymphatic system and traffic to the site of infection (2).

Several previous reports have identified dominant chemokine receptors that are expressed by T cells in order for proper migration to mucosal tissues. For example, CCR9 is critical for recruitment to the intestinal tract under many conditions (3), while CXCR3 directs T cell migration to the lungs following influenza virus infections (4, 5). Despite the increase in concern over the public health impact of sexually transmitted infections (STIs)(6), homing receptors for the genitourinary tract remain largely undefined. The most prevalent genital tract bacterial infection is caused by the obligate intracellular pathogen *Chlamydia trachomatis*. Clearance of *C. trachomatis* is primarily dependent on T cell secretion of IFNγ , which directly and indirectly targets the infected epithelial cells (7-15). However, the immune response to *C. trachomatis* is also responsible for tissue damage and the induction of sequelae such as infertility and ectopic pregnancy (7, 16). Understanding the trafficking of immune cells following an STI is key to the development of therapeutic interventions that lead to protection and prevent pathology.

In order to define how T cells respond to *C. trachomatis*, it is critical to elucidate what chemokine/chemokine receptor pairs promote proper activation and recruitment of T cells during infection. Reports examining the inflammatory conditions in the genital mucosa of mice following infection with the mouse-adapted species *Chlamydia muridarum* showed that the chemokines CCL5 and CXCL10 are upregulated and secreted at high levels from cells in the tissues (17-19). Another study examined samples from human patients and demonstrated an increase in CCR5

expression following *C. trachomatis* genital infections (20), while a different report showed mice deficient in CCR5 were unable to clear *C. muridarum* infections (21). Even though these data provide insight into expression dynamics following infection, they do not directly reveal which subsets of immune cells, such as T cells, are activated and recruited to the genital mucosa through the action of chemokine receptors. Furthermore, these studies are unable to distinguish the response of *C. trachomatis* specific lymphocytes from infiltrating bystander lymphocytes that respond in a non-specific manner to the general inflammatory conditions in the genital mucosa. In this study, we monitored $CD4^+$ *C. trachomatis*-specific T cells, which harbor a fixed TCR specific for the *C. trachomatis* antigen Cta1 (12). We were able to directly assess the impact of two chemokine receptors on the ability of *Chlamydia*-specific T cells to become activated and respond during infection of the genital tract. We find that concomitant expression of CXCR3 and CCR5 expression is required for antigen specific T cells to access, accumulate, and protect the genital tracts of mice from infection with *C. trachomatis*.

Results

CXCR3 and CCR5 are upregulated on lymphocytes during *C. trachomatis* infection. Previous studies have examined chemokines and chemokine receptors that are induced in whole tissue homogenates of the genital tract following *C. trachomatis* infection. Yet these studies could not differentiate non-specific homing, resulting from general inflammation, from the truly pathogen-specific lymphocytes responding to the genital mucosa. To determine which receptors are required for lymphocyte homing to the genital mucosa, we surveyed chemokine receptor mRNA expression in isolated lymphocytes from naïve vs. *C. trachomatis* infected mice. We extracted lymphocyte RNA isolated from the draining lymph node or genital tract in naïve mice or from mice infected in the uterus with 10^6 *C. trachomatis*. Using RT-PCR we examined the differences in expression of five different chemokine receptors on tissues from uninfected and infected mice. Analysis of the draining lymph node showed that only CXCR3 expression was increased following infection, showing a two-fold enhancement (Figure 3-1). In contrast, the lymphocytes isolated from the genital tract showed that expression of both CXCR3 and CCR5 was significantly induced following *C. trachomatis* infection. Expression of CXCR3 was increased more than ten-fold after infection, while CCR5 was upregulated by more than four-fold. In order for lymphocytes to exit the lymph node, they down-regulate CCR7, consistent with our observation that the level of this marker decreased on lymphocytes in both the draining lymph node and genital tract of infected mice (22). All other chemokine receptors examined showed no changes in expression levels following infection with *C. trachomatis*. Therefore, the expression of the chemokine receptors CXCR3 and CCR5 is upregulated in lymphocytes in response to a genital tract infection with *C. trachomatis*.

Mice deficient in CXCR3 or CCR5 have increased *C. trachomatis* burden following genital tract infection. The increase in the expression of CXCR3 and CCR5 on lymphocytes following genital tract infection with *C. trachomatis* suggested that both receptors might be important for

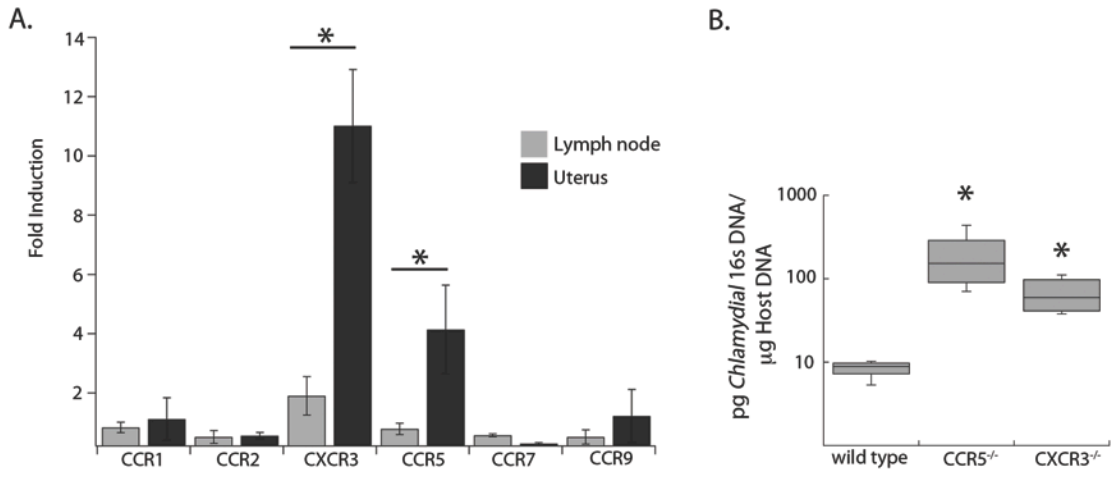

Figure 3-1. CXCR3 and CCR5 are upregulated in the genital tract during infection and necessary for clearance of *C. trachomatis*. A) RNA was isolated from tissues of uninfected and infected mice. RT-PCR was used to quantify the expression of five chemokine receptors relative to a GAPDH control. Fold-induction was calculated (relative expression infected)/(relative expression uninfected). The data shown are representative of three independent experiments. Each bar represents the average fold-induction ± SD of two pools of five mice for each condition B) Genomic DNA was isolated from the genital tract of wild-type, $CXCR3^{-/-}$, or $CCR5^{-/-}$ mice six days following infection. Quantitative PCR was used to calculate the levels of *C. trachomatis* 16s DNA relative to levels of host GAPDH. Shown is a box and whisker plot of two combined experiments each conducted with three mice per genotype. * = $p<0.05$

the resolution of infection. We therefore assessed the efficiency of *C. trachomatis* clearance from the genital tracts of mice deficient in either CXCR3 or CCR5 as compared to wild-type mice. Wild-type, CXCR3$^{-/-}$, and CCR5$^{-/-}$ mice were infected in the uterus with 10^6 IFU of *C. trachomatis,* and levels of bacteria in the genital tract were evaluated six days later by qPCR (Figure 3-1)(12). All wild-type mice had under 10 pg of bacterial 16s DNA per mg of host DNA, whereas both the CXCR3$^{-/-}$ and CCR5$^{-/-}$ mice had almost 8-fold higher levels of bacterial 16s DNA in the genital tract. Since there was no difference in bacterial load between CXCR3$^{-/-}$ or CCR5$^{-/-}$ mice, it suggests that both receptors may be needed for the proper resolution of genital tract infection with *Chlamydia*.

***Chlamydia* specific CD4$^+$ cells become activated and traffic normally to the genital tract in chemokine receptor-deficient hosts.** The high bacterial loads observed in the CXCR3 and CCR5 deficient mice could be due to an inability to properly prime an immune response (23, 24). To test this, we monitored wild-type *Chlamydia* specific TCR transgenic T cells during infection of wild-type, CXCR3$^{-/-}$, and CCR5$^{-/-}$ host mice inoculated with *C. trachomatis*. Seven days after infection, we found that wild-type pathogen-specific T cells showed no defect in trafficking to the spleen, draining lymph nodes, or the genital tract in hosts deficient for CXCR3 or CCR5 (Figure 3-2A). Thus, the recruitment and/or retention of pathogen specific T cells in the genital tract is independent of chemokine receptor expression in the host. To ensure that the *Chlamydia* specific T cells were activated normally, we stained the isolated T cells for CD62L, CD45Rb, and CD25 as markers of early and late activation (Figure 3-2B). When we compared cells isolated from mice expressing the chemokine receptors with those lacking expression, we found that the cells showed identical activation. Furthermore, these cells also secrete IFNγ to similar levels upon restimulation in vitro (data not shown). Most importantly, all the *Chlamydia*-specific T cells that were present in the genital tract were completely activated, indicating that

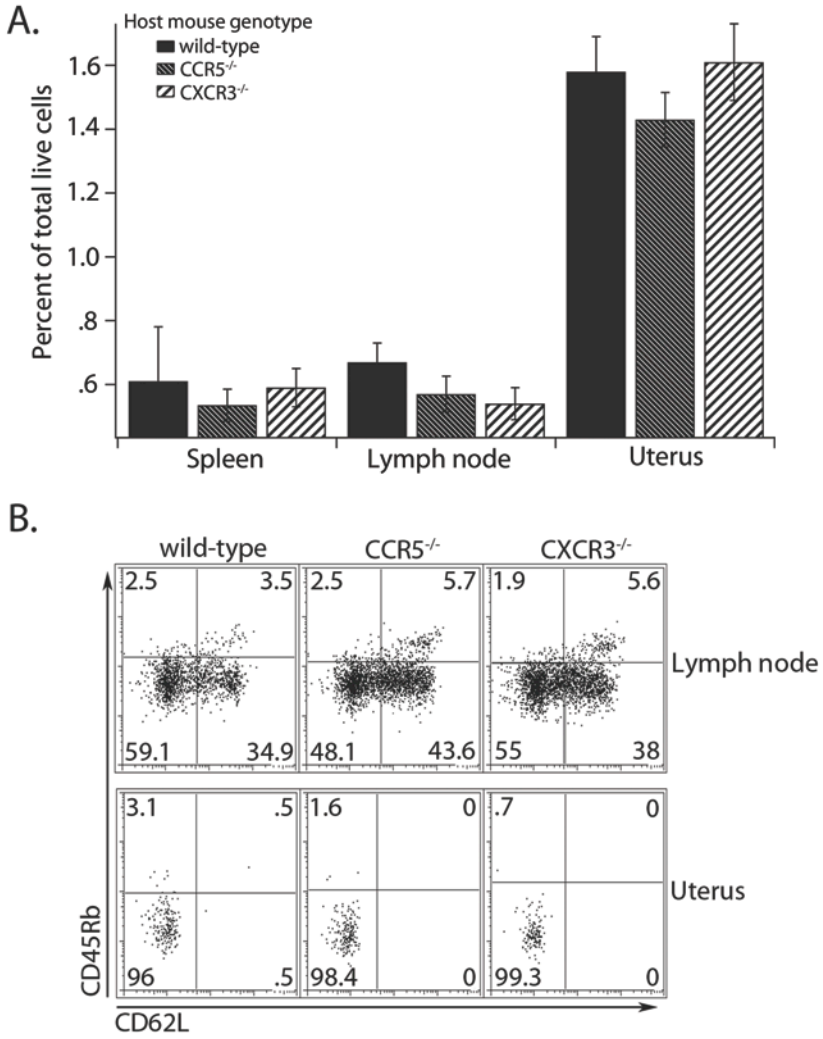

Figure 3-2. Wild-type *Chlamydia* specific CD4$^+$ T cells are recruited to the genital tract and become activated in CXCR3 or CCR5 deficient mice. A) Wild-type CD90.1$^+$ transgenic CD4$^+$ T cells were transferred into CD90.2 wild-type, CXCR3$^{-/-,}$ or CCR5$^{-/-}$ host mice. The following day, hosts were challenged in the genital tract with *C. trachomatis*. Seven days after infection the tissues were harvested and cells prepared for flow cytometry. Antigen specific CD4$^+$ T cells were identified as both CD4 and CD90.1 positive. The graph shows the percent of total live cells in each tissue examined and is representative of one experiment of two conducted. B) Surface levels of the activation markers CD45Rb and CD62L were examined by flow cytometry. All cells were pre-gated on CD4 and CD90.1 positive T cells. A representative plot from one of two independent experiments is shown.

even when the host bystander population is deficient in CXCR3 or CCR5 there is no deficiency in the priming of *Chlamydia* specific T cells.

Both CXCR3 and CCR5 are upregulated on *Chlamydia* specific T cells present in the genital mucosa. Because host deficiency in CXCR3 or CCR5 did not alter the priming or homing of wild type antigen specific T cells, we hypothesized that T cells responding to *C. trachomatis* antigens in the genital tract might be enriched for CXCR3 and/or CCR5. To test this, we examined the presence of CXCR3 and CCR5 on the surface of antigen specific transgenic T cells during infection. Naïve *Chlamydia* specific T cells were isolated from TCR transgenic mice and stained for CXCR3 and CCR5 (Figure 3-3). All naïve cells examined expressed low levels of both CXCR3 and CCR5. We then transferred these antigen specific T cells into mice that were infected in the uterus with *C. trachomatis*. Seven days after infection we isolated lymphocytes from the draining lymph nodes and genital mucosa and stained them for CXCR3 and CCR5. *Chlamydia* specific T cells from the lymph nodes were more than twenty percent positive for CXCR3 while all cells remained low for CCR5. However, almost all of the antigen specific T cells isolated from the genital tract were CXCR3 high and over 80 percent were now CCR5 positive. We observed two distinct CCR5 positive subsets in the genital tract, but the significance and phenotypic difference of these distinct populations is still unclear. These data suggest that in response to infection *Chlamydia* specific T-cells upregulate CXCR3 on their surface beginning in the draining lymph node. Upon exiting the lymph node, CXCR3 is further upregulated, and CCR5 now becomes expressed on the surface at high levels, resulting in their recruitment to or their retention in the genital tract. ***Chlamydia* specific $CD4^+$ T cells deficient in CXCR3 or CCR5 are unable to traffic normally to the genital tract.** As described above we found that CXCR3 and CCR5 are upregulated on *C. trachomatis* specific T cells in response to genital tract infection and that pathogen specific T cells activate normally in $CXCR3^{-/-}$ or $CCR5^{-/-}$ hosts. This led us to test whether the high *C. trachomatis* burden seen in

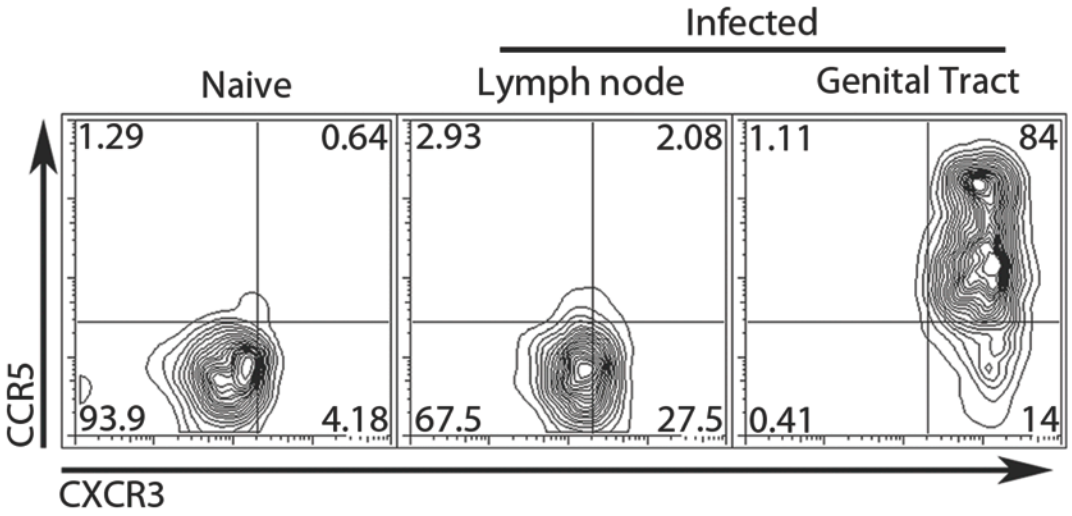

Figure 3-3. CXCR3 and CCR5 are upregulated on the surface of antigen specific CD4$^+$ T cells in a stepwise fashion following *C. trachomatis* infection. Wild-type CD90.1 *Chlamydia* specific CD4$^+$ T cells were transferred intravenously into CD90.2 hosts. Mice were challenged in the genital tract with *C. trachomatis* the following day. Seven days after infection the tissues were isolated and analyzed by flow cytometry. *Chlamydia* antigen specific cells were identified by CD4$^+$CD90.1$^+$ gating and assessed for surface expression of CXCR3 and CCR5 Shown is a representative plot from three independent experiments.

mice deficient in CXCR3 or CCR5 is due to an inability of pathogen specific T cells to traffic to the genital mucosa during infection. We obtained *Chlamydia* specific T cells that are deficient in CXCR3 or CCR5 and monitored their trafficking in mice during *C. trachomatis* genital tract infection. We transferred 10^5 wild-type, CXCR3$^{-/-}$, or CCR5$^{-/-}$ antigen specific T cells into CD90.1 wild-type hosts. The mice were then infected with *C. trachomatis* and the number of *Chlamydia* specific T cells in the genital tract was assessed at four time points (Figure 3-4A). Four days after infection there was no significant trafficking of any T cells into the genital tract. However, by six days following infection, wild-type *Chlamydia* specific T cells amassed in the genital tract, while cells from either CXCR3$^{-/-}$ or CCR5$^{-/-}$ mice failed to migrate to the site of infection. Eight days after infection the recruitment of wild-type cells to the genital tract continued to increase, whereas cells from CXCR3$^{-/-}$ and CCR5$^{-/-}$ mice showed no accumulation. Ten days following infection, when *C. trachomatis* is mostly cleared (data not shown), the number of wild-type cells in the genital tract began to contract, whereas pathogen specific T cells from the chemokine receptor deficient mice showed no signs of trafficking to the genital tract. These data illustrate that lack of either CXCR3 or CCR5 does not delay recruitment to the genital tract, rather it completely prevents homing to the site of infection.

Since our time-course data suggested that the loss of either CXCR3 or CCR5 blocks recruitment to the genital tract, we next wanted to assess whether a loss of both CXCR3 and CCR5 would further impede homing to the genital tract. We bred the TCR transgenic onto the CXCR3/CCR5 double knockout mouse background. We then transferred these antigen specific CXCR3$^{-/-}$ CCR5$^{-/-}$ T cells (as well as wild-type, CXCR3-deficient, and CCR5-deficient T cells) into CD90.1 wild-type hosts that were then infected with *C. trachomatis*. Eight days following infection, a time when we found the greatest difference in homing between wild-type and receptor-deficient cells, *Chlamydia* specific cells of all four genotypes accumulated equivalently

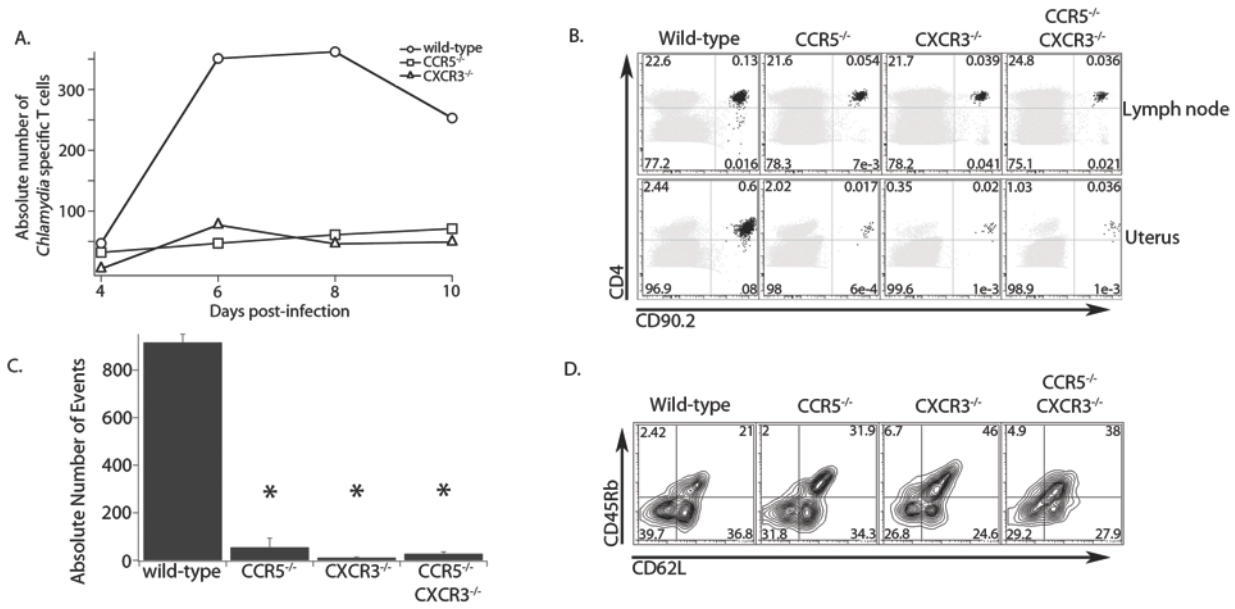

Figure 3-4. *Chlamydia* specific CD4$^+$ cells lacking CXCR3 and/or CCR5 are unable to traffic to the genital mucosa. A) Wild-type, CXCR3$^{-/-}$ or CCR5$^{-/-}$ CD90.2$^+$ *Chlamydia* specific T cells were transferred into CD90.1$^+$ host mice. Mice were challenged the following day with *C. trachomatis* in the genital tract. At the timepoints indicated, the genital tract was harvested and cells prepared for flow cytometry. The total number of antigen specific T cells was also quantified. Each data point represents the total number of cells from three mice for each genotype. The figure represents one experiment of two conducted. B) CD90.2$^+$ wild-type, CXCR3$^{-/-}$, CCR5$^{-/-}$, or CXCR3$^{-/-}$ CCR5$^{-/-}$ transgenic CD4$^+$ T cells were transferred into CD90.1$^+$ host mice and infected the following day with *C. trachomatis*. Eight days following infection the tissues were harvested and prepared for flow cytometry. Shown is a representative cytometry plot from one experiment of three conducted of the draining lymph node (top panel) and genital tract (bottom panel). The host CD4$^+$ T cell population is shown in grey and the antigen specific CD4$^+$ T cells are shown in black. The values presented are a percent of total live cells. C) Absolute total numbers of *Chlamydia* specific CD4$^+$ T cells in the genital tract were quantified from the experiment in B. D) Cells isolated from the draining lymph node were pre-gated for CD90.2$^+$ and CD4$^+$ positive populations and examined for surface staining of the activation markers CD45Rb and CD62L. Shown is a representative plot from one of two independent experiments. *=$p<0.05$

in the draining lymph nodes of infected mice (Figure 3-4B). However, in the genital tract, wild-type cells accumulated at levels more than twenty-fold higher than chemokine receptor-deficient cells (Figure 3-4B,C). All variants of the chemokine receptor-deficient *Chlamydia* specific T cells were unable to home correctly to the genital tract following infection, and the double knockout phenotype was identical to that of either single knockout. These data show that both CXCR3 and CCR5 are needed to properly direct antigen specific T cells following *C. trachomatis* infection in the genital mucosa.

While these data suggest that $CD4^+$ cells deficient for CXCR3 or CCR5 are not recruited efficiently to the genital tract following infection, we wanted to confirm they were activated normally in order to rule out any deficiency in T cell priming. We assessed the levels of CD62L and CD45Rb on all of the chemokine receptor-deficient *Chlamydia* specific T cells in the draining lymph node eight days after infection. Surface staining showed no significant difference in activation pattern between the chemokine receptor-deficient T cells and wild-type T cells even though there is a slight decrease in activation of chemokine receptor deficient T cells (Figure 3-4D). Taken together, loss of CXCR3, CCR5, or both severely inhibits trafficking of pathogen specific T cells to the genital mucosa even though these cells accumulate equivalently in the draining lymph node and are activated similarly to wild-type T cells.

***Chlamydia*-specific $CD4^+$ cells deficient for CCR5 or CXCR3 are unable to compete with WT cells in trafficking to the genital tract.** Since trafficking to the genital tract was completely ablated in transfer studies using single chemokine receptor knockouts, we were unable to determine if the $CXCR3^{-/-}$ $CCR5^{-/-}$ T cells exacerbated the homing deficiency to the genital mucosa. To test this we developed a competitive homing assay that would be more sensitive to subtle differences in T cell numbers homing to the genital mucosa. This approach allowed us to directly monitor the ability of wild-type and chemokine receptor deficient T cells to home to the genital tract under identical conditions in the same host (Figure 3-5A). We first transferred an

equal number of CD90.1 chemokine receptor sufficient and CD90.2 chemokine receptor deficient antigen specific T cells into CD45.1 hosts, which we then infected in the genital tract with *C. trachomatis*. Seven days after infection, we calculated a migration index [(% CD90.1)/ (% CD90.2)] for all the T cells transferred in both the draining lymph node and the genital tract (Figure 5B). T cells of all genotypes showed no statistical difference in the migration index in their draining lymph node. In contrast, when we calculated the migration index for T cells in the genital tract, only the wild-type T cell transfer yielded a migration index near 1. Pathogen specific T cells that were deficient in CCR5 migrated 30 percent less efficiently than wild-type cells, while T cells lacking CXCR3 were 20 percent less efficient. Interestingly, the antigen specific T cells lacking both chemokine receptors migrated ten fold less efficiently than wild-type cells suggesting an additive impact of both CXCR3 and CCR5. This indicates that while both single chemokine receptor knockouts are impaired in their ability to compete with wild-type T cells and be recruited to the genital tract, loss of both receptors may be more detrimental to their ability to access the genital mucosa.

***Chlamydia*-specific CD4^{+} cells deficient for CCR5 or CXCR3 are unable to protect mice from genital tract infection.** The experiments above show that loss of CXCR3 and/or CCR5 impairs the recruitment of *Chlamydia* specific T cells to the genital mucosa following infection. Therefore we predicted these T cells would not be able to protect mice from infection as well as wild-type T cells. To assess their protective capacity, we pre-activated wild-type, CXCR3$^{-/-}$, CCR5$^{-/-}$ and double deficient T cells in vitro, polarizing them to the Th1 phenotype and then transferred them into IFNγ -deficient hosts. Since the clearance of *C. trachomatis* in mice is dependent on IFNγ , and the only source of IFNγ was the transferred population of cells, we were able to directly ascertain the capacity of *Chlamydia* specific T cells to traffic to the site of infection, locally produce IFNγ, and reduce bacterial burden in the genital tract (8-10). Following in vitro TH1 skewing, all the chemokine receptor deficient T cells were competent at secreting

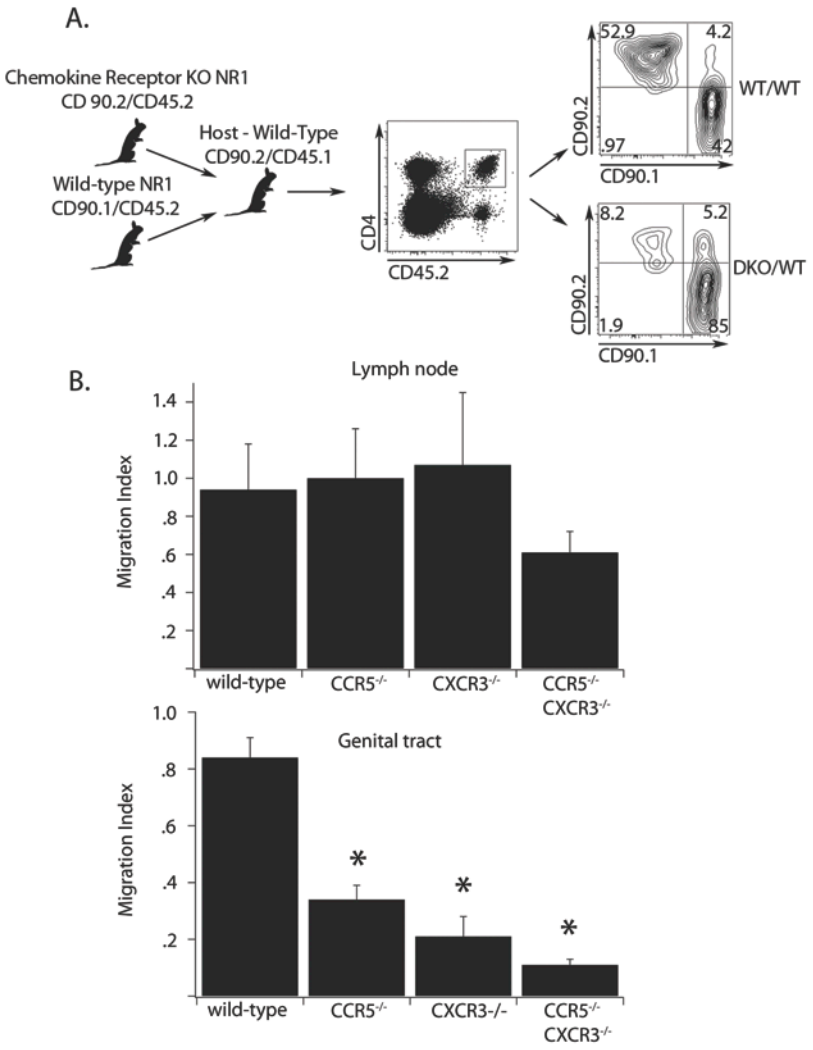

Figure 3-5. Chemokine receptor-deficient *Chlamydia* specific CD4+ T cells are unable to compete with wild-type cells in homing to the genital tract. A) A schematic of the competitive homing assay is shown. Equal numbers of antigen specific $CD4^+$ T cells from CD45.2/CD90.1 wild type mice and CD45.2/CD90.2 wild-type, $CXCR3^{-/-}$, $CCR5^{-/-}$, or $CXCR3^{-/-}$ $CCR5^{-/-}$ mice were transferred into CD45.1/CD90.2 host mice. The following day mice were infected in the genital tract with *C. trachomatis*. Seven days after infection tissues were harvested and prepared for flow cytometry. The strategy for gating is illustrated. We first gated CD4 and CD45.2 positive cells. Then we compared the percent of the gated cells that were CD90.1 or CD90.2 positive. Shown is a representative plot comparing the homing to the genital tract between the wild-type:wild-type cell mix and $CXCR3^{-/-}CCR5^{-/-}$:wild-type mix. Shown is one representative of four independent experiments. B) We calculated a migration index for each cell mix using the percent of CD90.2/CD90.1 positive cells present in the draining lymph node (top) and the percent of the CD90.2/CD90.1 positive cells in the genital tract (bottom). Error bars represent standard deviation and *=$p<0.05$

IFNγ equivalently to wild-type T cells (data not shown). Activated cells were transferred into mice, which were subsequently challenged with *C. trachomatis*. After 6 days of infection, the peak of antigen specific T cells recruitment to the site of infection (Figure 3-4A), we isolated the genital tract and determined the levels of *C. trachomatis* by qPCR (Figure 3-6). Mice that received wild-type T cells had more than two logs less *C. trachomatis* relative to mice receiving no T cells. However, mice receiving either CXCR3 or CCR5 single knockout T cells had ten-fold higher bacterial levels compared to wild-type cells. This showed that single receptor knockout cells partially protected the host, decreasing *Chlamydia* burden by over one log as compared to mice receiving no transfer. Therefore, both CXCR3$^{-/-}$ and CCR5$^{-/-}$ antigen specific T cells are capable of protecting host mice from *C. trachomatis* infection to some degree, albeit much less than wild-type. Surprisingly, mice that received CXCR3$^{-/-}$ CCR5$^{-/-}$ T cells did not protect host mice whatsoever and had levels of *C. trachomatis* in the genital tract identical to mice that received no transfer. These data indicate that, although loss of CXCR3 or CCR5 in antigen specific T cells leads to a deficiency in protecting mice from infection, loss of both receptors in concert results in total ablation of protection against *C. trachomatis*. This illustrates that optimal trafficking and protective function of *Chlamydia* specific T cells in the genital tract requires a cooperative interaction between CXCR3 and CCR5.

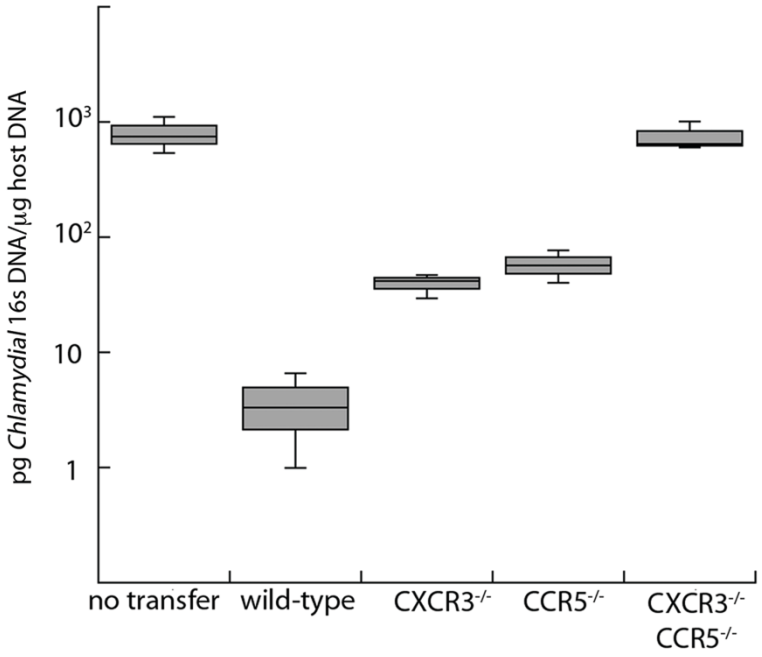

Figure 3-6. Antigen specific TH1 cells deficient in both CXCR3 and CCR5, have no protective capacity in vivo. Wild-type, CXCR3$^{-/-}$, CCR5$^{-/-}$, or CXCR3$^{-/-}$ CCR5$^{-/-}$ *Chlamydia* specific CD4^{+} T cells were skewed in vitro to the Th1 phenotype for five days. These pre-activated T cells were then transferred into IFNγ $^{-/-}$ host mice. The following day the mice were challenged with *C. trachomatis*. Six days after infection the genital tract was harvested and DNA was isolated. We used quantitative PCR to compare the levels of *Chlamydia* 16s DNA to host GAPDH DNA. Levels of *C. trachomatis* 16s DNA were converted into pg/μl. Shown is a box and whisker plot from one representative experiment of two conducted. In the graph shown all samples are significantly different ($p<0.05$) except for the comparison between the CXCR3$^{-/-}$ and CCR5$^{-/-}$ samples and CXCR3$^{-/-}$ CCR5$^{-/-}$ compared to “no transfer”.

Discussion

The ability of immune cells to traffic to sites of inflammation and infection is necessary for efficient clearance of invading pathogens. While chemokine receptors that are critical for directing T cells to the lungs and intestinal tract have been described previously(1, 4, 5), characterization of receptors that are necessary for recruitment to the genital tract has remained elusive. In this report, we show that a combination of CXCR3 and CCR5 is necessary for pathogen-specific $CD4^+$ T cells to respond to and clear *C. trachomatis* infection of the genital mucosa.

Previous studies showed that infection with the mouse specific pathogen *C. muridarum* led to elevated levels of the chemokines CXCL10 and CCL5 in the genital tract tissue(17). These chemokines, specific for the receptors CXCR3 and CCR5, promote the recruitment of immune cells to resolve infection. CCR5 has been implicated in genital mucosa homing because CCR5 deficient mice are unable to clear *C. muridarum* infections efficiently(21). However, one recent study suggested that CXCR3 may be important for $CD8^+$ T cells to respond to the vaginal tissue during herpes simplex virus infection(25). Therefore, we sought to determine the chemokine receptors that are necessary for pathogen specific T cells to clear a murine genital infection with the human bacterial pathogen *C. trachomatis*. Although mice clear *C. trachomatis* infection more efficiently than humans, we are able to demonstrate that T cells respond and migrate in the mouse following *C. trachomatis* infection. Therefore we could use *C. trachomatis*-specific TCR transgenic T cells to facilitate these experiments. It is possible that the rapid clearance of C. trachomatis from mice relative to humans affects the molecules responsible for T cell migration, but we have no evidence that this is the case.

Following stimulation and activation, pathogen specific T cells upregulate specific chemokine receptors to egress from the lymph node and respond rapidly to the infected tissue. Indeed, we saw a trend in CXCR3 and CCR5 expression at both the transcriptional level as well as expression through surface staining. In the draining lymph node there was a distinct

upregulation of only CXCR3. Meanwhile, in the genital mucosa there was a dramatic upregulation of both CXCR3 and CCR5, indicating that these receptors may be regulated in a step-wise fashion. Our current model proposes that the initial upregulation of CXCR3 in the draining lymph node allows efficient egress following T cell activation. Upon exiting the lymph node, antigen specific T cells upregulate CCR5 in order to migrate to the genital mucosa.

In this report we show that mice deficient in either CXCR3 or CCR5 are unable to clear genital tract infections with *C. trachomatis* as efficiently as wild-type mice. One possible hypothesis is that the loss of chemokine receptors may alter the development of a Th1 response that is critical for *Chlamydia* clearance. However, transfer of wild-type antigen specific T cells into CXCR3 or CCR5 deficient hosts resulted in no defect in T cell activation or accumulation in the draining lymph node. These T cells also arrive in the genital mucosa in similar numbers and are fully activated, showing that the chemokine receptor profile of any bystander T cells in the host does not affect the capacity of wild-type *Chlamydia* specific T cells to respond to infection normally. Furthermore these data suggest that the higher pathogen load seen in chemokine receptor-deficient mice is not due to a loss in T cell priming but rather a defect in trafficking to the infected tissue.

No previous reports had assessed whether a lack of CCR5 or CXCR3 impairs recruitment of antigen specific T cells to the genital mucosa during *C. trachomatis* infections. Our current study demonstrates that *Chlamydia*-specific $CD4^+$ T cells deficient for either CXCR3 or CCR5 are unable to accumulate in the genital tract over the course of infection. This highlights the importance of CXCR3 and CCR5, as loss of either chemokine receptor does not delay recruitment but rather, blocks trafficking to the genital mucosa altogether. Even though receptor-deficient T cells could not home to the genital mucosa, these cells trafficked normally to the draining lymph node, where they were properly primed with antigen. We did see a minor decrease in activation among all receptor deficient T cells that was not statistically significant in our studies. It is possible however that this slight reduction in activation may have a small effect

on the severe blockage of T cell recruitment, but it does not appear to be a major contributor. The more sensitive competitive homing assay bolstered our time course findings by showing that antigen specific chemokine receptor-deficient cells are significantly less efficient at trafficking to the genital tract than wild-type cells when they are both present in the same mouse. Furthermore, when mice received pre-activated antigen specific T cells deficient for either CXCR3 or CCR5, the T cells could not protect recipient mice to the same extent as wild-type cells, but each population was still able to reduce the *C. trachomatis* load in the genital tract 10-fold. Ultimately, these approaches identified both CXCR3 and CCR5 as necessary for proper homing of *Chlamydia* specific T cells to the genital mucosa and protecting mice from infection.

Previous reports have also examined a double deficiency of CXCR3 and CCR5 during virus infections of the lung and central nervous system (4, 26). These investigators concluded that CXCR3 and CCR5 might function antagonistically on T cells. However, in our study the data support a cooperative interaction between CXCR3 and CCR5 following a genital tract infection with *C. trachomatis*. Our single transfer and competitive homing studies showed that T cells lacking both CXCR3 and CCR5 were unable to be recruited to or retained in the genital mucosa after infection. Furthermore, transfer of pre-activated antigen specific T cells lacking both CXCR3 and CCR5 did not protect recipient mice at all. Together these data indicate that loss of both CXCR3 and CCR5 together is more detrimental than loss of either receptor individually. This finding does not result from a drastic T cell priming defect because all chemokine receptor deficient cells were able to accumulate in the draining lymph node and be activated similarly. Therefore we conclude that the inability of $CXCR3^{-/-}$ $CCR5^{-/-}$ antigen specific T cells to traffic to and be retained in the genital tract following infection with *C. trachomatis* eliminates all protective capacity of these cells.

In contrast to the generally accepted view of CXCR3 and CCR5 as “general TH1 inflammation chemokine receptors”, recent evidence in lung infection models have indicated

antigen specific cells do not utilize both receptors. Moreover, the expression of CCR5 was deleterious to TH1 T cell homing to the lung (4). This incongruity in the "general inflammation" model of homing suggests that monitoring antigen specific responses is required to elucidate lymphocyte homing to infections at disparate mucosal sites. It remains a possibility that the host bystander T cell population, that is present in all experiments, does play some role during the clearance of a genital tract infection. Our data suggests however, that these non-antigen specific T cells are not critical for the priming of *Chlamydia* specific T cells (Figure 3-2) and not needed for antigen specific T cells to protect host mice from infection (Figure 3-6). Our studies, characterizing homing to the genital tract, indicate that an antigen specific CD4 population requires both CXCR3 and CCR5 for homing and protection of the genital mucosa.

The distinct chemokine receptor profiles for each mucosal site, such as CCR9 for homing to the intestine or CCR4/10 for homing to the skin, illustrate a coordinated specificity by the host to ensure that activated T cells arrive in the correct tissues efficiently. Understanding the chemokine receptor repertoire required to access distinct mucosal sites may allow for the development of tissue specific therapeutics. With the identification of CCR5 as a major player in genital tract homing however, it is tempting to speculate that co-infection of patients with *C. trachomatis* would also lead to higher rates of HIV infection, where CCR5 is a major receptor for entry into T cells (27, 28). CCR5 has been proposed as a possible drug target to alter HIV infections, but it will be necessary to test these drugs for their impact on other infections of the genital tract to ensure that these HIV therapeutics do not promote other STIs (29).

With additional experimentation it will be possible to determine whether T cells responding to other pathogens of the genital tract depend on the same chemokine receptors we have identified during *C. trachomatis* infection. By characterizing the phenotypes of other STIs, as well as the immune responses that are necessary to properly clear these infections, therapeutics can be designed that not only control infections but also obviate disease pathologies.

Materials and Methods

Mice. C57BL/6, B6.PL-*Thy1*^{a} (CD90.1 congenic), B6.129S7-*IFNγ*^{tm1Agt} (IFNγ$^{-/-}$), C57BL/6, B6.SJL-*Ptprca* Pep3/BoyJ (*CD45*.1 congenic) B6.*Ccr5*$^{-/-}$B6.129P2-Ccr5^{tm1kuz}/J (CCR5-/-) B6.129P2-*Cxcr3*^{tm1Dgen}/J (CXCR3-/-) were purchased from The Jackson Laboratory (Bar Harbor, ME). We constructed *C. trachomatis* specific chemokine receptor deficient mice by breeding NR1 transgenic mice with either CCR5-/- or CXCR3-/- mice. All mice were maintained and cared for within the Harvard Medical School Center for Animal Resources and Comparative Medicine. All experiments were approved by Harvard's Institutional Animal Care and Use Committee.

Growth, isolation and detection of bacteria. *C. trachomatis* serovar L2 (434/Bu) was propagated within McCoy cell monolayers grown in Eagle's MEM (Invitrogen, Grand Island NY) supplemented with 10% FCS, 1.5 g/L sodium bicarbonate, 0.1 M nonessential amino acids, and 1 mM sodium pyruvate. Infected monolayers were disassociated from plates using .05% trypsin/EDTA and sonicated to disrupt the inclusion. EBs were purified by density gradient centrifugation as described(30). Aliquots were stored at -80°C in medium containing 250 mM sucrose, 10 mM sodium phosphate, and 5 mM L-glutamic acid and thawed immediately prior to use.

Flow cytometry. Tissues were mechanically disaggregated and immediately stained for activation markers. Cells were pre-incubated with anti-FcRγ (Bio X-Cell, West Lebanon, NH) before staining with anti-CD4 Pacific Blue (Biolegend, San Diego, CA), anti-CD90.1 peridinin chlorophyll-a protein (BD Bioscience, San Jose, CA), anti-CD90.2 (phycoerythrin or peridinin chlorophyll-a protein), and anti-CD45.2 (allophycocyanin). We used anti-CD45Rb phycoerythrin-cychrome 7 (Biolegend) anti-CD62L allophycocyanin-Alexa 750 (Ebioscience, San Diego, CA) in order to examine the activation levels of antigen specific T cells following

infection. Data were collected on a modified FACSCalibur (Cytek Development, Fremont CA) or an LSRII (BD Bioscience) and analyzed using FlowJo (Tree Star Industries, Ashland OR).

Transfer of Transgenic T cells, infection of mice, and preparation of tissue. Prior to transfer, *C. trachomatis* ($Cta1_{133-152}$)-specific $CD4^+$ T cells(12) were isolated from the peripheral lymphoid tissues of donor NR1 mice. Recipient mice were injected intravenously with either 10^5 or 10^6 cells from the donors. To infect the genital tract, mice were treated with 2.5 mg of medroxyprogestrone acetate subcutaneously and then infected one week later in the uterus with 10^6 IFU of *C. trachomatis* L2(8, 12). Intrauterine infection was done using the NSET device (http://paratechs.com/nset.htm). In short, 5μl of SPG containing 10^6 *C. trachomatis* was deposited using the NSET pipet tip through the NSET speculum. Infection occurs at the base of the uterine horns (including the cervix). Five days following infection, the lymph nodes, spleen, and uterine horns were collected. The uterus was digested with 1 mg/ml of type XI collagenase (Sigma) and 50 Kunitz/ml of DNase (Sigma, St Louis MO) for 45 min at 37 C. Single cell suspensions were prepared for staining via mechanical disaggregation.

Real time PCR. Tissue from two pools of five mice infected in the uterus with 10^6 IFU of *C. trachomatis* L2 (and corresponding tissue from uninfected controls) were harvested and processed as above. Isolated cells were resuspended in TRIzol (Invitrogen) and RNA was isolated using an RNeasy mini kit (Qiagen, Valencia CA). RNA was quantified and diluted to 5 ng/ul for real-time analysis. Primers for chemokine receptors were CCR1-Forward-5'-TCTGGACCCCCTACAATCTG-3', Reverse-5'-GGCAATCACCTCAGTCACCT3' CCR2-Forward-5'ACACCCTGTTTCGCTGTAGG-3', Reverse-5'-CCTGGAAGGTGGTCAAGAAG, CXCR3-Forward-5'GCCCTCACCTGCATAGTTGT-3', Reverse-5'-ATTGAGGCGCTGATCGTAGT-3', CCR5-Forward-5'-CGAAAACACATGGTCAAACG-3', Reverse-5'-GTTCTCCTGTGGATCGGGTA-3', CCR7-Forward-5'-

AACGGGCTGGTGATACTGAC-3', Reverse-5'-TAGGCCCAGAAGGGAAGAAT-3', CCR9-Forward-5'-TGACTCCACTGCTTCCACAG-3', Reverse-5'-GTGCCCACAATGAACACAAG-3', GAPDH-Forward-5'-GGTGCTGAGTATGTCGTGGA-3', Reverse-5'-CGGAGATGATGACCCTTTTG-3'. Real-time PCR was conducted using the Quantitect SYBR Green RT-PCR kit (Qiagen) and run on an ABI prism 7000 sequence detection system (Applied Biosystems). Resulting Ct values were normalized against GAPDH for each sample resulting in a relative expression for each tissue. Fold induction was calculated by dividing relative expression of infected tissue by relative expression of uninfected tissue.

Competitive homing. One million wild-type NR1 cells (CD45.2/CD90.1) were mixed with an equivalent number of wild-type, CCR5-/-, CXCR3-/-, or CCR5-/- CXCR3-/- NR1 cells (CD45.2/CD90.2) and transferred into CD45.1/CD90.2 hosts. Twenty-four hours following transfer, 10^6 IFU of *C. trachomatis* L2 were inoculated into the uterus. Tissues were harvested seven days post-infection and processed as described above.

Skewing of NR1 cells. $CD4^+$ T cells were purified from NR1 mice using a mouse CD4 negative isolation kit (Invitrogen) per the manufacturers directions. The T cells were cultured in RPMI-1640 (Invitrogen) supplemented with 10% FCS, L-glutamine, HEPES, 50 μM 2-mercaptoethanol, 50 U/ml penicillin, and 50 ug/ml streptomycin. To stimulate the T cells, irradiated feeder splenocytes were pulsed with 5 μM of $Cta1_{133-152}$ peptide and cocultured with the CD4-enriched NR1 cells at a stimulator to T cell ratio of 4:1. To polarize T cells towards the Th1 phenotype cells were incubated with 10 ng/ml of IL-12 (Peprotech, Rocky Hill NJ) and 10 μg/ml of anti-IL4 (Biolegend). Cells were stimulated for five days then 10^6 cells were transfered into naïve $CD90.2^+$ host mice. Twenty-four hours following transfer, mice were challenged in the uterus with 10^6 IFU of *C. trachomatis* L2.

Quantitative PCR. To assess the levels of *C. trachomatis* present, we used a previously described qPCR method(31). Briefly we isolated nucleic acid from genital tract homogenates using the QIAamp DNA mini kit from Qiagen. Mouse GAPDH DNA and *Chlamydia* 16S DNA were quantified by qPCR on an ABI Prism 7000 sequence detection system using primer pairs and dual-labeled probes. Using standard curves from known amounts of *Chlamydia* and mouse DNA, we calculated the amount (in picograms) of *Chlamydia* DNA per unit weight (in micrograms) of mouse DNA in the samples.

Statistical analysis. All groups were evaluated for statistical significance through the use of unpaired two-tailed *t* tests. Where it appeared necessary to highlight significant differences between data points, the level of significance is depicted as * = $p<0.05$

References

1. Sigmundsdottir, H., and E. C. Butcher. 2008. Environmental cues, dendritic cells and the programming of tissue-selective lymphocyte trafficking. *Nat Immunol* 9: 981-987.

2. Thelen, M. 2001. Dancing to the tune of chemokines. *Nat Immunol* 2: 129-134.

3. Stenstad, H., A. Ericsson, B. Johansson-Lindbom, M. Svensson, J. Marsal, M. Mack, D. Picarella, D. Soler, G. Marquez, M. Briskin, and W. W. Agace. 2006. Gut-associated lymphoid tissue-primed CD4+ T cells display CCR9-dependent and -independent homing to the small intestine. *Blood* 107: 3447-3454.

4. Fadel, S. A., S. K. Bromley, B. D. Medoff, and A. D. Luster. 2008. CXCR3-deficiency protects influenza-infected CCR5-deficient mice from mortality. *European journal of immunology* 38: 3376-3387.

5. Kohlmeier, J. E., T. Cookenham, S. C. Miller, A. D. Roberts, J. P. Christensen, A. R. Thomsen, and D. L. Woodland. 2009. CXCR3 directs antigen-specific effector CD4+ T cell migration to the lung during parainfluenza virus infection. *J Immunol* 183: 4378-4384.

6. Starnbach, M. N., and N. R. Roan. 2008. Conquering sexually transmitted diseases. *Nature reviews. Immunology* 8: 313-317.

7. Brunham, R. C., and J. Rey-Ladino. 2005. Immunology of Chlamydia infection: implications for a Chlamydia trachomatis vaccine. *Nat Rev Immunol* 5: 149-161.

8. Gondek, D. C., N. R. Roan, and M. N. Starnbach. 2009. T cell responses in the absence of IFN-gamma exacerbate uterine infection with Chlamydia trachomatis. *J Immunol* 183: 1313-1319.

9. Johansson, M., K. Schon, M. Ward, and N. Lycke. 1997. Genital tract infection with Chlamydia trachomatis fails to induce protective immunity in gamma interferon receptor-deficient mice despite a strong local immunoglobulin A response. *Infect Immun* 65: 1032-1044.

10. Perry, L. L., H. Su, K. Feilzer, R. Messer, S. Hughes, W. Whitmire, and H. D. Caldwell. 1999. Differential sensitivity of distinct Chlamydia trachomatis isolates to IFN-gamma-mediated inhibition. *J Immunol* 162: 3541-3548.

11. Rank, R. G., L. S. Soderberg, and A. L. Barron. 1985. Chronic chlamydial genital infection in congenitally athymic nude mice. *Infect Immun* 48: 847-849.

12. Roan, N. R., T. M. Gierahn, D. E. Higgins, and M. N. Starnbach. 2006. Monitoring the T cell response to genital tract infection. *Proceedings of the National Academy of Sciences of the United States of America* 103: 12069-12074.

13. Roan, N. R., and M. N. Starnbach. 2006. Antigen-specific CD8+ T cells respond to Chlamydia trachomatis in the genital mucosa. *J Immunol* 177: 7974-7979.

14. Starnbach, M. N., M. J. Bevan, and M. F. Lampe. 1994. Protective cytotoxic T lymphocytes are induced during murine infection with Chlamydia trachomatis. *J Immunol* 153: 5183-5189.

15. Williams, D. M., B. G. Grubbs, E. Pack, K. Kelly, and R. G. Rank. 1997. Humoral and cellular immunity in secondary infection due to murine Chlamydia trachomatis. *Infect Immun* 65: 2876-2882.

16. Rekart, M. L., and R. C. Brunham. 2008. Epidemiology of chlamydial infection: are we losing ground? *Sex Transm Infect* 84: 87-91.

17. Belay, T., F. O. Eko, G. A. Ananaba, S. Bowers, T. Moore, D. Lyn, and J. U. Igietseme. 2002. Chemokine and chemokine receptor dynamics during genital chlamydial infection. *Infect Immun* 70: 844-850.

18. Sakthivel, S. K., U. P. Singh, S. Singh, D. D. Taub, J. U. Igietseme, and J. W. Lillard, Jr. 2008. CCL5 regulation of mucosal chlamydial immunity and infection. *BMC Microbiol* 8: 136.

19. Shibahara, H., Y. Hirano, Ayustawati, K. Kikuchi, A. Taneichi, H. Fujiwara, S. Takamizawa, and I. Sato. 2003. Chemokine bioactivity of RANTES is elevated in the sera of infertile women with past Chlamydia trachomatis infection. *Am J Reprod Immunol* 49: 169-173.

20. Ficarra, M., J. S. Ibana, C. Poretta, L. Ma, L. Myers, S. N. Taylor, S. Greene, B. Smith, M. Hagensee, D. H. Martin, and A. J. Quayle. 2008. A distinct cellular profile is seen in the human endocervix during Chlamydia trachomatis infection. *Am J Reprod Immunol* 60: 415-425.

21. Barr, E. L., S. Ouburg, J. U. Igietseme, S. A. Morre, E. Okwandu, F. O. Eko, G. Ifere, T. Belay, Q. He, D. Lyn, G. Nwankwo, J. W. Lillard, Jr., C. M. Black, and G. A. Ananaba. 2005. Host inflammatory response and development of complications of Chlamydia trachomatis genital infection in CCR5-deficient mice and subfertile women with the CCR5delta32 gene deletion. *J Microbiol Immunol Infect* 38: 244-254.

22. Bromley, S. K., S. Y. Thomas, and A. D. Luster. 2005. Chemokine receptor CCR7 guides T cell exit from peripheral tissues and entry into afferent lymphatics. *Nat Immunol* 6: 895-901.

23. Chakravarty, S. D., J. Xu, B. Lu, C. Gerard, J. Flynn, and J. Chan. 2007. The chemokine receptor CXCR3 attenuates the control of chronic Mycobacterium tuberculosis infection in BALB/c mice. *J Immunol* 178: 1723-1735.

24. Manicone, A. M., K. M. Burkhart, B. Lu, and J. G. Clark. 2008. CXCR3 ligands contribute to Th1-induced inflammation but not to homing of Th1 cells into the lung. *Exp Lung Res* 34: 391-407.

25. Nakanishi, Y., B. Lu, C. Gerard, and A. Iwasaki. 2009. CD8(+) T lymphocyte mobilization to virus-infected tissue requires CD4(+) T-cell help. *Nature* 462: 510-513.

26. de Lemos, C., J. E. Christensen, A. Nansen, T. Moos, B. Lu, C. Gerard, J. P. Christensen, and A. R. Thomsen. 2005. Opposing effects of CXCR3 and CCR5 deficiency on CD8+ T cell-mediated inflammation in the central nervous system of virus-infected mice. *J Immunol* 175: 1767-1775.

27. Granelli-Piperno, A., B. Moser, M. Pope, D. Chen, Y. Wei, F. Isdell, U. O'Doherty, W. Paxton, R. Koup, S. Mojsov, N. Bhardwaj, I. Clark-Lewis, M. Baggiolini, and R. M. Steinman. 1996. Efficient interaction of HIV-1 with purified dendritic cells via multiple chemokine coreceptors. *J Exp Med* 184: 2433-2438.

28. Patterson, B. K., A. Landay, J. Andersson, C. Brown, H. Behbahani, D. Jiyamapa, Z. Burki, D. Stanislawski, M. A. Czerniewski, and P. Garcia. 1998. Repertoire of chemokine receptor expression in the female genital tract: implications for human immunodeficiency virus transmission. *Am J Pathol* 153: 481-490.

29. Telenti, A. 2009. Safety concerns about CCR5 as an antiviral target. *Curr Opin HIV AIDS* 4: 131-135.

30. Howard, L., N. S. Orenstein, and N. W. King. 1974. Purification on renografin density gradients of Chlamydia trachomatis grown in the yolk sac of eggs. *Appl Microbiol* 27: 102-106.

31. Bernstein-Hanley, I., Z. R. Balsara, W. Ulmer, J. Coers, M. N. Starnbach, and W. F. Dietrich. 2006. Genetic analysis of susceptibility to Chlamydia trachomatis in mouse. *Genes Immun* 7: 122-129.

Chapter 4: Integrin $\alpha 4\beta 1$ is necessary for $CD4^+$ T cell-mediated protection against genital *C. trachomatis* infection.

Attributions: The experiments in this chapter were done in collaboration with Sergio Davila

The data in this chapter has been prepared for submission as a manuscript

Introduction

Chlamydia trachomatis is the most common cause of bacterial sexually transmitted infection in the United States and the leading cause of preventable blindness worldwide(1). *C. trachomatis* is an obligate intracellular pathogen that infects epithelial cells of the genital tract and conjunctiva. In the upper genital tract, complications from *C. trachomatis* infection include pelvic inflammatory disease, ectopic pregnancy and infertility(2, 3). The high frequency of infection, low incidence of acquired immunity and lack of an effective vaccine make *C. trachomatis* a continuing public health concern.

Protection of the genital mucosa from *C. trachomatis* is dependent on the production of IFNγ(4). IFNγ protects through the upregulation of genes such as IDO, NOS and IRGs that interfere with various aspects of the pathogen's developmental cycle and reduce growth(5-8). Transfer of *Chlamydia*-specific $CD4^+$ T cells can protect naïve mice against challenge, and IFNγ production by the $CD4^+$ T cells is required. Mice that are deficient in IFNγ production or depleted of $CD4^+$ T cells have delayed resolution of infection in the genital mucosa(9). Overall it is well-appreciated that antigen-specific, IFNγ-secreting $CD4^+$ T cells must efficiently traffic to the genital mucosa in response to *Chlamydia* infection in order to drive protective immunity(10). Mechanisms suggesting how lymphocytes traffic to the gastrointestinal tract and central nervous system (CNS) have been demonstrated. Lymphocyte recruitment to the gastrointestinal tract is largely mediated by the chemokine receptor CCR9 and the integrin receptor α4β7(11). On the other hand, integrin α4β1 regulates trafficking to the CNS. In these models, interfering with α4β1 and α4β7 profoundly impairs immune cell recruitment to the respective tissues (12, 13). In fact, integrin-specific antibodies are used clinically to block infiltrating immune cells and provide relief from autoimmune diseases such as ulcerative colitis and multiple sclerosis(14)(15).

Unfortunately our understanding of how $CD4^+$ T cells traffic to the genital mucosa has been limited, including what combination of adhesion receptors is required.

In this study, we interrogated the importance of α4β1 and α4β7 integrin heterodimers in promoting *Chlamydia*-specific $CD4^+$ T cell recruitment to the genital mucosa and protecting mice from *C. trachomatis* infection. We show that integrin α4β1 is dramatically increased on the surface of both polyclonal and *Chlamydia*-specific $CD4^+$ T cells in the uterus following infection. We find that blocking or deleting integrin α4β1, but not α4β7, on pathogen-specific $CD4^+$ T cells results in the impairment of trafficking to the uterus and a decrease in the protective capacity of $CD4^+$ T cells. We conclude that integrin α4β1 is necessary for $CD4^+$ T cell-mediated protection against *C. trachomatis*. Identifying the receptors required for $CD4^+$ T cell trafficking to the genital tract in response to *C. trachomatis* is important in designing a vaccine that elicits sterilizing, long lasting immunity against the pathogen while limiting the extent of tissue pathology.

Results

C. trachomatis infection leads to robust integrin α4β1 surface expression on bulk $CD4^+$ T cells in the uterus

Previous studies differ regarding the levels of α4β1 and α4β7 expression on $CD4^+$ T cells in the uterus during *Chlamydia* infection. As a first step to resolve these discrepancies we examined the surface expression of α4, β1, and β7 on $CD4^+$ T cells responding to *Chlamydia* infection in the genital mucosa. Mice were infected transcervically with *C. trachomatis* and 7 days later we isolated the genital mucosa and examined the surface expression of integrins on endogenous polyclonal $CD4^+$ T cells by flow cytometry. We found that the integrins α4 and β1 were upregulated on the surface of $CD4^+$ T cells in the uterus relative to those in the draining (iliac) lymph nodes of infected mice (Figure 4-1A). In contrast, the surface expression of β7 was only modestly increased compared to β1 on $CD4^+$ T cells in the genital mucosa. We next wanted to examine the co-expression of integrins on the surface of $CD4^+$ T cells in the genital tract using flow cytometry. When we gated on either $\alpha4^+\beta1^+$ or $\alpha4^+\beta7^+$ expressing $CD4^+$ T cells in the genital mucosa we noted a higher number of $CD4^+$ T cells expressing $\alpha4^+\beta1^+$. To confirm this difference in the T cell population we quantified the absolute number of $CD4^+$ T cells expressing either $\alpha4^+\beta1^+$ or $\alpha4^+\beta7^+$ in infected or naïve animals 7 days after transcervical *Chlamydia* infection. We found few $CD4^+$ T cells in the uterus during steady state in naïve mice, as previously shown. Following infection with *C. trachomatis*, the absolute number of $\alpha4^+\beta1^+$ $CD4^+$ T cells in the upper genital tract significantly increased unlike the number of $\alpha4^+\beta7^+$ cells (Figure 4-1B). We next compared activation markers between $\alpha4^+\beta1^+$ or $\alpha4^+\beta7^+$ $CD4^+$ T cells responding to the genital mucosa. Interestingly, both the number of activated $\alpha4^+\beta1^+$ and $\alpha4^+\beta7^+$ $CD4^+$ T cells were significantly increased in infected animals relative to naïve controls (Figure 4-1C). Nonetheless, there was a more recruitment of activated $\alpha4^+\beta1^+$ $CD4^+$ T cells to infected uteri compared to $\alpha4^+\beta7^+$ $CD4^+$ T cells. Our results show that while both $\alpha4^+\beta1^+$ and $\alpha4^+\beta7^+$

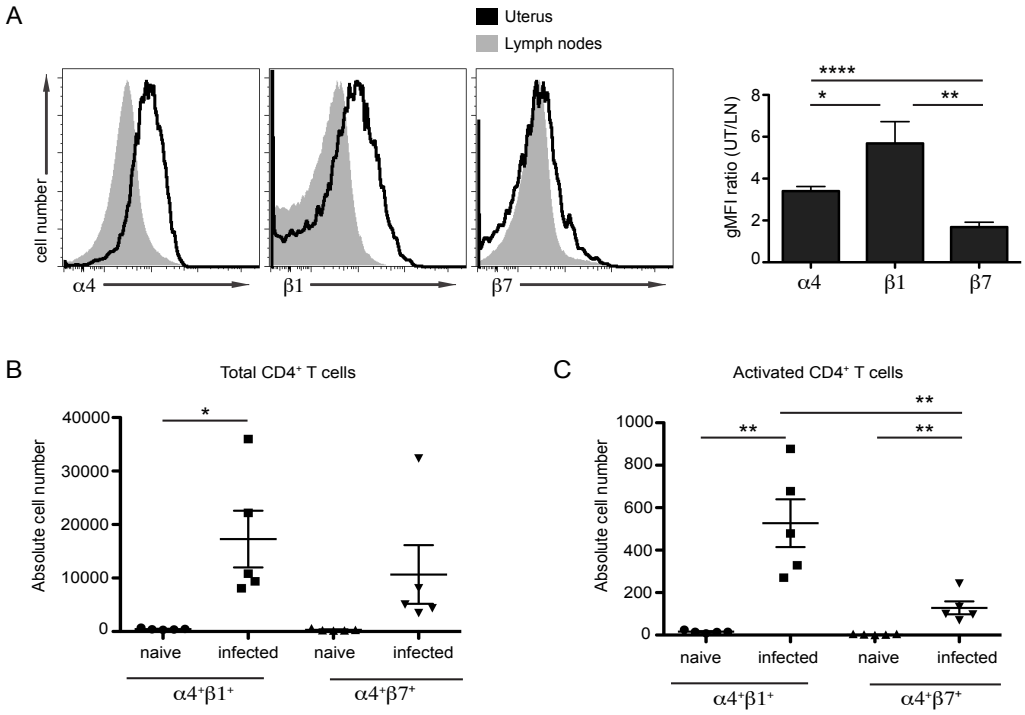

Figure 4-1. *C. trachomatis* infection leads to robust integrin α4β1 surface expression on bulk CD4$^+$ T cells in the uterus. C57BL/6 wild type mice were transcervically infected with 10^6 *C. trachomatis* IFUs. At day 7 after infection the uterus and draining lymph nodes were harvested and prepared for flow cytometry. CD3, CD4, α4, β1 and β7 positive staining as well as the exclusion of Live/Dead cell death stain was used as the gating strategy for the identification of live α4$^+$β1$^+$ and α4$^+$β7$^+$ CD4$^+$ T cells. **(A)** Integrin surface expression was analyzed by comparing the gMFI ratio of the uterine to lymph node localized CD4$^+$ T cells. **(B)** Total numbers of α4$^+$β1$^+$ and α4$^+$β7$^+$ CD4$^+$ T cells were evaluated in the uteri of naïve or infected mice. **(C)** The total number of activated α4$^+$β1$^+$ and α4$^+$β7$^+$ CD4$^+$ T cells was quantified in the uteri of naïve or infected mice; activation was determined by CD44$^+$ staining. Shown are representative results from one of two independent experiments. * $p < 0.05$, ** $p < 0.01$, and **** $p < 0.0001$.

$CD4^+$ T cells are found the infected genital mucosa β1 is more highly expressed. This suggests $\alpha4^+\beta1^+$ is the primary integrin driving $CD4^+$ T cell recruitment to genital mucosa in response to *C. trachomatis* infection.

Infection leads to increased α4β1 surface expression on *C. trachomatis*-specific $CD4^+$ T cells in the uterus

During *Chlamydia* infection, antigen-specific T cells are primed and recruited specifically to the genital tract. However, inflammatory cytokines also activate bystander T cells at the site of infection independently of antigen specificity(16). Previous work characterizing integrin receptors required for T cell recruitment to the genital mucosa used memory $CD4^+$ T cell lines(17), polyclonal $CD4^+$ T cells(18), or bulk $CD4^+$ T cells(19) but never examined naïve *C. trachomatis*-specific $CD4^+$ T cells. It is only possible to model primary infection using naïve antigen-specific T cells. To focus on the integrin profile of only the *Chlamydia*-specific $CD4^+$ T cell population, we took advantage of *C. trachomatis* specific TCR transgenic $CD4^+$ T cells that are locked into specificity for the *Chlamydia* antigen Cta1 (referred to subsequently as NR1 cells)(20). Based on the results from Figure 4-1, we hypothesized that NR1 cells would display significantly increased surface β1, rather than β7, upon trafficking to infected uteri. To test this, we transferred 10^6 NR1 cells intravenously into congenic naïve animals that were then infected transcervically the following day with *C. trachomatis*. As we observed using polyclonal $CD4^+$ T cells, at 8 days following infection there was over 10-fold increased surface expression of integrin β1 on NR1 cells in the uterus compared to NR1 cells in the draining lymph nodes (Figure 4-2A). The surface expression of integrins in the genital tract and iliac lymph nodes of *C. trachomatis* infected mice was examined at three time points following infection to understand the dynamics of integrin expression. NR1 cells were examined at 3, 8, and 13 days following infection to coincide with T cell activation, peak of infiltration, and contraction, respectively (Figure 4-2B and C). There was a surge of both $\alpha4^+\beta1^+$ and $\alpha4^+\beta7^+$ NR1 cells in infected

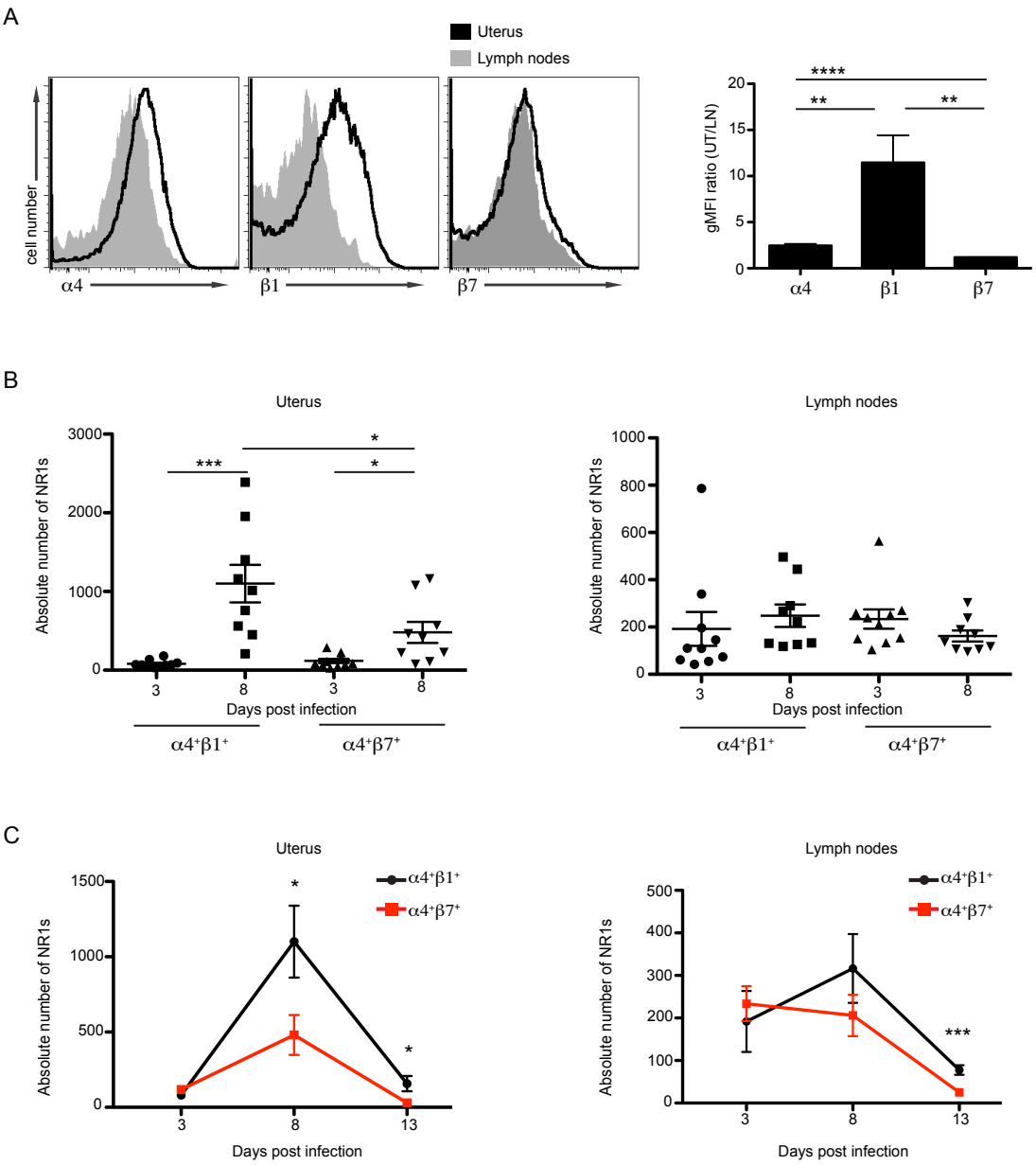

Figure 4-2. Infection leads to robust α4β1 surface expression on *C. trachomatis*-specific CD4$^+$ T cells in the uterus. 10^6 CD90.1$^+$ NR1 cells were transferred to CD90.2$^+$ recipient mice. The following day mice were transcervically infected with 10^6 *C. trachomatis* IFUs. The uterus and draining lymph nodes were harvested at different time points after infection and prepared for flow cytometry. Vα2 (transgenic TCR), CD4, CD90.1 and integrin positive staining as well as the exclusion of Live/Dead cell death stain was used as the gating strategy for the identification of live α4$^+$β1$^+$ and α4$^+$β7$^+$ NR1 cells. **(A)** Integrin surface expression was analyzed by comparing the gMFI ratio of the uterine to lymph node localized NR1 cells at 8 days post infection. **(B)** The total number of α4$^+$β1$^+$ and α4$^+$β7$^+$ NR1 cells was evaluated and compared at 3 and 8 days after infection in the uterus (left) and draining lymph nodes (right). **(C)** NR1 cell trafficking kinetics in the uterus (left) and draining lymph nodes (right) is depicted at 3, 8, and 13 days after infection. Shown are representative results from one of three independent experiments. * $p < 0.05$, ** $p < 0.01$, *** $p < 0.001$, and **** $p < 0.0001$.

uteri 8 days after infection compared to what was observed with these populations 3 days after infection (Figure 4-2B). Even though both NR1 populations increased during infection, the magnitude of infiltration of the $\alpha4^+\beta1^+$ NR1 cells to the uterus was far more robust (***$p<0.001$) than the $\alpha4^+\beta7^+$ population (*$p<0.05$) (Figure 4-2B, left). Surface integrin profiles on NR1 cells in the draining lymph node were found to have no statistical differences in integrin expression between these two time points (Figure 4-2B, right). Thirteen days after infection, the decline of NR1 cells (Figure 4-2C) corresponded to resolution of *C. trachomatis* infection in the genital mucosa(21). Even at this late time point, $\alpha4^+\beta1^+$ NR1 cells were found significantly more frequently than $\alpha4^+\beta7^+$ NR1 cells in the genital tract. This suggests that NR1 cells expressing $\alpha4^+\beta1^+$ are either recruited or retained in the uterus for a longer period of time than other T cell populations. Together these findings demonstrate that $CD4^+$ T cells preferentially express α4 and β1 on their surface in the genital mucosa in response to *C. trachomatis* infection.

Blocking integrin α4 but not α4β7 on Chlamydia-specific CD4+ T cells leads to an increase in *C. trachomatis* burden in genital mucosa

Since we identified a strong upregulation of α4β1 on the surface of T cells responding to *Chlamydia* infection, we next wanted to assess the functional role of β1 and β7 in promoting protective immunity. We have previously shown that transfer of *in vitro*-activated Th1-skewed NR1 cells into naïve mice confers significant protection from *Chlamydia* infection compared to mice that receive no T cells(10). We hypothesized that if specific integrins are required for recruitment to the genital mucosa, blocking these integrins on activated NR1 cells may alter their protective capacity. To test this and determine the relative contributions of β1 and β7 to $CD4^+$ T cell-mediated protection, we selectively blocked integrin receptors following infection using antibodies (Figure 4-3). NR1 cells from naïve mice were harvested and polarized *in vitro* to a Th1 phenotype. IFN-γ production by the cells was assayed to confirm their Th1 phenotype by flow cytometry prior to transfer (data not shown). One million NR1 Th1 cells were pre-treated

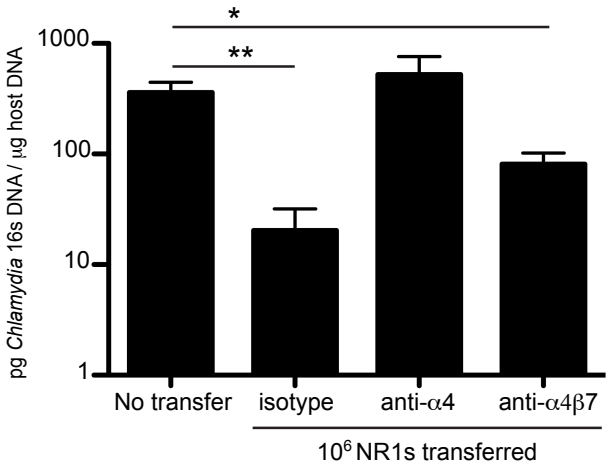

Figure 4-3. Blocking α4 but not α4β7 abolishes the protective capacity of *Chlamydia*-specific CD4+ T cells following *C. trachomatis* infection. To confer protection, NR1 cells were skewed *in vitro* to a Th1 phenotype for 5 days using cta1 peptide and irradiated splenocytes. 10^6 CD90.1$^+$ NR1 cells were transferred to CD90.2$^+$ recipients and the following day mice were transcervically infected with $5x10^6$ *C. trachomatis* IFUs. Groups were injected i.p. with the respective antibody at 1 and 3 days post infection. Genomic DNA was isolated from the uterus at 5 days after infection. Burden was determined by calculating the levels of *Chlamydia* 16S DNA relative to the levels of host GADPH using qPCR. Shown are representative results from one of two independent experiments. * $p < 0.05$, and ** $p < 0.01$.

with antibody that blocked α4 (blocks both α4β1 and α4β7), α4β7, or an isotype control and transferred intravenously into host mice that were transcervically infected with *C. trachomatis* the following day. To ensure robust blockade of integrins on NR1 cells each group of mice were also treated with antibody 1 and 3 days following infection. Five days after infection *C. trachomatis* burden in the uterus was measured using quantitative PCR (qPCR). Mice that were treated with blocking antibody against α4 had significantly higher *C. trachomatis* burden in the genital tract than isotype control treated animals, burdens similar to that found in mice that received no NR1 cells at all. On the other hand, mice treated with α4β7 blocking antibody showed lower levels of *C. trachomatis* in the genital mucosa similar to the isotype antibody treated mice. Despite the lack of an antibody that specifically blocks α4β1, we can infer the importance of α4β1 indirectly. Because blocking α4 with antibody prevents both α4β1 and α4β7 signaling, the differences observed in protection between α4 and α4β7 antibody treatment groups point towards a function of α4β1. Since the integrin α4 chain dimerizes with either β1or β7(22), the results shown in Figure 3 indirectly confirm that α4β1 is required for $CD4^+$ T cell mediated protection against *C. trachomatis* in the genital mucosa.

A reduction in $CD4^+$ T cells is responsible for the higher *C. trachomatis* burden in anti-α4 antibody-treated mice

Even though we found that blocking α4 was sufficient to prevent $CD4^+$ T cell mediated protection in the genital mucosa, we had not determined the mechanisms responsible for higher burden. We predicted that the loss of protection seen in mice treated with α4-blocking antibody was due to diminished recruitment of NR1 cells to the infected uterus. To test this possibility, we repeated the antibody blocking experiments and monitored the trafficking of NR1 cells to genital tract during infection using flow cytometry. NR1 cells were skewed to the Th1 phenotype *in vitro*, and then transferred into congenically mismatched host mice. The next day mice were infected transcervically with *C. trachomatis*. Prior to transfer, NR1 cells were pretreated with individual

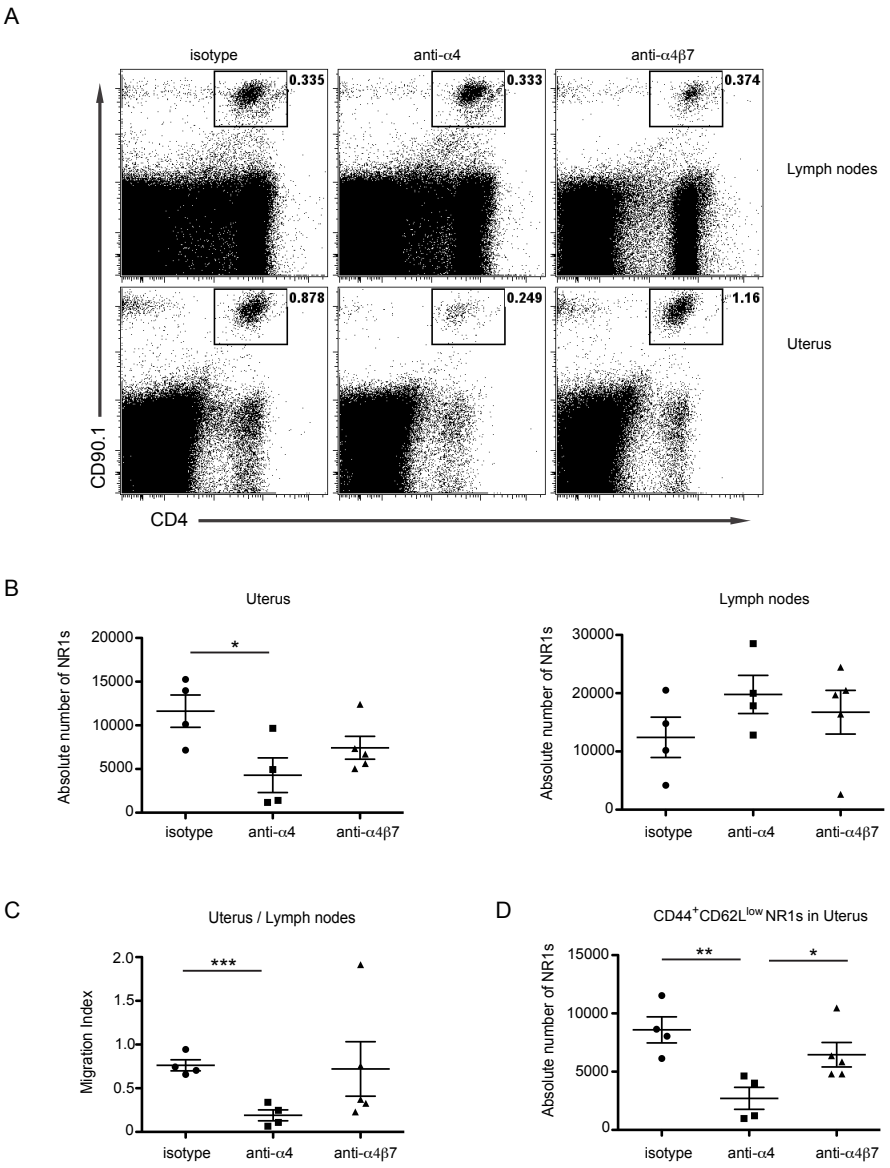

Figure 4-4. *C. trachomatis*-specific CD4$^+$ T cell trafficking to the genital tract is impaired in α4 but not α4β7 antibody treated mice following infection. To confer protection, NR1 cells were skewed *in vitro* to a Th1 phenotype for 5 days using cta1 peptide and irradiated splenocytes. 10^6 CD90.1$^+$ NR1 cells were transferred to CD90.2$^+$ recipients and the following day mice were transcervically infected with $5x10^6$ *C. trachomatis* IFUs. Groups were injected i.p. with the respective antibody at 1 and 3 days post infection. The uterus and draining lymph nodes were harvested at 5 days after infection and prepared for flow cytometry. Vα2, CD4, and CD90.1 positive staining as well as the exclusion of Live/Dead cell death stain was used as the gating strategy for the identification of live NR1 cells. **(A)** The percentages of NR1 cells are shown in the draining lymph nodes (top) and uterus (bottom). **(B)** Absolute numbers were quantified in the uterus (left) and draining lymph nodes (right). **(C)** The migration index was calculated by comparing the absolute number of NR1 cells in the uterus relative to the draining lymph nodes within the same animal. A higher ratio indicated more NR1 cells in the uterus. **(D)** The absolute numbers of effector NR1 cells was determined by examining the CD44$^+$CD62L^{low} gated population. Shown are representative results from one of two independent experiments. * $p < 0.05$, ** $p < 0.01$, and *** $p < 0.001$

integrin blocking antibodies or an isotype control. Mice were also treated with the same blocking antibody or isotype control 1 and 3 days after infection. Five days after infection, we examined the number of NR1 cells present in the uterus and draining lymph nodes by flow cytometry. We noted that the number of NR1 cells in the genital mucosa was significantly diminished following treatment with the α4 blocking antibody relative to the isotype treated mice (Figure 4-4A and B). In contrast, α4β7 antibody treatment did not impact NR1 cell recruitment to the genital tract as absolute numbers were similar between isotype and α4β7-treated groups. The absolute numbers of NR1 cells present in the iliac lymph nodes were not significantly different between the groups suggesting no general defect in trafficking of NR1 cells following α4β7 antibody treatment. We also calculated a migration index (the ratio of live NR1 cells in the uteri to iliac lymph nodes within the same animal) to normalize for mouse-to-mouse variability. We found that the migration index was profoundly decreased in mice treated with α4 blocking antibody compared to isotype treated mice (Figure 4-4C). These results show that blocking α4 prevents efficient $CD4^+$ T cell trafficking to the genital tract following *C. trachomatis* infection. Since the migration index of mice treated with α4β7 antibody was no different from isotype control treated mice it suggests α4β7 plays a limited role in NR1 cell trafficking to the genital mucosa.

We then assessed what population of $CD4^+$ T cells was being afflicted after antibody treatment and thus unable to protect the uteri against *C. trachomatis* infection. NR1 cells were stained for CD44 and CD62L in order to evaluate the presence of effector $CD4^+$ T cells at the site of the infection. The absolute number of $CD44^+$CD62Llow NR1 cells in the uterus was significantly decreased only in the α4 antibody-treated group compared to isotype-treated mice (Figure 4-4D). Moreover, α4β7 antibody treatment did not decrease the absolute number of effector NR1 cells in the uteri. The results shown in Figure 4 allowed us to conclude that the lack of $CD4^+$ T cell trafficking to the genital tract following α4 blockade is primarily due to the inhibition of α4β1. These observations demonstrate that disrupting the integrin α4β1 on NR1 cells during *C. trachomatis* infection is sufficient to eliminate $CD4^+$ T cell-mediated protection.

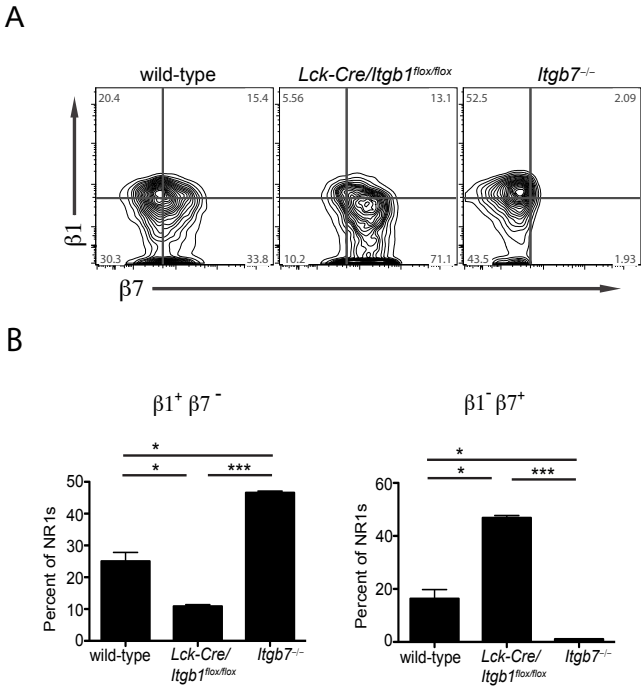

Figure 4-5. CD4$^+$ T cells from *C. trachomatis*-specific integrin deficient mice show altered integrin surface expression. Integrin sufficient or deficient NR1 cells were skewed *in vitro* to a Th1 phenotype for 5 days using cta1 peptide and irradiated splenocytes. **(A)** After stimulation, live NR1 cell were gated to show the percentage of $\beta1^+\beta7^-$ and $\beta1^-\beta7^+$ populations within each group. **(B)** The quantification of $\alpha4^+\beta1^+\beta7^-$ or $\alpha4^+\beta1^-\beta7^+$ NR1 cells is shown as percentage of total NR1 cells. Shown are representative results from one of two independent experiments. * $p < 0.05$ and *** $p < 0.001$.

Integrin β1-deficient *C. trachomatis*-specific CD4$^+$ T cells are unable to protect the uterus

To complement the antibody-blocking experiments showing that α4β1 is required for *Chlamydia*-specific CD4$^+$ T cells to home to and protect the genital mucosa, we generated TCR transgenic mice in which the T cells are deficient in either integrin β1 or β7. Because loss of β1 results in embryonic lethality, we used a CRE-Flox system to generate NR1 cells conditionally deficient in β1. NR1 transgenic mice were crossed to Lck-CRE and Itgb1flox/flox animals such that only the lymphocytes were deficient in β1. We also crossed NR1 transgenic mice with Itgb7-/- mice to generate *Chlamydia*-specific CD4$^+$ T cells deficient in β7. We first confirmed that integrin surface expression was significantly altered for each knockout T cell genotype (Figure 4-5A and B). Interestingly, loss of β1 led to a concomitant increase of surface β7 on NR1 cells similar to a previous report showing that α4β7 heterodimers form more readily in the absence of the β1 chain(23). The loss of β7 also led to an increase of the percentage of β1$^+$ NR1 cells after in vitro activation. We next confirmed that NR1 cells deficient in individual integrins were normally activated. Integrin-deficient NR1 cells were harvested from the knockout mice and polarized in vitro for 5 days to a Th1 phenotype. We found no significant difference between groups in the total number of recovered NR1 cells 5 days following activation, demonstrating that all the genotypes are viable (data not shown). We next examined the activation and cytokine production for each group. For all genotypes examined, NR1 cells were robustly activated as determined by staining for the activation markers CD25 and CD44 (Figure 4-6A). When we assayed the cytokine profiles of each NR1 genotype using intracellular cytokine staining we found similar levels of the cytokines IFN-γ and TNF-α from all groups, suggesting that loss of integrin β chains does not negatively impact Th1 differentiation (Figure 4-6B). Therefore the absence of either β1 or β7 does not interfere with activation, expansion, and Th1 cytokine production of NR1 cells *in vitro*.

Upon showing that the various genotypes of NR1 cells had normal effector phenotypes, we asked whether deficiency in either the β1 or β7 chain would adversely affect the protective

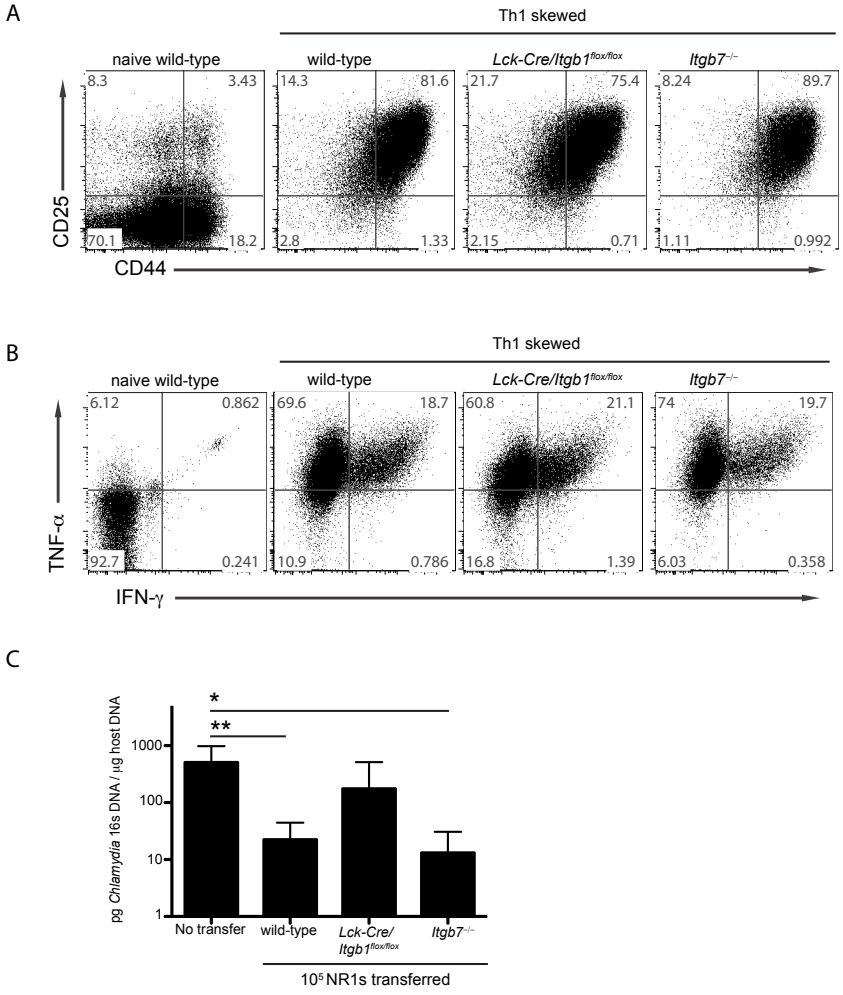

Figure 4-6. *C. trachomatis*-specific CD4$^+$ T cells deficient in integrin β1 are unable to protect the genital tract following infection. To provide protection, integrin sufficient or deficient NR1 cells were skewed *in vitro* to a Th1 phenotype for 5 days using cta1 peptide and irradiated splenocytes. (A) The activation status of live NR1 cells was assessed by gating for the CD25$^+$CD44$^+$ population. (B) Th1 cytokine production was measure by intracellular cytokine staining for TNF-α and IFN-g. After 5 days of stimulation, 10^5 CD90.2 NR1 cells were transferred to CD90.1 recipients. The following day, mice were transcervically infected with $5x10^6$ *C. trachomatis* IFUs. Genomic DNA was isolated from the uterus at 5 days after infection. (C) Burden was determined by calculating the levels of *Chlamydia* 16S DNA relative to the levels of host GADPH using qPCR. Shown are representative results from one of three independent experiments. * $p < 0.05$ and ** $p < 0.01$.

capacity of *Chlamydia*-specific CD4$^+$ T cells. Based on our previous results from antibody blocking experiments, we hypothesized that β1-deficient NR1 cells would be unable to protect the genital mucosa from *C. trachomatis* infection. To test this prediction, we transferred 105 wildtype, β 1-/- or β 7-/- Th1-skewed NR1 cells into naïve mice 1 day prior to transcervical infection with *C. trachomatis* (Figure 4-6C). Five days after infection we harvested the uteri and quantified the levels of *C. trachomatis* using qPCR. As expected, mice that received wildtype NR1 cells showed a dramatic reduction in *Chlamydia* burden compared to mice that received no transfer. Mice that received β1-deficient NR1 cells were not protected against *Chlamydia* infection and had burdens similar to mice receiving no transferred T cells. In line with our previous findings using antibody blockade, we found that mice receiving β 7-/- NR1 cells were significantly protected against *C. trachomatis* infection relative to mice that received no transfer, and trended toward being more protective than even wild-type NR1 cells. These findings definitively show that integrin β7 on NR1 cells is dispensable for protecting the uterus from *Chlamydia* infection. In summary, integrin β1, but not β7, is necessary for *Chlamydia*-specific CD4$^+$ T cells to protect against infection in the genital mucosa.

Integrin β1 deficiency impairs *C. trachomatis*-specific CD4$^+$ T cell homing to the uterus

We next sought to understand the mechanisms responsible for the loss of protective capacity in β1-/- *Chlamydia*-specific CD4$^+$ T cells. Our previous data using antibody blocking showed that T cell trafficking to the genital mucosa was inhibited and therefore provided little protection. We used a competitive homing assay to test the trafficking potential of integrin-deficient *Chlamydia*-specific CD4$^+$ T cells. Here we directly compared the migration of integrin-sufficient and deficient NR1 cells under identical conditions within the same infected host. We transferred an equal ratio of CD45.2/CD90.2 β1-/-, β7-/- or wildtype NR1 cells and CD45.2/CD90.1 wildtype NR1 cells into congenically mismatched CD45.1 recipients. The next day we infected the mice transcervically with *C. trachomatis*. Seven days after infection, we

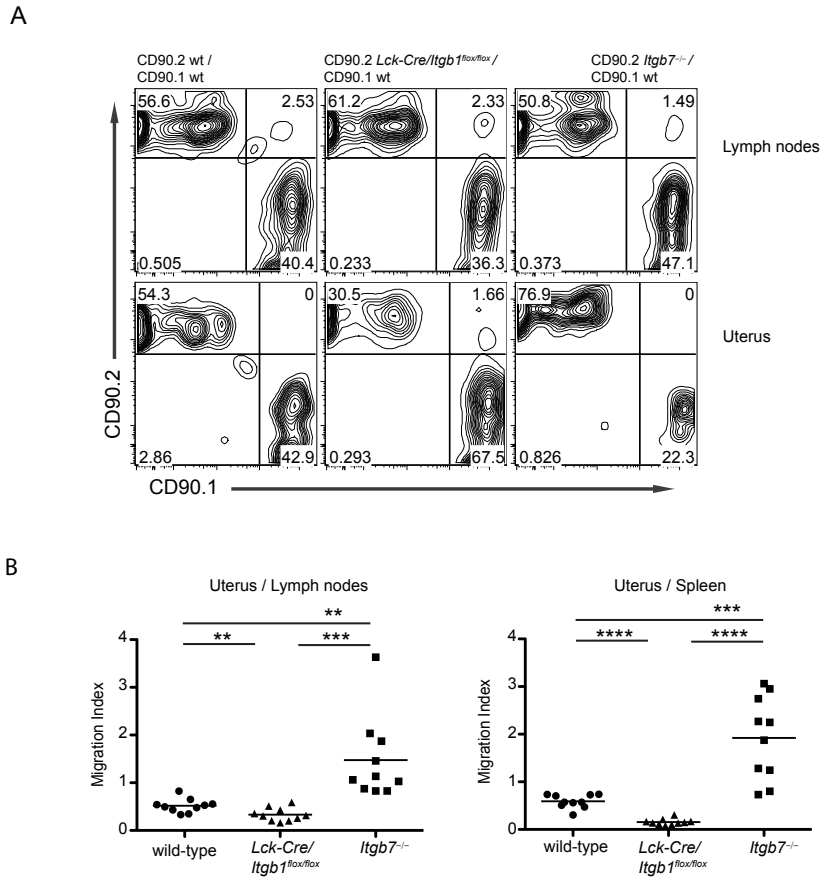

Figure 4-7. *C. trachomatis*-specific CD4$^+$ T cells deficient in β1 are unable to traffic efficiently to the genital mucosa. An equivalent number of CD45.2/CD90.1 integrin wt and CD45.2/CD90.2 wt, β1 deficient, or β7 deficient NR1 cells were transferred to CD45.1/CD90.2 recipient mice. The next day, mice were transcervically infected with *C. trachomatis*. The uterus, draining lymph nodes and spleen was harvested at 7 days post infection and analyzed by flow cytometry. Live NR1 cells were identified by gating for the Live/Dead negative population that was positive for CD45.2, va2 and CD4 staining. Trafficking competition within the host was determined by gating for CD90.1$^+$ or CD90.2$^+$ NR1 cells. (A) Shown are representative plots of integrin wt and deficient NR1 cells in the draining lymph nodes (top) and uterus (bottom). (B) The migration index within each group was calculated by comparing the percentage of CD90.2$^+$ to CD90.1$^+$ NR1 cells in the uterus to the same ratio in the lymph nodes (left) or spleen (right). Shown are representative results from one of three independent experiments. ** $p < 0.01$, *** $p < 0.001$, and **** $p < 0.0001$.

isolated and processed tissues to quantify the numbers of both NR1 populations using flow cytometry. We found that β1-/- NR1 cells were far less efficient than wildtype NR1 cells in trafficking to the genital mucosa, while β7-/- NR1 cells outcompeted their wildtype counterparts (Figure 4-7A). None of the experimental groups showed defects in their migration to the iliac lymph node. Interestingly, we noted a higher percentage of β1-deficient NR1 cells in the lymph nodes compared to the wildtype NR1 cells, inverse of what we observed in the genital mucosa. These results are likely due to a decreased ability of β1-/- NR1 cells to leave the circulation to enter the infected uterine mucosa. To normalize for mouse-to-mouse variation in absolute T cell numbers, we calculated a migration index for each mouse by comparing the ratio of the two transferred NR1 populations in the uterus (integrin deficient CD90.2% : integrin sufficient CD90.1%) to the ratio of the transferred populations in the draining lymph nodes or spleen within the same animal (Figure 4-7B). A smaller the migration index indicated less efficient trafficking of integrin-deficient NR1 cells specifically to the site of infection relative to the circulation. We found a dramatically lower migration index for β1-/- NR1 cells demonstrating that trafficking to the uterus during infection was significantly impaired relative to wildtype NR1 cells. Intriguingly, the migration index for β7-/- NR1 cells was significantly higher than wildtype, demonstrating enhanced homing of *Chlamydia*-specific $CD4^+$ T cells to the uterus in the absence of integrin β7. These results suggest that integrin β7 is not only dispensable, but that deficiency of β7 enhances antigen-specific $CD4^+$ T cell migration to the genital tract during *C. trachomatis* infection. Together our findings reveal that integrin β1 plays a crucial in trafficking of $CD4^+$ T cells to the genital mucosa and that absence of β1 negatively affects the protective capacity of *C. trachomatis*-specific $CD4^+$ T cells.

Discussion

The orchestration of events required for a successful T cell response determines whether an intracellular pathogen will be eliminated from the host. In the case of *C. trachomatis* infection, a robust $CD4^+$ Th1 cell response that homes to the genital tract provides the vigorous IFN-γ response necessary for bacterial clearance(10). The integrin receptors important for *C. trachomatis*-specific $CD4^+$ T cell-mediated protection had not been previously described. Using *C. trachomatis*-specific $CD4^+$ T cells, we demonstrated that perturbing integrin α4β1 but not α4β7, through antibody blockade or genetic deletion, results in a loss of protective capacity and increased bacterial burden in the genital tract. We attributed the impaired protection to the decreased trafficking of antigen-specific $CD4^+$ T cell to the genital mucosa. Together these observations demonstrate that integrin α4β1 is necessary for $CD4^+$ T cell-mediated protection against *C. trachomatis* infection in the murine genital tract.

We previously demonstrated that the chemokine receptors CXCR3 and CCR5 are required for *Chlamydia*-specific $CD4^+$ T cells to home to and protect the genital mucosa following infection with *C. trachomatis* (24). Here we extended these studies to identify integrin receptors that are important for $CD4^+$ T cell mediated protection. Previous studies demonstrated that surface β1 is upregulated on lymphocytes localized in the genital tract but not in the intestinal mucosa following vaginal infection with the mouse-adapted species *Chlamydia* muridarum (19). In contrast, separate studies observed an enrichment of surface β7 on a transferred $CD4^+$ T cell line in the genital tract following C. muridarum infection(17). However, these studies were unable to assess the functional consequences of perturbing integrin signaling on $CD4^+$ T cells, such as loss of protective capacity. These studies also made use of bulk or memory $CD4^+$ T cell lines that are unable to recapitulate the initial activation events as naïve antigen-specific T cells recognize *C. trachomatis* during primary infection.

When we examined the surface expression of β1 and β7 on both bulk and antigen-specific $CD4^+$ T cells, we found that relative β1 expression was dramatically increased on the

majority of $CD4^+$ T cells found in the uterus following *Chlamydia* infection (Figure 4-1A and 4-2A). However, we consistently did note a smaller population of $CD4^+$ T cells expressing intermediate levels of surface β7 in the genital mucosa (Figure 4-1B and 4-2B). The presence of two populations with distinct integrin profiles is consistent with previous reports that showed the surface expression of α4β1 and α4β7 on $CD4^+$ T cells in the genital tract. When examining bulk lymphocytes, Perry et al observed that β1 surface expression was significantly increased in the genital tract 14 days after infection. Although most $CD4^+$ T cells were expressing high levels of surface integrin β1, this group also noted a minor percentage of $\beta7^+$ $CD4^+$ T cells in the genital tract(19). Separate reports suggested that α4β7 was the dominant integrin receptor expressed on $CD4^+$ T cells in the genital tract. However these studies had significant experimental constraints that limit their interpretation. For example, Kelly et al did not interrogate the integrin profile during the primary response or differentiate between antigen-specific and bystander $CD4^+$ T cells in the genital tract(25). Another report examined the surface integrin receptors on a memory $CD4^+$ T cell line in culture following stimulation but did not assess in vivo integrin dynamics. In addition, $CD4^+$ T cells in this study were analyzed only 18 hours after adoptive transfer(17). Memory $CD4^+$ T cells can exert effector activities with greater ease than primary T cells(26), therefore examining memory cells is not indicative of the trafficking properties T cells in a primary response. More importantly, these studies did not perturb integrins on *C. trachomatis*-specific $CD4^+$ T cells to establish their necessity for protection.

The results presented here show that α4β1-expressing $CD4^+$ T cells mediate protective immunity in the genital mucosa. Even so, we did identify a second $\beta7^+$ population that did not alter immunity in the genital mucosa. The existence of two NR1 cell populations with distinct integrin profiles and identical TCR specificity shows that integrin levels are not hardwired into cells but rather imprinted during T cell activation as has been suggested previously(27). Our results also suggest that only $CD4^+$ T cells with the correct integrin profile can extravasate into the infected genital mucosa. We speculate that while α4β1-expressing T cells can enter the

infected tissue efficiently, the α4β7^{+} CD4^{+} T cells remain in the circulation, failing to provide protection in the genital mucosa, but perhaps contributing to immunity elsewhere in the mouse. Because the entire uterus, including its associated vasculature, was harvested in all experiments it was not possible to distinguish between those T cells present in blood vessels and those that had completed transendothelial migration. Interestingly, one recent report uncovered a mechanism that drives distinct integrin expressing T cell populations in the lungs of mice. Ruane et al found that a subset of residing dendritic cells (DCs) can imprint lung T cells to express α4β7 instead of α4β1. The T cells expressing α4β7 do not mediate protection in the lungs but rather provide systemic mucosal immunity(28). Given that a subset of lung DCs can imprint a population of α4β7 on T cells, we speculate a similar process occurs also occurs in the genital tract. While the majority of CD4^{+} T cells are primed to express α4β1, which mediates immunity in the genital mucosa during *C. trachomatis* infection, perhaps a subset of uterine DCs also imprints α4β7 CD4^{+} T cell population that may provide systemic mucosal immunity. This hypothesis will need to be examined in future experiments.

It is well established that integrin α4β1 adheres to the addressin VCAM-1 and the extracellular matrix protein fibronectin. Surface VCAM-1 increases on endothelial cells lining microvessels following inflammation(22). For example, patients with CNS autoimmune disorders are often treated with natalizumab, an α4 antibody that blocks α4β1 interaction with its ligands. Natalizumab treatment decreases undesirable inflammation in the CNS by interfering with α4β1 mediated immune cell recruitment to this sensitized area in the body(29). Previous studies have also shown that surface VCAM-1 becomes abundant on murine and human genital mucosa following *Chlamydia* infection. In contrast, the expression of the mucosal addressin cell adhesion molecule-1 (MAdCAM-1), the binding partner for α4β7, has been reported to be expressed robustly in the gut but only modestly in the genital tract(19, 30). The noticeable increase of surface VCAM-1 in the genital mucosa following *C. trachomatis* infection

corresponds to the upregulation of surface α4β1 on *Chlamydia*-specific $CD4^+$ T cells in the uterus observed in this study.

Several other signals stimulate the rapid increase of VCAM-1 on vaginal epithelial cells including IFNγ treatment and herpes simplex virus infection(31). Given that VCAM-1 expression can be selectively upregulated on both endothelial and non-endothelial cells, $CD4^+$ T cells may require α4β1 signaling for multiple steps in protection. Previous studies have characterized the importance of α4β1 to slow/arrest lymphocytes in the blood vessel, but additionally α4β1 may mediate the interactions between effector $CD4^+$ T cells and infected epithelial cells as has been suggested to occur during *Chlamydia* infection (32). It remains unknown whether *C. trachomatis*-specific $CD4^+$ T cells directly interact with infected epithelial cells in the genital mucosa or if their antimicrobial effects occur by altering the cytokine milieu at the site of infection. Here we observed that integrin β1 and β7 were dispensable for proliferation and differentiation to a Th1 phenotype, as IFNγ production and recovery of live NR1 cells was similar between wildtype and knockout cells (Figure 4-6A and B). Consequently, we conclude that the function of β1 in mediating protection is to allow successful *Chlamydia*-specific $CD4^+$ T cell trafficking to the uterus rather than playing a role in activation or production of IFNγ. Future studies must further explore the interaction between IFNγ-producing $CD4^+$ T cells and the infected epithelium to determine whether β1 is required for cellular interactions in vivo at the genital mucosa.

Our group previously identified the chemokine receptors important for antigen-specific $CD4^+$ T cells to home to and protect the uterus following *C. trachomatis* infection(24). The results obtained through this study further elucidate the essential trafficking receptors required for an effective $CD4^+$ T cell defense in the genital mucosa. It remains to be determined whether $CD4^+$ T cells responding to other pathogens in the genital tract also require the same adhesion receptors we have identified (CXCR3, CCR5 and α4β1) for successful trafficking. Generating a robust and long-lived protective T cell response is crucial to clear infection and avoid recurrent

cycles of inflammation and associated pathology. Vaccine efforts against intracellular pathogens should examine whether the appropriate T cell population, with the necessary homing molecules, is being generated to ensure protection and minimize pathology. In addition to the current treatments for autoimmune diseases in the gut and the CNS, integrin and chemokine receptor targeted therapies could be used to selectively shape the recruitment of desired T cells to other mucosal tissues.

Materials and Methods

Mice

C57BL/6, B6.PL-Thy1a (CD90.1 congenic), C57BL/6, B6.SJL-Ptprca Pep3/BoyJ (CD45.1 congenic), B6.Cg-Tg548Jxm/J (Lck-CRE), C57BL/6-Itgb7tm1Cgn/J (Itgb7-/-), and B6;129-Itgb1tm1Efu/J (Itgb1flox/flox) mice were purchased from the Jackson Laboratory (Bar Harbor, ME) and NR1 mice were previously described(33). *C. trachomatis*-specific integrin-deficient mice were generated by breeding NR1 mice to either Lck-CRE and Itgb1flox/flox or Itgb7-/- mice. All mice were maintained in facilities managed by the Harvard Medical School Center for Animal Resources and Comparative Medicine. To normalize for the murine estrous cycle, mice were treated subcutaneously with 2.5 mg of medroxyprogesterone 7 days prior to infection. Harvard's Institutional Animal Care and Use Committee approved all the experiments described. A minimum of 4 mice per group was used in each experiment.

Growth, isolation and detection of *C. trachomatis*

C. trachomatis serovar L2 (434/Bu) was propagated using McCoy cell monolayers grown in Eagle's MEM (Invitrogen, Grand Island, NY) plus 10% FCS, 1.5 g/l sodium bicarbonate, 0.1 M nonessential amino acids, and 1 mM sodium pyruvate. Infected McCoy cells were detached from plates using sterile glass beads and then sonicated to disrupt *C. trachomatis* inclusions. Density gradient centrifugation was used to purify elementary bodies(24). Aliquots were stored at -80˚C in a medium containing 250 mM sucrose, 10 mM sodium phosphate, and 5 mM L-glutamic acid.

Transfer of NR1 cells, infection of mice, and tissue preparation

C. trachomatis-specific $CD4^+$ T cells were isolated from the lymph nodes and spleens of naïve donor NR1 mice. Recipient mice received 10^6 NR1 cells and were infected the following day with 10^6 *C. trachomatis* inclusion forming units (IFU) in 10 ml of sucrose-phosphate-glutamate media. We used the NSET device (ParaTechs) to bypass the cervix and directly infect the uterine horns(34). The uterus was harvested and disaggregated by digestion with 1 mg/ml of

type XI collagenase (Sigma, St. Louis, MO) and 50 Kunitz/ml of DNase (Sigma) for 30 min at 37˚C. Single cell suspensions from tissues were obtained by mechanical disaggregation prior to staining. Suspensions of splenocytes were treated with a hypotonic buffer to lyse red blood cells prior to use.

Flow cytometry

Single cell suspensions were stained immediately for activation markers or stimulated for 5 hours with 100 ng/ml PMA (Alexis Biochemical) and 1 mg/ml ionomycin (Calbiochem) in brefeldin A (BD Biosciences) for intracellular cytokine staining. Cells were treated with anti-FcgR (BioXCell) before staining with combinations of the following antibodies: anti-b1 Pacific Blue, anti-b7 FITC, anti-TCRva2 allophycocyanin, anti-CD90.1 Peridinin Chlorophyll Protein, anti-CD45.2 phycoerythrin (PE), anti-CD90.2 FITC, anti-IFN-g PE, anti-TNF-a PE-cy7, anti-CD25 PE, anti-CD44 PE or Pacific Blue, anti-CD62L FITC (Biolegend), anti-CD3e allophycocyanin, anti-a4 PE (BD Biosciences), anti-CD4 Qdot605 and a LIVE/DEAD dead cell stain kit (Invitrogen). For cytokine staining, cells were permeabilized using a Cytofix/Cytoperm Plus Kit following manufacturer's instructions (BD Biosciences). Cell number was determined with AccuCheck Counting Beads (Invitrogen). Flow cytometry data were collected on a modified FACSCalibur (Cytek Development) or an LSRII (BD Biosciences) and analyzed using FlowJo (Tree Star).

Th1 polarization and protection against *C. trachomatis*

$CD4^+$ T cells were harvested from the lymph nodes and spleens of naïve NR1 mice and enriched with a mouse CD4 negative isolation kit (Invitrogen) following the manufacturer's protocol. $CD4^+$ T cells were cultured in media consisting of RPMI 1640 (Invitrogen), 10% FCS, L-glutamine, HEPES, 50 mM 2-ME, 50 U/ml penicillin, and 50 mg/ml streptomycin. NR1 cells were activated by co-culture with irradiated or mitomycin-treated splenocytes pulsed with 5 mM of Cta1133-152 peptide at a stimulator:T cell ratio of 4:1. Th1 polarization was achieved by supplying cultures with 10 ng/ml of IL-12 (Peprotech, Rocky Hill, NJ) and 10 mg/ml of anti-IL-4

antibody (Biolegend). After 5 days of stimulation, NR1 Th1 cells were transferred i.v. into naïve recipient mice. In integrin antibody blocking experiments, NR1 cells were treated with 100 ug of anti-α4, anti-α4β7 or isotype antibody (BioXCell) for 1 hour at room temperature prior to transfer into recipients. The next day, mice were challenged with 5x106 *C. trachomatis* IFUs and the upper genital tract was analyzed for burden 5 days after infection. Mice were treated i.p. with 200 ug of the respective antibody at 1 and 3 days post-infection for integrin blocking experiments.

Competitive homing

For this assay(35) an equivalent number of integrin wildtype NR1 cells (CD45.2/CD90.1) and congenic wildtype, Lck-CRE/Itgb1flox/flox, or Itgb7-/- NR1 cells (CD45.2/CD90.2) were combined and transferred into congenically mismatched CD45.1 hosts. The following day, mice were transcervically infected with 5x106 *C. trachomatis* IFUs. Tissues were harvested and analyzed 7 days after infection.

Quantitative PCR

Bacterial burden was evaluated by quantifying *C. trachomatis* 16S DNA relative to mouse GADPH DNA(33). The uterus was homogenized and DNA was extracted using the DNeasy blood and tissue kit (Qiagen). DNA was analyzed using *C. trachomatis*- and mouse-specific primer pairs and dual-labeled probes. Threshold values were detected by an ABI Prism 7000 sequence system. The ratio of *C. trachomatis* to host DNA was obtained using a standard curve.

Statistical analysis

Statistical significance between groups was determined using an unpaired two-tailed t test and depicted within figures as * $p < 0.05$, ** $p < 0.01$, *** $p < 0.001$, and **** $p < 0.0001$.

References

1. Brunham R, Rey-Ladino J. Immunology of Chlamydia infection: implications for a Chlamydia trachomatis vaccine. Nature reviews Immunology. 2005;5(2):149-61. doi: 10.1038/nri1551.

2. Cohen C, Brunham R. Pathogenesis of Chlamydia induced pelvic inflammatory disease. Sexually transmitted infections. 1999;75(1):21-4.

3. Roan N, Starnbach M. Immune-mediated control of Chlamydia infection. Cellular microbiology. 2008;10(1):9-19. doi: 10.1111/j.1462-5822.2007.01069.x.

4. Perry L, Su H, Feilzer K, Messer R, Hughes S, Whitmire W, et al. Differential sensitivity of distinct Chlamydia trachomatis isolates to IFN-gamma-mediated inhibition. Journal of immunology (Baltimore, Md : 1950). 1999;162(6):3541-8.

5. Thomas S, Garrity L, Brandt C, Schobert C, Feng G, Taylor M, et al. IFN-gamma-mediated antimicrobial response. Indoleamine 2,3-dioxygenase-deficient mutant host cells no longer inhibit intracellular Chlamydia spp. or Toxoplasma growth. Journal of immunology (Baltimore, Md : 1950). 1993;150(12):5529-34.

6. Mayer J, Woods M, Vavrin Z, Hibbs J. Gamma interferon-induced nitric oxide production reduces Chlamydia trachomatis infectivity in McCoy cells. Infection and Immunity. 1993;61(2):491-7.

7. Nelson D, Virok D, Wood H, Roshick C, Johnson R, Whitmire W, et al. Chlamydial IFN-gamma immune evasion is linked to host infection tropism. Proceedings of the National Academy of Sciences of the United States of America. 2005;102(30):10658-63. doi: 10.1073/pnas.0504198102.

8. Coers J, Bernstein-Hanley I, Grotsky D, Parvanova I, Howard J, Taylor G, et al. Chlamydia muridarum evades growth restriction by the IFN-gamma-inducible host resistance factor Irgb10. Journal of immunology (Baltimore, Md : 1950). 2008;180(9):6237-45.

9. Gondek D, Roan N, Starnbach M. T cell responses in the absence of IFN-gamma exacerbate uterine infection with Chlamydia trachomatis. Journal of immunology (Baltimore, Md : 1950). 2009;183(2):1313-9. doi: 10.4049/jimmunol.0900295.

10. Gondek D, Olive A, Stary G, Starnbach M. CD4+ T cells are necessary and sufficient to confer protection against Chlamydia trachomatis infection in the murine upper genital tract. Journal of immunology (Baltimore, Md : 1950). 2012;189(5):2441-9. doi: 10.4049/jimmunol.1103032.

11. Mora J, Bono M, Manjunath N, Weninger W, Cavanagh L, Rosemblatt M, et al. Selective imprinting of gut-homing T cells by Peyer's patch dendritic cells. Nature. 2003;424(6944):88-93. doi: 10.1038/nature01726.

12. Yednock T, Cannon C, Fritz L, Sanchez-Madrid F, Steinman L, Karin N. Prevention of experimental autoimmune encephalomyelitis by antibodies against alpha 4 beta 1 integrin. Nature. 1992;356(6364):63-6. doi: 10.1038/356063a0.

13. Bauer M, Brakebusch C, Coisne C, Sixt M, Wekerle H, Engelhardt B, et al. Beta1 integrins differentially control extravasation of inflammatory cell subsets into the CNS during autoimmunity. Proceedings of the National Academy of Sciences of the United States of America. 2009;106(6):1920-5. doi: 10.1073/pnas.0808909106.

14. Feagan B, Greenberg G, Wild G, Fedorak R, Paré P, McDonald J, et al. Treatment of ulcerative colitis with a humanized antibody to the alpha4beta7 integrin. The New England journal of medicine. 2005;352(24):2499-507. doi: 10.1056/NEJMoa042982.

15. Steinman L. Blocking adhesion molecules as therapy for multiple sclerosis: natalizumab. Nature reviews Drug discovery. 2005;4(6):510-8. doi: 10.1038/nrd1752.

16. Di Genova G, Savelyeva N, Suchacki A, Thirdborough S, Stevenson F. Bystander stimulation of activated CD4+ T cells of unrelated specificity following a booster vaccination with tetanus toxoid. European journal of immunology. 2010;40(4):976-85. doi: 10.1002/eji.200940017.

17. Hawkins R, Rank R, Kelly K. Expression of mucosal homing receptor alpha4beta7 is associated with enhanced migration to the Chlamydia-infected murine genital mucosa in vivo. Infection and Immunity. 2000;68(10):5587-94. doi: 10.1128/iai.68.10.5587-5594.2000.

18. Kelly K, Chan A, Butch A, Darville T. Two different homing pathways involving integrin β7 and E-selectin significantly influence trafficking of CD4 cells to the genital tract following Chlamydia muridarum infection. American journal of reproductive immunology (New York, NY : 1989). 2009;61(6):438-45. doi: 10.1111/j.1600-0897.2009.00704.x.

19. Perry L, Feilzer K, Portis J, Caldwell H. Distinct homing pathways direct T lymphocytes to the genital and intestinal mucosae in Chlamydia-infected mice. Journal of immunology (Baltimore, Md : 1950). 1998;160(6):2905-14.

20. Roan N, Gierahn T, Higgins D, Starnbach M. Monitoring the T cell response to genital tract infection. Proceedings of the National Academy of Sciences of the United States of America. 2006;103(32):12069-74. doi: 10.1073/pnas.0603866103.

21. Gondek DC, Olive AJ, Stary G, Starnbach MN. CD4+ T cells are necessary and sufficient to confer protection against Chlamydia trachomatis infection in the murine upper genital tract. J Immunol. 2012;189(5):2441-9. Epub 2012/08/03. doi: 10.4049/jimmunol.1103032. PubMed PMID: 22855710; PubMed Central PMCID: PMC3690950.

22. von Andrian U, Mackay C. T-cell function and migration. Two sides of the same coin. The New England journal of medicine. 2000;343(14):1020-34. doi: 10.1056/nejm200010053431407.

23. DeNucci C, Pagán A, Mitchell J, Shimizu Y. Control of alpha4beta7 integrin expression and CD4 T cell homing by the beta1 integrin subunit. Journal of immunology (Baltimore, Md : 1950). 2010;184(5):2458-67. doi: 10.4049/jimmunol.0902407.

24. Olive A, Gondek D, Starnbach M. CXCR3 and CCR5 are both required for T cell-mediated protection against C. trachomatis infection in the murine genital mucosa. Mucosal immunology. 2011;4(2):208-16. doi: 10.1038/mi.2010.58.

25. Kelly K, Rank R. Identification of homing receptors that mediate the recruitment of CD4 T cells to the genital tract following intravaginal infection with Chlamydia trachomatis. Infection and Immunity. 1997;65(12):5198-208.

26. Croft M, Bradley L, Swain S. Naive versus memory CD4 T cell response to antigen. Memory cells are less dependent on accessory cell costimulation and can respond to many antigen-presenting cell types including resting B cells. Journal of immunology (Baltimore, Md : 1950). 1994;152(6):2675-85.

27. Iwata M, Hirakiyama A, Eshima Y, Kagechika H, Kato C, Song S-Y. Retinoic acid imprints gut-homing specificity on T cells. Immunity. 2004;21(4):527-38. doi: 10.1016/j.immuni.2004.08.011.

28. Ruane D, Brane L, Reis B, Cheong C, Poles J, Do Y, et al. Lung dendritic cells induce migration of protective T cells to the gastrointestinal tract. The Journal of experimental medicine. 2013;210(9):1871-88. doi: 10.1084/jem.20122762.

29. von Andrian U, Engelhardt B. Alpha4 integrins as therapeutic targets in autoimmune disease. The New England journal of medicine. 2003;348(1):68-72. doi: 10.1056/NEJMe020157.

30. Johansson E, Rudin A, Wassén L, Holmgren J. Distribution of lymphocytes and adhesion molecules in human cervix and vagina. Immunology. 1999;96(2):272-7. doi: 10.1046/j.1365-2567.1999.00675.x.

31. Parr M, Parr E. Interferon-gamma up-regulates intercellular adhesion molecule-1 and vascular cell adhesion molecule-1 and recruits lymphocytes into the vagina of immune mice challenged with herpes simplex virus-2. Immunology. 2000;99(4):540-5. doi: 10.1046/j.1365-2567.2000.00980.x.

32. Jayarapu K, Kerr M, Ofner S, Johnson RM. Chlamydia-specific CD4 T cell clones control Chlamydia muridarum replication in epithelial cells by nitric oxide-dependent and -independent mechanisms. J Immunol. 2010;185(11):6911-20. Epub 2010/11/03. doi: 10.4049/jimmunol.1002596. PubMed PMID: 21037093; PubMed Central PMCID: PMC3073083.

33. Roan N, Gierahn T, Higgins D, Starnbach M. Monitoring the T cell response to genital tract infection. Proceedings of the National Academy of Sciences of the United States of America. 2006;103(5b5eacd0-ed49-5337-2e9d-21ca71f1089c):12069-143. doi: 10.1073/pnas.0603866103.

34. Gondek D, Olive A, Stary G, Starnbach M. CD4+ T Cells Are Necessary and Sufficient To Confer Protection against Chlamydia trachomatis Infection in the Murine Upper Genital Tract. Journal of immunology (Baltimore, Md : 1950). 2012(b592258e-6d58-45f6-046d-1dc90ef462ba). doi: 10.4049/jimmunol.1103032.

35. Olive A, Gondek D, Starnbach M. CXCR3 and CCR5 are both required for T cell-mediated protection against C. trachomatis infection in the murine genital mucosa. Mucosal immunology. 2011;4(1b375027-c9c5-6c09-5dfa-d26184570326):208-24. doi: 10.1038/mi.2010.58.

Chapter 5: Quantitative proteomics reveals pathogen-induced changes to the host proteome, independent of changes in host transcription, that are required for intracellular bacterial growth.

Contributions

The Quantitative Mass Spectrometry was executed and analyzed by Dr. Ronghu Wu and Dr. Edward Huttlin from the laboratory of Dr. Steven Gygi.

Dr. Jeffery Barker helped to complete the cellomics high content imaging analysis.

Madeleine Haff helped to execute immunoblots throughout this chapter.

Dr. Andrew McClusky and Madeleine Haff helped to run and to analyze the amino acid incorporation assay.

The results of this chapter have been prepared as a manuscript for submission

Introduction

Intracellular bacterial pathogens infect host cells and manipulate cellular processes in order to gain nutrients, evade the immune response, and promote bacterial growth and survival. *Chlamydia trachomatis*, is a gram-negative obligate intracellular pathogen that must survive within cells to productively infect mammallian hosts. Although most investigators studying the effects of bacteria on host cells appreciate that gene regulation and protein turnover are both key to understanding how bacteria alter host cell functions, there has been a bias towards the study of gene regulation rather than protein stability. This bias is the result of the availability of microarrays and other tools that allow the simultaneous measurement of thousands of individual host cell gene transcripts during a particular stage of cell infection in a high throughput fashion.

Previous work examined how infection with *Chlamydia trachomatis* alters the host transcriptional landscape in human epithelial cells. The results from these studies showed that during infection there is a strong upregulation of transcriptional networks that drive the initial immune response and inflammation. While these studies informed our understanding of the intial stages of the immune detection of *Chlamydia* and the early host response to infection, they cannot discern between changes in host transcription that are driven actively by *Chlamydia* or are a result of TLR/NLR signaling. Furthermore, it remains possible that the changes in transcription identified in these studies do not entirely reflect changes to protein levels. To address how the host proteome is altered during infection requires quantitative proteomic approaches that examine the levels of host proteins directly.

Although proteomics is an active area of investigation, the ability to monitor changes in protein abundance on a global level is limited. Approaches to study protein levels globally usually involve pulse-chase experiments, the administration of protease inhibitors followed by biochemical analysis, or biochemically trapping individual protein-protein interactors. These approaches are inherently limited in the number of proteins that can be monitored at one time, and are not scalable to make them “more global”. In the case of *C. trachomatis*, modern

proteomic approaches have never been used to characterize changes in host cell proteins (only studies using 2-D gels have been performed (1)), despite a general appreciation that the pathogen manipulates host cell proteins during infection (2-7). We have been interested in understanding how *C. trachomatis* manipulates host cell protein function and turnover to successfully replicate what occurs in the cell, but we were frustrated by the inavailability of methodology to study changes in host cell protein stability at the scale available for the study of transcriptional changes.

The quantitative mass spectrometry approach known as stable isotope labeling with amino acids in culture (SILAC) is a highly innovative method to globally monitor levels of endogenous proteins in mammalian cells. Here we adapted SILAC in combination with global transcriptional profiling as a new approach to understand host-pathogen interactions in mammalian cells (8). We found that *Chlamydia* infection dramatically alters the makeup of the host cellular proteome. Surprisingly, we found that the majority of proteins that were altered during infection remained unchanged in parallel transcriptional analysis. When we examined the mechanisms driving the discordant levels of mRNA and protein, we found that during infection with *Chlamydia,* host cell translation is significantly decreased. Finally, using a gain-of-function screen, we identified individual host proteins alterations that are required for efficient *Chlamydia* replication. Taken together, these results highlight the important role that proteomic studies play in developing a better understanding of the host pathways that are targeted by pathogens and are critical for intracellular growth. Better characaterization of host-pathogen interactions that occur during infection will significantly increase our ability to target and cure infectious disease.

Results

Identification of host proteins altered following infection with *C. trachomatis*

Chlamydia trachomatis has been shown to directly alter host-cell proteins, yet the scale of these changes and the identity of many host targets remains unknown (9). In order to identify host proteins that are altered during infection on a large scale, we used the quantitative proteomic approach known as stable isotope labeling of amino acids in cell culture (SILAC) to compare levels of all identified host proteins in infected and uninfected cells (10). For these studies we used HEK293T cells, which lack almost all TLRs and NLRs, and therefore will not mount a robust initial immune response. We reasoned that using these cells would allow us to examine the direct effects of *Chlamydia* infection on human cells in the absence of host responses that are not driven specifically by *C. trachomatis*. We infected ^{13}C-lysine ("heavy") labeled human HEK293T cells with *C. trachomatis* and cultured ^{12}C-lysine ("light") labeled uninfected cells in parallel. At 4, 14 and 24 hours after infection, we mixed lysates from the heavy labeled infected cells with lysates from the uninfected light labeled cells at a 1:1 ratio. (Figure 5-1A). These mixed lysates were then digested with trypsin and analyzed via tandem mass spectrometry to identify individual peptides and to compare their relative abundances in the presence and absence of *C. trachomatis* infection. Peptides were identified by comparing MS/MS fragmentation patterns with human protein sequences and were quantified by comparing the intensities of the heavy and light forms (11). Peptides were then grouped by their protein of origin and used to infer relative levels of protein abundance under each condition. We found that at four hours after infection, over 100 proteins were altered more than two-fold (Figure 5-1B). This increased to almost 200 proteins at 14 hours post-infection. By 24 hours post-infection we saw an additional significant increase in the number of host proteins that were altered more than two-fold, suggesting that *C. trachomatis* dramatically alters the host-proteome during infection (Figure 5-1B). In order to increase our confidence in the protein alterations that we identified, we performed an independent biological replicate at 24 hours post-infection

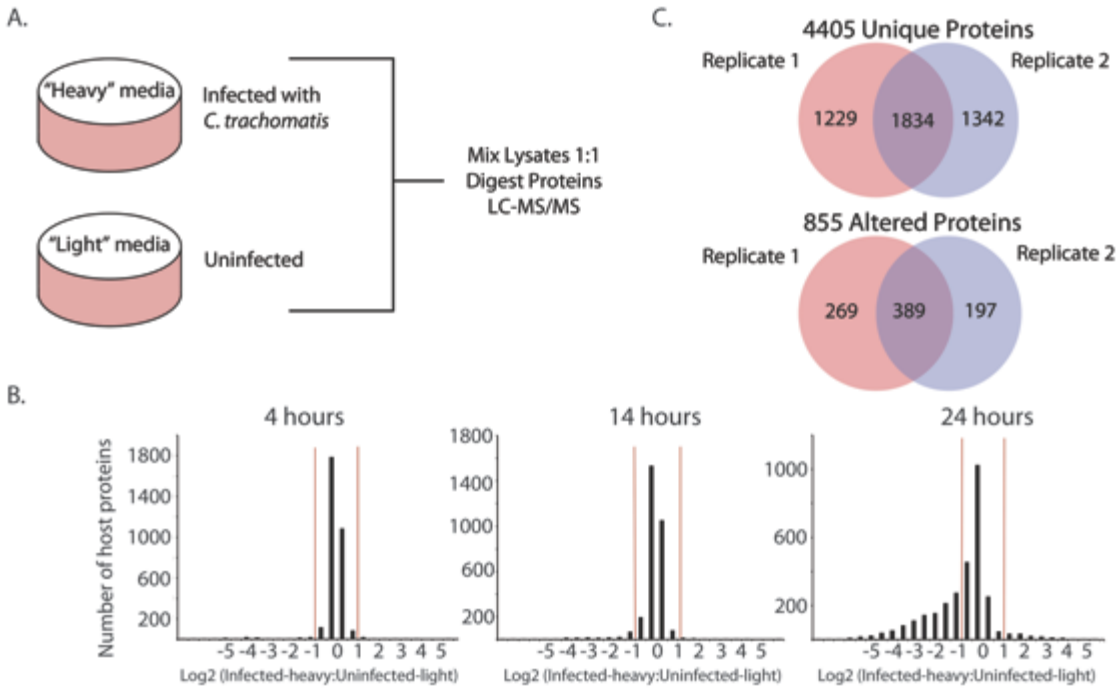

Figure 5-1. SILAC identifies host proteins altered during infection with *C. trachomatis*.
A) Schematic representation of the SILAC proteomic screen.
B) The differential levels (log_2 ratio on the x-axis) of all proteins quantified by LC-MS/MS at 4, 14, and 24 hours post-infection. Red bars indicate changes of two-fold (left: destabilized; right: stabilized).
C) Top: The overlap of total proteins between two independent replicates 24 hours after infection with *C. trachomatis*. Bottom: The overlap of proteins between the two replicates at 24 hours after infection with *C. trachomatis*, limited to those altered more than two-fold.

(Figure 5-1C). Between the two 24 hour replicates, we identified 1834 common proteins (of 4405 total proteins identified in both replicates), from which we identified 389 common altered proteins (of 805 total altered proteins identified in both replicates). We binned potential hits into low and high confidence groups depending on whether they were found in one or both replicates, respectively (Table S5-1). These data reveal that *C. trachomatis* alters the host proteome to a scale not previously appreciated. Interestingly, the number of host proteins altered increases as infection progresses, suggesting that *C. trachomatis* actively manipulates host cells throughout its developmental cycle. In order to validate the dataset directly, we examined changes in protein levels throughout infection by immunoblot analysis. In all cases where antibodies were available to detect the protein of interest, the immunoblot confirmed the changes measured by SILAC in the screen (Figure 5-2).

Through the use of quantitative mass spectrometry we identified a large number of host proteins whose levels were altered following infection with *C. trachomatis*. We next used bioinformatic analysis to gain a better understanding of how individual hits fit into the larger context of host cell biology. We conducted DAVID functional annotation clustering to identify gene ontology groups and host pathways that were significantly enriched during *Chlamydia* infection. We used host proteins that were identified as high confidence hits at 24 hours following infection with *Chlamydia* for our analysis. Among the top enriched cluster groups, we identified proteins involved in cytoskeleton/microtubule networks, RNA processing and translation, as well as organelles such as the Golgi apparatus and nuclear lumen (Summarized in Table S5-2). Previous work has suggested that *Chlamydia* directly alters the Golgi during infection via fragmentation, highlighting the utility of our data for identifying larger host cell interactions beyond the individual proteins that were found in the SILAC screen. We were surprised to find the strong impact of *Chlamydia* infection on RNA splicing and host protein translation because these processes have not been widely implicated as targeted during *Chlamydia* infection. Our data suggested that changes in host protein levels may not mirror

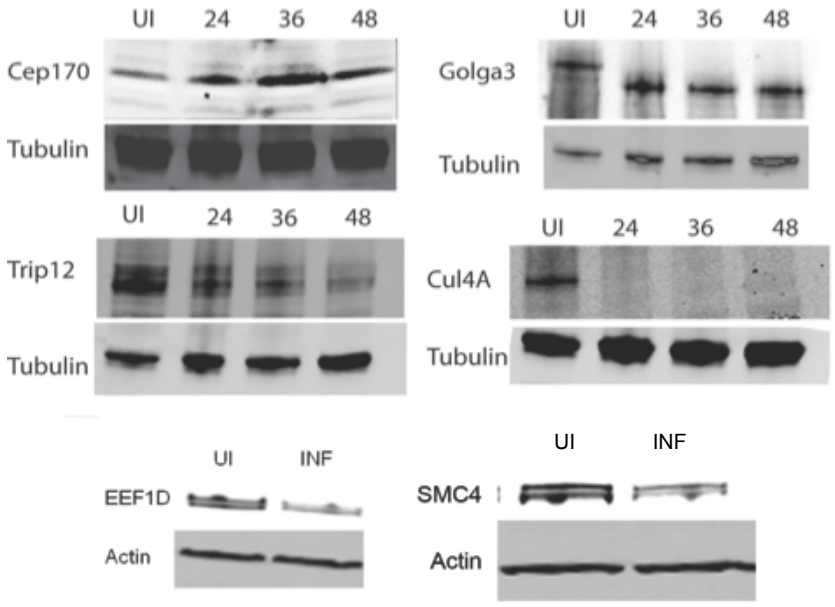

Figure 5-2. Validation data for the SILAC proteomic screen.
293T cells were mock-infected or infected with *C. trachomatis* for the indicated amount of time. Immunoblots were performed using antibodies for selected proteins (Cep170, Golga3, Trip12, Cul4A, EEF1D, and SMC4) and beta-Tubulin or beta-Actin (loading control).

changes in mRNA levels.

Identification of genes altered transcriptionally following infection with *C. trachomatis*

If specific host cellular processes, such as RNA stability and translation, are directly altered during infection with *Chlamydia*, it suggests that the changes that we identified at the protein level using SILAC may differ from the changes that have been identified at the transcriptional level. Our initial quantitative proteomic experiments showed that *C. trachomatis* alters hundreds of host proteins following infection, and we wanted to determine which genes were also changed at the transcriptional level. In order to address this question, we performed transcriptional analysis of the host cells at the same time points after infection at which we conducted SILAC analysis (Table S5-1). Our microarray analysis overlapped with previously published studies of host cells infected with *C. trachomatis,* with the exception of some differences in the upregulation of a number of pro-inflammatory genes (12, 13). These differences were expected because our studies were performed in HEK293T cells, which lack the majority of innate sensing genes (14). This also suggests that most of our observations are not the result of innate immune responses. Similar to what we observed in the SILAC time course described above, we saw an increase in the total number of genes whose transcription was altered more than two-fold as the infection progressed (Figure 5-3A).

Our initial transcriptional analysis identified only a handful of host genes that were altered significantly during *Chlamydia* infection in HEK293T cells, and few of these genes appeared to overlap with the protein changes that were identified using SILAC. We next wanted to independently validate our microarray findings using a more sensitive quantitative RT-PCR approach. We took advantage of the Bio-Rad PrimePCR resource to investigate changes in mRNA expression for a wide-range of host genes in a single 384 well plate assay format. We isolated mRNA from HEK 293T cells mock-infected or infected with *C. trachomatis* for 30 hours and reverse-transcribed total mRNA into cDNA. Using pre-mixed primer pairs for 90 host genes, we amplified individual genes by RT-PCR in technical duplicates to analyze changes in

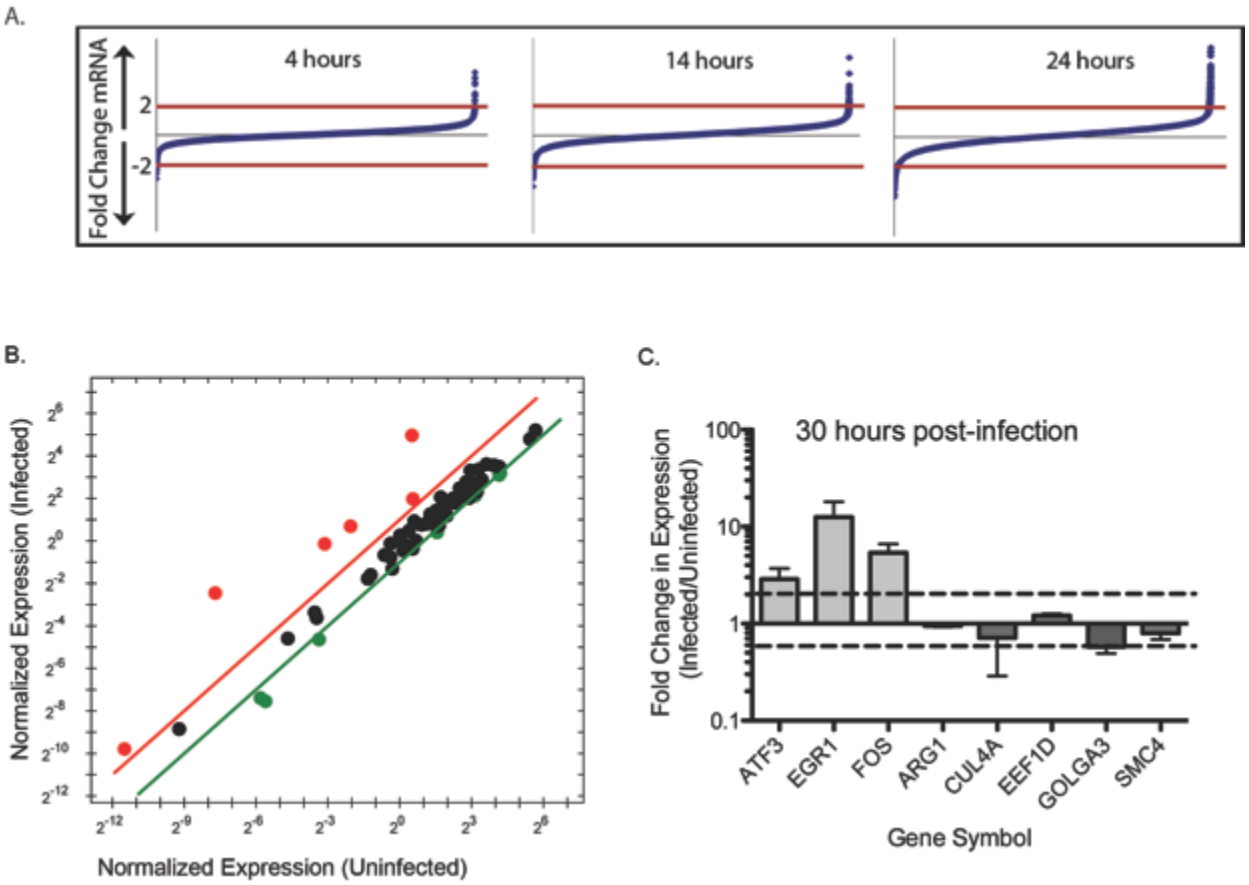

Figure 5-3. Transcriptional analysis and validation of host cells infected with *C. trachomatis*

A)The differential levels (log_2 ratio on the y-axis) of all genes quantified by microarray for mRNA levels at 4, 14, and 24 hours post-infection compared to uninfected controls. Red bars indicate changes of two-fold (Below: Down-regulated; Above: Up-regulated).

B) 293T cells were mock-infected or infected with *C. trachomatis* for 30 hours. Isolated RNA was transcribed into cDNA and analyzed by quantitative RT-PCR using PrimePCR high throughput analysis and normalized to Actin. Bars indicate changes of two-fold. Positive control genes not related to SILAC are indicated with +.

C) Shown is the fold-change in gene expression following *C. trachomatis* infection for a representative group of genes. Light gray bars represent positive controls as determined by initial microarray analysis. Dark gray bars represent genes that were altered in the SILAC analysis.

transcription. Eighty of the genes we chose to examine were high confidence hits identified in the initial SILAC screen (31 stabilized and 49 destabilized). We also included 5 positive controls and 5 negative controls consisting of genes that were found to be differentially altered at the transcriptional level during infection, but were not found to be altered at the protein level in the SILAC screen.

We found that the mRNA levels for only four genes of the eighty tested from proteins altered in SILAC were altered more than two-fold following infection with *C. trachomatis* (Figure 5-3B, Table S5-1). In contrast, all 5 positive control genes were altered significantly following *Chlamydia* infection and no negative controls. Together these data suggest that the transcriptional changes to the host that occur during infection with C. trachomatis may not be predictive of changes that occur directly in protein levels.

Many changes in host protein levels are not predicted by transcriptional profiling

Since we found very few proteins that were altered transcriptionally in our RT-PCR validation, we next wanted to globally assess how each individual protein was altered at both the transcriptional level and the protein level. This analysis aimed to identify changes to host proteins that are occurring independently of transcription, and therefore may be directly targeted during infection with *C. trachomatis*. We plotted the changes in each gene at the transcriptional level versus changes in that same gene at the protein level (Figure 5-4). Surprisingly, we noticed that over 90% of the protein changes identified were occurring independently of changes in host transcription. One explanation for this is that changes in transcription may occur prior to changes in the protein level. However, when we compared differing time points (SILAC at 24 hr vs. transcription at 14 hr) we saw no evidence of such a delay being responsible for the lack of correlation between the array data and SILAC data (data not shown). We conclude that infection with *C. trachomatis* extensively alters the host proteome independently of its effects on the host transcriptome.

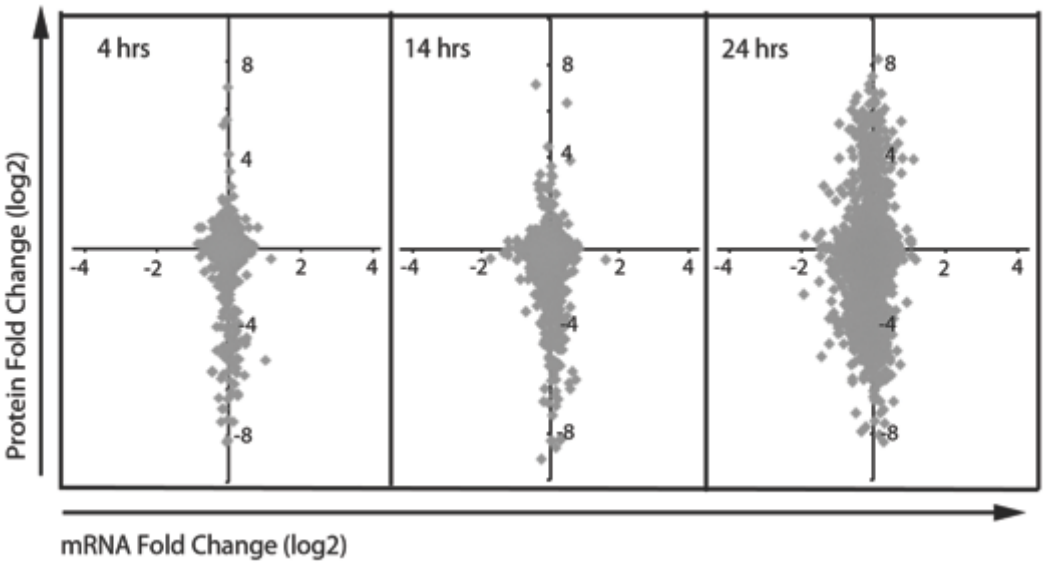

Figure 5-4. Changes in host protein levels do not correlate with changes in host mRNA levels during *C. trachomatis* infection.
Scatter plots show the correlation between changes in mRNA levels as determined by microarray analysis and protein levels as determined by SILAC at three timepoints after infection of HEK293T cells with *C. trachomatis*.

C. trachomatis infection alters host translation efficiency late during infection

Our data presented up to this point demonstrate that changes to the host proteome are discordant with changes to host transcription. This suggests that *Chlamydia* infection is able to alter levels of host proteins in a manner independent of changes in transcription. Our bioinformatics analysis of host proteins that were identified as altered in our SILAC screen showed a strong enrichment for genes involved in ribosome function and in host protein translation efficiency. This hinted that infection with *C. trachomatis* might alter the host cell's ability to translate proteins. Several bacterial pathogens have been shown to directly inhibit host protein translation through the action of toxins or effector proteins in order to promote pathogen survival. Furthermore, previous studies have shown that *Chlamydia* replicates more efficiently in the presence of low levels of the antibiotic cyclohexamide, which inhibits eukaryotic protein translation. We hypothesized that one mechanism by which *Chlamydia* infection may differentially alter mRNA and protein levels is by preventing robust host translation throughout the developmental cycle, phenocopying cyclohexamide treatment.

To examine the impact of infection on host translation, we employed a protein translation assay that measures the incorporation of radioactive amino acids in cells that are either mock-infected or infected with *C. trachomatis*. HeLa cells were mock-infected or infected with *C. trachomatis* for 30 hours, were then washed, and the media was replaced with [^{3}H]-leucine and media containing defined antibiotics that inhibit either host or bacterial translation. Cells were incubated in the radioactive media for one hour to allow for the incorporation of amino acids into proteins. Cells were then washed extensively, placed in scintillation fluid, and the level of radioactivity in each well was determined. We found that in the absence of antibiotics, the total incorporation of radioactive leucine was significantly decreased in cells infected with *C. trachomatis,* with levels that were almost two-fold lower than in the mock-infected cells (Figure 5-5). In the untreated condition, the total radioactivity is representative of the sum of the translation of both host and bacterial proteins. In order to assess how either host or bacterial

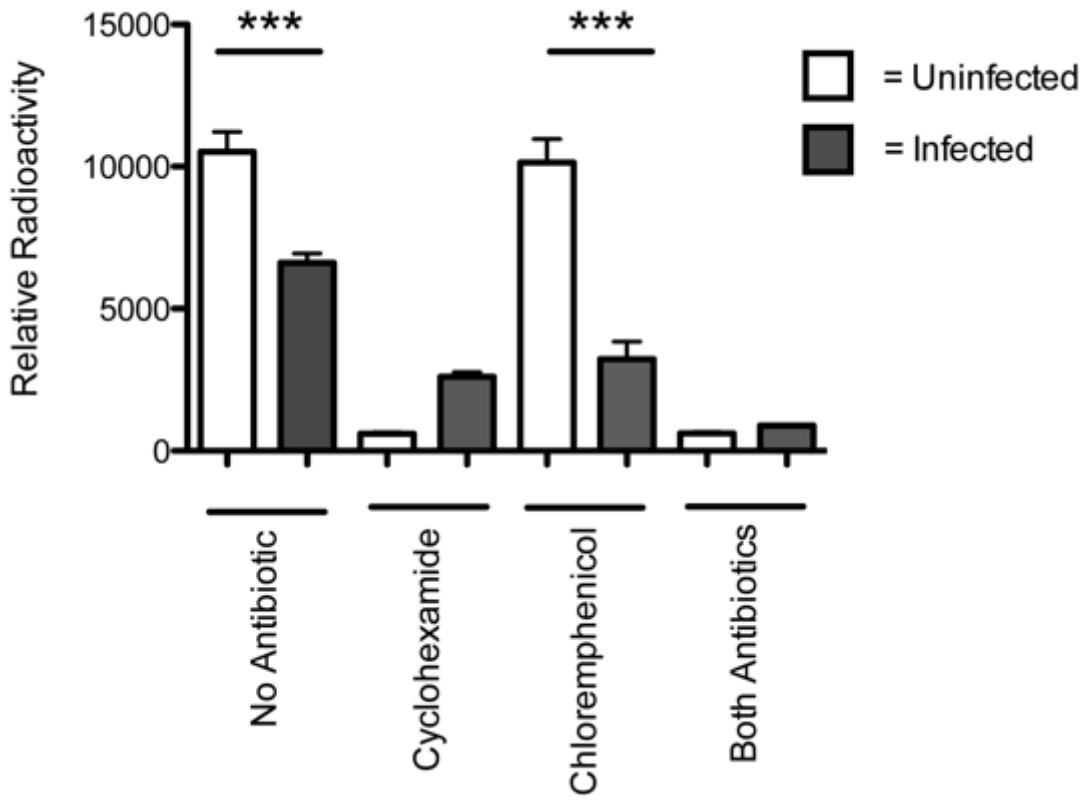

Figure 5-5. Infection with *C. trachomatis* decreases host protein translation efficiency. HeLa cells were mock-infected or infected with *C. trachomatis* (MOI=10) for 29 hours. Cells were then treated with 100μg of the indicated antibiotic. 30 hours following infection cells were were washed and fresh media with [^{3}H]-leucine was added to all cells for 1 hour. Cells were then lysed and the level of radioactivity in each well was determined. Shown is a representative of 3 independent experiments (n=4). *** denotes p<.001 by unpaired students t-test.

translation is altered, we treated cells with the antibiotic cyclohexamide, chloramphenicol, which inhibits bacterial protein translation, or both. In cells that were treated with cyclohexamide, we found that incorporation of radioactive amino acids is entirely inhibited in uninfected cells, but that there is a small level of incorporation in infected cells. This level of incorporation represents the translation that occurs in *Chlamydia* in host cells. In cells treated with chloramphenicol, which inhibits *C. trachomatis* translation, any radioactivity detected should represent only host amino acid incorporation. We found significantly lower levels of radioactive incorporation between infected and uninfected cells. Furthermore we found that cells treated with chloramphenicol, and therefore only examine host protein translation, had even less amino acid incorporation than cells with no drug treatment. As a control to ensure that our drug concentrations effectively inhibited translation, we examined the incorporation of radioactive leucine in cells treated with both antibiotics. We found almost no radioactive incorporation in the dual-treated controls compared to untreated cells, demonstrating that our drug treatments are at sufficient to inhibit translation in this assay. Taken together, these data suggest that host translation efficiency is lowered in cells infected with *C. trachomatis*. This underscores one mechanism driving discordant levels in host proteins and mRNA in *Chlamydia*-infected cells.

Overexpression of destabilized host proteins inhibits the growth of *C. trachomatis*

Our proteomic analysis identified pathways that were significantly altered during infection with *C. trachomatis*, and found that many host proteins that were altered would not have been predicted by examining changes in mRNA alone. However, it remained unclear whether these changes in host proteins directly impacted the ability of *Chlamydia* to aquire nutrients and to grow efficiently inside host cells. We next wanted to examine the individual role of the proteins that were identified as altered in our protemic screen. We hypothesized that a subset of *C. trachomatis*-induced changes may be essential for *C. trachomatis* infection to progress

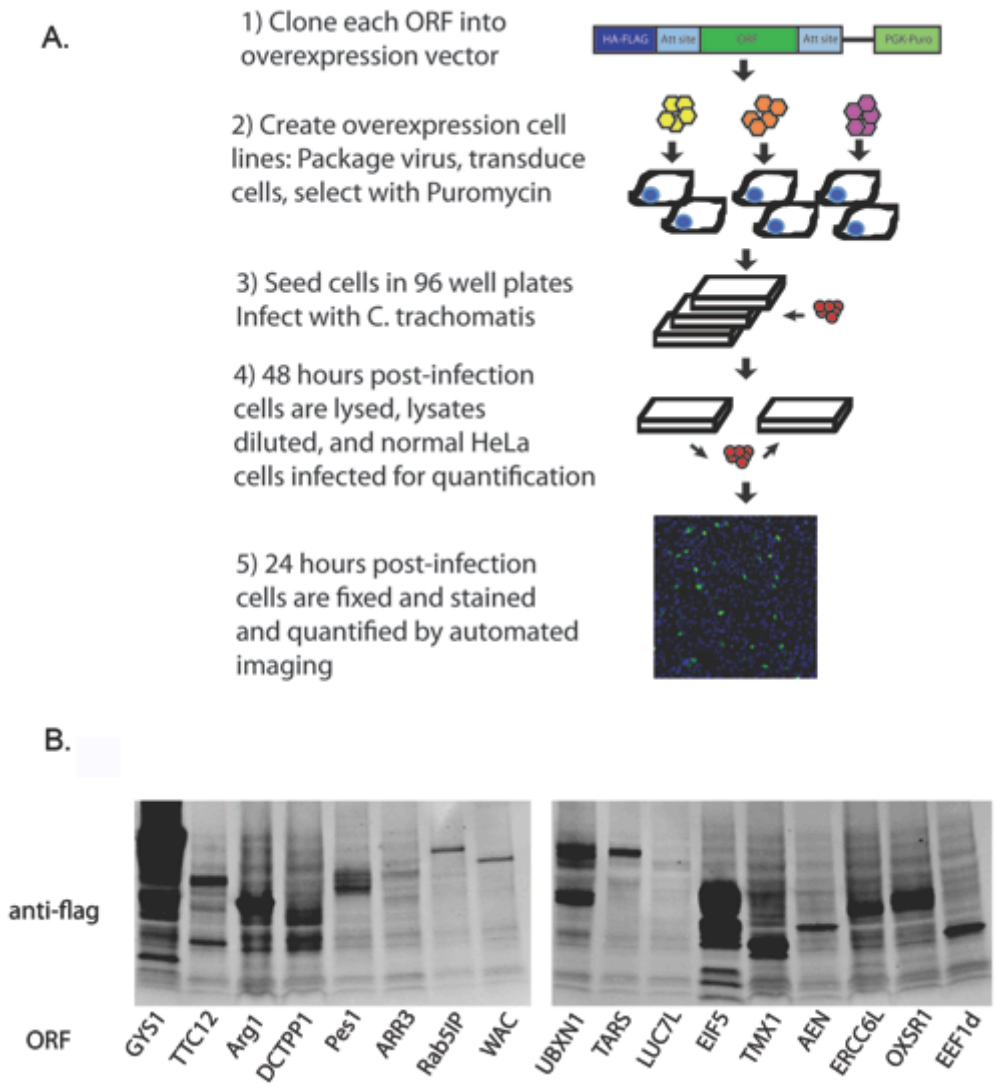

Figure 5-6. Optimization of gain-of-function screen protocol and cell lines.
A) Schematic representation of the constitutive expression screen.
B) A random subset of 293T constitutive expression cell lines were analyzed by immunoblot for the indicated ORFs. 10mg of cell lysates were probed for tagged proteins using an anti-flag antibody.

normally. To test this hypothesis, we piloted a gain-of-function screen which functionally reversed the specific protein changes that were driven by *C. trachomatis* (Figure 5-6A). Initially, we focused on proteins that were shown to be destabilized following infection. We reasoned that if destabilizing a particular host protein is essential for *Chlamydia* replication that over-expression of this protein may overwhelm the capacity of *C. trachomatis* to destabilize the protein and thus restrict bacterial growth. The general scheme for the overexpression screen is depicted in Figure 5-6A. We picked three hundred destabilized proteins from our hit list and cloned each protein into a retroviral flag-tagged over-expression vector. As a "neutral" control, we also cloned 50 randomly chosen proteins that were identified in our screens as unchanged following infection and 12 negative controls that contained the empty vector. We then created stable lines in HEK 293T cells that over-expressed each protein to levels well above the endogenous levels. We randomly selected 20 experimental cell lines and confirmed that the majority of cell lines were overexpressing a flag-tagged protein (Figure 5-6B). An important caveat to this methodology is that similar to large-scale siRNA experiments, over-expression efficiency was variable between cells lines, which could lead to false negatives due to low expression of individual proteins. We infected each cell line in duplicate with *C. trachomatis* for 48 hours. Cells were then lysed, diluted in media, and titered using normal HeLa cells as targets. After 24 hours, the cells were fixed and stained for the *C. trachomatis* major outer membrane protein (MOMP) and for host cell nuclei. We then used high content imaging to quantify the number of inclusions for each sample. Each well was normalized and the fold change in growth was calculated for each cell line containing an overexpressed host protein (Figure 5-7). The position within the distribution of experimental samples where the neutral and negative controls fall is noted in the figure. Importantly, all negative controls (0%) and all but one neutral control (2%) had changes in bacterial growth of less than 1.5 fold. In contrast, we identified 35 experimental proteins (12%) that inhibited *C. trachomatis* growth by over 1.5 fold. Because changes in protein stability as determined by GPS or SILAC may be caused by several

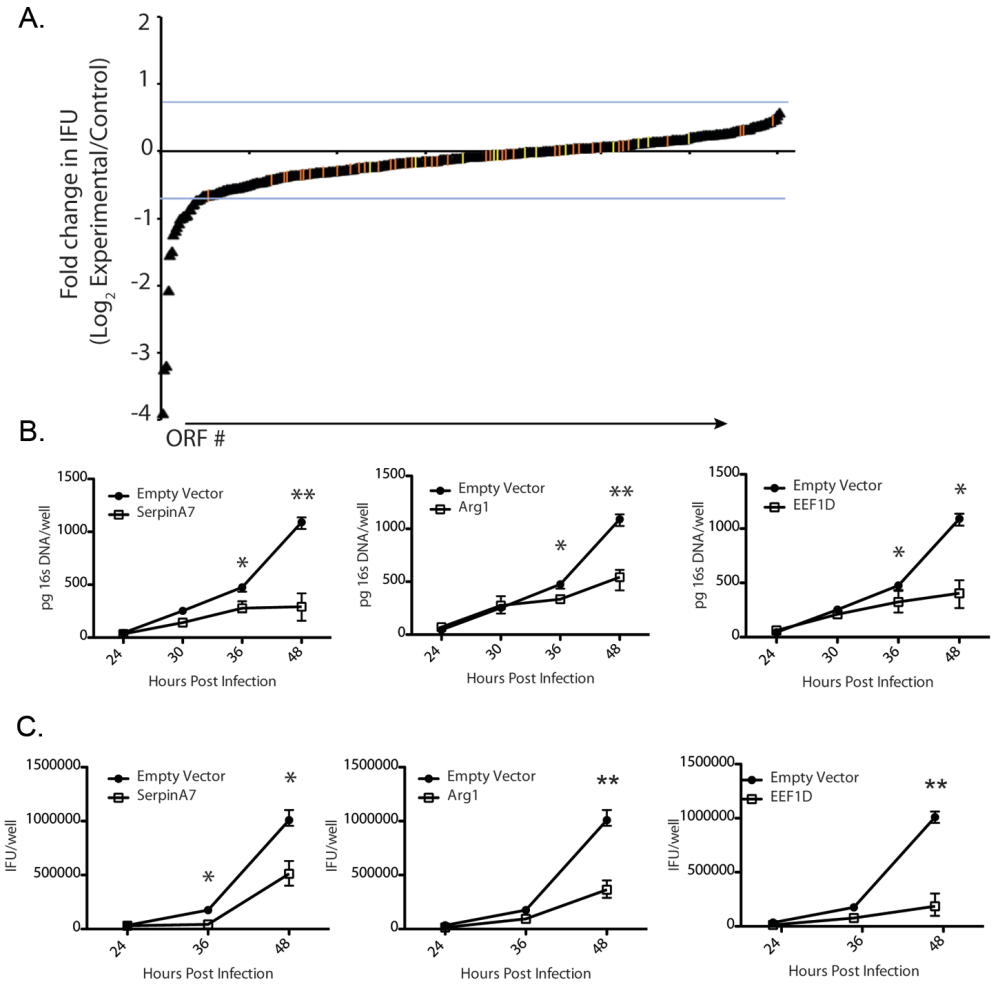

Figure 5-7. Gain-of-function screen identifies destabilized host proteins that are necessary for *C. trachomatis* growth and propagation.
A) Distribution of the mean fold change in *C. trachomatis* IFU production. All data points are shown in black triangles. The distributions of vector controls (yellow hash through the triangle) or neutral controls (orange hash through the triangle) were overlayed on the primary screen. Blue lines indicate 1.5 fold changes in *C. trachomatis* IFU.
B) A subset of overexpression cell lines was infected with *C. trachomatis* for the indicated timepoints. Levels of *C. trachomatis* were determined by qPCR of the 16s gene and compared to vector control cells. The graphs show the mean levels of *C. trachomatis* from triplicate samples +/- the standard deviation (*p<.05, **p<.01 by paired student t-test) (n=3).
C) A subset of overexpression cell lines was infected with *C. trachomatis* for the indicated timepoints. Levels of *C. trachomatis* were determined by IFU production and compared to vector control cells. The graphs show the mean IFU of *C. trachomatis* produced from triplicate samples +/- the standard deviation (*p<.05, **p<.01 by paired student t-test) (n=3).

factors such as phosphorylation, ubiquitination or protein complex formation, we would not expect to see growth defects for the majority of cell lines containing overexpressed host proteins.

We then further validated the capacity of these 35 transduced cell lines to inhibit *C. trachomatis* growth (Table S5-3). These validation studies verified 16 cell lines that reproducibly inhibited the ability of *C. trachomatis* to grow by at least 1.5 fold following infection (Table S5-3). We then selected 3 of these cell lines and examined their ability to inhibit *C. trachomatis* through an infection time course. We examined the levels of *C. trachomatis* by quantitative PCR, as well as the capacity of the cells to produce progeny by counting inclusion forming units (IFU). In all of these cases, overexpression of a single host protein decreased the levels of *C. trachomatis* present during primary infection (Figure 5-7B), as well as the ability of the pathogen to produce infectious elementary bodies (Figure 5-7C). These data suggest that a subset of proteins that appeared destabilized in our screens actually must be destabilized in order for efficient replication of *C. trachomatis* to occur in host cells.

Discussion

Infections with intracellular pathogens lead to a reorganization of host cells directed both by the host response to infection and by active mechanims employed by the invading bacteria. In order for investigators to develop novel antibiotics that target pathogenic mechanims occuring during infection, we must broadly characterize how host cells are directly altered during infection and understand which of those changes are directed by the pathogen. Recently, investigators have focused on transcriptome analysis to identify global changes in host mRNA expression during infection. In this study, we combined quantitative proteomic and global transcriptional analysis to characterize changes that occur to host cells during infection with *C. trachomatis*. Our results show that *Chlamydia* broadly rearranges the host proteome independently of changes in host transcription beyond levels previously appreciated. It also demonstrates that several of these host protein changes are essential for bacterial growth.

For the intracellular pathogen *Chlamydia trachomatis,* global transcription studies have led to the identification of transcriptional networks that are broadly altered throughout infection. Unfortunately, these analyses have limited ability to identify host processes that are targeted directly by *C. trachomatis* throughout the developmental cycle. First, all transcriptional studies examining *C. trachomatis* infection to date have used cultured cell lines that are competent in the majority of innate immune signaling pathways. When analyzing these data, it is clear that many genes that are transcriptionally altered during infection are in fact related to the host response to infection that occurs following most intracellular infections. In the data presented here, we circumvented innate sensing pathways in all our global analysis by using HEK293T cells, which lack almost all TLRs and NLRs. The lack of these signaling molecules prevents robust innate activation following infection, and should allows for the identification of changes in host processes that are the direct result of *C. trachomatis* infection. Our transcriptional analysisof HEK293T cells throughout infection with *Chlamydia* supports this hypothesis, as we identified far fewer genes that were altered at the mRNA level than previous studies and

importantly, several of the genes that were unaltered transcriptionally in our study were pro-inflammatory genes such as IL-8, which are predicted to be driven by the host response. Therefore using HEK293T cells as a screening tool enhances our ability to identify changes to human cells directed by *C. trachomatis* and to bypass the effects of the innate immune response.

While transcriptional analysis is a robust starting point to charactize host-pathogen interactions, ultimately the levels of host proteins, which are the molcules of action in cells, may be a better indicator of host cell alterations. In this study, for the first time quantitative proteomics were used to characterize ways in which the host cell proteome is altered during infection with *Chlamydia trachomatis*. Previous work examining changes to host proteins have relied on 2D-Gel electrophoresis and targeted immunoblot analysis, providing limited information about proteomic changes that occur during *Chlamydia* infection. Our results show that there are a dramatic number of host proteins that are altered even as early as four hours following infection, compared to uninfected cells. As infection progresses, the changes in the host proteome become exacerbated. After 24 hours of *Chlamydia* infection, we identified over 380 host proteins that were reproducibly altered by more than two-fold. These changes were far more robust than we anticipated based on our transcriptional analysis, and suggest that *Chlamydia* broadly alters the host proteome during infection. One caveat to these experiments is they were done withiout inhibiting CPAF, which may have lead to unintended changes in host proteins that are not representative of physiological interactions. However, because only the 24 hour timepoint when CPAF would be expressed in these experiments, and with the combination of two biological replicates and immunoblot validation done under CPAF inhibiting conditions, we are confident that the majority of the protein changes identified are not artificial CPAF substrates. Therefore, broad changes to the host proteome occur during infection with *Chlamydia* to levels not previously appreciated.

When we examined the changes in host transcription and host proteins levels from the

same infected cells, we noted that there was a very low correlation between the two. In fact, over 90% of the host protein changes found in SILAC were altered independently of changes in host transcription. We further validated a subset of high confidence SILAC hits by quantitative RT-PCR and found none of thes proteins were altered transcriptionally during *C. trachomatis* infection. It is an intriguing finding that *C. trachomatis* broadly elicits changes in host proteins idependent of changes to host transcription. We hypothesized that one way *C. trachomatis* may accomplish this is by altering the efficiency of host translation. Bioinformatic analysis of the host proteins altered following infection with *C. trachomatis* identified a number of ribosomal proteins and other translation regulating proteins. Supporting this hypothesis, we identified that constitutive expression of elongation factor EEF1D reduced replication of *C. trachomatis* in host cells. EEF1D is a guanine nucleotide exchange factor that is needed to deliver aminoacyl tRNAs to the ribosome. Loss of EEF1d represses the translation efficiency of host proteins, as seen during HIV infection (15). Likewise, it is known that treatment of cells with cyclohexamide promotes increased *C. trachomatis* replication (16). When we examined amino acid incorporation into proteins in cells that were mock-infected or infected with *C. trachomatis,* we found that a significant inhibition of host translation occurs during infection. This is one potential mechanism that drives the discordant levels of mRNA and protein observed during the *Chlamydia* infectious cycle. It will be important to begin studies to understand whether *C. trachomatis* encodes effectors that directly target the ribosome, similar to another intracellular pathogen, *Legionella pneumophila* (17). This could provide evidence that repression of host cell translation may be a common strategy employed by bacterial pathogens to promote growth within host cells.

Another mechanism by which *C. trachomatis* may directly alter host proteins independent of transcription is by altering the host cell ubiquitin landscape. One hit identified in the SILAC screen was the E3 ubiquitin ligase component Cul4A (18). We confirmed Cul4A is destabilized following infection by immunoblot. While our ongoing studies are examining

individual Cul4 substrates that may be altered, we hypothesize that by targeting the removal of a single E3 ubiquitin ligase or host deubiquitinating enzyme, *C. trachomatis* may be able to indirectly change the rate of turnover of specific host proteins or classes of host proteins. Further studies must begin to take advantage of resources that have helped characterized the mammalian ubiquitin system and apply them to identify specific host ubiquitin ligases or deubiquitinating enzymes that are critical for *C. trachomatis* replication. Our current study shows that *C. trachomatis* broadly alters host proteins post-transcriptionally and this may be a broad mechanism used by bacterial pathogens to promote survival.

While our study identified hundreds of host proteins that are altered during infection, the majority of these proteins were not essential for normal bacterial replication to occur. There are a number of possibilities for why we did not see a higher number of host proteins that are critical for normal growth to occur. One potential pitfall using a single gene gain-of-function approach is the inability to account for redundant host pathways that may circumvent the perturbations on a single protein tested. Another possibility for false-negative results is the inherent limitations to precisely control the expression of genes in our gain-of-function screen. Furthermore, we predict that a number of host protein alterations that we identified are not targeted directly by *C. trachomatis,* but rather are indirect consequences of other events such as the induction of host stress responses and therefore are not essential for growth. Finally some alterations may be important for other survival mechanisms that are not tested by the assays presented here, such as immune evasion. It is critical that we expand on our findings presented here to identify which essential protein changes are directed by *C. trachomatis*. By identifying specific host proteins that are essential for infection to occur normally, we can develop host-based antibiotics that disrupt pathogen interactions with the host cell, rather than poisoning the organism directly. A proof-of-principle of this concept was recently described for *Mycobacterium tuberculosis* (19). In this study investigators targeted host tyrosine kinases using the drug imatinib (Gleevec) and showed a reduction in both bacterial load and in the

development of granulomas. The potential of host-based therapeutics is an exciting possibility that has also been pursued for viral infection, because it may be very difficult for the pathogen to evolve resistance to these compounds (20). Overall applying these new global approaches will help us better understand pathogenesis and prevent disease.

Materials and Methods

Tissue Culture, Reagents, and General Procedures

HeLa, and 293T cells were maintained in Dulbecco's Minimum Essential Media supplemented with Penicillin/Streptomycin and 10% fetal bovine serum (Invitrogen). HeLa cells stably expressing CrpA-EGFP or EGFP alone were passaged in the medium described plus 200 µg/ml G418. For hypoxia-like induction experiments cells were cultured in DMEM containing 200 uM $CoCl_2$ for the indicated amount of time. 293T and HeLa cells were transfected using the TransIT transfection reagent (Mirus). Retroviruses were packaged in 293T cells transfected with the plasmid of interest as well as plasmids expressing VSVg and Gag-pol (Luo et al., 2009). Viral infections were supplemented with hexadimethrine bromide at a concentration of 8 µg/ml. Transfection of siRNA oligonucleotides was performed with Dharmafect (Dharmacon) lipid transfection reagent according to the manufacturer's protocols. siRNA were purchased from Dharmacon as smart pools. A complete list of immunological reagents used in this study is below. Flow cytometry was performed on a BD-LSRII Flow Cytometer (Becton Dickinson). Data were collected using BD FACS Diva software (Becton Dickinson) and analysis was performed using FloJo software.

Validation was performed by individually picking ORFeome clones and cloning them using gateway recombination into the GPS vector. All inserts were sequenced using the primer: 5'-AGCTGTACAAGTCCGAACTCGT-3'. The vectors were used to package virus and used to generate cell lines expressing individual GPS-ORFs. For immunoblot validation of endogenous proteins after *Chlamydia* infection, cells were lysed at the indicated time points.

EBs of *C. trachomatis* serovar L2 434/Bu were propagated within McCoy cell monolayers. A combination of glass bead disruption and sonication was used to release EBs from infected McCoy cells. EBs were further purified by ultracentrifugation over Renograffin gradients, as previously described (15). Aliquots of *C. trachomatis* EBs were

stored at -80° C in SPG buffer (250 mM sucrose, 10 mM sodium phosphate, and 5 mM L-glutamic acid, pH 7.2). Prior to infection with *C. trachomatis*, cells were cultured for 12-24 h in their respective media minus antibiotics. Cells were infected with *C. trachomatis* by adding media containing dilute EBs to host cells. Centrifugation was not used unless specified in the text. The multiplicity of infection (MOI) used for *C. trachomatis* was 3:1 unless indicated. DMEM alone was used for mock-infected cells.

Immunoblot analysis. For immunoblot analysis, cells were lysed at indicated timepoints following infection in glycerol lysis buffer (10 mM HEPES, 150 mM NaCl, 0.1% NP-40, 10% glycerol) in the presence of a complete protease inhibitor cocktail (Roche Applied Science, Indianapolis, IN) and phosphatase inhibitor. Lysates were normalized for total protein content by measuring absorption at 280 nm or using a BCA test (Pierce). Normalized samples were subjected to SDS-PAGE analysis (TGX gels, BD), transferred to nitrocellulose, and immunoblotted with the following antibodies:

Actin (Licor), Cep170 (AbCam), Cul4A (Cell Signaling), EEF1D (Santa Cruz) Flag (Invitrogen), Golga3 (AbCam), Trip12 (AbCam), Tubulin (Licor), SMC4 (AbCam)

Automated image analysis. Stained cells were imaged with a Cellomics ArrayScan VTI automated microscope. Six fields per well of a 96-well plate were imaged at 20x magnification. First, cells were identified by their nuclei staining in channel 1 of Cellomics. Cells that scored positive in channel 1 were analyzed for Alexa-488 (inclusions) in channel 2. A minimum average intensity in the Alexa-488 channel was calculated by manual inspection and applied to each selected object. The selected objects that were above this threshold are shown in blue while those that were below are shown in orange. Once the threshold was determined, all of the plates were subjected to data analysis using vHCS Scan Target Activation software v5.1.2.

Data were obtained by using vHCS View software and the number of inclusions in the well was identified as “valid object count” (VOC).

Quantitative PCR. To assess the levels of *C. trachomatis* present, we used a previously described qPCR method (21). Briefly, we isolated nucleic acid from infected cells using the DNeasy kit (Qiagen). *Chlamydia* 16S DNA was quantified by qPCR on an ABI Prism 7000 sequence detection system using primer pairs and dual-labeled probes. Using standard curves from known amounts of *Chlamydia* the levels of 16s DNA per well was calculated.

Microarray analysis. To compare relative levels of RNA expression, HEK293T cells were grown in DMEM (10% FBS). Cells were then infected with *C. trachomatis* or left uninfected. Cells were harvested at three time points after infection (4, 14, and 24 hours). Cells were then lysed using a Trizol (Invitrogen) and RNA was isolated using RNeasy kit (Qiagen) according to manufacturer’s instructions. RNA levels and quality was analyzed using an Agilent Bioanalyzer. RNA was then fragmented, labeled, and hybridized onto an Affymetrix GeneChip Human Gene 1.0 ST Array. Chips were read using an Affymetrix chip reader and were normalized and analyzed using GeneSpring software. Normalized expression levels were compared between conditions and two-fold changes were identified across all genes.

Overexpression Screen. Candidate proteins expression constructs were made by individually picking ORFeome clones and cloning them using gateway recombination into the iTAP vector. Each clone was sequenced using the primer: 5’-CGTGTACGGTGGGAGGTCTA-3’. For each ORF, retrovirus we made as described above. 293T cells were transduced individually in one well of a six-well plate. 48 hours later cells were selected with puromycin. Following selection cells were plated into duplicate 96 well plates with 10^4 cells per well. Cells were then infected with *C. trachomatis* at an MOI of 1:1. Forty-eight hours after infection cells were lysed and the

lysate was diluted 1:1000 and re-seeded into 96-well plates containing 10^4 normal HeLa cells. Twenty-four hours after inoculation with the lysate, cells were fixed with ice-cold MeOH for 30 minutes. Cells were washed two times with PBS containing 0.1% tween. Cells were then stained for with DAPI and *C. trachomatis* was stained using the antibody to the outer membrane protein MOMP contained in the *C. trachomatis* pathfinder diagnosis kit (Roche). Cells were quantified by automated microscopy as described above. The mean number of IFU produced by vector control samples was calculated, along with the mean IFU produced for each experimental ORF. A fold-change in *C. trachomatis* growth was calculated against the vector controls for each sample. Cells that inhibited growth more than 1.5-fold were maintained and used for subsequent infection studies.

RT-PCR analysis

Predesigned primers were selected from the BioRad human PrimePCR collection. Primers were pre-aliquoted in quadruplicates across a 384 well plate. HeLa cells were mock-infected or infected with C. trachomatis for 30 hours. Cells were then lysed in Trizol (Invitrogen) and RNA was isolated using RNeasy purification (Qiagen). cDNA was then synthesized using an iScript Advanced cDNA Synthesis Kit for RT-qPCR. SsoAdvanced SYBR Green Supermix was then used to amplify cDNA by RT-PCR using an ABI Prism 7000 sequence detection system in technical duplicates. All wells were normalized to host beta-actin and analyzed using CFX Manager Software (BioRad).

Protein translation assay

HeLa cells were plated in DMEM at 10^4 cells per well in a 96-well plate and incubated overnight at 37 C. The following day, cells were mock-infected or infected with 10^5 C. trachomatis for 29 hours. Cells were then washed and fresh media was added that contained no antibiotics, or contained 100ug Cyclohexamide and/or 10ug Chloramphenicol. After a one hour incubation,

the medium was removed and replaced with leucine-deficient medium supplemented with 1 **m**Ci of [^{3}H]-leucine/ml (PerkinElmer, Billerica, Massachusetts) and the same antibiotics as before. Cells were then incubated for an additional hour. Plates were washed twice with cold PBS (200 ul) prior to the addition of 200 ul of scintillation fluid. The amount of [^{3}H]-leucine incorporated was determined by scintillation counting using a Wallac MicroBeta TriLux 1450 LSC (PerkinElmer, Waltham, MA).

Mass Spectrometric Comparison of Protein Abundances via SILAC. To compare relative levels of protein expression, HEK293T cells were grown in DMEM (10% FBS) prepared with either ^{13}C-labeled or normal ^{12}C lysine. After 14 days of growth in these media, we achieved complete labeling of cellular proteins in the ^{13}C medium as verified by mass spectrometry analysis. Cells grown in ^{13}C-lysine were then infected with *C. trachomatis* while ^{12}C-lysine-labeled cells were left uninfected. Both infected and non-infected cells were harvested at three time points after infection (4, 14, and 24 hours). Cells were then lysed using a glycerol lysis buffer containing protease and phosphatase inhibitor cocktails, and mixed at a 1:1 ratio based on total protein concentration as measured by the BCA assay. The combined lysates from each timepoint were then separated via SDS-PAGE, followed by excision and division of the gel into 12 bands with roughly equal protein content as judged by visual inspection of Coomassie staining patterns. Bands subsequently underwent digestion in-gel with endoproteinase Lys-C (Wako). Finally, peptides extracted from each gel band were resuspended in 5% acetonitrile/5% formic acid for mass spectrometric analysis.

Peptides extracted from each gel band were identified and quantified via LC-MS/MS analysis using an LTQ-Orbitrap mass spectrometer (Thermo Fisher Scientific) equipped with a Famos autosampler (LC Packings) and an Agilent 1100 binary HPLC pump (Agilent Technologies) essentially as described previously (22). Briefly, a gradient from 6-30% acetonitrile in 0.125% formic acid was used to separate peptides via reversed phase

chromatography at approximately 300 nl/min over 70 minutes (total run time was 90 minutes). After acquisition of each high-resolution survey scan in the Orbitrap, low resolution MS/MS spectra were collected in data-dependent mode to match the top twenty most intense precursors following collision-induced dissociation within the linear ion trap. A minimum signal of 500 counts and a well-defined isotopic envelope were required for MS/MS selection, while singly charged peptides and peptides with unknown charge states were excluded. Ions were excluded from further sequencing for 30 seconds following MS/MS selection.

After LC-MS analysis, RAW files were converted to mzXML format and data were loaded into our in-house system for storage and processing of proteomics data. Features selected for MS/MS sequences were examined to ensure accurate monoisotopic mass determination and to optimize mass measurements. The Sequest search algorithm (11) was then used to match MS/MS spectra with peptides drawn from the human proteome (IPI; version 3.6) (23). Sequences of common protein contaminants including endoproteinase Lys-C were included as well. Sequences of all proteins were considered in both forward and reversed orientations to enable subsequent estimation of peptide and protein false discovery rates via the target-decoy method (24). The following parameters were used for database searching: 100 ppm precursor ion tolerance; 1.0 Da fragment ion tolerance; Lys-C digestion with up to 2 missed cleavages; fixed carbamidomethylation of cysteine (+57.0214); and variable methionine oxidation (+15.9949) and $^{13}C_6$-labeling of Lysine (+6.0201). Peptide identifications were filtered to a preliminary false discovery rate of 1% using the target-decoy method and linear discriminant analysis to distinguish correct and incorrect peptide identifications based on multiple metrics including Sequest's Xcorr and DCn scores, mass error, charge state, and peptide length (25). Probabilistic scores were then determined for each protein based on its matching peptides and the entire dataset was further filtered to achieve a final protein-level false discovery rate of 2%. After this additional protein-level filtering, the resulting peptide-level false discovery rate was reduced to well below 1%.

Relative quantitation of each identified peptide was accomplished using the Vista algorithm (26), as described previously (22). To be eligible for quantification, each quantified peptide was required to earn a Vista score of at least 79, and isotopic envelopes for both heavy and light forms were required to achieve a minimum signal-to-noise ratio of 3. Alternatively, if one form was found to have a S/N ratio less than 3, its partner was required to have a S/N ratio exceeding 5. In cases where only a single isotopic form (heavy or light) was observed, it was required to attain a minimum S/N ratio of 5; such peptides were quantified based on their signal-to-noise ratio since its corresponding isotopic pair could not be found. Furthermore, to limit quantitation of false identifications, peptides matching such 'exclusive' peptide identifications were required attain Q-values of 0.001 or better, meaning that they had to be identified at a minimum false discovery rate of no greater than 0.1%. Relative protein abundance levels were inferred from the median ratio of all matching peptides. To correct for minor errors in sample mixing, raw abundance ratios were normalized to ensure that the median Log(2)-transformed protein ratio was 0, corresponding to 1:1 mixing of heavy and light samples.

References

1. Savijoki K, Alvesalo J, Vuorela P, Leinonen M, Kalkkinen N. Proteomic analysis of Chlamydia pneumoniae-infected HL cells reveals extensive degradation of cytoskeletal proteins. FEMS Immunol Med Microbiol. 2008;54(3):375-84. Epub 2008/12/04. doi: FIM488 [pii] 10.1111/j.1574-695X.2008.00488.x. PubMed PMID: 19049650.

2. Balsara ZR, Misaghi S, Lafave JN, Starnbach MN. Chlamydia trachomatis infection induces cleavage of the mitotic cyclin B1. Infect Immun. 2006;74(10):5602-8. Epub 2006/09/22. doi: 74/10/5602 [pii] 10.1128/IAI.00266-06. PubMed PMID: 16988235; PubMed Central PMCID: PMC1594933.

3. Misaghi S, Balsara ZR, Catic A, Spooner E, Ploegh HL, Starnbach MN. Chlamydia trachomatis-derived deubiquitinating enzymes in mammalian cells during infection. Molecular microbiology. 2006;61(1):142-50. Epub 2006/07/11. doi: 10.1111/j.1365-2958.2006.05199.x. PubMed PMID: 16824101.

4. Pirbhai M, Dong F, Zhong Y, Pan KZ, Zhong G. The secreted protease factor CPAF is responsible for degrading pro-apoptotic BH3-only proteins in Chlamydia trachomatis-infected cells. J Biol Chem. 2006;281(42):31495-501. Epub 2006/08/31. doi: M602796200 [pii] 10.1074/jbc.M602796200. PubMed PMID: 16940052.

5. Brumell JH, Scidmore MA. Manipulation of rab GTPase function by intracellular bacterial pathogens. Microbiology and molecular biology reviews : MMBR. 2007;71(4):636-52. Epub 2007/12/08. doi: 10.1128/MMBR.00023-07. PubMed PMID: 18063721; PubMed Central PMCID: PMC2168649.

6. Chellas-Gery B, Linton CN, Fields KA. Human GCIP interacts with CT847, a novel Chlamydia trachomatis type III secretion substrate, and is degraded in a tissue-culture infection model. Cell Microbiol. 2007;9(10):2417-30. Epub 2007/05/30. doi: CMI970 [pii] 10.1111/j.1462-5822.2007.00970.x. PubMed PMID: 17532760.

7. Rockey DD, Scidmore MA, Bannantine JP, Brown WJ. Proteins in the chlamydial inclusion membrane. Microbes Infect. 2002;4(3):333-40. Epub 2002/03/23. doi: S1286457902015460 [pii]. PubMed PMID: 11909744.

8. Grabbe C, Dikic I. Cell biology. Going global on ubiquitin. Science. 2008;322(5903):872-3. Epub 2008/11/08. doi: 322/5903/872 [pii] 10.1126/science.1166845. PubMed PMID: 18988833.

9. Betts-Hampikian HJ, Fields KA. The Chlamydial Type III Secretion Mechanism: Revealing Cracks in a Tough Nut. Frontiers in microbiology. 2010;1:114. Epub 2010/01/01. doi: 10.3389/fmicb.2010.00114. PubMed PMID: 21738522; PubMed Central PMCID: PMC3125583.

10. Ong SE, Blagoev B, Kratchmarova I, Kristensen DB, Steen H, Pandey A, et al. Stable isotope labeling by amino acids in cell culture, SILAC, as a simple and accurate approach to expression proteomics. Molecular & cellular proteomics : MCP. 2002;1(5):376-86. Epub 2002/07/16. PubMed PMID: 12118079.

11. Eng JK, McCormack AL, Yates JR. An approach to correlate tandem mass-spectral data of peptides with amino-acid-sequences in a protein database. J Am Soc Mass Spectrom. 1994;5(11):976-89. PubMed PMID: ISI:A1994PP71300004.

12. Xia M, Bumgarner RE, Lampe MF, Stamm WE. Chlamydia trachomatis infection alters host cell transcription in diverse cellular pathways. The Journal of infectious diseases. 2003;187(3):424-34. Epub 2003/01/29. doi: 10.1086/367962. PubMed PMID: 12552426.

13. Ren Q, Robertson SJ, Howe D, Barrows LF, Heinzen RA. Comparative DNA microarray analysis of host cell transcriptional responses to infection by Coxiella burnetii or Chlamydia trachomatis. Annals of the New York Academy of Sciences. 2003;990:701-13. Epub 2003/07/16. PubMed PMID: 12860710.

14. Medvedev AE, Vogel SN. Overexpression of CD14, TLR4, and MD-2 in HEK 293T cells does not prevent induction of in vitro endotoxin tolerance. Journal of endotoxin research. 2003;9(1):60-4. Epub 2003/04/15. doi: 10.1179/096805103125001360. PubMed PMID: 12691621.

15. Xiao H, Neuveut C, Benkirane M, Jeang KT. Interaction of the second coding exon of Tat with human EF-1 delta delineates a mechanism for HIV-1-mediated shut-off of host mRNA translation. Biochemical and biophysical research communications. 1998;244(2):384-9. Epub 1998/03/26. doi: 10.1006/bbrc.1998.8274. PubMed PMID: 9514931.

16. Ripa KT, Mardh PA. Cultivation of Chlamydia trachomatis in cycloheximide-treated mccoy cells. Journal of clinical microbiology. 1977;6(4):328-31. Epub 1977/10/01. PubMed PMID: 562356; PubMed Central PMCID: PMC274768.

17. Fontana MF, Banga S, Barry KC, Shen X, Tan Y, Luo ZQ, et al. Secreted bacterial effectors that inhibit host protein synthesis are critical for induction of the innate immune response to virulent Legionella pneumophila. PLoS pathogens. 2011;7(2):e1001289. Epub 2011/03/11. doi: 10.1371/journal.ppat.1001289. PubMed PMID: 21390206; PubMed Central PMCID: PMC3040669.

18. Emanuele MJ, Elia AE, Xu Q, Thoma CR, Izhar L, Leng Y, et al. Global identification of modular cullin-RING ligase substrates. Cell. 2011;147(2):459-74. Epub 2011/10/04. doi: 10.1016/j.cell.2011.09.019. PubMed PMID: 21963094; PubMed Central PMCID: PMC3226719.

19. Napier RJ, Rafi W, Cheruvu M, Powell KR, Zaunbrecher MA, Bornmann W, et al. Imatinib-sensitive tyrosine kinases regulate mycobacterial pathogenesis and represent therapeutic targets against tuberculosis. Cell host & microbe. 2011;10(5):475-85. Epub 2011/11/22. doi: 10.1016/j.chom.2011.09.010. PubMed PMID: 22100163; PubMed Central PMCID: PMC3222875.

20. Brass AL, Dykxhoorn DM, Benita Y, Yan N, Engelman A, Xavier RJ, et al. Identification of host proteins required for HIV infection through a functional genomic screen. Science. 2008;319(5865):921-6. Epub 2008/01/12. doi: 10.1126/science.1152725. PubMed PMID: 18187620.

21. Coers J, Gondek DC, Olive AJ, Rohlfing A, Taylor GA, Starnbach MN. Compensatory T cell responses in IRG-deficient mice prevent sustained Chlamydia trachomatis infections. PLoS pathogens. 2011;7(6):e1001346. Epub 2011/07/07. doi: 10.1371/journal.ppat.1001346. PubMed PMID: 21731484; PubMed Central PMCID: PMC3121881.

22. Wu R, Dephoure N, Haas W, Huttlin EL, Zhai B, Sowa ME, et al. Correct interpretation of comprehensive phosphorylation dynamics requires normalization by protein expression

changes. Mol Cell Proteomics. 2011;10(8):M111 009654. Epub 2011/05/10. doi: M111.009654 [pii]
10.1074/mcp.M111.009654. PubMed PMID: 21551504.

23. Kersey PJ, Duarte J, Williams A, Karavidopoulou Y, Birney E, Apweiler R. The International Protein Index: an integrated database for proteomics experiments. Proteomics. 2004;4(7):1985-8. Epub 2004/06/29. doi: 10.1002/pmic.200300721. PubMed PMID: 15221759.

24. Elias JE, Gygi SP. Target-decoy search strategy for increased confidence in large-scale protein identifications by mass spectrometry. Nat Methods. 2007;4(3):207-14. doi: 10.1038/nmeth1019. PubMed PMID: ISI:000244715100013.

25. Huttlin EL, Jedrychowski MP, Elias JE, Goswami T, Rad R, Beausoleil SA, et al. A tissue-specific atlas of mouse protein phosphorylation and expression. Cell. 2010;143(7):1174-89. Epub 2010/12/25. doi: 10.1016/j.cell.2010.12.001. PubMed PMID: 21183079; PubMed Central PMCID: PMC3035969.

26. Bakalarski CE, Elias JE, Villen J, Haas W, Gerber SA, Everley PA, et al. The Impact of peptide abundance and dynamic range on stable-isotope-based quantitative proteomic analyses. J Proteome Res. 2008;7(11):4756-65. doi: 10.1021/pr800333e. PubMed PMID: ISI:000260792000015.

Chapter 6: Pathogen-induced alterations to the host cell proteome are broadly required for intracellular growth

Contributions:

Dr. Michael Emmanuel and Laura Sack aided with microarray hybridization, validation approaches and the ORFeome library

Dr. Jeffery Barker helped execute the cellomics high content imaging screen

Madeline Haff was essential for most of the immunoblots presented in this chapter

The results of this chapter have been submitted for publication.

Introduction

Intracellular bacterial pathogens have evolved to exploit host cells in order to survive, replicate, and spread from mammalian hosts (1-3). Many of these bacterial pathogens reside in host-cell vacuoles and translocate virulence factors directly into the host cytosol through specialized secretion systems (4-6). This allows bacterial pathogens to avoid destruction by the endocytic pathway and enables them to replicate within the host cell (7, 8). The activities of secreted effectors and their impact on host cell functions are areas of intense investigation, however significant progress has been hindered because there is redundancy among bacterial effector proteins as well as the host pathways they target (9-11). To completely understand how secreted effectors exploit host cell functions during infection, investigators must study multiple aspects of host cell protein regulation (12). Over the last decade there has been a major focus on understanding changes in host transcription following infection (13). The availability of microarrays has allowed analysis of global changes to thousands of gene transcripts simultaneously. These approaches have probed host transcriptional responses to infection and identified host responses that bacterial pathogens manipulate in order to promote survival (14).

Most bacterial manipulations of host cell proteins however cannot be identified through transcriptional arrays alone. Many of the effectors that have been identified modify or alter the stability of host proteins directly (15-17). Unfortunately, studies examining global changes to proteins following bacterial infection have been limited. Investigators have used pulse-chase experiments as well as 2D-Gel electrophoresis coupled with mass spectrometry to identify proteins that are altered during infection (18). Even with the advances in quantitative proteomics, few studies have assessed changes to entire proteomes following infection (19-21).

Here, we take advantage of global proteomic and genomic techniques to identify host proteins that are altered in stability following infection with *Chlamydia trachomatis*. *Chlamydia* is the leading cause of bacterial sexually transmitted disease in the United States, and the leading cause of preventable blindness worldwide (22). *C. trachomatis* has two developmental forms;

the elementary body (EB) that is infectious, but metabolically inactive, and the reticulate body (RB) that is the replicating, metabolically active form. EBs are taken up into host cell vacuoles, and once inside EBs rapidly convert to RBs (23). Replication occurs within the vacuole (known as the "inclusion") over approximately 36-48 hours. Just before the cell becomes compromised, the RBs convert back to EBs so that infection of neighboring cells can occur. Our lab and others have shown that some *C. trachomatis* proteins can be translocated into cells by the type III secretion systems (TTSS) of other pathogens (24-26). This provides some of the evidence leading to the conclusion that inclusion-bound *C. trachomatis* traffic bacterial proteins across the vacuolar membrane into the host cell cytosol. Among the proteins secreted into the cytosol by *C. trachomatis* are two deubiquitinating enzymes and several secreted proteases, suggesting that *C. trachomatis* directly manipulates host protein levels during infection (16, 27, 28).

Because *C. trachomatis* is dependent on the host cell for survival, it is an ideal bacterial pathogen to begin using global approaches to study how it alters the host cell proteome. Here, we used both quantitative proteomics and transcriptional analysis during infection to identify changes in host proteins that occur independently of changes in transcription. In parallel, we adapted a recently developed global protein stability (GPS) platform to screen the human ORFeome for changes in host protein stability following infection with *C. trachomatis* (29, 30). Using these approaches we identified hundreds of host proteins that are altered in stability following infection. We next used a multi-pronged approach, consisting of bioinformatics, gain-of-function and loss-of-function screens, as well as directed bacterial effector-host substrate identification in order to understand *Chlamydia*-induced changes to host proteins. Our results indicate that *C. trachomatis* dramatically alters the host proteome in order to successfully replicate, and that a subset of these changes are driven by secreted effectors and are essential for bacterial replication. By understanding how intracellular bacterial infections directly alter the proteome of host cells, we will become equipped to discover new interventions that block changes to host proteins required by pathogens and ultimately prevent infection and disease.

Results

The global protein stability platform identifies hundreds of host proteins that are altered following infection with *C. trachomatis*

To begin a search for host proteins whose stability might be altered following infection with *C. trachomatis*, we adapted the Global Protein Stability (GPS) screening platform. GPS is a system originally designed as a fluorescent protein-based method to identify the substrates of mammalian ubiquitin ligases (30, 31). The GPS platform is a pooled library of HEK293T cells each expressing a single copy of a reporter cassette that contains DsRed, an internal ribosome entry site (IRES), and a human ORF fused to EGFP (Figure 6-1A). This allows the expression of both reporters as a single mRNA from a CMV promoter, making transcription constant and differences in EGFP/DsRed reflective of differences in protein levels. Over 10,000 unique human ORFs are represented in the library with each cell expressing a single EGFP-ORF fusion protein. Cells in the library were sorted by FACS into seven bins corresponding to lowest to highest EGFP:DsRed ratio a reflection of the stability of each human ORF in the library (29, 31). In order to identify what ORFs are present in each bin we amplified the ORFs from a genomic DNA sample from each bin and then applied them to a custom microarray composed of probes to each of the 10,000 ORFs. This allowed us to determine the relative number of cells expressing each ORF contained in each bin. A protein stability index (PSI) was assigned to each ORF based on the weighted average of the bin numbers containing cells expressing that ORF (29). After confirming that infection of cells with *C. trachomatis* does not alter the inherent stability of either DsRed or EGFP, we performed the identical experiment described above after infecting the GPS library with *C. trachomatis* for 24 hours (Figure 6-1B). Using the PSI value for each protein in the library under uninfected and infected conditions, we calculated the ΔPSI resulting from infection (Figure 6-1C). We then used a priority rank system to order the proteins from most stabilized to most destabilized identifying over 600 proteins (out of 8000 that passed initial filtering from the microarrays) that are altered in stability (ΔPSI < -.25 or ΔPSI > .25)

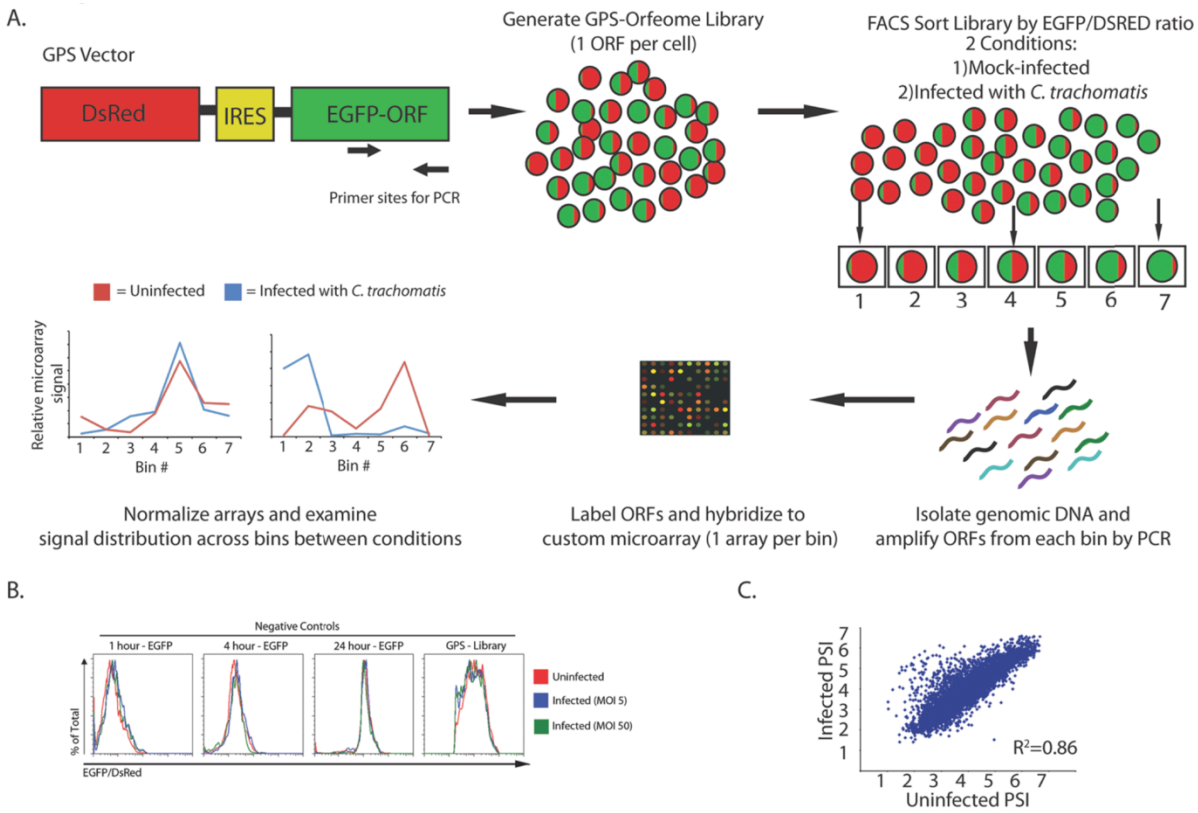

Figure 6-1. GPS profiling identifies host proteins altered during *C. trachomatis* infection.
A) Schematic representation of the GPS screen.
B) Histograms show the EGFP/DsRed ratio for cells expressing GFP for varying half-life and the entire GPS library. The cell lines were mock-infected (red line) or infected with *C. trachomatis* at an MOI of 5 (blue line) or 50 (green line) for 24 hours and analyzed by flow cytometry.
C) Scatter plot for the PSI for each probe in the screen under the two conditions (mock-infected vs. infected).

following infection with *C. trachomatis* (Table S6-1 and described in detail in the methods). This was far more proteins than we anticipated based on previously reported transcription data and suggested that *C. trachomatis* was profoundly remodeling the host proteome upon infection (32). In order to determine the overall validation rate of the GPS screen we randomly chose a subset of 175 ORFs from the 600 initial hits and created unique GPS reporter cell lines each expressing a single EGFP-ORF fusion. This validation approach was designed to ensure an unbiased estimate of the reproducibility of the entire GPS screen. Reporter cell lines were either mock-infected or infected with *C. trachomatis* for 24 hours, and then analyzed by flow cytometry for changes in the EGFP:DsRed ratios. We found that 109 cell lines (62%) had altered ratios reproducibly following infection (Figure 6-2A, Figure 6-2B and Table S6-1). To confirm that some of these ORFs were altered by infection we used immunoblots specific for an epitope tag on the host protein (14 of 20 confirmed) or using endogenous antibodies (7 of 9 confirmed) (Figure 6-3A, Figure 6-3B and Table S6-1). Interestingly, we found that while the GFP fusions accurately informed us when a specific protein was altered, they did not always predict whether a protein was stabilized or destabilized. For example, we identified the host protein SNCG as stabilized following infection with *C. trachomatis* using the GPS reporter, yet immunoblot analysis showed that this protein is actually cleaved following infection (Figure 6-3A and 6-3B). These data suggest that cleavage of host proteins in the GPS platform can remove specific degrons, leading to the stabilization of the EGFP reporter even though cleavage has occurred.

To help integrate our GPS hit data into the overall biology of the host cell we conducted bioinformatics analysis using DAVID clustering analysis (details are described in the methods)(33). Within the most enriched clusters in our analysis we identified host proteins that have been previously described to be important for *Chlamydia* infection (Table S6-2). These included chromatin remodeling proteins, the Golgi apparatus, cell cycle control proteins, and host cytoskeleton networks, supporting the concept that our GPS data can identify pathways important for *Chlamydia* growth (Table S6-2) (34-38). When we examined top clusters that

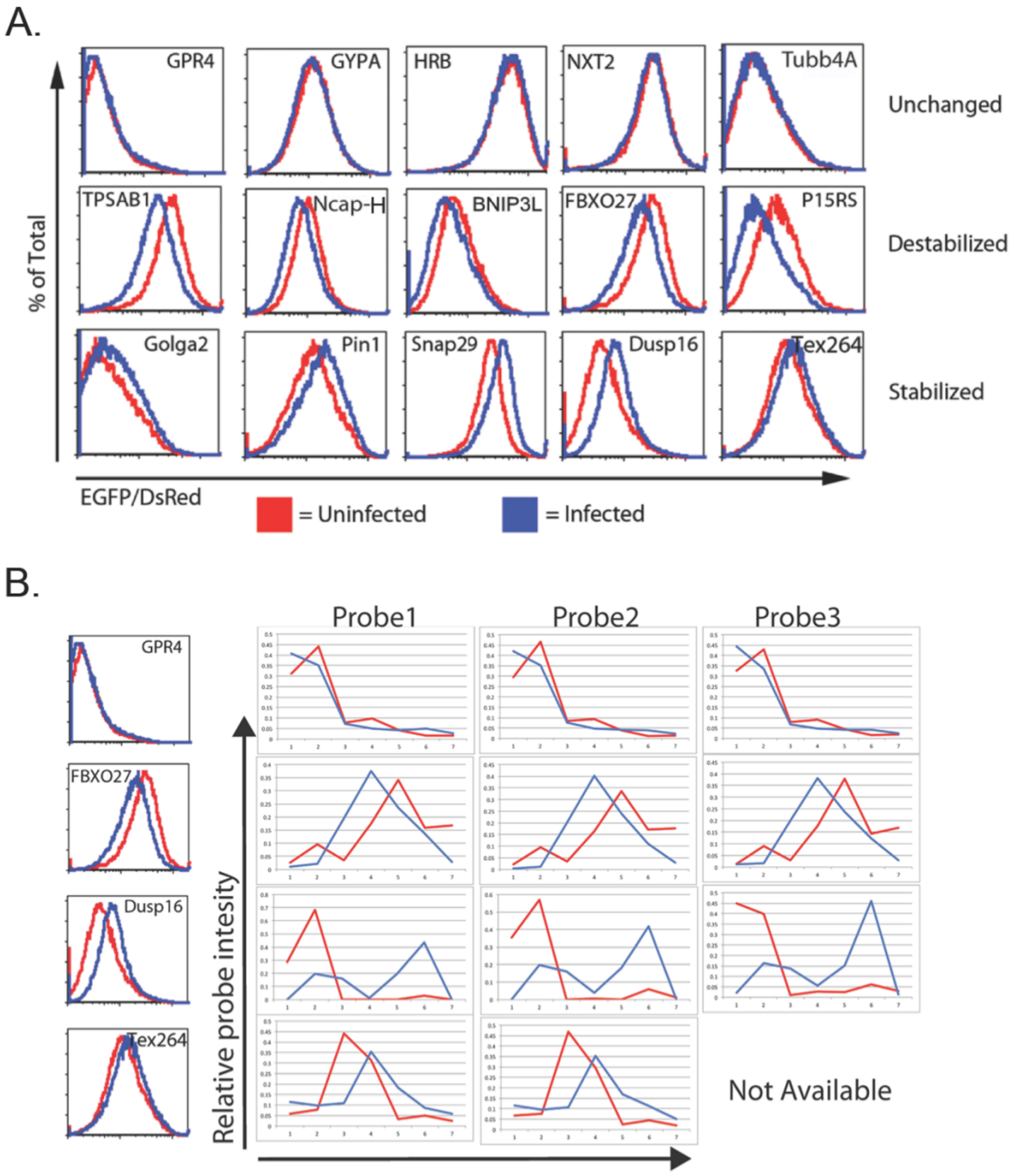

Figure 6-2. Infection of clonal GPS cell lines recapitulates screen phenotypes.
A) A subset of candidates that were tested by expressing the host gene in HEK293T cells. Cells were mock-infected (red line) or infected with *C. trachomatis* (blue line) for 24 hours and evaluated using flow cytometry.
B) Infected 293T cells expressing the indicated ORFs in the GPS vector were analyzed by flow cytometry after 24 hours. The microarray probe distributions are shown at the right for probes of the indicated ORFs. A complete list of the validation status of tested proteins can be found in Table 6-2.

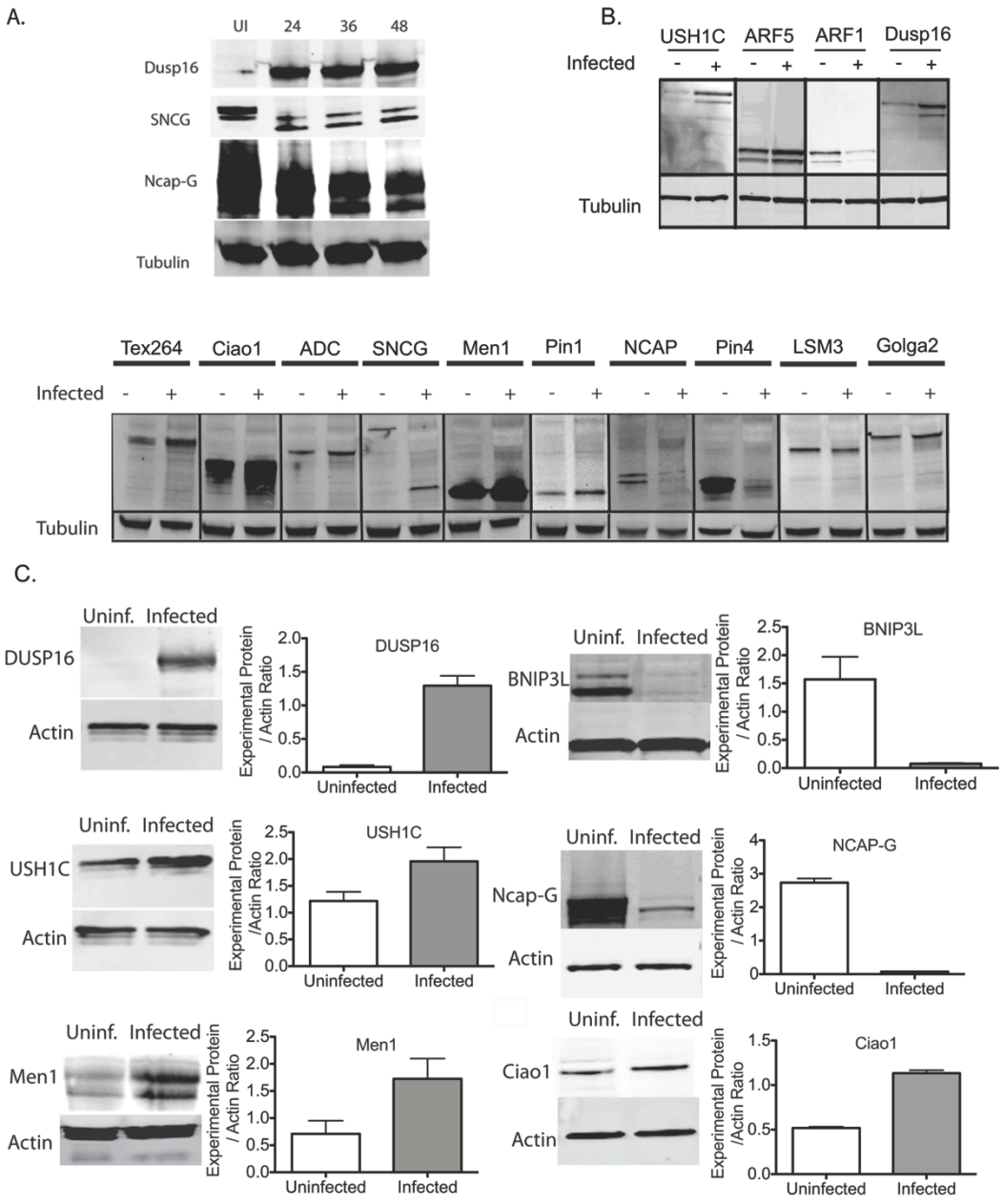

Figure 6-3. Immunoblot validation of proteins identified in GPS.
A) HEK293T cells were mock-infected or infected with *C. trachomatis* for the indicated amount of time. Cells were analyzed by immunoblot for the expression of the experimental proteins (Dusp16, SNCG, and NCAP-G) as well as beta-tubulin (loading control).
B) A subset of HEK293T cells expressing tagged versions of potential GPS targets were mock-infected or infected with *C. trachomatis* for 24 hours. Cell lysates were analyzed by immunoblot for the indicated experimental proteins and beta tubulin (loading control).
C) 293T cells were mock-infected or infected with *C. trachomatis* for the 30 hours when cells were lysed in 8M Urea. Shown are representative immunoblots for selected proteins (Ciao1, USH1C, DUSP16, Men1, NCAP-G and BNIP3L) and beta-actin (loading control). Replicate samples were quantified using the Odyssey infrared imaging system or imageJ and the relative intensities were plotted in the graphs.

contained protein families not previously associated with *Chlamydia* infection, we found an enrichment of protein families containing transcription factors, host-signaling cascades such as JNK, and vesicular trafficking components (Table S6-2). We also found a number of proteins that were enriched in the nuclear membrane or mitochondria suggesting that *Chlamydia* infection directly alters the makeup of these intracellular organelles (Table S6-2).

We next used the data from the GPS screen and our bioinformatics analysis to execute a small-scale proof-of-principle study to test the whether the interactions between *Chlamydia* and host cells we identified could reveal broader alterations to these pathways that occur during infection. To do this we mined the GPS dataset for proteins that had robust shifts in EGFP:DsRed, were members of a larger family of proteins, and where only a small percentage of the larger "family" were identified as hits in the initial screen. Two protein families we explored were the dual specificity phosphatases (Dusps) and nuclear pore proteins (Nups) that both had family members shift (Dusp15/16 and Nup50/160) in the GPS screen (Table S6-1), but did not have broad coverage of the entire protein family in our screen. To test whether *Chlamydia* infection more broadly alters this protein family we cloned a larger panel of Dusps (12 members) and Nups (8 members) into the GPS vector and created stable reporter cell lines for each member. We then infected these cells with *Chlamydia* and examined the shift of EGFP:DsRed 24 hours later by flow cytometry. We found that infection with *Chlamydia* broadly influenced the stability of 11 out of 12 Dusps and 6 out of 8 Nups suggesting this family of proteins may be broadly altered during infection (Figure 6-4B). These data show further utility of the GPS platform to drive additional studies that should reveal mechanisms in play during *Chlamydia* interaction with the host.

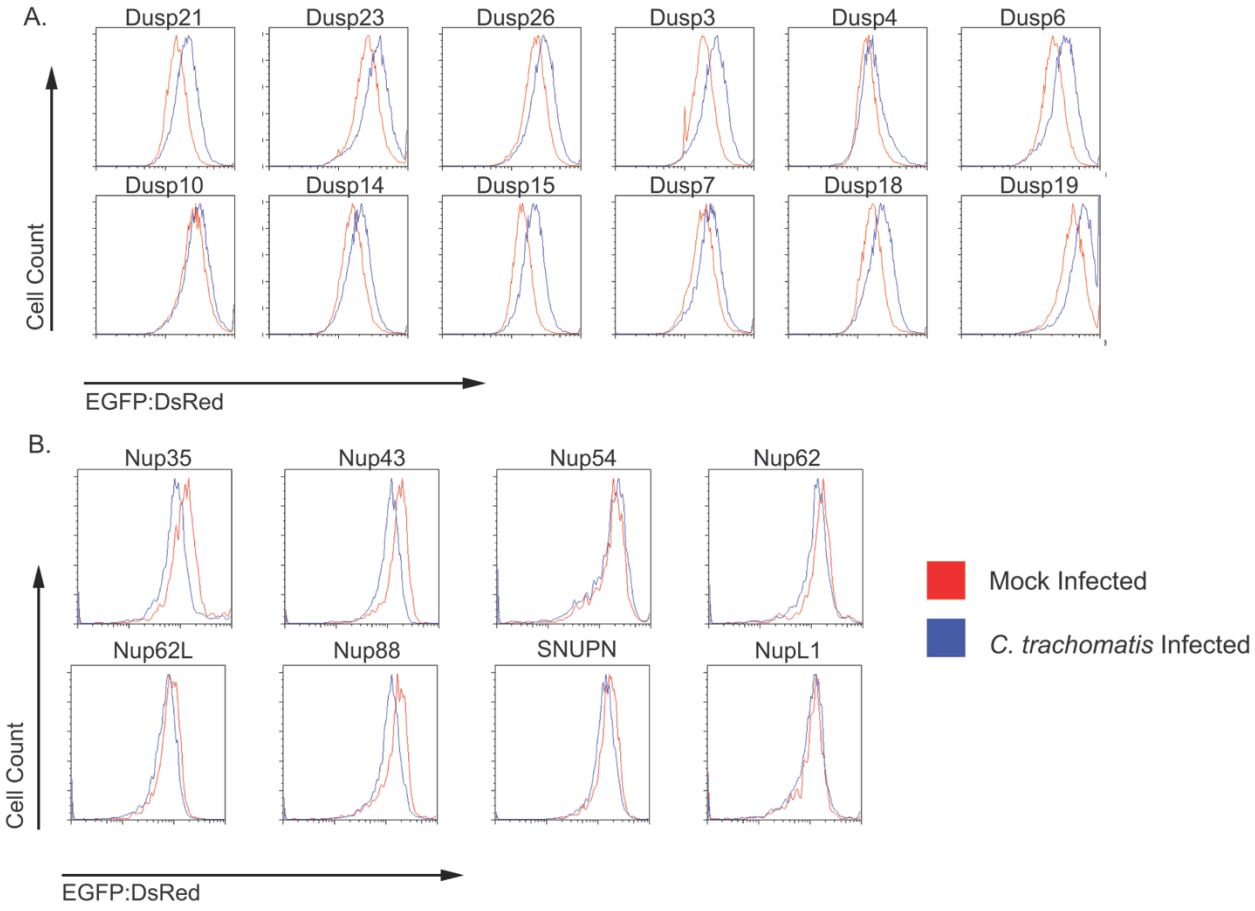

Figure 6-4. Identification of protein families altered broadly during infection using GPS.
A) The entire Dusp family was selected from the ORFeome library and cloned into the GPS vector. 293T cells expressing the indicated ORFs from the Dusp family were made by lentiviral transduction and were analyzed by flow cytometry after 24 hours following infection. Shown are representative plots from one of three independent experiments.
B) The entire Nup family was selected from the ORFeome library and cloned into the GPS vector. 293T cells expressing the indicated ORFs from the Nup family were made using the GPS vector and were analyzed by flow cytometry 24 hours following infection. Shown are representative plots from one of three independent experiments.

Knockdown of a subset of altered host proteins inhibits the growth of *C. trachomatis*

While infection-mediated alterations in the proteome were extensive in the GPS screen, it was unclear which, if any, of these changes were critical for infection to occur normally. We predicted that a subset of host proteins were altered following infection in order for *C. trachomatis* to evade immunity and/or acquire nutrients and therefore might be required for normal growth. To explore the consequences of the host protein changes we uncovered, we sought to functionally "undo" the changes in individual proteins by preventing those changes from occurring following infection. We reasoned that a loss-of-function screen, reducing expression of proteins stabilized following infection, might uncover host factors important for *C. trachomatis* growth and lead us to identify host pathways that could be targeted pharmacologically. We optimized an imaging based siRNA protocol using siRNA targeting PTEN as a positive control and a non-targeting siRNA as a negative control (Figure 6-5A) (39). Cells were transfected with pools of 4 siRNAs for 72 hours, infected with *C. trachomatis*, and subsequently evaluated for growth by measuring the production of infectious progeny (Inclusion forming units, IFU). In triplicate, we conducted a siRNA screen of 200 human genes. Of those, 147 were genes encoding proteins we had identified as stabilized following infection with *C. trachomatis* (and were available to us in a local siRNA library) while the remaining 50 genes were randomly chosen among those we scored as unchanged in the original GPS screen. We hypothesized that siRNA-mediated knockdown of stabilized host proteins might functionally undo *Chlamydia*-driven alterations and identify host proteins that are essential for intracellular replication. We initially found 26 host genes that inhibited *C. trachomatis* growth two-fold or more compared to non-targeting siRNA controls (Figure 6-5B and Table S6-3). Importantly, of the 50 control host proteins we included that were unchanged in their stability following infection, only two reduced *Chlamydia* growth more than two-fold. This suggested that these proteins were host factors needed for bacterial growth (Table S6-3). To validate these findings, we conducted a screen that contained four individual duplexes per gene and identified 13 host

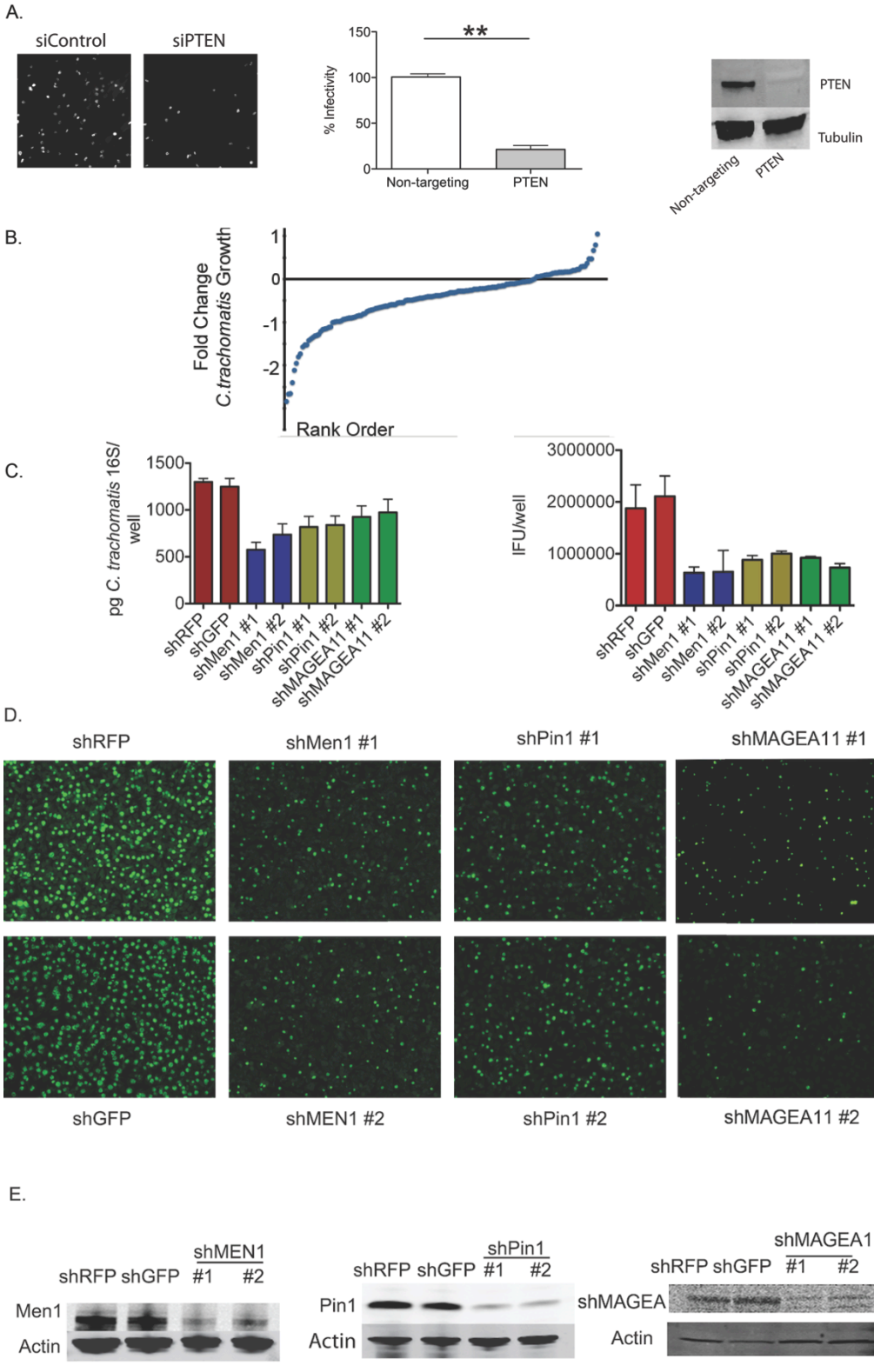

Figure 6-5. Loss-of-function screen of stabilized proteins to identify host factors that alter C. trachomatis growth. A) Optimization of a loss-of-function screen to identify host factors important for *Chlamydia* infection**.** HeLa cells were treated with non-targeting siRNA or siPTEN. Graphs show the mean infectivity relative to the non-targeting siRNA +/- the standard

Figure 6-5 (Continued) deviation (**p<.01)(n=3). Immunoblot analysis of PTEN and tubulin (loading control) after 72 hour treatment with non-targeting siRNA or siPTEN.
B) Distribution of the mean fold-change in *C. trachomatis* IFU production in experimental siRNA knockdown cell lines relative to negative controls.
C) A subset of stable shRNA knockdown cell lines was infected with *C. trachomatis* for 48 hours. Levels of *C. trachomatis* were determined by qPCR of the 16s gene and compared to non-targeting controls (left) and IFU production (right). The graphs show the mean levels of *C. trachomatis* from two independent hairpins from triplicate samples +/- the standard. All experimental hairpins are p<.05 compared to control knockdown by one way ANOVA (n=3).
D) Representative immunofluorescence micrographs from IFU analysis in (D) (Mag 10x) (n=3).
E) Immunoblot analysis to confirm the knockdown of indicated proteins compared to control hairpins. Actin is used as a loading control.
genes that inhibited *C. trachomatis* growth with at least two independent duplexes (Table S6-3).

These data illustrate that a subset of host proteins that were identified as stabilized following infection are required for normal *Chlamydia* growth, and suggests that these are host proteins or pathways that could be targets for host-based therapeutics.

We next wanted to independently confirm that the suppression of a subset of genes identified in our screen would alter *C. trachomatis* growth using an alternative knockdown method. We selected three genes, Pin1, Men1 and MAGEA11 that were stabilized in the GPS screen and created stable knockdown cell lines using two independent lentivirus-delivered shRNAs for each gene of interest or for control genes. Positive transductants were selected with puromycin, and knockdown was confirmed using immunoblot (Figure 6-5E). We then examined the ability of *C. trachomatis* to grow and produce infectious progeny in each knockdown cell line. To differentiate between bacterial replication and infectivity we employed two distinct assays. We used qPCR to examine bacterial replication by quantifying the number of *Chlamydia* genomes present and we also determined the number of infectious progeny produced by titering lysates from infected cells. This allowed us to query the entire *Chlamydia* life cycle, including re-differentiation into EBs from the same samples. When we examined the levels of *C. trachomatis* by qPCR, we found modest but reproducible 1.5-2-fold defects in replication in each knockdown (Figure 6-5C). However, these deficiencies were amplified when we examined the production of infectious progeny, with some knockdowns causing almost a ten-fold reduction in IFU (Figures 6-5C). We also examined the development of inclusions in knockdown cells by fluorescence microscopy. Thirty hours after infection there was no significant difference in the morphology of inclusions between control and experimental knockdown cells. When we quantified inclusion size, there was trend toward smaller inclusions yet no differences reached statistical significance. This suggests that the pathways interacting with these host proteins may be required for late bacterial replication and/or the re-differentiation of RBs to EBs. Together these data confirm that a subset of proteins that are stabilized during infection with *C. trachomatis* are also required for intracellular growth of the pathogen.

AP-1 dependent transcription is activated following infection with *C. trachomatis*

The bioinformatics analysis of the GPS screen showed a strong enrichment in kinase signaling cascades and transcription factors. When we individually examined the role of the 13 genes identified in the loss-of-function screen using natural language processing we also found several genes, including Pin1 and Men1 that directly influence the activation and amplitude of the host transcription factor AP-1 (40-43)(Figure 6-6A). AP-1 is a heterodimeric transcription factor that regulates the expression of a large range of host genes related to inflammation, stress, and cell survival (44). The AP-1 complex is activated following infection with a wide range of bacterial pathogens but its role in *C. trachomatis* intracellular growth has not been described. We first wanted to examine whether AP-1 dependent transcription occurred following infection by *C. trachomatis*. By understanding the timing of AP-1 dependent transcription, we can begin to understand the requirements for upstream host signaling cascades that activate AP-1 and may be needed during *C. trachomatis* growth and development. To determine if AP-1 driven transcription occurs during infection, we used a reporter cell line that expresses EGFP in an AP-1 dependent manner. We mock-treated these reporter cells, treated cells with PMA (a known activator of AP-1 driven transcription), or infected them with *C. trachomatis*. Thirty-six hours after PMA treatment or infection we analyzed cells by flow cytometry in order to determine the levels of EGFP. Relative to controls there was distinct upregulation of EGFP in cells treated with PMA that was even more pronounced in cells infected with *C. trachomatis* (Figure 6-6B). We quantified the mean fluorescence intensity (MFI) of each population, and found a greater than three-fold increase in the MFI of EGFP in cells infected with *C. trachomatis* compared to control cells (Figure 6-6C). These data show that following infection with *C. trachomatis*, AP-1-directed transcription is activated.

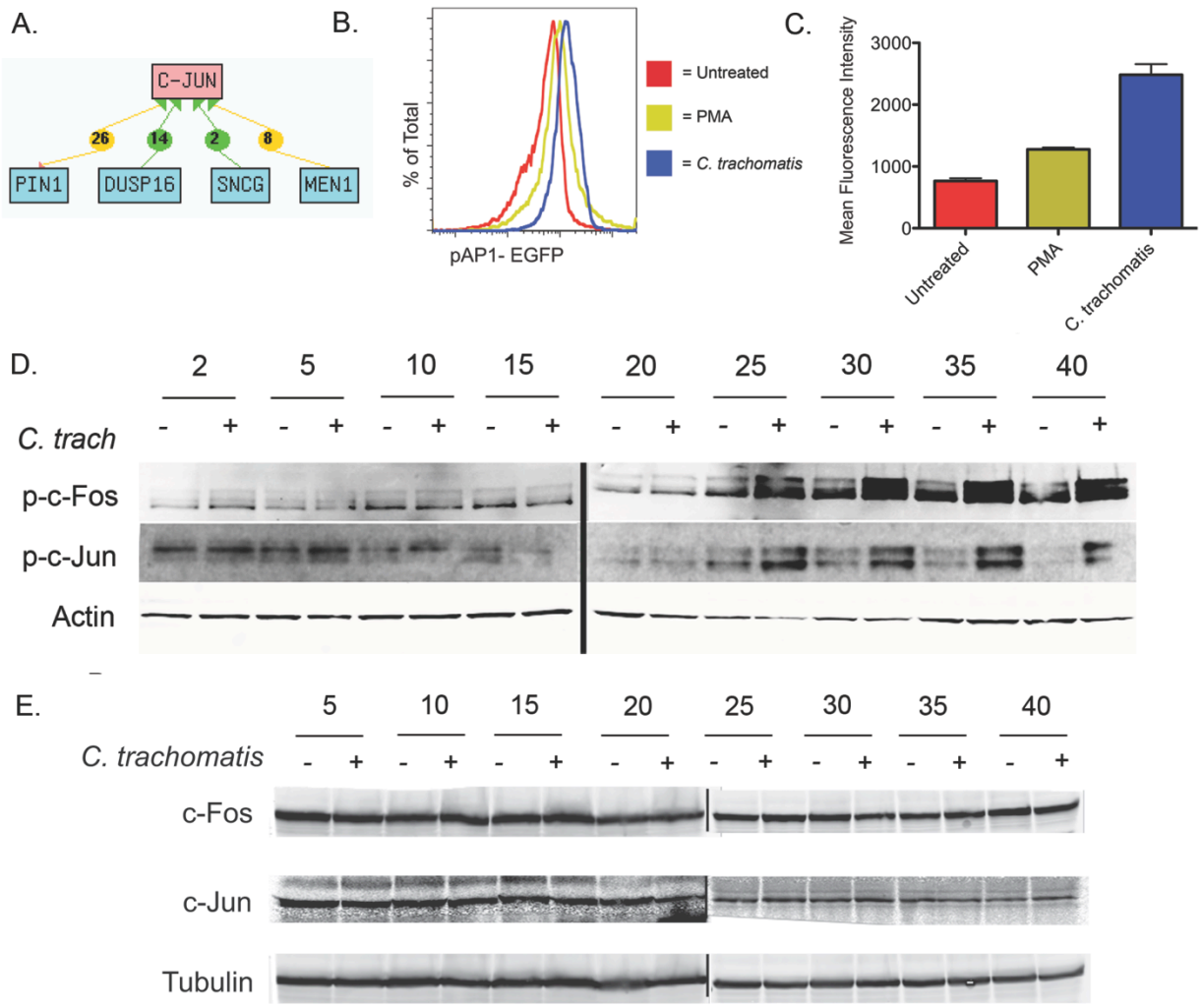

Figure 6-6. The transcription complex AP-1 is activated during *C. trachomatis* infection.
A) Natural language processing of top hits from the loss-of-function screen point towards a role for AP-1 signaling. Chilibot analysis was used in a candidate gene approach to examine interactions of loss-of-function hits and host signaling pathways. Shown are interactions of 4 hits that all interact with c-Jun based on literature analysis. Green arrows mean all sources show positive regulation while yellow means there are differing reports.
B) pAP-1 EGFP reporter cells were mock-infected, infected with *C. trachomatis*, or treated with PMA. Thirty hours later EGFP expression was determined by flow cytometry; A representative plot overlaying the three conditions is shown (n=3).
C) Quantification of the mean-fluorescence intensity for each condition from (A) +/- the standard deviation (n=3). $p<.05$ compared to Mock by two-tailed students t-test (n=3).
D) Immunoblot analysis of and phosphorylated (top) c-Fos and (Bottom) c-Jun in mock-infected HeLa cells or HeLa cells infected with *C. trachomatis* every five hours for 40 hours. Loading was normalized to Actin. Shown is representative blot from one of three independent experiments.
E) Total c-Jun and c-Fos remain unchanged during infection with *Chlamydia*. HeLa cells were infected with *Chlamydia* or mock-infected. At the indicated timepoints cells were lysed and analyzed for total levels of c-Fos and c-Jun. All lysates were normalized using tubulin. Shown is a representative blot from three independent experiments.

One step required for AP-1 dependent transcription is the phosphorylation of AP-1 components including the proteins c-Jun and c-Fos, which leads to direct transcriptional activation of target genes. We next wanted to examine the phosphorylation of both c-Jun and c-Fos over time in cells infected with *C. trachomatis*. We mock-infected or infected HeLa cells with *C. trachomatis* and examined the levels of total and phosphorylated c-Jun and c-Fos by immunoblot every five hours throughout infection (Figure 6-6D). Cells infected with *C. trachomatis* showed minimal phosphorylation of c-Fos or c-Jun for the first 20 hours of infection. However, 20-25 hours after infection, there was a significant increase the phosphorylation of both c-Fos and c-Jun that increased in magnitude through the remainder of the timecourse (Figure 6-6D). When we examined the levels of total c-Jun and c-Fos we found minimal changes in the overall levels of both proteins (Figure 6-6E). These experiments validated our findings using the AP-1 reporter and showed that AP-1 is activated late in host cells infected with *C. trachomatis*.

As mentioned above, our loss-of-function screen identified genes that altered C. *trachomatis* growth and also influence AP-1 signaling (Fig 6-6A). We were curious whether one potential mechanism for *Chlamydia* restriction in these knockdown cells might be alterations in the activation of AP-1. To test this, we mock infected or infected stable control knockdown cells or cells containing shRNA against Men1 or Pin1 with *C. trachomatis* for 40 hours. Cells were then lysed and probed for the activation of AP-1 components by immunoblot. Both shPin1 and shMen1 knockdown cells showed a significant decrease in the phosphorylation of c-Fos and c-Jun (Fig 6-7A) compared to shGFP controls. These data show a direct link between the loss-of-function data and the activation of the AP-1 signaling cascade and suggests one potential mechanism preventing efficient *Chlamydia* growth in these cells.

If AP-1 dependent transcription is required for *C. trachomatis* growth, we hypothesized that upstream signaling components would also be activated during infection. We next wanted to examine what signaling pathways may be modulated by infection in order to activate the AP-1

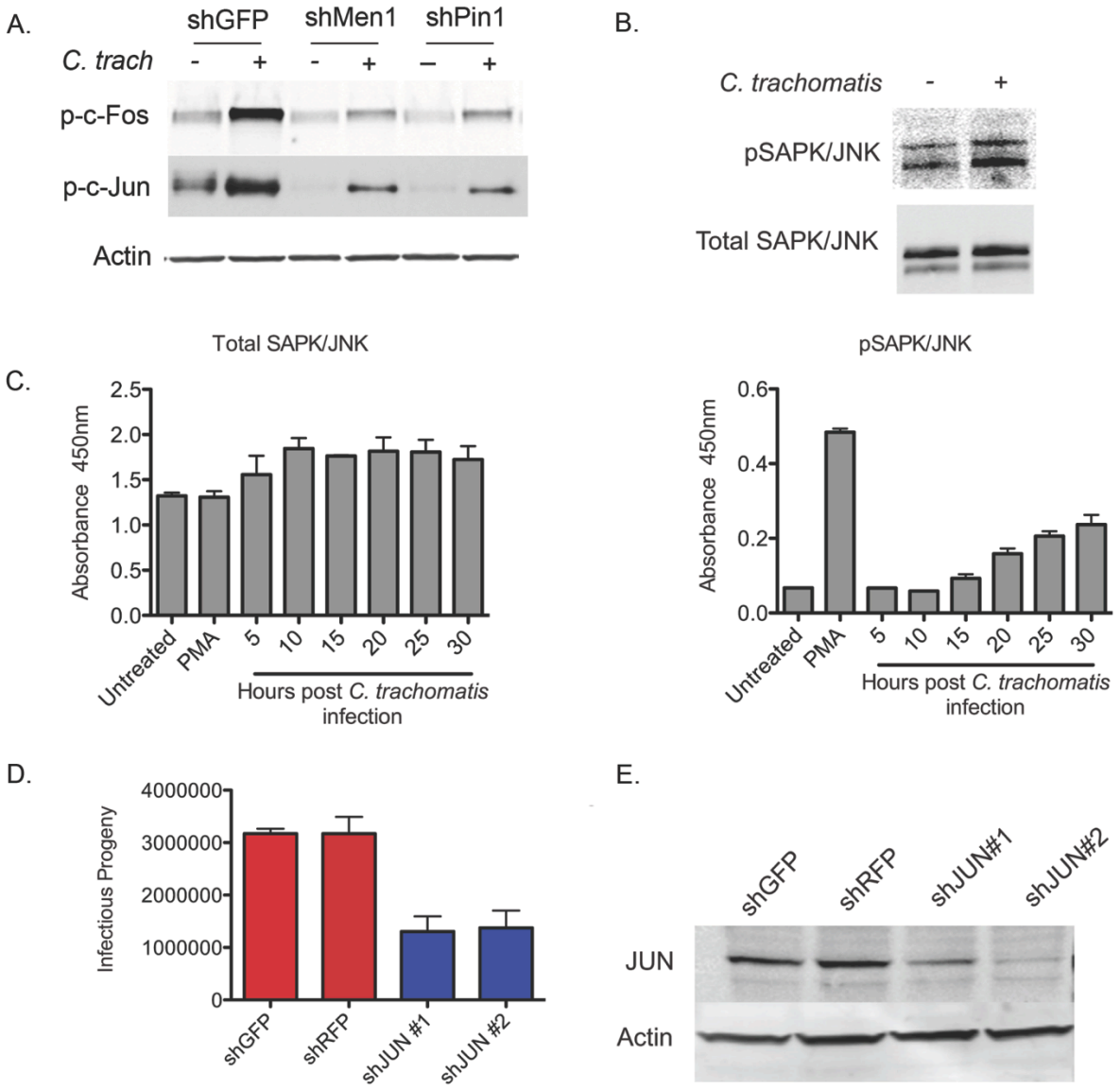

Figure 6-7. Loss of AP-1 activation alters *C. trachomatis* replication.
A) Indicated shRNA knockdown cells were infected or mock-infected with *Chlamydia* for 40 hours. Cells were lysed and the levels of phosphorylated c-Fos and c-Jun were determined by immunoblot. Loading was normalized to host Actin. Shown is a representative blot from three.
B) Immunoblot analysis of cells mock-infected or infected with *C. trachomatis* for 30 hours to determine the levels of total SAPK/JNK (bottom) and phosphorylated SAPK/JNK (top) (n=4).
C) ELISA analysis to determine the levels of total SAPK/JNK (top) and phosphorylated SAPK/JNK (bottom) in cells left untreated, treated with PMA, or infected with *C. trachomatis* for the indicated times. Bars represent standard deviation from triplicate samples from one of two independent experiments.
D) shJUN knockdowns were infected with *C. trachomatis* for 48 hours. Levels of *C. trachomatis* were determined by IFU production and compared to non-targeting control hairpins. The graphs show the mean IFU of *C. trachomatis* produced from triplicate samples +/- the standard deviation for each individual hairpin. All experimental hairpins have $p<.05$ compared to control knockdown by one way ANOVA (n=3).
E) Immunoblot analysis to confirm the knockdown of JUN compared to control hairpins. Actin is used as a loading control.

complex. The MAPK pathways p38, ERK, and JNK, have previously been shown to mediate c-Jun phosphorylation and both p38 and ERK are activated throughout infection with *C. trachomatis* (45, 46). However, one previous study showed that inhibition of ERK and p38 leads to continued c-Jun phosphorylation (46). We hypothesized that the JNK pathway may also play a role in this process. Two previous studies examined JNK activation early following infection with *C. trachomatis* but did not observe activation. However these reports may have overlooked subtle activation of this cascade that occurs later during infection (45, 46). Therefore, we examined JNK activation throughout infection with *C. trachomatis*. We infected HeLa cells with *C. trachomatis* and then lysed the cells at various timepoints. These lysates were then used to perform a sandwich ELISA to detect total levels of SAPK/JNK as well as phosphorylated levels of SAPK/JNK. We found that following infection with *Chlamydia* there was a negligible change in the levels of total SAPK/JNK (Figure 6-7C). However, there was a general accumulation in the levels of phosphorylated SAPK/JNK that increased as infection progressed similar to what was observed with c-Fos and c-Jun (Figure 6-7C). We confirmed these findings by immunoblot and determined that infection with *C. trachomatis* leads to the phosphorylation of SAPK/JNK compared to mock-treated cells (Figure 6-7B). Taken together these data show that infection with *C. trachomatis* induces AP-1 dependent transcription late in the developmental cycle and may be influenced by the JNK signaling cascade.

Since AP-1 complex regulators and robust AP-1 activation were found to be required for normal *Chlamydia* growth, we next directly tested the necessity of AP-1 components for *Chlamydia* replication. We created shRNA knockdowns of c-Jun using two independent hairpins (Figure 6-6E) and compared the production of infective *C. trachomatis* progeny in these cells compared to control shRNA knockdowns (Figure 6-6D). Consistent with the knockdowns of AP-1 regulating components depletion of c-Jun significantly reduced the production of IFU. These data confirm that AP-1 is activated late during infection and required for *C. trachomatis* to efficiently complete its developmental cycle.

AP-1 activation is required for *C. trachomatis* growth *in vitro* and *in vivo*

One goal of the GPS screen was to identify host proteins or pathways that may be targetable by small molecules to inhibit bacterial growth. As shown above, the AP-1 complex is activated during infection with *C. trachomatis* and through loss-of-functions screens we identified that AP-1 activation is required for growth. We hypothesized that pharmacological inhibitors of this pathway might directly inhibit the growth and replication of *C. trachomatis*. To test this we used two distinct inhibitors to prevent AP-1 dependent transcription and determine their effects on *C. trachomatis* growth and development. We used a JNK inhibitor (SP600125) that blocks upstream activation of the AP-1 complex as well as Juglone a specific inhibitor of Pin1, which prevents prolonged amplification of AP-1 dependent transcription (47). Because we found that Pin1 is required for *C. trachomatis* replication by shRNA it suggested Pin1 as a target for inhibition (Figure 6-5). We infected HeLa cells with *C. trachomatis* for one hour then added media containing various concentrations of SP600125, Juglone or the vehicle in which they were prepared (DMSO or EtOH alone) and examined bacterial replication by determining the quantity of *C. trachomatis* genomes present in the samples using qPCR 24 and 48 hours following infection. The presence of either SP600125 or Juglone at concentrations of 1 uM or higher significantly decreased the levels of *C. trachomatis* by qPCR at 48 hours post-infection (Figure 6-9A) yet low concentrations of either inhibitor (100 nM) did not alter *C. trachomatis* growth compared to control treatments. When we examined inclusions in the presences of inhibitors using immunofluorescence microscopy, we noted a significant decrease in the size of inclusions (Figure 6-9B). These data suggest that inhibiting AP-1 activation can directly alter *C. trachomatis* growth.

We next wanted to confirm that both SP600125 and Juglone inhibited the activation of AP-1 components during *Chlamydia* infection. We infected cells with C. *trachomatis* then treated them with vehicle alone, 1uM of SP600125, or 1uM of Juglone. We also included a washout condition for the reversible inhibitor SP600125 to determine if removal allowed recovery of AP-1

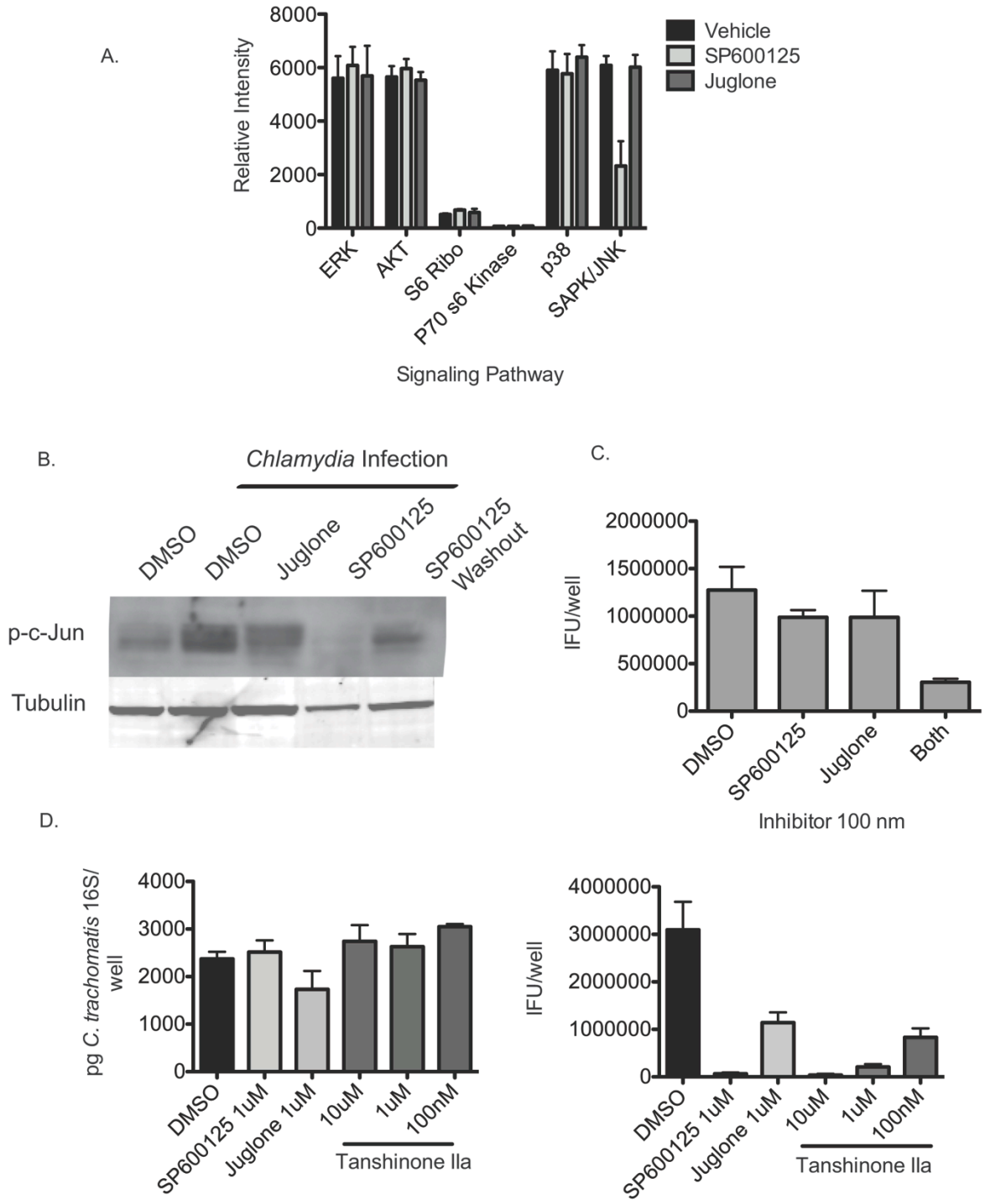

Figure 6-8. Characterization of chemical inhibitors on signaling pathways during *C. trachomatis* infection.

A) HeLa cells were infected with *C. trachomatis* and treated with vehicle alone, SP600125, or Juglone 20 hours post-infection. Thirty hours after infection cells were lysed and applied to PathScan Intracellular signaling arrays in duplicate per condition. Arrays were read and

Figure 6-8 (Continued) analyzed using the Odyssey infrared imaging system. The relative intensity of each spot was calculated using Odyssey software. Shown are the mean fluorescent intensities for each phosphorylated MAPK pathway for all inhibitor conditions +/- the standard deviation.
B) SP600125 or Juglone inhibits the phosphorylation of c-Jun during infection with *C. trachomatis*. HeLa cells were infected with *Chlamydia*, and 10 hours post-infection cells were treated with the indicated inhibitor or vehicle control. For the washout cells were washed 20 hours post-infection to remove the inhibitor. Cells were then lysed 35 hours post-infection and analyzed for total p-c-Jun in cells. Loading was normalized to tubulin. Shown is a representative immunoblot from one of three independent experiments.
C) Combining both inhibitors at low concentrations increases growth inhibition. Cells were infected with *Chlamydia* and treated with the indicated vehicle alone or inhibitor 10 hours post-infection. 40 hours post-infection cells were lysed and titered onto fresh HeLa cells. Shown is the mean IFU produced from each condition from one independent experiment of three (n=4). $p<.05$ for treatment with both inhibitors by one-way ANOVA.
D) AP-1 transcription is needed for *C. trachomatis* growth. Cells were infected Cells were infected with *Chlamydia* and treated with the indicated vehicle alone or inhibitor 10 hours post-infection. Only for Tanshione IIa were multiple concentrations used. 40 hours post-infection cells were lysed and titered onto fresh HeLa cells. 24 hours following re-infection cells were fixed and stained for *C. trachomatis* and the number of inclusions following each treatment was enumerated. (Left) Shown is the mean pg C. trachomatis 16s DNA per condition (n=4). No comparison is significant. (Right)Shown is the mean IFU produced from one independent experiment of three. All conditions $p<.05$ compared to DMSO control by one-way ANOVA.

activation. We examined the phosphorylation of c-Jun by immunoblot 40 hours post-infection for all conditions. In the presence of either SP600125 or Juglone, there was a significant decrease in the phosphorylation of c-Jun compared to the vehicle control, indicating the inhibitors directly alter AP-1 signaling. Importantly, removal of SP600125 20 hours post-infection led to the recovery of c-Jun phosphorylation (Figure 6-8B). In order to examine potential off target effects of these inhibitors we conducted phospho-array analysis of infected lysates in the presence and absence of vehicle alone or inhibitors. We determined that the presence of either 1uM SP600125 or juglone did not alter the phosphorylation state of other major signaling cascades including the MAPK pathways p38 or ERK (Figure 6-8A). While this does not eliminate the possibility of potential off target effects not included in the phosphoarray, it suggests the inhibition of c-Jun phosphorylation is partially dependent on JNK signaling.

We next examined IFU production following treatment with these compounds and found that either inhibitor significantly decreased the production of infectious progeny at all concentrations tested (Figure 6-9C). This was surprising based on our data showing no growth defect as measured by qPCR when using 100 nM concentrations of either inhibitor, yet these data were consistent with those obtained using shRNA knockdowns where the defects in replication were also more pronounced when measured as IFU (Figure 6-5). We further inhibited infectious progeny production by combining both inhibitors even at low concentrations (Figure 6-8C). We next speculated that AP-1 should only be required late in *C. trachomatis* infection in line with our timecourse analysis of activation. In order to test this we first conducted a washout experiment where an inhibitor was removed at certain timepoints after infection. Because Juglone is a non-reversible inhibitor we chose to run these experiments only with the reversible JNK inhibitor. Cells were infected with *C. trachomatis* in the presence of 1 uM SP600125 or DMSO. Ten, 15 or 20 hours after infection the media was removed, cells were washed, and fresh media lacking the inhibitor was added. After allowing the infection to continue to 48 hours, the cells were lysed and the levels of *C. trachomatis* were determined by both

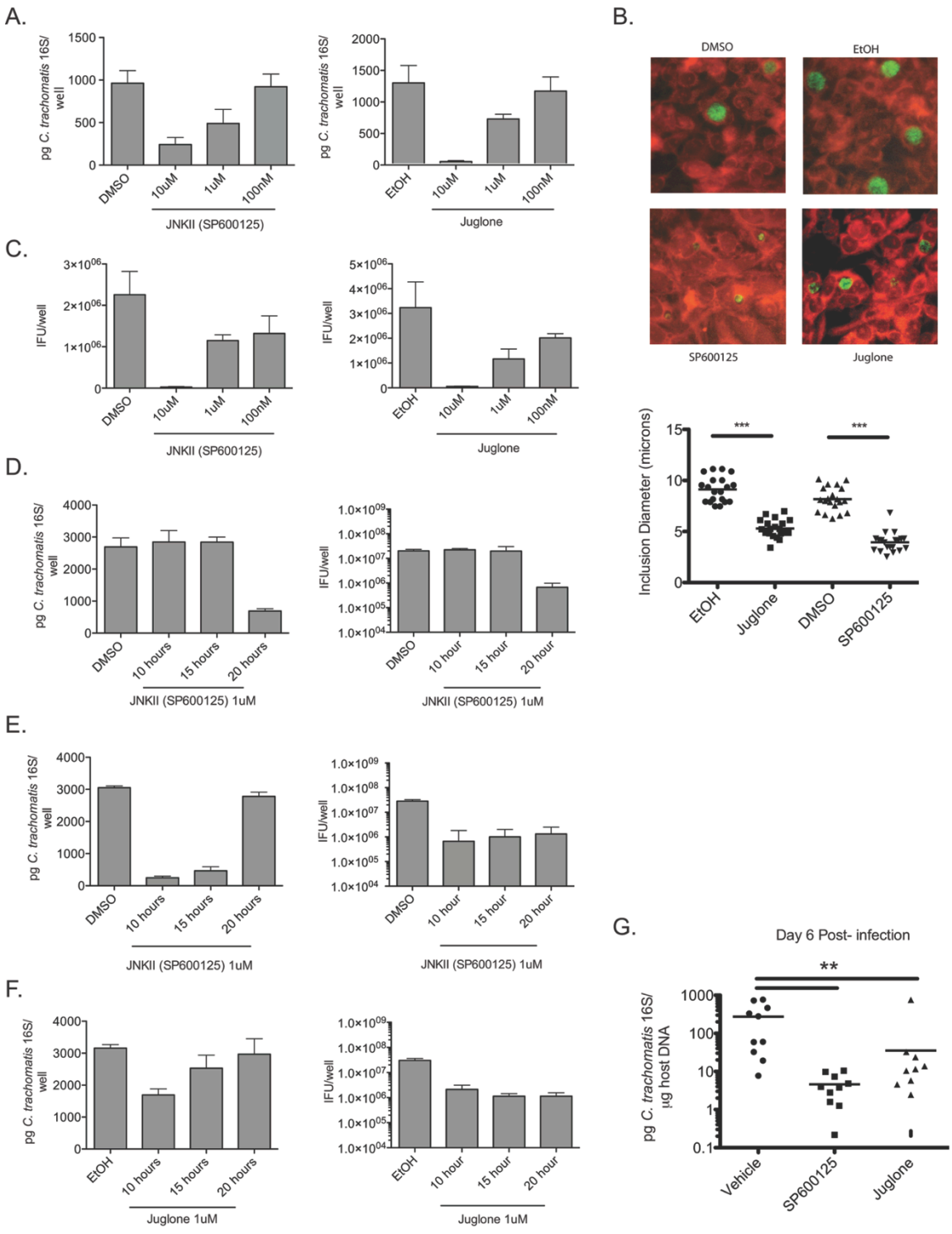

Figure 6-9. Inhibition of AP-1 signaling prevents *C. trachomatis* growth and the production of elementary bodies.
A) HeLa cells were infected with *C. trachomatis* and then treated with the indicated concentration of JNK inhibitor (SP600125), Pin1 inhibitor (Juglone), or vehicle alone (DMSO or EtOH). The number of *Chlamydia* genomes was quantified using qPCR at 48 hours post-infection (n=4).

Figure 6-9 (Continued) B) Infected HeLa cells were treated with vehicle alone or indicated inhibitors and fixed 30 hours post-infection. Cells were stained for *C. trachomatis* major outer membrane protein (MOMP). (Top) Representative images of *C. trachomatis* inclusions treated with DMSO, EtOH, SP600125 or Juglone (1 uM each at Magnification 20x). (Bottom) Quantification of average inclusion diameter following inhibitor treatment. $p<.001$ by students t-test (n=2).
C) Production of IFU from cells infected with *C. trachomatis* then treated with the indicated inhibitors for 48 hours (n=4).
D) HeLa cells were infected with *C. trachomatis* and then treated with SP600125. At the indicated times post-infection, the inhibitor was removed and replaced with fresh media. *C. trachomatis* levels were determined by qPCR (Left) and IFU analysis (Right) 48 hours post-infection (n=3).
E) HeLa cells were infected with *C. trachomatis* and at the indicated timepoints were treated with SP600125. 48 hours post infection cells were lysed and the levels of *C. trachomatis* were determined by qPCR (Left) and IFU analysis (Right) (n=3).
F) HeLa cells were infected with *C. trachomatis,* and then at the indicated timepoints the cells were treated with Juglone. 48 hours post infection cells were lysed and the levels of *C. trachomatis* were determined by qPCR (Left) and IFU production (Right).
In all experiments the graphs represent the mean level of *C. trachomatis* +/- the standard deviation (n=3).
G) Mice were infected transcervically with 10^6 IFU of *C. trachomatis*. Twenty-four, 48 and 72 hours post-infection mice were treated with indicated inhibitors or vehicle alone. Six days after infection the levels of *C. trachomatis* were determined using qPCR. Graphs show bacterial levels in individual mice and mean distribution for each treatment group $p< 0.01$ (n=2).

qPCR and determination of IFU (Figure 6-9D). When we removed the inhibitor as late as 15 hours post-infection we found no effect on *C. trachomatis* growth or IFU production. However, if we removed the inhibitor 20 hours following infection, we saw a profound defect in *Chlamydia* levels and IFU production. These data suggest that AP-1 dependent transcription is not required early in *C. trachomatis* infection, yet it is required by 20 hours post-infection.

As a complement to these experiments we next wanted to determine the effect of adding inhibitors at certain time points after infection. Cells were infected with *C. trachomatis* and SP600125, Juglone, or vehicle alone were added 10, 15 or 20 hours post-infection. Forty-eight hours after infection, the cells were lysed and we determined the levels of *C. trachomatis* by qPCR and by measuring IFU (Figure 6-9E and 6-9F). Similar to the washout experiment, addition of either SP600125 or Juglone to infected cells at 10 or 15 hours post-infection reduced *C. trachomatis* levels and IFU production. Interestingly, addition of either inhibitor 20 hours post-infection had a negligible effect on the growth of *C. trachomatis* by qPCR yet caused a significant decrease in the production of IFU, similar to the defect seen following inhibitor addition at earlier timepoints. These data show that AP-1 signaling is required for efficient *C. trachomatis* growth *in vitro*.

It remained possible that the activation of AP-1 components, but not AP-1 mediated transcription, was all that was required for *Chlamydia* growth. To examine whether AP-1 mediated transcription was also required for intracellular survival we employed a third inhibitor, Tanshinone IIa, which allows AP-1 phosphorylation but prevents DNA binding and subsequent transcriptional activity (48). Cells were infected with *C. trachomatis* for 20 hours then treated with various concentrations of Tanshione IIa to limit the time of inhibitor treatment. Cells were then lysed at 48 hours post-infection and bacterial levels and the production of infectious progeny were determined by qPCR and IFU analysis respectively. We saw minimal defects in bacterial growth by qPCR but observed a significant inhibition in the production of infectious progeny in a dose-dependent manner (Figure 6-8D). These data show that preventing AP-1

mediated transcription directly inhibits the ability of *Chlamydia* to complete the developmental cycle.

We next wanted to determine whether activation of this pathway would also be required for *C. trachomatis* growth *in vivo*. We have recently described a murine model of *C. trachomatis* infection that allows the use of human *Chlamydia* strains in mice, and recapitulates many aspects of human disease in the upper genital tract (49). Using this model we infected mice transcervically with *C. trachomatis* and 24, 48 and 72 hours post-infection mice were treated with vehicle alone, SP600125, or Juglone by both IP injection and transcervical application. Six days post-infection, mice were sacrificed, the upper genital tract was isolated, and the burden of *C. trachomatis* in the tissue was determined using qPCR. Treatment of mice with either SP600125 or Juglone led to a 10-100 fold decrease in the levels of *C. trachomatis* in the upper genital mucosa compared to vehicle alone (Figure 6-9G). This suggests that *C. trachomatis* requires AP-1 dependent signaling in order to survive in the murine upper genital mucosa. Together these results show that *C. trachomatis* manipulates host signaling cascades that are required for bacterial growth both *in vitro* and *in vivo*.

Discussion

During infection with intracellular pathogens, the host proteome is broadly remodeled (12). However, changes in host protein stability during bacterial infection have not previously been evaluated globally. Most studies focusing on host alterations following *C. trachomatis* infection have examined only transcriptional changes (50). Here we employed systematic methodology to globally identify host proteins that were altered in stability following infection with *C. trachomatis*, characterized which of these host proteins were necessary for growth, and identified host pathways that are necessary for normal infection to occur.

In this report we applied GPS, a system designed to identify substrates of human ubiquitin ligases, to evaluate how infection with a bacterial pathogen directly alters host protein stability. Investigators studying various aspects of mammalian cell biology commonly use ORFeome-based screens to understand how global dynamics change following specific perturbations (30). Our study takes advantage of the human ORFeome as a resource to understand bacterial pathogenesis by evaluating over 12,000 proteins simulatenously. Using the GPS platform we uncovered a dramatic shift in the host proteome that occurs during *C. trachomatis* infection. The GPS platform is also lysis independent and is not subject to potential post-lysis effects of the *Chlamydia* protease CPAF that have recently been described (51). By coupling the global coverage of ORFeome screens with a systematic validation scheme we identified a large number of host proteins that are altered in stability following *C. trachomatis* independently of changes in host transcription and may be required for bacterial growth.

The proteins we identified are involved in a wide-range of host cell functions, revealing new insights into how *C. trachomatis* alters the host in order to successfully replicate. The GPS platform identified host proteins such as Mcl1 that were previously shown to be stabilized during *C. trachomatis* infection and uncovered host cell processes, such as histone modifications and the Golgi functions that are known to be altered during infection with *Chlamydia* (34, 36-38, 52). This shows that GPS is well suited to identify *C. trachomatis*-

mediated alterations to host proteins that occur independently of host transcription. We further used bioinformatics analysis along with focused GPS experiments to uncover entire protein families such as Dusps and Nups that were altered in concert during infection. Among proteins that are stabilized during infection we identified a strong enrichment in host transcription pathways, nuclear components, and vesicular trafficking (Table S6-2). We also found that mitochondrial and ubiquitin related proteins were enriched among destabilized proteins. While it remains unclear whether these host cell processes are directly or indirectly altered during infection, it suggests *Chlamydia* infection broadly disrupts host cell functions. Future studies will be required to uncover the mechanisms underlying individual protein changes as well as identify specific *Chlamydia* virulence determinants that target particular host cell functions. For example, while Golgi fragmentation occurs following infection and is necessary for normal *C. trachomatis* growth, we still do not understand bacterial proteins driving this cellular change (36, 51). Several strong hits in the GPS screen were golgi proteins including Golga2 and Golga4. This highlights the functionality of the GPS system as a possible screening platform to identify (through gain-of-function approaches) *C. trachomatis* effector/s that are responsible for golgi fragmentation. Future work will be focused on applying these technologies to better understand the host targets of individual virulence determinants that *Chlamydia* secretes into host cells in order to infect cells and promote intracellular growth.

In order to elucidate potential host pathways that may regulate *C. trachomatis* infection we combined bioinformatics analysis and a loss-of-function screen to suppress individual host proteins identified through GPS. We identified a subset of host proteins that are required for *C. trachomatis* growth (Figure 6-5). In exploring intracellular survival of *Chlamydia*, our bioinformatics analysis of the GPS screen and natural language processing analysis of the loss-of-function screen pointed towards a critical role of MAPK signaling and specific host transcription factors including AP-1. Therefore we focused our attention on AP-1 activation and

function throughout *Chlamydia* infection. When we inhibited AP-1 activation using a JNK inhibitor (SP600125) or a Pin1 inhibitor (Juglone) throughout infection, we saw a dramatic decrease in *C. trachomatis* growth. Using add-in and washout experiments we further showed that AP-1 activity is required later than 20 hours after infection in order for normal IFU production to occur. One of the most intriguing findings was that addition of either inhibitor later during infection had dramatic effects on IFU production. This suggests that AP-1 activity may be required for RB replication and/or re-differentiation into the EB form. One might imagine that the intracellular growth of *C. trachomatis* might trigger host stress responses, and that *C. trachomatis* may have mechanisms that sense these host stress pathways to initiate differentiation and exit from the failing host cell.

The AP-1 complex is a critical transcription factor that regulates the expression of a large range of host genes in response to diverse stimuli (44). The AP-1 complex is targeted by several bacterial pathogens to alter cellular survival or prevent inflammation and cytokine production, with some pathogens preventing activation and some inducing activation of host signaling cascades (53). However, it has not previously been shown to play a role during *C. trachomatis* infection (54). Previous studies have shown both ERK and p38 MAPK activation is required for a normal pro-inflammatory cytokine response during *Chlamydia* infection (54, 55). We confirmed that AP-1 activation occurs during infection with *C. trachomatis* and found a role for the JNK signaling cascade in this process. Even though previous reports have not observed JNK activation during *C. trachomatis* infection, these studies only examined early timepoints and were focused on IL-8 signaling, not bacterial growth (54). Our results show that JNK is activated late in infection, albeit less robustly than ERK (data not shown). This may explain why the JNK signaling cascade has been overlooked as playing a role in *C. trachomatis* pathogenesis. Interestingly, a recent report using *C. pneumoniae* suggested that AP-1 activation is responsible for inflammation seen *in vivo* (56). While the effect of AP-1 on inflammation during infection *in vivo* remains to be confirmed for *C. trachomatis*, these data together suggest

that finely tuned AP-1 signaling is required for robust intracellular growth. Our current model speculates that too much AP-1 activation and the inflammation may overwhelm bacterial growth while too little signaling prevents the production of infectious progeny. We hypothesize that AP-1 activity influences *Chlamydia* growth through either the induction of specific gene product/s that are required by *Chlamydia*, or by altering the overall cellular state which in turn triggers final *Chlamydia* replication and re-differentiation. Future studies are required to elucidate the mechanisms underlying *Chlamydia* dependence on AP-1 as well as to better understand the balance between AP-1 dependent bacterial survival and inflammation *in vivo*.

Overall, the methods described here are widely applicable to a variety of pathogens and can also be adapted to examine less dramatic perturbations to host cells. For example, comparing changes in host proteins altered only in the presence of specific secretion systems, such as a type III secretion system, should enrich for host protein changes altered directly by the secreted effectors of the system. GPS screens can also be used to examine changes to the host proteome resulting from the expression of a single virulence determinant. This may allow the identification of substrates notoriously difficult to identify such as E3 ubiquitin ligases or deubiquitinating enzymes (12, 16, 57, 58). Examining how pathogens (or commensals) directly alter the host proteome is essential to understanding basic mechanisms of bacterial-host cell interactions. It also may drive the development of novel therapeutics that target host functions required for growth of pathogens, resulting in antimicrobials that will have less impact on natural flora and where drug resistance would not develop.

Materials and Methods

Tissue Culture, Reagents, and General Procedures HeLa, and 293T cells were maintained in Dulbecco's Minimum Essential Media supplemented with Penicillin/Streptomycin and 10% fetal bovine serum (Invitrogen). 293T and HeLa cells were transfected using the TransIT transfection reagent (Mirus). Lentiviruses were packaged in 293T cells transfected with the plasmid of interest as well as plasmids expressing VSVg and Gag-Pol-Rev (Luo et al., 2009). Viral infections were supplemented with hexadimethrine bromide at a concentration of 8 µg/ml. Transfection of siRNA oligonucleotides was performed with Dharmafect (Dharmacon) lipid transfection reagent according to the manufacturer's protocols. siRNA were purchased from Dharmacon as smart pools. A complete list of immunological reagents used in this study is below. Flow cytometry was performed on a BD-LSRII Flow Cytometer (Becton Dickinson). Data were collected using BD FACS Diva software (Becton Dickinson) and analysis was performed using FloJo software.

Validation was performed by individually picking ORFeome clones and cloning them using gateway recombination into the GPS vector. All inserts were sequenced using the primer: 5'-AGCTGTACAAGTCCGAACTCGT-3'. The vectors were used to package virus and used to generate cell lines expressing individual GPS-ORFs. For immunoblot validation of endogenous proteins after *Chlamydia* infection, cells were lysed at the indicated time points.

EBs of *C. trachomatis* serovar L2 434/Bu were propagated within McCoy cell monolayers. A combination of glass bead disruption and sonication was used to release EBs from infected McCoy cells. EBs were further purified by ultracentrifugation over Renograffin gradients, as previously described (15). Aliquots of *C. trachomatis* EBs were stored at -80° C in SPG buffer (250 mM sucrose, 10 mM sodium phosphate, and 5 mM L-glutamic acid, pH 7.2). Prior to infection with *C. trachomatis*, cells were cultured for 12-24 h in their respective media minus antibiotics. Cells were infected with *C. trachomatis* by

adding media containing dilute EBs to host cells. Centrifugation was not used unless specified in the text. The multiplicity of infection (MOI) used for *C. trachomatis* was 3:1 unless indicated. DMEM alone was used for mock-infected cells.

Immunoblot analysis. For immunoblot analysis, cells were lysed at indicated timepoints following infection in Urea lysis buffer unless otherwise indicated (8M Urea, 150 mM NaCl, 0.1% NP-40) in the presence of a complete protease inhibitor cocktail (Roche Applied Science, Indianapolis, IN) and phosphatase inhibitor (Cell Signaling). Lysates were normalized for total protein content by measuring absorption at 280 nm or using a BCA test (Pierce). Normalized samples were subjected to SDS-PAGE analysis (BD and Lonza), transferred to nitrocellulose or PVDF (Licor), and immunoblotted with the following antibodies:

Actin (Licor), BNIP3L (AbCam), Ciao1 (AbCam), Dusp16 (AbCam), JNK (Cell signaling), p-JNK (Cell signaling), Jun (Cell signaling), p-JUN (Cell Signaling) Men1 (AbCam), Ncap-G (Santa Cruz), Pin1 (Cell Signaling), PTEN (AbCam), SNCG (AbCam), Stk24 (AbCam), Tubulin (Licor), USH1C (AbCam)

Automated image analysis. Infected cells were fixed and permeabilized with MeOH and stained for *Chlamydia* MOMP (FITC-MOMP, BioRad) for 1 hour. Stained cells were imaged with a Cellomics ArrayScan VTI automated microscope. Six fields per well of a 96-well plate were imaged at 20x magnification. First, cells were identified by their nuclei staining in channel 1 of Cellomics. Cells that scored positive in channel 1 were analyzed for Alexa-488 (inclusions) in channel 2. A minimum average intensity in the Alexa-488 channel was calculated by manual inspection and applied to each selected object. The selected objects that were above this threshold were shown in blue while those that were below are shown in orange. Once the threshold was determined, all of the plates were subjected to data analysis using vHCS Scan Target Activation software v5.1.2. Data were obtained by using vHCS View software and the number of inclusions in the well was identified as “valid object count” (VOC).

Immunofluorescence analysis. Cells were seeded on coverslips in 24 well dishes. The next day cells were infected with *C. trachomatis* at an MOI of 3. 24 hours following infection cells were fixed using paraformaldehyde and permeablized using .1% tween in PBS. We then stained cells with anti-*Chlamydia* antibody linked to FITC and DAPI. Cells were analyzed at 20x using a NIKON Eclipse 200. At least 10-20 images were captured per coverslip. We then analyzed the average diameter of inclusions using imageJ analysis.

Quantitative PCR. To assess the levels of *C. trachomatis* present, we used a previously described qPCR method (59). Briefly, we isolated nucleic acid from infected cells using the DNeasy kit (Qiagen). *Chlamydia* 16S DNA was quantified by qPCR on an ABI Prism 7000 sequence detection system using primer pairs and dual-labeled probes. Using standard curves from known amounts of *Chlamydia* the levels of 16s DNA per well was calculated. For *in vivo* experiments the upper genital tract was isolated and DNA was isolated and the levels of *C. trachomatis* were determined relative to levels of host DNA as described previously (49).

AP-1 complex activation. For examination of AP-1 dependent transcription an AP-1 driven EGFP reporter cell line was created using pre-made Lentivirus (SAbioscience). After puromycin selection cells were infected or treated PMA and examined by flow cytometry using a FACs Calibur (BD). Plots were analyzed using FlowJo software.

JNK and p-JNK Activation. Cell lysates from cells infected for the indicated times were used as samples in a sandwich ELISA to detect levels of total JNK and p-JNK following infection (Cell Signaling). The manufacturer instructions were followed. Samples were tested for their absorbance 450 nm.

Chemical Inhibitors. The JNK inhibitor (SP600125) and Pin1 inhibitor (Juglone) were purchased from EMD Millipore for pathway analysis and used at the indicated concentrations. Tanshione IIa was purchased from (Santa Cruz). For *in vitro* experiments Juglone was resuspended in EtOH, for *in vivo* experiments Juglone was resuspended in DMSO. SP600125

and tanshione IIa were dissolved in DMSO for all experiments. Vehicle controls contain the appropriate solvent for each experiment.

Phospho-Array. Cells infected with *C. trachomatis* for 20 hours were treated with vehicle alone, SP600125, or Juglone for 10 hours. Cells were processed and the arrays were conducted by following manufacturers directions for the Pathscan Intracellular Signaling Array Kit (Cell Signaling). Arrays were scanned and quantified using an Odyssey Infrared Imaging system and software (LiCor).

siRNA Screen. siRNA smart pools were cherry picked into 96 well plates from the complete Dharmacon siRNA genome set at the Harvard Institute of Chemistry and Cell Biology (ICCB). The outer wells of each plates were excluded. Each plate contained 6 non-targeting controls and 6 positive controls used to optimize the assay. HeLa cells were seeded at a density of $2.5x10^3$ into 96-well plates. Each siRNA was transfected in triplicate for 72 hours. Cell viability was examined at 72 hours and scored on 0-5 scale (0=all cells dead 5=no obvious cell death). Cells that scored 2 or less were not analyzed further. Cells were then infected with 10^4 IFU of *C. trachomatis* for 48 hours. Cells were then lysed and dilute 1:1000 and re-seeded into 96 well plates containing 10^4 normal HeLa cells. Twenty-four hours following infection, cells were fixed with ice-cold MeOH for 30 minutes. Cells were washed two times with PBS containing 0.1% tween. Cells were then stained using DAPI and an antibody to *C. trachomatis* MOMP. Cells were quantified by automated microscopy as described above. The mean number of IFU produced by non-targeting controls for each plate was calculated. A fold-change in *C. trachomatis* growth was calculated against non-targeting mean for each plate. A mean fold-change was then calculated for all triplicate samples. Cells that inhibited growth more than 2-fold were picked for a deconvolution screen. Individual shRNA(2 per gene) were then purchased from the TRC library. Lentiviral particles were packaged transduced and selected as above. The identical infection protocol was used as described above.

GPS Screen. The GPS screen was conducted essentially as described (Yen et al., 2008). Cells

were mock-infected or infected with *C. trachomatis* for 24 hours. Infection was confirmed visually by the presence of inclusions in almost all cells. The general workflow of the GPS screen is as follows. 293T cell libraries were sorted into either 7 bins, based on their EGFP/DsRed ratio. Approximately equal numbers of cells were sorted into each bin, with the outermost bins receiving slightly fewer cells than those in the middle. We sorted a minimum of 1.2 million cells per bin. Sorting was carried out at the Immune Diseases Institute at Harvard Medical School with the assistance of Natasha Barteneva. Following sorting, cells were pelleted and frozen at −80°C. Pellets were subsequently thawed and lysed in 10 mM Tris pH 8.0, 10 mM EDTA, 0.5% SDS, and 0.2 mg/ml Proteinase K at 55°C overnight with agitation. Genomic DNA (gDNA) was extracted using Phaselock tubes with phenol:chloroform and then chloroform. RNase A was added to a final concentration of 25 µg/ml and following incubation overnight at 37°C, gDNA was extracted using Phaselock tubes, as above. DNA was ethanol precipitated (with glycogen), recovered by centrifugation, and washed three times with 75% ethanol. The dried, resuspended pellet was PCR amplified with Takara hot start polymerase (Takara RR006B) using common PCR primers as described (Yen and Elledge, 2008). PCR amplified DNA was transcribed with T7 using Ambion MEGAscript and purified with Qiagen RNeasy kits. RNA was labeled with a ULS labeling kit (Kreatech: unsorted samples-Cy5, sorted samples-Cy3). Hybridization was performed on custom Agilent DNA microarrays printed as 4 x 44k arrays according to manufacturer's protocols. The probe sequences used are listed in the supplemental table. Microarrays were read using an Agilent scanner. The GPS screen was performed using version 3.1 of the ORFeome collection. PSI was calculated as described (Yen et al., 2008). Percent shift was calculated by summing absolute values of the subtracted relative abundance from probes across all bins.

GPS Data Analysis. Probes were first filtered by removing probes with signals below five-time the average background signal. Probes with signals less than zero were reset to zero.

Microarrays from each bin were normalized within each screen based on their spike-in control signals. After filtering low signal probes and normalizing, we examined the EGFP signals for all probes within a single bin between treated and untreated conditions for every bin to confirm probe and hybridization reliability. We next calculated the PSI for each probe and compared those between treated and untreated conditions. These numbers are reported in the supplementary table. The average PSI of all probes, for each condition, was determined and normalization was performed as necessary. A ΔPSI was calculated by subtracting the PSI numbers of the uninfected from those of the infected. We rank ordered probes based on ΔPSI and used a custom macro in Microsoft Excel to graph the distribution for every probe across bins, comparing infected and uninfected conditions on each graph, for every probe that passed our low signal cut-off (Table S6-1). We have included a blank excel file with the coding for this macro as supplementary table S6-4. Visual inspection of the graphs was essential for high validation rates and to easily discriminate against hits that are influenced by noise seen in microarray studies. Graphs were ranked based on the ΔPSI and were visually inspected one at a time to determine if there was a significant probe shift. We have listed those ORFs that had a sufficient ΔPSI and passed visual inspection. We often found that a high ΔPSI could be attributed to erroneous noise in outside bins, making visual inspection essential. Genes that showed a significant shift from multiple probes (when available) were designated for further study and are listed in Table S6-1 worksheet 2.

Bioinformatic Analysis. We used DAVID bioinformatics resources to identify enriched annotation clusters within the GPS dataset as done previously (33). We uploaded our stabilized and destabilized protein lists independently into DAVID and used the human proteome as the background list. We used cluster analysis to identify redundant enriched terms for each group through several categories including KEGG pathway and Gene Ontology terms. We listed the top enriched clusters including enrichment scores and genes identified in Table S6-2.

We also used natural language processing analysis in a candidate gene approach to identify connections in the published literature among genes found in the loss-of-function screen as done by others previously (43). We used Chilibot freeware and searched for interactions between c-Jun and loss-of-function hits and create a graphic representation of these interactions (60).

Mice and *in vivo* inhibitor treatment

C57BL/6 were purchased from The Jackson Laboratory and were maintained and cared for within the Harvard Medical School Center for Animal Resources and Comparative Medicine (Boston, MA). All mice were treated with 2.5mg of medroxyprogesterone subcutaneously seven days prior to infection in order to normalize the murine estrous cycle. Mice were infected transcervically with 10^6 IFU of *C. trachomatis*. For inhibitor treatments mice were injected IP and transcervically with vehicle alone, 10 mg/kg of SP600125 per injection route (61), and 1 mg/kg of Juglone per injection route (62) similar to previous studies. All experiments were approved by Institutional Animal Care and Use Committee. In all experiments ten mice per group were used.

References

1. Ashida H, Ogawa M, Kim M, Mimuro H, Sasakawa C. Bacteria and host interactions in the gut epithelial barrier. Nature chemical biology. 2012;8(1):36-45. Epub 2011/12/17. doi: 10.1038/nchembio.741. PubMed PMID: 22173358.

2. Ham H, Sreelatha A, Orth K. Manipulation of host membranes by bacterial effectors. Nature reviews Microbiology. 2011;9(9):635-46. Epub 2011/07/19. doi: 10.1038/nrmicro2602. PubMed PMID: 21765451.

3. Rohmer L, Hocquet D, Miller SI. Are pathogenic bacteria just looking for food? Metabolism and microbial pathogenesis. Trends in microbiology. 2011;19(7):341-8. Epub 2011/05/24. doi: 10.1016/j.tim.2011.04.003. PubMed PMID: 21600774; PubMed Central PMCID: PMC3130110.

4. Ge J, Shao F. Manipulation of host vesicular trafficking and innate immune defence by Legionella Dot/Icm effectors. Cellular microbiology. 2011;13(12):1870-80. Epub 2011/10/11. doi: 10.1111/j.1462-5822.2011.01710.x. PubMed PMID: 21981078.

5. Cornelis GR. The type III secretion injectisome, a complex nanomachine for intracellular 'toxin' delivery. Biological chemistry. 2010;391(7):745-51. Epub 2010/05/21. doi: 10.1515/BC.2010.079. PubMed PMID: 20482311.

6. Bingle LE, Bailey CM, Pallen MJ. Type VI secretion: a beginner's guide. Current opinion in microbiology. 2008;11(1):3-8. Epub 2008/02/22. doi: 10.1016/j.mib.2008.01.006. PubMed PMID: 18289922.

7. Barry AO, Mege JL, Ghigo E. Hijacked phagosomes and leukocyte activation: an intimate relationship. Journal of leukocyte biology. 2011;89(3):373-82. Epub 2010/08/20. doi: 10.1189/jlb.0510270. PubMed PMID: 20720162.

8. Cossart P, Roy CR. Manipulation of host membrane machinery by bacterial pathogens. Current opinion in cell biology. 2010;22(4):547-54. Epub 2010/06/15. doi: 10.1016/j.ceb.2010.05.006. PubMed PMID: 20542678; PubMed Central PMCID: PMC2975266.

9. McDermott JE, Corrigan A, Peterson E, Oehmen C, Niemann G, Cambronne ED, et al. Computational prediction of type III and IV secreted effectors in gram-negative bacteria. Infection and immunity. 2011;79(1):23-32. Epub 2010/10/27. doi: 10.1128/IAI.00537-10. PubMed PMID: 20974833; PubMed Central PMCID: PMC3019878.

10. Galan JE. Common themes in the design and function of bacterial effectors. Cell host & microbe. 2009;5(6):571-9. Epub 2009/06/17. doi: 10.1016/j.chom.2009.04.008. PubMed PMID: 19527884; PubMed Central PMCID: PMC2729653.

11. O'Connor TJ, Adepoju Y, Boyd D, Isberg RR. Minimization of the Legionella pneumophila genome reveals chromosomal regions involved in host range expansion. Proceedings of the National Academy of Sciences of the United States of America. 2011;108(36):14733-40. Epub 2011/08/30. doi: 10.1073/pnas.1111678108. PubMed PMID: 21873199; PubMed Central PMCID: PMC3169125.

12. Ribet D, Cossart P. Pathogen-mediated posttranslational modifications: A re-emerging field. Cell. 2010;143(5):694-702. Epub 2010/11/30. doi: 10.1016/j.cell.2010.11.019. PubMed PMID: 21111231.

13. Burrack LS, Higgins DE. Genomic approaches to understanding bacterial virulence. Current opinion in microbiology. 2007;10(1):4-9. Epub 2006/12/13. doi: 10.1016/j.mib.2006.11.004. PubMed PMID: 17161645.

14. Arbibe L, Kim DW, Batsche E, Pedron T, Mateescu B, Muchardt C, et al. An injected bacterial effector targets chromatin access for transcription factor NF-kappaB to alter transcription of host genes involved in immune responses. Nature immunology. 2007;8(1):47-56. Epub 2006/12/13. doi: 10.1038/ni1423. PubMed PMID: 17159983.

15. Mukherjee S, Keitany G, Li Y, Wang Y, Ball HL, Goldsmith EJ, et al. Yersinia YopJ acetylates and inhibits kinase activation by blocking phosphorylation. Science. 2006;312(5777):1211-4. Epub 2006/05/27. doi: 10.1126/science.1126867. PubMed PMID: 16728640.

16. Misaghi S, Balsara ZR, Catic A, Spooner E, Ploegh HL, Starnbach MN. Chlamydia trachomatis-derived deubiquitinating enzymes in mammalian cells during infection. Molecular microbiology. 2006;61(1):142-50. Epub 2006/07/11. doi: 10.1111/j.1365-2958.2006.05199.x. PubMed PMID: 16824101.

17. Ensminger AW, Isberg RR. E3 ubiquitin ligase activity and targeting of BAT3 by multiple Legionella pneumophila translocated substrates. Infection and immunity. 2010;78(9):3905-19. Epub 2010/06/16. doi: 10.1128/IAI.00344-10. PubMed PMID: 20547746; PubMed Central PMCID: PMC2937443.

18. Savijoki K, Alvesalo J, Vuorela P, Leinonen M, Kalkkinen N. Proteomic analysis of Chlamydia pneumoniae-infected HL cells reveals extensive degradation of cytoskeletal proteins. FEMS immunology and medical microbiology. 2008;54(3):375-84. Epub 2008/12/04. doi: 10.1111/j.1574-695X.2008.00488.x. PubMed PMID: 19049650.

19. Vogels MW, van Balkom BW, Heck AJ, de Haan CA, Rottier PJ, Batenburg JJ, et al. Quantitative proteomic identification of host factors involved in the Salmonella typhimurium infection cycle. Proteomics. 2011;11(23):4477-91. Epub 2011/09/16. doi: 10.1002/pmic.201100224. PubMed PMID: 21919203.

20. Shi L, Adkins JN, Coleman JR, Schepmoes AA, Dohnkova A, Mottaz HM, et al. Proteomic analysis of Salmonella enterica serovar typhimurium isolated from RAW 264.7 macrophages: identification of a novel protein that contributes to the replication of serovar typhimurium inside macrophages. The Journal of biological chemistry. 2006;281(39):29131-40. Epub 2006/08/09. doi: 10.1074/jbc.M604640200. PubMed PMID: 16893888.

21. Shi L, Chowdhury SM, Smallwood HS, Yoon H, Mottaz-Brewer HM, Norbeck AD, et al. Proteomic investigation of the time course responses of RAW 264.7 macrophages to infection with Salmonella enterica. Infection and immunity. 2009;77(8):3227-33. Epub 2009/06/17. doi: 10.1128/IAI.00063-09. PubMed PMID: 19528222; PubMed Central PMCID: PMC2715674.

22. Holmes KK. Sexually transmitted diseases. 4th ed. New York: McGraw-Hill Medical; 2008. xxv, 2166 p. p.

23. Moulder JW. Interaction of chlamydiae and host cells in vitro. Microbiological reviews. 1991;55(1):143-90. Epub 1991/03/01. PubMed PMID: 2030670; PubMed Central PMCID: PMC372804.

24. Subtil A, Delevoye C, Balana ME, Tastevin L, Perrinet S, Dautry-Varsat A. A directed screen for chlamydial proteins secreted by a type III mechanism identifies a translocated protein and numerous other new candidates. Molecular microbiology. 2005;56(6):1636-47. Epub 2005/05/27. doi: 10.1111/j.1365-2958.2005.04647.x. PubMed PMID: 15916612.

25. Ho TD, Starnbach MN. The Salmonella enterica serovar typhimurium-encoded type III secretion systems can translocate Chlamydia trachomatis proteins into the cytosol of host cells. Infection and immunity. 2005;73(2):905-11. Epub 2005/01/25. doi: 10.1128/IAI.73.2.905-911.2005. PubMed PMID: 15664932; PubMed Central PMCID: PMC547017.

26. Fields KA, Hackstadt T. Evidence for the secretion of Chlamydia trachomatis CopN by a type III secretion mechanism. Molecular microbiology. 2000;38(5):1048-60. Epub 2000/12/21. PubMed PMID: 11123678.

27. Chellas-Gery B, Linton CN, Fields KA. Human GCIP interacts with CT847, a novel Chlamydia trachomatis type III secretion substrate, and is degraded in a tissue-culture infection model. Cellular microbiology. 2007;9(10):2417-30. Epub 2007/05/30. doi: 10.1111/j.1462-5822.2007.00970.x. PubMed PMID: 17532760.

28. Zhong G. Chlamydia trachomatis secretion of proteases for manipulating host signaling pathways. Frontiers in microbiology. 2011;2:14. Epub 2011/06/21. doi: 10.3389/fmicb.2011.00014. PubMed PMID: 21687409; PubMed Central PMCID: PMC3109274.

29. Yen HC, Xu Q, Chou DM, Zhao Z, Elledge SJ. Global protein stability profiling in mammalian cells. Science. 2008;322(5903):918-23. Epub 2008/11/08. doi: 10.1126/science.1160489. PubMed PMID: 18988847.

30. Emanuele MJ, Elia AE, Xu Q, Thoma CR, Izhar L, Leng Y, et al. Global identification of modular cullin-RING ligase substrates. Cell. 2011;147(2):459-74. Epub 2011/10/04. doi: 10.1016/j.cell.2011.09.019. PubMed PMID: 21963094; PubMed Central PMCID: PMC3226719.

31. Yen HC, Elledge SJ. Identification of SCF ubiquitin ligase substrates by global protein stability profiling. Science. 2008;322(5903):923-9. Epub 2008/11/08. doi: 10.1126/science.1160462. PubMed PMID: 18988848.

32. Xia M, Bumgarner RE, Lampe MF, Stamm WE. Chlamydia trachomatis infection alters host cell transcription in diverse cellular pathways. The Journal of infectious diseases. 2003;187(3):424-34. Epub 2003/01/29. doi: 10.1086/367962. PubMed PMID: 12552426.

33. Huang da W, Sherman BT, Lempicki RA. Systematic and integrative analysis of large gene lists using DAVID bioinformatics resources. Nature protocols. 2009;4(1):44-57. Epub 2009/01/10. doi: 10.1038/nprot.2008.211. PubMed PMID: 19131956.

34. Balsara ZR, Misaghi S, Lafave JN, Starnbach MN. Chlamydia trachomatis infection induces cleavage of the mitotic cyclin B1. Infection and immunity. 2006;74(10):5602-8. Epub 2006/09/22. doi: 10.1128/IAI.00266-06. PubMed PMID: 16988235; PubMed Central PMCID: PMC1594933.

35. Rejman Lipinski A, Heymann J, Meissner C, Karlas A, Brinkmann V, Meyer TF, et al. Rab6 and Rab11 regulate Chlamydia trachomatis development and golgin-84-dependent Golgi fragmentation. PLoS pathogens. 2009;5(10):e1000615. Epub 2009/10/10. doi: 10.1371/journal.ppat.1000615. PubMed PMID: 19816566; PubMed Central PMCID: PMC2752117.

36. Heuer D, Rejman Lipinski A, Machuy N, Karlas A, Wehrens A, Siedler F, et al. Chlamydia causes fragmentation of the Golgi compartment to ensure reproduction. Nature. 2009;457(7230):731-5. Epub 2008/12/09. doi: 10.1038/nature07578. PubMed PMID: 19060882.

37. Chumduri C, Gurumurthy RK, Zadora PK, Mi Y, Meyer TF. Chlamydia infection promotes host DNA damage and proliferation but impairs the DNA damage response. Cell host & microbe. 2013;13(6):746-58. Epub 2013/06/19. doi: 10.1016/j.chom.2013.05.010. PubMed PMID: 23768498.

38. Hybiske K, Stephens RS. Mechanisms of Chlamydia trachomatis entry into nonphagocytic cells. Infection and immunity. 2007;75(8):3925-34. Epub 2007/05/16. doi: 10.1128/IAI.00106-07. PubMed PMID: 17502389; PubMed Central PMCID: PMC1952008.

39. Gurumurthy RK, Maurer AP, Machuy N, Hess S, Pleissner KP, Schuchhardt J, et al. A loss-of-function screen reveals Ras- and Raf-independent MEK-ERK signaling during Chlamydia trachomatis infection. Science signaling. 2010;3(113):ra21. Epub 2010/03/18. doi: 10.1126/scisignal.2000651. PubMed PMID: 20234004.

40. Park JE, Lee JA, Park SG, Lee DH, Kim SJ, Kim HJ, et al. A critical step for JNK activation: isomerization by the prolyl isomerase Pin1. Cell death and differentiation. 2012;19(1):153-61. Epub 2011/06/11. doi: 10.1038/cdd.2011.82. PubMed PMID: 21660049; PubMed Central PMCID: PMC3252824.

41. Chen CB, Ng JK, Choo PH, Wu W, Porter AG. Mammalian sterile 20-like kinase 3 (MST3) mediates oxidative-stress-induced cell death by modulating JNK activation. Bioscience reports. 2009;29(6):405-15. Epub 2009/07/17. doi: 10.1042/BSR20090096. PubMed PMID: 19604147.

42. Ikeo Y, Yumita W, Sakurai A, Hashizume K. JunD-menin interaction regulates c-Jun-mediated AP-1 transactivation. Endocrine journal. 2004;51(3):333-42. Epub 2004/07/17. PubMed PMID: 15256779.

43. Chittenden TW, Howe EA, Culhane AC, Sultana R, Taylor JM, Holmes C, et al. Functional classification analysis of somatically mutated genes in human breast and colorectal cancers. Genomics. 2008;91(6):508-11. Epub 2008/04/25. doi: 10.1016/j.ygeno.2008.03.002. PubMed PMID: 18434084; PubMed Central PMCID: PMC2492759.

44. Schonthaler HB, Guinea-Viniegra J, Wagner EF. Targeting inflammation by modulating the Jun/AP-1 pathway. Annals of the rheumatic diseases. 2011;70 Suppl 1:i109-12. Epub 2011/02/26. doi: 10.1136/ard.2010.140533. PubMed PMID: 21339212.

45. Buchholz KR, Stephens RS. The extracellular signal-regulated kinase/mitogen-activated protein kinase pathway induces the inflammatory factor interleukin-8 following Chlamydia trachomatis infection. Infection and immunity. 2007;75(12):5924-9. Epub 2007/09/26. doi: 10.1128/IAI.01029-07. PubMed PMID: 17893134; PubMed Central PMCID: PMC2168325.

46. Chen F, Cheng W, Zhang S, Zhong G, Yu P. [Induction of IL-8 by Chlamydia trachomatis through MAPK pathway rather than NF-kappaB pathway]. Zhong nan da xue xue bao Yi xue ban = Journal of Central South University Medical sciences. 2010;35(4):307-13. Epub 2010/05/08. doi: 10.3969/j.issn.1672-7347.2010.04.005. PubMed PMID: 20448351.

47. Lee NY, Choi HK, Shim JH, Kang KW, Dong Z, Choi HS. The prolyl isomerase Pin1 interacts with a ribosomal protein S6 kinase to enhance insulin-induced AP-1 activity and cellular transformation. Carcinogenesis. 2009;30(4):671-81. Epub 2009/01/27. doi: 10.1093/carcin/bgp027. PubMed PMID: 19168580.

48. Lee CY, Sher HF, Chen HW, Liu CC, Chen CH, Lin CS, et al. Anticancer effects of tanshinone I in human non-small cell lung cancer. Molecular cancer therapeutics. 2008;7(11):3527-38. Epub 2008/11/13. doi: 10.1158/1535-7163.MCT-07-2288. PubMed PMID: 19001436.

49. Gondek DC, Olive AJ, Stary G, Starnbach MN. CD4+ T cells are necessary and sufficient to confer protection against Chlamydia trachomatis infection in the murine upper genital tract. J Immunol. 2012;189(5):2441-9. Epub 2012/08/03. doi: 10.4049/jimmunol.1103032. PubMed PMID: 22855710.

50. Lad SP, Fukuda EY, Li J, de la Maza LM, Li E. Up-regulation of the JAK/STAT1 signal pathway during Chlamydia trachomatis infection. J Immunol. 2005;174(11):7186-93. Epub 2005/05/21. PubMed PMID: 15905563.

51. Chen AL, Johnson KA, Lee JK, Sutterlin C, Tan M. CPAF: a Chlamydial protease in search of an authentic substrate. PLoS pathogens. 2012;8(8):e1002842. Epub 2012/08/10. doi: 10.1371/journal.ppat.1002842. PubMed PMID: 22876181; PubMed Central PMCID: PMC3410858.

52. Rajalingam K, Sharma M, Lohmann C, Oswald M, Thieck O, Froelich CJ, et al. Mcl-1 is a key regulator of apoptosis resistance in Chlamydia trachomatis-infected cells. PloS one. 2008;3(9):e3102. Epub 2008/09/05. doi: 10.1371/journal.pone.0003102. PubMed PMID: 18769617; PubMed Central PMCID: PMC2518856.

53. Alto NM, Orth K. Subversion of cell signaling by pathogens. Cold Spring Harbor perspectives in biology. 2012;4(9):a006114. Epub 2012/09/07. doi: 10.1101/cshperspect.a006114. PubMed PMID: 22952390.

54. Buchholz KR, Stephens RS. Activation of the host cell proinflammatory interleukin-8 response by Chlamydia trachomatis. Cellular microbiology. 2006;8(11):1768-79. Epub 2006/06/29. doi: 10.1111/j.1462-5822.2006.00747.x. PubMed PMID: 16803583.

55. Vignola MJ, Kashatus DF, Taylor GA, Counter CM, Valdivia RH. cPLA2 regulates the expression of type I interferons and intracellular immunity to Chlamydia trachomatis. The Journal of biological chemistry. 2010;285(28):21625-35. Epub 2010/05/11. doi: 10.1074/jbc.M110.103010. PubMed PMID: 20452986; PubMed Central PMCID: PMC2898388.

56. Wang A, Al-Kuhlani M, Johnston SC, Ojcius DM, Chou J, Dean D. Transcription factor complex AP-1 mediates inflammation initiated by Chlamydia pneumoniae infection. Cellular microbiology. 2012. Epub 2012/11/21. doi: 10.1111/cmi.12071. PubMed PMID: 23163821.

57. Mesquita FS, Thomas M, Sachse M, Santos AJ, Figueira R, Holden DW. The Salmonella deubiquitinase SseL inhibits selective autophagy of cytosolic aggregates. PLoS pathogens. 2012;8(6):e1002743. Epub 2012/06/22. doi: 10.1371/journal.ppat.1002743. PubMed PMID: 22719249; PubMed Central PMCID: PMC3375275.

58. Rytkonen A, Poh J, Garmendia J, Boyle C, Thompson A, Liu M, et al. SseL, a Salmonella deubiquitinase required for macrophage killing and virulence. Proceedings of the National Academy of Sciences of the United States of America. 2007;104(9):3502-7. Epub 2007/03/16. doi: 10.1073/pnas.0610095104. PubMed PMID: 17360673; PubMed Central PMCID: PMC1802004.

59. Coers J, Gondek DC, Olive AJ, Rohlfing A, Taylor GA, Starnbach MN. Compensatory T cell responses in IRG-deficient mice prevent sustained Chlamydia trachomatis infections. PLoS pathogens. 2011;7(6):e1001346. Epub 2011/07/07. doi: 10.1371/journal.ppat.1001346. PubMed PMID: 21731484; PubMed Central PMCID: PMC3121881.

60. Chen H, Sharp BM. Content-rich biological network constructed by mining PubMed abstracts. BMC bioinformatics. 2004;5:147. Epub 2004/10/12. doi: 10.1186/1471-2105-5-147. PubMed PMID: 15473905; PubMed Central PMCID: PMC528731.

61. Wang W, Shi L, Xie Y, Ma C, Li W, Su X, et al. SP600125, a new JNK inhibitor, protects dopaminergic neurons in the MPTP model of Parkinson's disease. Neuroscience research. 2004;48(2):195-202. Epub 2004/01/27. PubMed PMID: 14741394.

62. Kim SE, Lee MY, Lim SC, Hien TT, Kim JW, Ahn SG, et al. Role of Pin1 in neointima formation: down-regulation of Nrf2-dependent heme oxygenase-1 expression by Pin1. Free radical biology & medicine. 2010;48(12):1644-53. Epub 2010/03/24. doi: 10.1016/j.freeradbiomed.2010.03.013. PubMed PMID: 20307651.

Chapter 7: Discussion

Chlamydia trachomatis is a persistent bacterial pathogen that has infected humans for thousands of years (1). Over time, *Chlamydia* has adapted to survive and evade immune mechanisms initiated by the human host to avoid clearance and blunt protective immunity (2). In turn, the host becomes susceptible to the development of severe disease sequelae that are major public health threats, such as ectopic pregnancy and infertility (3). The majority of *Chlamydia* infections remain asymptomatic, complicating diagnosis and treatment. Because of this, there is a great need to develop a long-lived protective vaccine that will not only protect against *C. trachomatis,* but will also prevent immunopathologies. This dissertation examined both host mechanisms that drive protective immunity in the genital mucosa, as well as bacterial strategies that are used to manipulate host cells in order to promote intracellular growth and survival. Together these findings uncover important aspects of *C. trachomatis* host-pathogen interactions that now open new avenues of study that will lead to the development of a protective vaccine.

Mouse models of *Chlamydia trachomatis* genital infection

As a first step towards developing a *Chlamydia* vaccine, there is a need to develop small animals models that can be used to test vaccine candidates *in vivo*. In order to be useful the small animal models must recapitulate many aspects of human disease, including the development of chronic infections and immune sequelae. Unfortunately, current murine models of *Chlamydia* infection remain limited (4).

Many investigators studying immunity to *C. trachomatis* use the murine-adapted *Chlamydia muridarum* as a surrogate pathogen in mice (5-7). As described in Chapter 2, while *C. muridarum* infections robustly colonize mice via the intravaginal route of infection and lead to the development of immune pathologies, there are several aspects of this model that cannot recapitulate human disease and therefore limit its utility (8). It is clear that a protective vaccine against *C. trachomatis* must drive cell-mediated immunity, as antibodies are not broadly

protective (7, 9). Antibody-based vaccines against *C. trachomatis* did not induce protection in early clinical trials, leading investigators to pursue strategies that robustly activate T cell responses (10). Unfortunately *C. muridarum*-derived peptides differ from human strains of *C. trachomatis* to a large enough degree that protective peptides from one species many times do not exist in the other (8). Therefore, the development of infection models in mice using human strains of *C. trachomatis* is an area of study that is required to more rapidly progress with vaccine development.

Previous studies in which mice were infected intravaginally with *C. trachomatis* described weak colonization, ascension to the upper genital tract, and minimal development of immune sequelae (11, 12). In Chapter 2 of this dissertation, I described data showing that these previous findings were mostly because human stains of *Chlamydia* are unable to withstand the lower genital tract environment in mice. However, using a novel transcervical infection method that deposits *Chlamydia* directly into the upper genital mucosa, I found robust colonization of the upper genital tract, induction of immune pathologies, and development of protective immunity. The disease course seen following transcervical infection with *C. trachomatis* closely mirrors that seen following infection with *C. muridarum*, only with shorter duration due to restriction by murine IFNγ responses. Unfortunately, mice that were infected transcervically with *C. trachomatis* did not develop the chronic infections that are associated with human disease. Therefore, while transcervical infection with *C. trachomatis* can now be used to model several aspects of acute disease seen in humans, it does not currently recapitulate persistent phases of infection. Future studies will need to investigate methods to further improve the transcervical model in order to make it more representative of human infections.

One important topic that remains to be examined in depth in the transcervical model is the disease course of various clinical strains of human *C. trachomatis*. For my initial characterization of the transcervical infection model I exclusively used the lymphogranuloma venereum (LGV) strain L2. In humans, L2 is among the most virulent strains of *C. trachomatis*

that infects the human genital mucosa. However, after colonizing the genital tract, L2 infection spreads systemically to the lymphatic system, causing severe inflammation in these tissues (13). L2 infections of the genital tract may not be the most accurate model of persistent genital infections. In the context of public health, infections with LGV make up a small percentage of documented *C. trachomatis* infections, limiting the direct clinical relevance of studies using this strain (13). The majority of human *C. trachomatis* genital infections are caused by serovars D-K. Intravaginal infection with serovar D has previously been shown to cause hydrosalpinx in mice, unlike intravaginal infection with L2 (3). This suggests that serovar D may be better adapted to persist in the genital mucosa than L2. We are now pursuing experiments to determine whether transcervical infections of mice with *C. trachomatis* serovar D lead to more robust and extended colonization of the upper genital tract, ascend more efficiently to the ovaries, and promote the development of more consistent immunopathologies than transcervical infection with L2. These studies will help to improve our small animal infection model so that it better recapitulates the most common type of *C. trachomatis* infection seen in the clinic.

The next step in refining murine models of human *C. trachomatis* infection will be to develop methods that also induce long-term chronic infections *in vivo*. Since *C. muridarum* does not cause persistent infections, new chronic infection models will need to use human *C. trachomatis* strains in order to recapitulate the persistent disease state. One reason that human strains of *C. trachomatis* are rapidly cleared from mice is that they are sensitive to the murine IFNγ response , which induces the IRG system (14). Work performed by our lab and others showed that mouse cells that are stimulated with IFNγ direct IRGs to restrict *C.* trachomatis (15-17). In contrast, IFNγ stimulation of human epithelial cells, which do not possess IFNγ inducible IRGs, induce IDO expression (18). This in turn leads to intracellular tryptophan depletion. The differential response to IFNγ between mice and humans leads to dramatically different outcomes of infection. We hypothesized that performing transcervical infection in mice deficient

in IRGs may lead to persistent *Chlamydia* infection. However, in IRG-deficient mice, we found enhanced bacterial replication early during infection, which ultimately led to an exacerbated $CD4^+$ T cell response and infection clearance within two weeks (19). This suggests that unimpeded replication may ultimately be detrimental to the induction of quiescent *Chlamydia* infections.

Human strains of *C. trachomatis* have adapted to withstand to the human IFNγ response, allowing for their survival even under high levels of IDO and subsequent tryptophan depletion (18). Therefore, we speculate that a more physiological murine infection model that recapitulates all aspects of human disease will not only require the removal of murine specific IFNγ responses, but also require the addition of human IFNγ responses. The laboratory of Dr. Jorn Coers, in collaboration with our laboratory, has recently developed a "humanized" knock-in mouse model, which removes the murine IRG system while knocking in a cassette that enhances the expression of IDO to levels seen in human epithelial cells (data not shown) (20). We will now begin to examine the transcervical infection model using these humanized mice to determine if we are able to more closely recapitulate all aspects of the human disease. Ultimately, the development of these models is necessary to safely evaluate the potential of candidate vaccine formulations that drive protective immunity against *C. trachomatis* and prevent the induction of immune sequelae.

Immunity in the genital mucosa: implications for vaccine development

Since the transcervical infection model is a robust and reproducible model of *C. trachomatis* infection, it has opened new avenues of research that will increase our understanding of the mechanisms responsible for protection in the genital mucosa. By characterizing the factors that mediate long-term protective immunity, I hypothesized that I could uncover hallmarks of the immune response that are associated with protective immunity in the genital mucosa. These

findings could then be leveraged during vaccine development to promote a broadly protective immunization strategy. As a first step in this process, I characterized the cellular populations that afford protection in the genital mucosa following transcervical infection with *C. trachomatis*. Through these studies I found that $CD4^+$ T cells drove the majority of protection that is observed following *C. trachomatis* infection in the upper genital tract. When I depleted $CD4^+$ T cells from mice that had been previously infected with *C. trachomatis,* the mice were not protected against subsequent *C. trachomatis* challenge and harbored similar bacterial levels to naïve mice following primary infection. In addition, transferring *Chlamydia*-specific $CD4^+$ T cells into naïve mice afforded significant protection to *C. trachomatis* infection in the genital tract. Other recent work in our lab investigated the role of $CD8^+$ T cells and B cells during infection and found them to both be dispensable for protection from *C. trachomatis* in the genital tract (data not shown). These studies showed that transfer of serum or purified $CD8^+$ T cells from immune mice into naïve mice affords no protection, in contrast to $CD4^+$ T cells. Taken together, these data demonstrate that during use of the transcervical model there is a critical role for $CD4^+$ T cells in protecting the murine genital tract from infection with *C. trachomatis*. Therefore, in order for a *Chlamydia* vaccine candidate to be efficient, it must stimulate a robust Chlamydia-specific $CD4^+$ T cell response in the genital mucosa.

Despite the fact that these experiments showed a critical role for $CD4^+$ cells in the long-term protection of the genital mucosa, the steps that lead to the activation, recruitment and retention of T cells in the genital tract remained ambiguous. In order for $CD4^+$ T cells to mediate protection in the genital tract they must be activated in the iliac lymph node by antigen presenting cells, traffic into the genital tissue where infection occurs, and release effector cytokines such as IFNγ that promote clearance (21). In Chapters 3 and 4 of this dissertation, I characterized homing molecules that are required for *Chlamydia*-specific $CD4^+$ T cells to traffic efficiently to the genital tract and to afford protection from *C. trachomatis* infection. Loss of the chemokine receptors CXCR3 and CCR5, or the integrin $\alpha4\beta1$ on *Chlamydia*-specific $CD4^+$ T

cells, negatively impacted both T cell recruitment to the genital tract and the T cells' protective capacity. While previous studies suggested potential chemokine receptors and integrins that promote T cell recruitment to the genital mucosa, these studies examined bulk T cells and were unable to track *Chlamydia*-specific T cells. Previous studies also failed to examine the role of individual receptors on the protective capacity of T cells. In this dissertation, the use of antigen specific techniques and the transcervical infection model allowed for the identification and characterization of CXCR3, CCR5 and $\alpha 4\beta 1$ in promoting a robust and protective $CD4^+$ T cell response following *C. trachomatis* infection in the genital mucosa.

As the mechanisms that promote protective $CD4^+$ T cell responses in the genital mucosa are elucidated, we can begin to optimize vaccine strategies that promote the development of these protective cellular populations following immunization. Based on the findings in Chapters 2, 3, and 4, I hypothesize that a vaccine that induces $CD4^+$ T cells with the proper chemokine receptor and integrin profiles would be the most protective immunization strategy. One way to leverage these findings as a vaccine approach may be to use a "prime and pull" method that attracts T cells of the correct homing molecule profile to the mucosal site of interest. This strategy has recently been used successfully in a herpes infection model in the genital tract of mice (22). In this vaccine approach, an initial immunization is given systemically in mice to prime pathogen-specific T cells. Then the chemokines CXCL9 and CXCL10, which bind to the receptor CXCR3, are topically applied to the genital tract. This chemokine then pulls activated antigen specific T cells that express CXCR3 from the periphery to the genital mucosa, where they can develop into long-term memory cells. It is possible that the same vaccine strategy could be used to protect from infections with *C. trachomatis*, and may even be further enhanced by including chemokines that bind CXCR3 and CCR5.

The prime and pull strategy is successful because it enhances the recruitment of activated pathogen-specific T cells that express specific homing molecules to the genital mucosa following vaccination (22). However, studies have yet to examine how different

immunization strategies influence the expression of homing molecules on protective $CD4^+$ T cells following vaccination. A vaccine that maximally primes pathogen-specific T cells to express critical homing molecules following immunization will promote more efficient “pulling” of protective cells to the genital mucosa, where they can develop into memory cells. Ultimately, enhanced T cell recruitment and retention in the genital mucosa may increase the protective capacity of vaccination. In order to examine how homing molecule expression on T cells is regulated, investigators must examine all aspects of T cell priming, including initial activation. Interactions between distinct antigen presenting cells and naïve T cells have been shown to influence the expression of homing molecules on the surface of antigen-specific T cells during priming. Previous studies showed that the activation of naïve T cells by dendritic cells cultured with intestinal tissues imprints T cells differently than dendritic cells alone. Co-culture of T cells with intestinal DCs induced a homing profile on activated T cells that promoted trafficking to the intestines through the upregulation of CCR9 and $\alpha4\beta7$ (23, 24). Unlike APC populations from the intestine, the influence of distinct genital mucosa resident APC populations on the induction of homing molecules on *Chlamydia*-specific T cells remains almost entirely unexplored. Future studies will need to examine how initial priming events can enhance or inhibit the upregulation of CXCR3, CCR5, and $\alpha4\beta1$ on *Chlamydia*-specific T cells and evaluate how various vaccine strategies specifically alter these interactions. Once APC populations that positively influence T cell recruitment to the infected genital mucosa are identified, we can then dissect these interactions to elucidate the mechanisms responsible for changes in homing receptor expression. Ultimately, identifying vaccine compositions that promote the enhanced expression of homing markers that are specific for the genital tract may improve the efficacy of protection afforded by immunization.

Even though the data presented in this dissertation demonstrate the protective role of $CD4^+$ T cells during natural infection of mice, human immunity to *C. trachomatis* appears to be

less robust, resulting in limited protective memory. In human disease, the absence of protective immunity is not due to a lack of $CD4^+$ T cell activation or homing to the genital tract, but rather it is the result of a failure to maintain a stable long-lived memory pool that can protect from reinfection (25). The underlying mechanisms that lead to this deficit in memory potential in humans are not understood and remain to be investigated experimentally. Future studies will need to shift their focus from primary infections to the dissection of how initial activation events, homing receptor expression, and the genital tract environment influence the memory potential of *Chlamydia*-specific $CD4^+$ T cells differently in humans and mice. As described above, one major difference between humans and mice is the robust induction of IDO following IFNγ stimulation in human epithelial cells. While IDO is thought of as a host-mechanism to restrict infection, the metabolite byproducts of the IDO response may also have detrimental impacts on $CD4^+$ T cells (26). High levels of kynurenines have been shown to directly impact the $CD4^+$ T cell response to *Mycobacterium tuberculosis* during lung infections. During *M. tuberculosis* infection, mice that are unable to induce IDO expression develop an exacerbated Th17 response, a response that is directly inhibited by kynurenines (27). Recent work in cancer biology further supports the immunosuppressive role of these molecules by showing that tumors can upregulate expression of IDO and kynurenine metabolites in order to induce tolerance and prevent T cell-mediated tumor clearance and memory development (26, 28). A similar situation may occur in the genital tract during *C. trachomatis* infections. I hypothesize that high expression of IDO has a two-pronged effect that promotes *C. trachomatis* survival. The first effect of IDO expression, as discussed previously, is the induction of a quiescent form of *C. trachomatis* that survives tryptophan depletion. The second and currently unexplored effect of IDO expression, is the direct immunosuppressive and tolerogenic influences that kynurenines, IDO derived metabolites, have on $CD4^+$ T cells. Infection with *C. trachomatis* induces the recruitment of IFNγ secreting $CD4^+$ T cells to the genital mucosa, which in turn induces IDO expression, increases

the levels of kynurenines, and depletes tryptophan stores. In response to tryptophan depletion, *C. trachomatis* differentiates into the well-described quiescent state, "tricking" the immune system into the perception of clearance. At the same time, high levels of kynurenines may directly inhibit the development of a robust Th1 response, similar to what has been described for other pathogens at other mucosal sites. Future studies are needed to test these hypotheses and to determine what impact high IDO expression and high kynurenine levels have on $CD4^+$ T cell-mediated protection against *C. trachomatis* in the murine genital mucosa. Taken together, while great progress is being made in the development of animals models of *C. trachomatis* and in understanding protective immunity in the genital mucosa of mice, we must now turn our attention to gaining a better understanding of what leads to robust memory induction and how infection with *C. trachomatis* alters immune development.

Chlamydia infection alters host cells to promote growth and evade immunity

C. trachomatis is superbly adapted to replicate in human cells and persist over time in human hosts (1). While *C. trachomatis* has evolved mechanisms that alter immune development, characterizing these virulence mechanisms has remained challenging. On one hand, *C. trachomatis* is unable to evade or manipulate host processes unique to mice, such as the IRG response to IFNγ stimulation (19). On the other hand, infections of mice with *C. trachomatis* may also mask immune evasion strategies that are present in humans but not mice, such as the induction of quiescence under low tryptophan levels following IDO induction (20). Therefore, *in vivo* mouse studies alone are not sufficient to fully characterize the virulence strategies employed by *C. trachomatis* in humans. In order to understand the strategies used by *C. trachomatis* to acquire nutrients and evade immune clearance, we must characterize how infection with *C. trachomatis* directly alters human cells using *in vitro* or *ex vivo* models. I hypothesized that understanding the mechanisms used by *C. trachomatis* to promote

intracellular growth may help us to better find strategies to drive bacterial clearance as well as lead to the development of host based therapeutics.

Previous studies have shown that *C. trachomatis* directly alters host proteins and pathways by secreting effector proteins directly into the host cytosol. These virulence factors have been shown to impact a wide-variety of host-cell processes, such as NF-κB signaling, cytoskeletal structure, cell cycle state, golgi function, and histone methylation (29-32). However, the handful of well-studied effectors is only a fraction of the almost 100 proteins predicted to be substrates of the type III secretion system, the majority of which have no known enzymatic function or host cell target (33). I speculated that large-scale discovery of host proteins targeted during infection might give insight into cellular processes manipulated by *C. trachomatis*. In Chapters 5 and 6 of this dissertation I applied two parallel proteomic and genomic techniques to broadly identify host proteins whose levels are altered as a result of infection. The first approach combined quantitative mass spectrometry, using SILAC and microarray transcriptional analysis, to identify host proteins that are altered following infection. Using this system I determined that the vast majority of these changes did not appear to result from changes in transcription. As a complimentary approach, I used the GPS screening platform to probe the human ORFeome collection for host proteins that whose stability was altered following infection. SILAC and GPS are inherently different screening platforms that independently may not achieve the global depth that is possible when they are used together. A strength of SILAC is its ability to assess changes in protein abundance with exceptional quantitative precision at endogenous levels of expression, providing us with a method to examine changes to proteins at physiological levels on a large scale. However, the effectiveness of SILAC has been limited because its protein abundance measurements reflect the combined influences of transcription, protein synthesis, and post-translational effects. Its performance has also been restricted due to incomplete proteome coverage, though ongoing

technological improvements are continually increasing the depth of its reach. GPS complements these shortcomings by assessing a larger number of host proteins (many of which weren't identified in SILAC), and examines each ORF independently of transcriptional regulation. Furthermore, because GPS uses intact cells it prevents non-specific protease activity driven by CPAF, which is characteristic of *Chlamydia* infected cells (34).

When I applied SILAC and GPS to identify host proteins that were altered during *C. trachomatis* infection, I found that almost 1,000 total host proteins were altered. Bioinformatic analysis on both datasets revealed host processes that were enriched among the altered host proteins from the screens. In both the SILAC and the GPS screens, we found a strong enrichment of host genes involved in Golgi Apparatus function, host transcriptional regulation, and cyotosolic trafficking networks. It was not surprising to identify the Golgi proteins as altered during *C. trachomatis* infection, as several studies have examined the fragmentation of Golgi stacks that occurs as intracellular bacterial replication progresses (31). Interestingly, bioinformatic analysis of both screens uncovered several host processes that have not been previously implicated during *C. trachomatis* infection. Among these annotated clusters were proteins involved in microtubule formation, mitochondrial function, protein degradation, protein translation and RNA splicing. Surprisingly, there was also a strong enrichment of genes involved in nucleus structure and in transcription factors, suggesting that *C. trachomatis* infection broadly alters host cell processes. It will be important for new studies to examine whether secreted bacterial effectors directly mediate the specific changes in host cell proteins that occur during *C. trachomatis* infection. One approach to identify these host-pathogen interactions is to take advantage of the GPS reporter cell lines that exhibited altered protein stability during infection with *C. trachomatis*. Using these reporter cell lines to identify individual effector proteins that can recapitulate the protein stability changes that are seen during infection may be a powerful screening tool. As a proof-of-principle for these approaches, I have recently executed a small-scale screen (described in Appendix B) where I

discovered that the *Chlamydia* protein CrpA destabilizes the host protein BNIP3L in order to alter the host cell response. These types of analyses can now be executed with a broader panel of *Chlamydia* effector and host proteins to identify potential host-pathogen interactions that could then be targeted to disrupt *Chlamydia* intracellular development.

One of the more intriguing findings from the SILAC and GPS experiments is that a large number of host protein levels are altered independent of changes in host transcription. In the SILAC analysis, I coupled quantitative proteomic screening with transcriptional array analysis and found that over 90% of the protein changes identified in the SILAC analysis occurred without concomitant changes in mRNA expression. Furthermore, changes identified using the GPS screening platform were entirely independent of changes in transcriptional regulation, as all the proteins were expressed off of a CMV promoter (35). Together these findings suggest that *C. trachomatis* infection broadly alters host proteins independent of changes in host transcription. While the mechanisms driving the differential changes in mRNA and protein level is not entirely clear, I have uncovered two potential mechanisms that may promote this discordance. First, I identified that *C. trachomatis* infection of human cells inhibits the translation efficiency of host ribosomes. By inhibiting translation, *Chlamydia* can prevent the accumulation of pro-inflammatory cytokines and can generate a larger pool of free amino acids, which are needed for the pathogen to survive in cells. In fact, in the gain-of-function screen described in Chapter 5, I found that overexpression of the elongation factor EEF1D prevents efficient *C. trachomatis* replication. These data indicate that alterations of host translation are required for *C. trachomatis* intracellular growth. The second mechanism that may drive differences in host protein and mRNA levels is a direct manipulation of the ubiquitin/proteasome system. In the SILAC screen, I found that the host ubiquitin ligase adaptor Cul4a was strongly destabilized during *C. trachomatis* infection. Loss of individual ubiquitin networks likely lead to distinct changes in host proteins that would not be found by examining transcriptional analysis alone. Furthermore, *Chlamydia* encodes two

deubiquitinating enzymes that are secreted into the host cytoplasm during infection that can directly alter ubiquitination in the host (36). Manipulating the ubiquitin landscape in host cells would allow *C. trachomatis* to toggle levels of a broad range of host proteins in infected cells to the benefit of the pathogen. More broadly speaking, decoupling transcription and translation in host cells may allow *C. trachomatis* to prevent robust activation of specific immune pathways that become transcriptionally activated during infection that may be detrimental to intracellular growth of the pathogen. It is also possible that inhibition of host translation ensures that there are adequate levels of the nutrients needed by *C. trachomatis* to survive. Future work will need to dissect these individual mechanisms and to identify potential host-pathogen interactions that drive these processes.

Together GPS and SILAC identified host proteins that are directly altered by *C. trachomatis* during infection. These screens identified many host proteins that are altered in stability following infection, but they did not address the biological impact of the individual host protein alterations. I hypothesized that if prevention a specific protein from being altered by *C. trachomatis* inhibited growth, then that protein might represent a potential choke point in the host cell that could be targeted to restrict infection. To identify the changes that are required for growth, we conducted an overexpression screen for host proteins that were destabilized by infection and a siRNA screen for those host proteins that were stabilized by infection. This is the first large-scale overexpression screen used to identify pathogen-induced changes that are required for the growth of a pathogen in mammalian cells. The proteins that we identified are involved in a wide-range of host cell functions, suggesting that *C. trachomatis* alters host cells broadly. Future studies will be conducted to individually characterize how these proteins alter *C. trachomatis* intracellular growth. To gain insight into potential mechanisms by which *C. trachomatis* growth is altered, I grouped hits into common pathways or protein networks. For example, I identified that several hits identified in the loss-of-function screen were related to the AP-1 transcription complex. AP-1 signaling is known to alter cellular processes, immune

activation and cellular survival programs (37). Several bacterial pathogens have been shown to manipulate these pathways to alter immune responses and intracellular survival. In fact, one recent study identified that *Salmonella* infections directly alter host transcription in a type III secretion system dependent manner, including the activation of AP-1 components, in order to allow intracellular development late during infection (41). My mechanistic analysis presented in Chapter 6 identified that AP-1 activation occurs 24 hours following *C. trachomatis* infection, and that AP-1 activation is required for efficient intracellular growth *in vitro* and *in vivo*. It currently remains unknown precisely which AP-1 targets are needed for *Chlamydia* replication and what underlying mechanisms drive AP-1 activation. However, it is interesting that *C. trachomatis* activates AP-1 in host cells when this pathway is also implicated in the inflammation in response to *Chlamydia* infection (37). It is tempting to speculate that *Chlamydia* manipulates AP-1 activation and other host signaling cascades to not only promote intracellular growth, but also to directly alter the host immune response. It is possible that the high levels of inflammation induced by *C. trachomatis* may lead to ineffective T cell responses, directly linking changes in infected epithelial cells to alterations in host immunity. Current work in our lab is investigating the interactions between infection induced inflammation and T cell protection in order to address these outstanding questions. Ultimately, it will be important to examine many of the host proteins and pathways identified as altered during *C. trachomatis* infection in the SILAC or GPS screens in an *in vivo* setting, in order to determine their influence on protective immunity in the genital mucosa.

Using proteomic approaches to characterize novel host-pathogen interactions

In Chapters 5 and 6 of this dissertation, I showed that *C. trachomatis* dramatically alters the proteomic landscape of host cells during infection. Previous studies have used quantitative proteomic techniques to study host interactions with bacterial pathogens (38, 39). While these studies were successful in identifying some host factors altered during infection,

the proteome coverage was limited (1000-2000 total host proteins) compared to our current study (>10,000 total host proteins). With the success of small-scale studies examining *Salmonella,* combined with the extensive study presented here, investigators should have a renewed interest in understanding the impact of intracellular pathogens directly on host cell proteins. Investigators studying varying aspects of mammalian cell biology have commonly used large-scale proteomic and ORFeome-based screens to understand how global dynamics change following specific perturbations (35). Our study is the first to take advantage of the human ORFeome as a resource to understand bacterial pathogenesis. By coupling ORFeome screens with quantitative mass-spectrometry we achieved over five times greater coverage than previous studies focused on the effects that bacterial pathogens have on the human proteome.

It is not hard to imagine several applications of these proteomic approaches to characterize unknown host-pathogen interactions. First, several other bacterial pathogens encode secretion systems that inject virulence determinants into host cells to manipulate host proteins. For example, among others, *Salmonella typhimurium* and *Shigella flexneri* encode ubiquitin modifying proteins that are secreted into the host cell during infection (40). Investigators can now use the approaches described in this dissertation to compare how infection directly alters host proteins during each bacterial infection. Using either GPS or SILAC, investigators can also begin to identify host proteins whose levels are directly mediated by bacterial effectors, by comparing changes to the proteome that occur during infection with wild-type bacteria or bacterial lacking specific virulence loci, such as type III or type IV secretion systems. In these screens, the proteins that shift following wild-type infection, but not during infection with virulence mutants, are the proteins that are likely to be directly targeted by secreted bacterial effectors. I anticipate that this screening approach would uncover far fewer total altered proteins, but will provide more targeted identification of specific host-pathogen interactions than screens that only compare changes in infected and

uninfected cells. Unfortunately, because targeted genetics remains difficult in *C. trachomatis,* this virulence mutant screen would still be challenging. In the absence of genetic techniques, it is possible to use a gain-of-function approach to identify the host targets of individual virulence determinants. In a gain-of-function approach, individual bacterial effectors or control vectors would be expressed in host cells and the host proteins that are altered would be compared between the two conditions. For example we can use the GPS screening platform to identify substrates of bacterial derived ubiquitin modifying proteins ChlaDub1 and ChlaDub2, which are encoded by *C. trachomatis* (36). Together, the experimental approaches described in this dissertation provide a blueprint for cataloging host proteins and pathways that are altered by pathogens. By screening a broad range of bacterial pathogens, we could begin to identify potential host proteins that are targeted by several pathogens. These common pathways would reveal host targets that are particularly ripe for the development of host-based antibiotic therapies that could prevent pathogen survival and the dissemination of disease.

Summary

Overall, the work described in this dissertation elucidated critical mechanisms that drive host immunity, as well as bacterial virulence strategies that directly alter the host during infection with *C. trachomatis*. The next step in developing a broadly protective vaccine that promotes immunity and prevents pathology will require the integration of both immunology and cellular microbiology, in a fashion similar to the approaches described here. By combining these approaches we will be able to develop a vaccine that not only activates the proper protective cellular populations following immunization, but also prevents immune evasion mechanisms that are employed by *C. trachomatis* during infection. Ultimately, these approaches can be applied to a wide range of pathogens that remain problematic worldwide to develop novel therapeutic strategies that can prevent infection altogether.

References

1. Roan NR, Starnbach MN. Immune-mediated control of Chlamydia infection. Cellular microbiology. 2008;10(1):9-19. Epub 2007/11/06. doi: 10.1111/j.1462-5822.2007.01069.x. PubMed PMID: 17979983.

2. Stephens RS, Kalman S, Lammel C, Fan J, Marathe R, Aravind L, et al. Genome sequence of an obligate intracellular pathogen of humans: Chlamydia trachomatis. Science. 1998;282(5389):754-9. Epub 1998/10/23. PubMed PMID: 9784136.

3. Starnbach MN, Roan NR. Conquering sexually transmitted diseases. Nature reviews Immunology. 2008;8(4):313-7. Epub 2008/03/01. doi: 10.1038/nri2272. PubMed PMID: 18309315.

4. O'Meara CP, Andrew DW, Beagley KW. The mouse model of Chlamydia genital tract infection: A review of infection, disease, immunity and vaccine development. Current molecular medicine. 2013. Epub 2013/10/10. PubMed PMID: 24102506.

5. Kelly KA, Chan AM, Butch A, Darville T. Two different homing pathways involving integrin beta7 and E-selectin significantly influence trafficking of CD4 cells to the genital tract following Chlamydia muridarum infection. Am J Reprod Immunol. 2009;61(6):438-45. Epub 2009/04/28. doi: 10.1111/j.1600-0897.2009.00704.x. PubMed PMID: 19392981; PubMed Central PMCID: PMC2888875.

6. Morrison SG, Morrison RP. In situ analysis of the evolution of the primary immune response in murine Chlamydia trachomatis genital tract infection. Infection and immunity. 2000;68(5):2870-9. Epub 2000/04/18. PubMed PMID: 10768984; PubMed Central PMCID: PMC97499.

7. Morrison SG, Morrison RP. Resolution of secondary Chlamydia trachomatis genital tract infection in immune mice with depletion of both CD4+ and CD8+ T cells. Infection and immunity. 2001;69(4):2643-9. Epub 2001/03/20. doi: 10.1128/IAI.69.4.2643-2649.2001. PubMed PMID: 11254630; PubMed Central PMCID: PMC98202.

8. Gondek DC, Olive AJ, Stary G, Starnbach MN. CD4+ T cells are necessary and sufficient to confer protection against Chlamydia trachomatis infection in the murine upper genital tract. J Immunol. 2012;189(5):2441-9. Epub 2012/08/03. doi: 10.4049/jimmunol.1103032. PubMed PMID: 22855710; PubMed Central PMCID: PMC3690950.

9. Morrison SG, Su H, Caldwell HD, Morrison RP. Immunity to murine Chlamydia trachomatis genital tract reinfection involves B cells and CD4(+) T cells but not CD8(+) T cells. Infection and immunity. 2000;68(12):6979-87. Epub 2000/11/18. PubMed PMID: 11083822; PubMed Central PMCID: PMC97807.

10. Longbottom D, Livingstone M. Vaccination against chlamydial infections of man and animals. Vet J. 2006;171(2):263-75. Epub 2006/02/24. doi: 10.1016/j.tvjl.2004.09.006. PubMed PMID: 16490708.

11. Johansson M, Lycke N. Immunological memory in B-cell-deficient mice conveys long-lasting protection against genital tract infection with Chlamydia trachomatis by rapid recruitment of

T cells. Immunology. 2001;102(2):199-208. Epub 2001/03/22. PubMed PMID: 11260325; PubMed Central PMCID: PMC1783171.

12. Morrison SG, Farris CM, Sturdevant GL, Whitmire WM, Morrison RP. Murine Chlamydia trachomatis genital infection is unaltered by depletion of CD4+ T cells and diminished adaptive immunity. The Journal of infectious diseases. 2011;203(8):1120-8. Epub 2011/02/16. doi: 10.1093/infdis/jiq176. PubMed PMID: 21321103; PubMed Central PMCID: PMC3068022.

13. Belland R, Ojcius DM, Byrne GI. Chlamydia. Nature reviews Microbiology. 2004;2(7):530-1. Epub 2004/07/14. doi: 10.1038/nrmicro931. PubMed PMID: 15248311.

14. Bernstein-Hanley I, Coers J, Balsara ZR, Taylor GA, Starnbach MN, Dietrich WF. The p47 GTPases Igtp and Irgb10 map to the Chlamydia trachomatis susceptibility locus Ctrq-3 and mediate cellular resistance in mice. Proceedings of the National Academy of Sciences of the United States of America. 2006;103(38):14092-7. Epub 2006/09/09. doi: 10.1073/pnas.0603338103. PubMed PMID: 16959883; PubMed Central PMCID: PMC1599917.

15. Nelson DE, Virok DP, Wood H, Roshick C, Johnson RM, Whitmire WM, et al. Chlamydial IFN-gamma immune evasion is linked to host infection tropism. Proceedings of the National Academy of Sciences of the United States of America. 2005;102(30):10658-63. Epub 2005/07/16. doi: 10.1073/pnas.0504198102. PubMed PMID: 16020528; PubMed Central PMCID: PMC1180788.

16. Coers J, Bernstein-Hanley I, Grotsky D, Parvanova I, Howard JC, Taylor GA, et al. Chlamydia muridarum evades growth restriction by the IFN-gamma-inducible host resistance factor Irgb10. J Immunol. 2008;180(9):6237-45. Epub 2008/04/22. PubMed PMID: 18424746.

17. Haldar AK, Saka HA, Piro AS, Dunn JD, Henry SC, Taylor GA, et al. IRG and GBP host resistance factors target aberrant, "non-self" vacuoles characterized by the missing of "self" IRGM proteins. PLoS pathogens. 2013;9(6):e1003414. Epub 2013/06/21. doi: 10.1371/journal.ppat.1003414. PubMed PMID: 23785284; PubMed Central PMCID: PMC3681737.

18. Beatty WL, Belanger TA, Desai AA, Morrison RP, Byrne GI. Tryptophan depletion as a mechanism of gamma interferon-mediated chlamydial persistence. Infection and immunity. 1994;62(9):3705-11. Epub 1994/09/01. PubMed PMID: 8063385; PubMed Central PMCID: PMC303021.

19. Coers J, Gondek DC, Olive AJ, Rohlfing A, Taylor GA, Starnbach MN. Compensatory T cell responses in IRG-deficient mice prevent sustained Chlamydia trachomatis infections. PLoS pathogens. 2011;7(6):e1001346. Epub 2011/07/07. doi: 10.1371/journal.ppat.1001346. PubMed PMID: 21731484; PubMed Central PMCID: PMC3121881.

20. Coers J, Starnbach MN, Howard JC. Modeling infectious disease in mice: co-adaptation and the role of host-specific IFNgamma responses. PLoS pathogens. 2009;5(5):e1000333. Epub 2009/05/30. doi: 10.1371/journal.ppat.1000333. PubMed PMID: 19478881; PubMed Central PMCID: PMC2682201.

21. Roan NR, Gierahn TM, Higgins DE, Starnbach MN. Monitoring the T cell response to genital tract infection. Proceedings of the National Academy of Sciences of the United States of America. 2006;103(32):12069-74. Epub 2006/08/02. doi: 10.1073/pnas.0603866103. PubMed PMID: 16880389; PubMed Central PMCID: PMC1567698.

22. Shin H, Iwasaki A. A vaccine strategy that protects against genital herpes by establishing local memory T cells. Nature. 2012;491(7424):463-7. Epub 2012/10/19. doi: 10.1038/nature11522. PubMed PMID: 23075848; PubMed Central PMCID: PMC3499630.

23. Mora JR, Bono MR, Manjunath N, Weninger W, Cavanagh LL, Rosemblatt M, et al. Selective imprinting of gut-homing T cells by Peyer's patch dendritic cells. Nature. 2003;424(6944):88-93. Epub 2003/07/04. doi: 10.1038/nature01726. PubMed PMID: 12840763.

24. Edele F, Molenaar R, Gutle D, Dudda JC, Jakob T, Homey B, et al. Cutting edge: instructive role of peripheral tissue cells in the imprinting of T cell homing receptor patterns. J Immunol. 2008;181(6):3745-9. Epub 2008/09/05. PubMed PMID: 18768825.

25. Vicetti Miguel RD, Reighard SD, Chavez JM, Rabe LK, Maryak SA, Wiesenfeld HC, et al. Transient detection of Chlamydial-specific Th1 memory cells in the peripheral circulation of women with history of Chlamydia trachomatis genital tract infection. Am J Reprod Immunol. 2012;68(6):499-506. Epub 2012/09/01. doi: 10.1111/aji.12008. PubMed PMID: 22934581; PubMed Central PMCID: PMC3493686.

26. Munn DH. Indoleamine 2,3-dioxygenase, Tregs and cancer. Current medicinal chemistry. 2011;18(15):2240-6. Epub 2011/04/27. doi: 0929-8673/11 $58.00+.00. PubMed PMID: 21517755.

27. Desvignes L, Ernst JD. Interferon-gamma-responsive nonhematopoietic cells regulate the immune response to Mycobacterium tuberculosis. Immunity. 2009;31(6):974-85. Epub 2010/01/13. doi: 10.1016/j.immuni.2009.10.007. PubMed PMID: 20064452; PubMed Central PMCID: PMC2807991.

28. Liu X, Newton RC, Friedman SM, Scherle PA. Indoleamine 2,3-dioxygenase, an emerging target for anti-cancer therapy. Current cancer drug targets. 2009;9(8):938-52. Epub 2009/12/23. PubMed PMID: 20025603.

29. Le Negrate G, Krieg A, Faustin B, Loeffler M, Godzik A, Krajewski S, et al. ChlaDub1 of Chlamydia trachomatis suppresses NF-kappaB activation and inhibits IkappaBalpha ubiquitination and degradation. Cellular microbiology. 2008;10(9):1879-92. Epub 2008/05/28. doi: 10.1111/j.1462-5822.2008.01178.x. PubMed PMID: 18503636.

30. Balsara ZR, Misaghi S, Lafave JN, Starnbach MN. Chlamydia trachomatis infection induces cleavage of the mitotic cyclin B1. Infection and immunity. 2006;74(10):5602-8. Epub 2006/09/22. doi: 10.1128/IAI.00266-06. PubMed PMID: 16988235; PubMed Central PMCID: PMC1594933.

31. Heuer D, Rejman Lipinski A, Machuy N, Karlas A, Wehrens A, Siedler F, et al. Chlamydia causes fragmentation of the Golgi compartment to ensure reproduction. Nature. 2009;457(7230):731-5. Epub 2008/12/09. doi: 10.1038/nature07578. PubMed PMID: 19060882.

32. Pennini ME, Perrinet S, Dautry-Varsat A, Subtil A. Histone methylation by NUE, a novel nuclear effector of the intracellular pathogen Chlamydia trachomatis. PLoS pathogens. 2010;6(7):e1000995. Epub 2010/07/27. doi: 10.1371/journal.ppat.1000995. PubMed PMID: 20657819; PubMed Central PMCID: PMC2904774.

33. Samudrala R, Heffron F, McDermott JE. Accurate prediction of secreted substrates and identification of a conserved putative secretion signal for type III secretion systems. PLoS pathogens. 2009;5(4):e1000375. Epub 2009/04/25. doi: 10.1371/journal.ppat.1000375. PubMed PMID: 19390620; PubMed Central PMCID: PMC2668754.

34. Chen AL, Johnson KA, Lee JK, Sutterlin C, Tan M. CPAF: a Chlamydial protease in search of an authentic substrate. PLoS pathogens. 2012;8(8):e1002842. Epub 2012/08/10. doi: 10.1371/journal.ppat.1002842. PubMed PMID: 22876181; PubMed Central PMCID: PMC3410858.

35. Emanuele MJ, Elia AE, Xu Q, Thoma CR, Izhar L, Leng Y, et al. Global identification of modular cullin-RING ligase substrates. Cell. 2011;147(2):459-74. Epub 2011/10/04. doi: 10.1016/j.cell.2011.09.019. PubMed PMID: 21963094; PubMed Central PMCID: PMC3226719.

36. Misaghi S, Balsara ZR, Catic A, Spooner E, Ploegh HL, Starnbach MN. Chlamydia trachomatis-derived deubiquitinating enzymes in mammalian cells during infection. Molecular microbiology. 2006;61(1):142-50. Epub 2006/07/11. doi: 10.1111/j.1365-2958.2006.05199.x. PubMed PMID: 16824101.

37. Wang A, Al-Kuhlani M, Johnston SC, Ojcius DM, Chou J, Dean D. Transcription factor complex AP-1 mediates inflammation initiated by Chlamydia pneumoniae infection. Cellular microbiology. 2013;15(5):779-94. Epub 2012/11/21. doi: 10.1111/cmi.12071. PubMed PMID: 23163821; PubMed Central PMCID: PMC3593943.

38. Shi L, Adkins JN, Coleman JR, Schepmoes AA, Dohnkova A, Mottaz HM, et al. Proteomic analysis of Salmonella enterica serovar typhimurium isolated from RAW 264.7 macrophages: identification of a novel protein that contributes to the replication of serovar typhimurium inside macrophages. The Journal of biological chemistry. 2006;281(39):29131-40. Epub 2006/08/09. doi: 10.1074/jbc.M604640200. PubMed PMID: 16893888.

39. Shi L, Chowdhury SM, Smallwood HS, Yoon H, Mottaz-Brewer HM, Norbeck AD, et al. Proteomic investigation of the time course responses of RAW 264.7 macrophages to infection with Salmonella enterica. Infection and immunity. 2009;77(8):3227-33. Epub 2009/06/17. doi: 10.1128/IAI.00063-09. PubMed PMID: 19528222; PubMed Central PMCID: PMC2715674.

40. Collins CA, Brown EJ. Cytosol as battleground: ubiquitin as a weapon for both host and pathogen. Trends in cell biology. 2010;20(4):205-13. Epub 2010/02/05. doi: 10.1016/j.tcb.2010.01.002. PubMed PMID: 20129784.

41. Hannemann S, Gao B, Galán JE. *Salmonella* Modulation of Host Cell Gene Expression Promotes Its Intracellular Growth. 2013;9(10):e1003668. Epub 2013/10/03. PubMed PMID: 24098123.

Appendix A: A Luman/CREB3–ADP-ribosylation factor 4 (ARF4) signaling pathway mediates the response to Golgi stress and susceptibility to pathogens

Contributions

Appendix A is the result of an exciting collaboration with Dr. Jan Reiling a post-doctoral fellow in the laboratory of David Sabatini at the Whitehead Institute. Initially, Jan characterized a host cell response to Golgi stress that involved the host protein ARF4 that he discovered using a haploid cell line gene trap screen. He found loss of ARF4 prevented the disruption of the Golgi complex using pharmaceutical compounds. Golgi disruption is a major virulence mechanism used by several intracellular pathogens to subvert host responses and acquire nutrients needed for survival. We tested the interesting hypothesis that blocking a general Golgi stress pathway in cells may also prevent pathogens from manipulating Golgi function. We found this to be the case for two pathogens *Shigella flexneri* and *Chlamydia trachomatis*. What follows in Appendix A is the entire manuscript that is now in press with Nature Cell Biology. The majority of the manuscript (Figures A1-A11) were experiments conducted almost entirely by Dr. Jan Reiling with small contributions by me. I then repeated the same mechanistic experiments and workflow used by Jan to characterize Golgi stress responses to examine phenotypes of intracellular bacterial pathogens, which is summarized in Figures A12 and A13.

INTRODUCTION

The processing, sorting and transport of proteins and lipids in the Golgi to their destined intracellular site of action is of fundamental importance to the maintenance and functions of subcellular compartments. The Golgi fulfills several other functions beyond regulation of vesicular transport of cargo such as serving as an important signaling platform where different stimuli converge and by bringing multiple factors together(1-5). Moreover, correct Golgi positioning is essential for several directed cell movements including wound healing, secretion or maintenance of cell polarity(6, 7).

Brefeldin A (BFA) was first described as a molecule with antiviral, antibiotic, and antifungal activity and is used as pharmacological tool to interrogate vesicular transport processes(8). BFA also showed anticancer effects against several human tumor cell lines and was explored as lead chemotherapeutic compound(9-12). BFA treatment of cells inhibits ER-Golgi transport, impedes protein secretion, and disperses the Golgi.

The ADP-ribosylation factors (ARFs) are evolutionarily conserved and ubiquitously expressed guanosine triphosphatases (GTPases), which belong to the Ras superfamily of small G proteins. They fulfill critical roles in the secretory pathway for transport of cargo between ER and Golgi or between different Golgi cisternae and in the endocytic system by recruiting coat proteins, activating lipid-modifying enzymes, and by regulating the cytoskeleton dynamics(13, 14). The effects of BFA are largely ascribed to the inhibition of ARF small G protein-guanine nucleotide exchange factor (GEF) complexes. BFA acts as uncompetitive inhibitor by binding in a hydrophobic cavity formed between ARF-GDP and a subset of GEFs thereby trapping the interaction partners in an unproductive conformation, which prevents exchange of GDP for GTP(15). The BFA-sensitive group of large GEFs includes GBF1, BIG1 and BIG2 that exert their functions at distinct sites throughout the Golgi complex.

Although there is substantial degree of sequence homology between different ARFs, the family of five small ARF G proteins found in humans is further divided into three classes based

on amino acid similarity: class I is composed of ARF1 and ARF3, ARF4 and ARF5 belong to class II, and class III contains a sole member, ARF6. A further distinctive feature is their subcellular localization. With the exception of ARF6, the most distantly related ARF that is present at the plasma membrane and on endosomes(16, 17), the other ARFs are mainly localized at the ER-Golgi interface, with ARF1, 4 and 5 found predominantly at the early Golgi and ERGIC, and ARF3 at the trans-Golgi and trans-Golgi network (TGN). ARFs also differ in their abundance, e.g. ARF1 and ARF3 are expressed 3-10-fold higher than ARF4-6(18). The high sequence conservation between the class I and II ARFs (>80%), their overlapping biochemical activities upon overexpression, and their similar expression pattern has hampered progress to unambiguously assign defined roles to the individual ARFs.

Here, we conducted a large scale insertional mutagenesis screen in a near-haploid human chronic myeloid leukemia cell line to identify genes essential for BFA-induced apoptosis and thereby uncovered C5orf44/TRAPPC13, and, unexpectedly, ARF4. Despite the previously reported redundancy between different ARF members, our study uncovers a role for ARF4 in response to BFA not shared with other ARF isoforms. We functionally dissected the mechanism of BFA resistance in ARF4-depleted cells and demonstrate that this occurs through upregulation of other ARF members such as ARF1 and ARF5, and also requires GBF1. Furthermore, we uncovered a signaling module involving the CREB3/Luman transcription factor and ARF4 whose expressions correlate with Golgi integrity and might be part of a Golgi stress response. The physiological importance of these results is indicated by additional findings revealing that ARF4 is critical for pathogenicity of *Chlamydia trachomatis* and *Shigella flexneri*, which infect millions each year.

RESULTS

To identify genes involved in BFA-induced toxicity, we employed a gene trap (GT)-based insertional mutagenesis approach using the near-haploid KBM7 cell line(19, 20). A heterogeneous population of approximately 100 million cells containing random knockout

mutations was assessed for their ability to resist cell death induced by chronic (3 weeks) BFA treatment. BFA-resistant GT cells were pooled at the end of the experiment, their DNA isolated, and the individual insertions mapped to the genome using deep sequencing(21). Two genes were enriched for GT insertions and associated with highly significant p-values (Figure A-1): 37 GTs mapped to *ARF4* ($p<8.39x10^{-110}$) and 12 to *C5orf44/TRAPPC13* ($p<7.86x10^{-29}$). For the remainder of this article we will focus on ARF4, and findings related to C5orf44/TRAPPC13 will be described elsewhere.

Using several lentivirally-transduced shRNA hairpins targeting ARF4, resistance to BFA was recapitulated in multiple cell lines including A549, HeLa, HT29, U251, PANC1, PC3, DU145, 786-0, MCF7 and MDA-MB231, thereby revealing an essential, conserved role for ARF4 in mediating BFA susceptibility (Figure A-1 and data not shown). Loss of ARF4 did not significantly alter proliferation or cell cycle phases relative to control cells (data not shown). To elucidate whether loss of ARF4 protects against other Golgi-disrupting agents, cells were treated for several days with Golgicide A (GCA) or Exo1. Similar to BFA treatment, ARF4 KD cells were largely protected from undergoing apoptosis upon GCA or Exo1 exposure in comparison to control cells (Figure A-1C). ARF4-depleted cells were, however, not resistant to other ER stress inducers including Tunicamycin, Thapsigargin, or A23187 pointing to a specific function of ARF4 in the secretory pathway (Figure A-2).

The ARFs may act pairwise or in a sequential manner to reinforce or diversify secretory transport processes, because earlier RNA interference (RNAi) studies revealed that only pairwise KD of different ARF isoforms caused aberrations in the secretory pathway(22-24). The finding that ARF4 loss alone was sufficient to render cells BFA-resistant was therefore not anticipated and hinted at a discrete role of ARF4 not shared with other ARFs. Our screen recovered GT integrations only in *ARF4* but not in any other *ARF* locus. To rule out the possibility that all ARFs but ARF4 were false negatives either due essentiality of the other ARFs

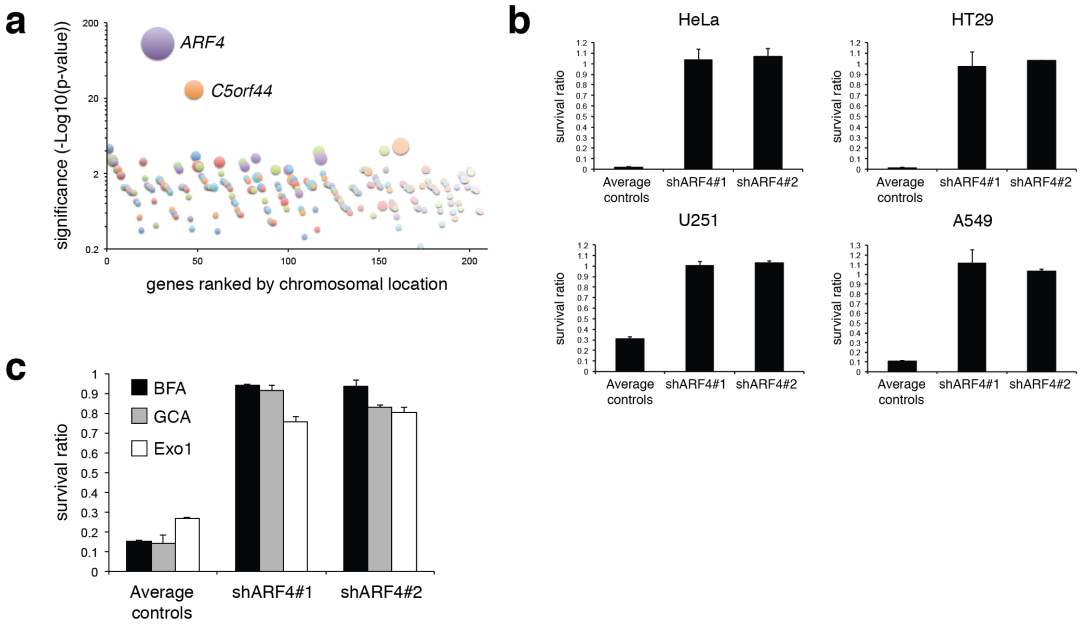

Figure A-1. Loss of ARF4 provides resistance to several Golgi-disrupting agents
(a) Mutagenized KBM7 cells were grown for 3 weeks in the presence of 50 ng/mL (180 nM) BFA after which genomic DNA of the surviving cells was isolated, and the GT insertion sites determined by deep sequencing and alignment to the genome. The number of independent insertions per gene was determined (represented by the circle size) and compared with that of an unselected mutagenized cell population from which enrichment scores (p-values) were derived (y axis). GT insertions were ordered along the x axis based on their chromosomal position. The two genes that were most enriched compared with an untreated control dataset were *ARF4* (37 GTs; $p<8.39\times10^{-110}$) and *C5orf44/TRAPPC13* (12 GTs; $p<7.86\times10^{-29}$).
(b) Viability of several cancer cell lines infected with control or ARF4 hairpins in response to BFA. Survival ratio was calculated by dividing cell numbers of BFA-treated cells by their corresponding counterparts under untreated conditions (with the exception of U251 cells whose viability was measured using the CellTiterGlo (CTG) assay). Shown are the means and S.D. of ARF4 KD and control cells and are examples of multiple representative experiments with n=2 for each condition and genotype with the exception of U251 ARF4 KD and their respective control cells for which n=10. Average controls refers to the averaged mean survival ratio of two to four different control hairpin-infected cell lines (shLUC, shRFP, shGFP) whose survival ratio is shown as the mean and S.E.M. Treatment duration, BFA concentrations, and p-values are as follows: HeLa: 3 days 30 ng/mL BFA treatment, $p<0.04$ for both ARF4 shRNAs; HT29: 5 days 30 ng/mL BFA treatment; $p<0.033$ for both ARF4 shRNAs; U251: 3 days 30 ng/mL BFA treatment, $p=1.06\times10^{-14}$ (for shARF4#1) and $p=5.72\times10^{-23}$ for shARF4#2); A549: 3 days 40 ng/mL BFA treatment, $p<0.005$ for both ARF4 shRNAs. Significance was determined using student's 2-tailed t-test (1-tailed for HT29 KD cells).
(c) Survival ratios of control and ARF4-depleted cells in response to BFA, Exo1 and GCA treatment as determined by counting surviving cells under treated and untreated conditions. Concentrations of compounds used were 20 ng/mL BFA, 2 μM GCA or 75 μM Exo1, treatment duration was 3 days. P-values are as follows (n=3): 2 μM GCA: $p<0.0003$ for both ARF4 shRNAs; 20 ng/mL BFA: $p<0.018$ for both ARF4 shRNAs; 75 μM Exo1: $p<0.00025$ for both ARF4 shRNAs.

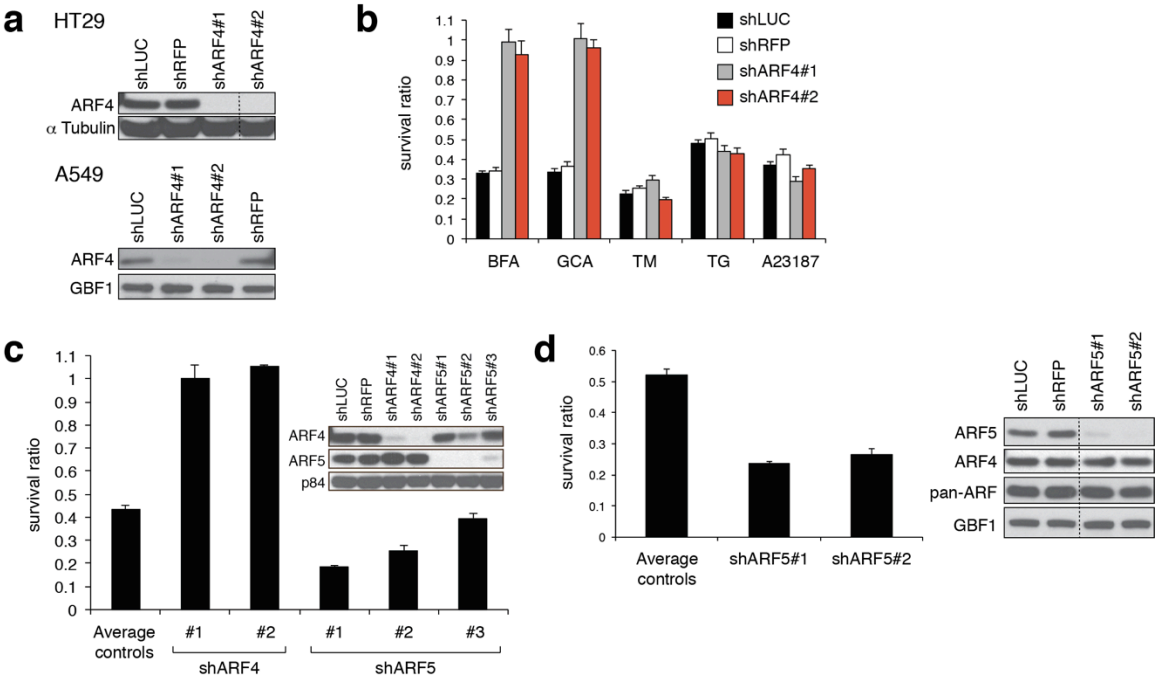

Figure A-2. Effect of BFA and other compounds on ARF4 and ARF5 knockdown cells
(a) ARF4 knockdown validation of HT29 and A549 cells infected with ARF4 hairpins.
(b) U251 cells lentivirally-transduced with control or ARF4 shRNAs were seeded in 96-well plates and treated for 3 days with or without indicated drugs before assessing cell viability using the CTG assay. ARF4 KD cells are protected against BFA and GCA but not against TM, TG, or A23187 compared with control cells. Drug concentrations used and abbreviations are: 30 ng/mL Brefeldin A (BFA), 3 μM Golgicide A (GCA), 500 ng/mL Tunicamycin (TM), 5 nM Thapsigargin (TG) and 1 μg/mL A23187.
(c) ARF4 or ARF5 depletion in HeLa cells causes resistance and hypersensitivity to BFA, respectively. Cells were left untreated or treated for 3 days with 7.5 ng/mL BFA, and the survival ratio was calculated by counting the number of surviving cells in the presence and absence of BFA. It is likely that the ARF4 antibody used for Western blotting also weakly recognizes ARF5 which is 90% identical to ARF4 (full length ARF4 was used as immunogen for antibody production) as there seems to be a slight ARF4 signal reduction upon ARF5 depletion in this particular cell line.
(d) KD of ARF5 in PANC1 cells shows that its loss makes cells more BFA-sensitive similar as in (c). Treatment duration was 4 days and 40 ng/mL BFA was used. Viability score was calculated as in (c).

or potential limitations associated with our screening approach such as insertion site preferences of the retroviral GT vector, we depleted several cell lines individually of each ARF family member by transduction with lentiviral hairpins. Reassuringly, when we knocked down ARF5, the other class II ARF, in HeLa or PANC1 cells, no BFA-resistance was observed. Instead, these cells were more sensitive to BFA than controls (Figure A-2C and 2D). Lentivirus-mediated depletion of ARF1 using multiple independent hairpins caused lethality in A549, HeLa, MCF7, PC3, HEK293T and PANC1 cells indicating that ARF1 function is essential (data not shown). We therefore repeated the infection with a several-fold lower virus titer to generate cells with reduced ARF1 expression yet compatible with survival. Reminiscent of ARF5 loss of function cells, ARF1-depleted cells were hypersensitive to BFA treatment. Therefore, loss of ARF4 protects against whereas loss of ARF1 or ARF5 sensitizes to BFA suggesting a unique function for ARF4 in BFA-resistance.

Given the protection of ARF4 KD cells from the cell-lethal effects of lower BFA concentrations, Golgi morphology was assessed next by immunofluorescence (IF). No obvious difference was detected between control and ARF4 KD cells under untreated conditions when stained for Giantin, GM130, or GBF1 (Figure A-3A and Figure A-4A). BFA treatment of cells infected with control hairpins promoted a diffuse appearance of the Golgi markers throughout the cytoplasm indicative of Golgi disassembly. Strikingly, most cells depleted of ARF4 displayed a normal Golgi morphology after BFA application similar to Golgi staining pattern in untreated conditions (Figure A-3 and Figure A-4B). In agreement with these results, general protein secretion was not inhibited by BFA in cells lacking ARF4 compared with control cells (Figure A-3B). Moreover, Hemagglutinin (HA) glycan maturation of cells infected with influenza A virus or class I MHC receptor trafficking was blocked in BFA-treated control cells but not in ARF4 KD cells (Figure A-3C and Figure A-4C). Thus, the integrity and functionality of the Golgi and secretory pathway following treatment with low BFA concentrations are preserved in ARF4-depleted cells. Under acute short-term treatment with high BFA

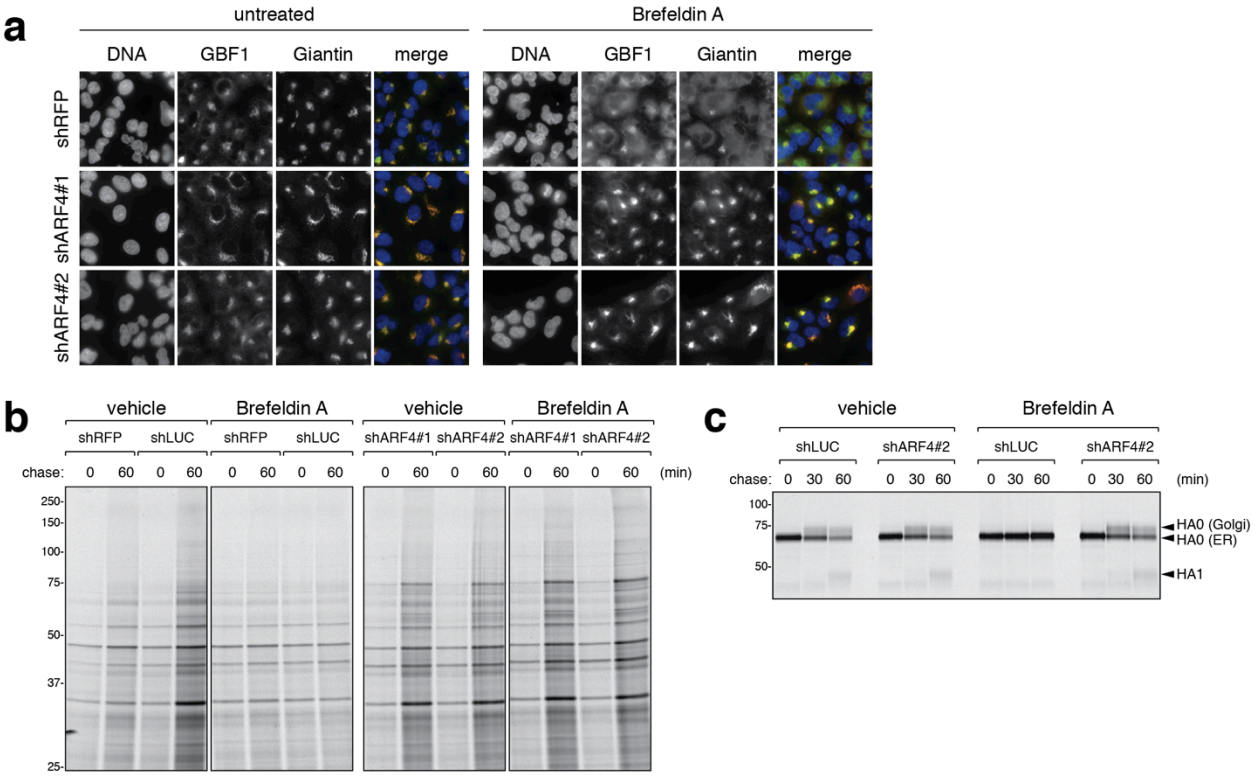

Figure A-3: ARF4 depletion preserves Golgi morphology and protein trafficking upon BFA treatment

(a) Representative IF images of one control and two ARF4 KD A549 cell lines reveal that ARF4 function is critical for Golgi dispersal upon BFA treatment as assessed by staining for the Golgi and ERGIC markers GBF1 and Giantin. Cells were treated with 20 ng/mL BFA for 29 hours.
(b) HeLa cells infected with either of two control (shLUC and shRFP) or ARF4 hairpins were metabolically labeled for 4 hours, and the amount of total proteins secreted into the culture media was assessed by SDS-PAGE. In the presence of 50 ng/mL BFA secretory trafficking persists in cells without ARF4 but not in the control cells.
(c) Control or ARF4-depleted cells were infected with influenza A virus at low pH. Influenza-derived Hemagglutinin A (HA)-trafficking through the secretory system was analyzed after a pulse of radioactive-labeled Met/Cys followed by a chase with cold Met/Cys. The results show that HA glycan-processing is not disrupted in the presence of BFA in cells without ARF4. HA0 is the full length HA that forms in the ER and trafficks through the Golgi. HA1 refers to HA that has reached the cell surface and is cleaved by Trypsin added to the chase media. See Methods section for further details.

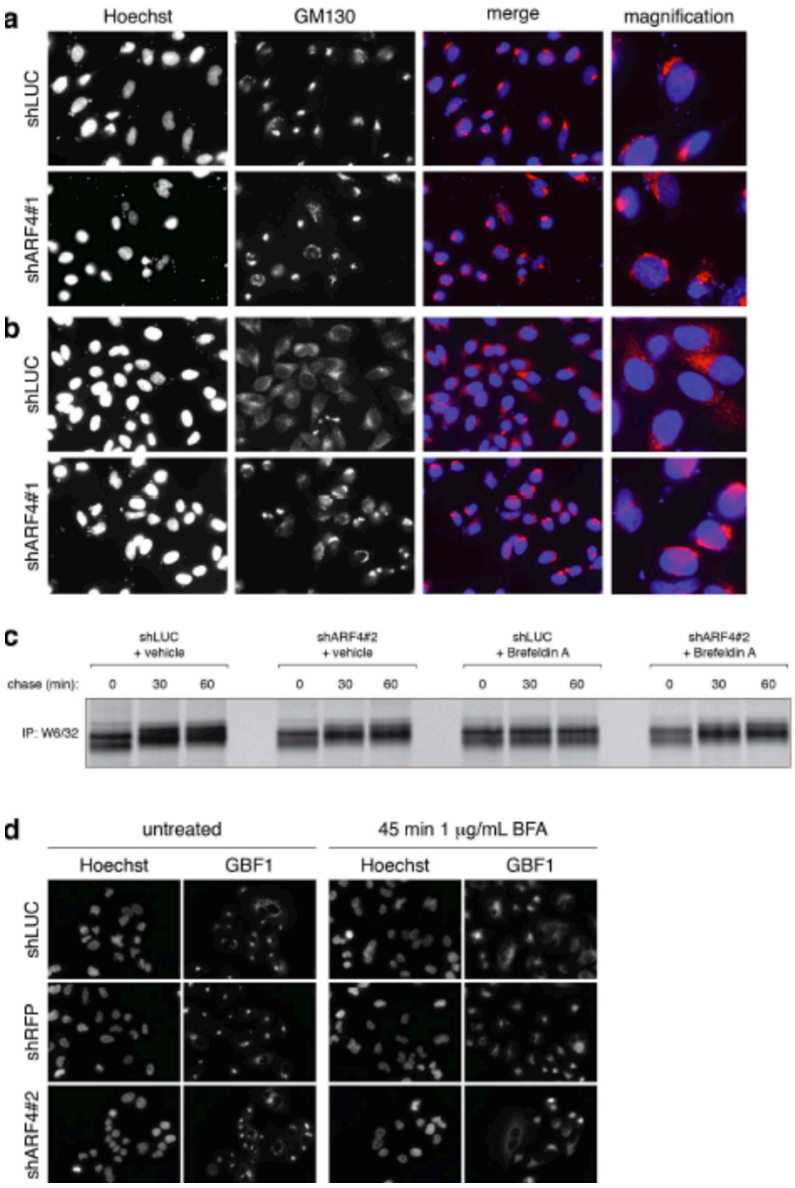

Figure A-4. Protection against BFA treatment upon loss of ARF4 in HeLa cells
(a, b) Golgi morphology is preserved in ARF4-depleted cells but not control cells upon treatment with low BFA concentrations. Shown are IF images of cells stained for the cis-Golgi marker GM130 and DNA (Hoechst). BFA treatment fragments the Golgi complex in control but not in ARF4 KD cells. (a) Cells left untreated, and (b) cells treated for one hour with 40 ng/mL BFA.
(c) Pulse/chase labeling experiment following MHC class I receptor trafficking (revealed by immunoprecipitation with the W6/32 antibody) with or without BFA treatment demonstrates that a functional secretory pathway persists in ARF4 KD HeLa cells despite the presence of 50 ng/mL BFA.
(d) Short term treatment with a high BFA dose of A549 cells transduced with indicated hairpins disperses the Golgi both in control and ARF4 KD cells.

concentrations, however, GBF1 staining appeared dispersed in ARF4 KD cells similar to controls indicative of a disrupted Golgi (Figure A-4D).

Compensatory ARF upregulation in cells with downregulated ARF4 function

Expression of activated forms of ARF1 or Rab1 and increased GBF1 or BIG2 expression were described to protect against Golgi disintegration upon BFA application(25-29). However, no obvious alterations in expression levels of GBF1, BIG1 and BIG2, several Golgi-matrix proteins (GM130, GRASP65, Giantin, Golgin-84), or Rab1b were detected under basal conditions in ARF4 KD protein lysates (Figure A-5A and 5B). The ARF1 monoclonal 1D9 antibody is a pan-ARF antibody recognizing ARF1, ARF3, ARF5, ARF6, and to lesser extent ARF4. Using this antibody, increased expression was observed in multiple cancer cell lines including U251, PC3, DU145, HT29, 786-0, MDA-MB231, PANC1, and HeLa cells (Figure A-5A-C). We also tested a panel of additional ARF antibodies that discriminate ARF isoforms. Enhanced ARF1, ARF3, and ARF5 expression but not ARF6 was detected upon ARF4 loss (Figure A-5A and 5B). To assess whether increased ARF levels translated into activity changes, an ARF-pull-down assay was employed(30). In agreement with the observed pan-ARF expression changes, ARF activity increased 1.5-2 fold in untreated or BFA-treated HeLa and PC3 ARF4 KD cells compared with control cells (Figure A-5A and 5B).

Based on these findings, we surmised that increased ARF1, ARF3 and ARF5 expression might play causative roles in ARF4-depleted cells levels endowing them with the capacity to withstand BFA toxicity. Accordingly, stable overexpression of either ARF1 or ARF5 alone but not ARF4 was sufficient to enhance cellular survival in the presence of BFA (Figure A-7). We next asked whether blocking ARF1, ARF3, or ARF5 function in cells without ARF4 might reverse BFA resistance. To test this we re-infected stable ARF4 KD or control cells with lentiviral ARF1, ARF3, or ARF5 hairpin vectors carrying different antibiotic markers to select for double-KD (DKD) cells. ARF1 ARF4 DKD and control cells were then grown in the presence or absence of BFA for several days, and their survival ratio was calculated. Strikingly, while ARF4

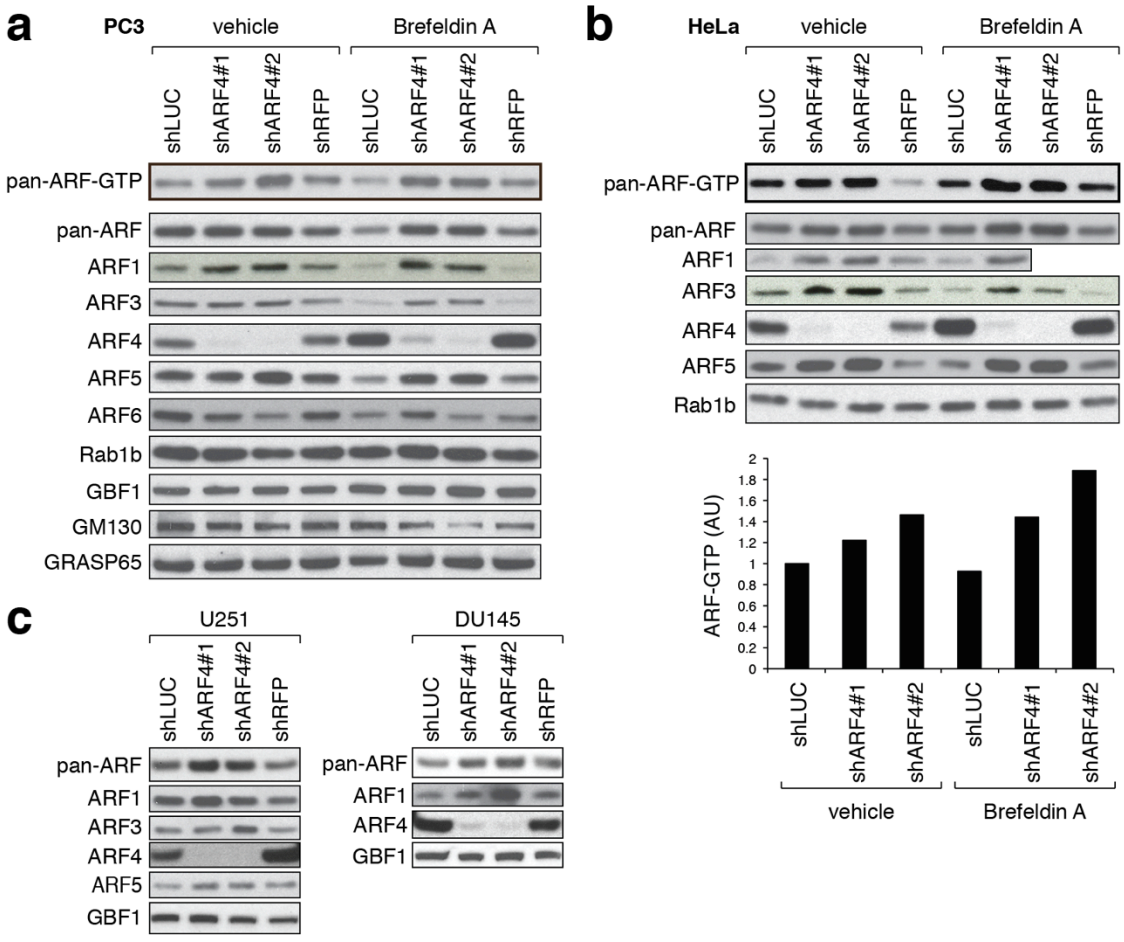

Figure A-5. Compensatory upregulation of other ARF family members in ARF4 knockdown cells

(a-c) Several cancer cell lines were transduced with lentiviral control hairpins or shRNAs against ARF4, and cell lysates were probed with the indicated antibodies.

(a, b) Stable hairpin-control or ARF4 KD PC3 (a) or HeLa (b) cells were analyzed for total ARF-GTP levels in the absence or presence of 20 ng/mL BFA (24 hours treatment) using a GST-VHS-GAT pull-down assay. In this assay, increased ARF binding to VHS-GAT, a truncated GGA3 form and ARF-substrate that is bound only when ARFs are GTP-loaded, serves as proxy for ARF activity. A representative example of a quantification of ARF-GTP levels in HeLa cells is shown (n=2; note that we omitted the shRFP control in the bar graph for this particular analysis. AU= arbitrary units). The corresponding protein lysates for the samples used in (a) and (b) were tested with indicated antibodies.

(c) Two additional examples (DU145 and U251 cells) showing upregulated (pan-) ARF levels in ARF4-depleted cells.

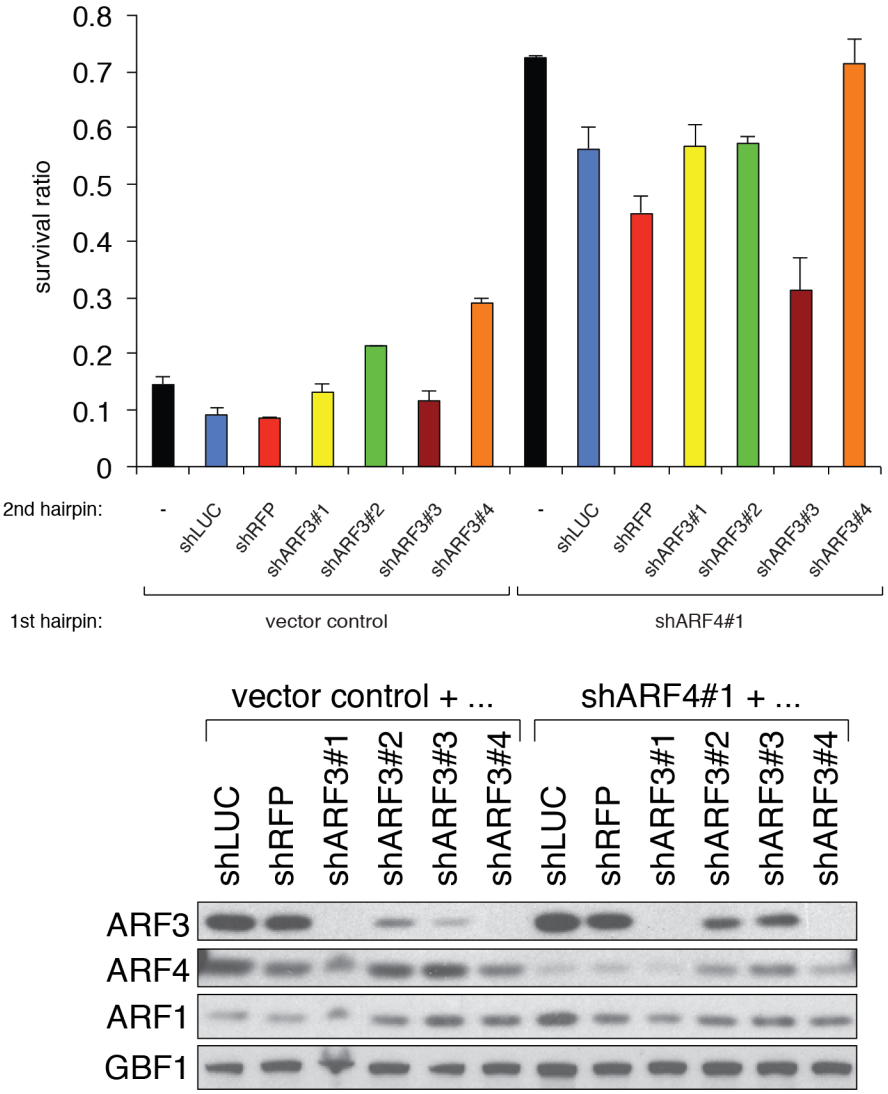

Figure A-6: ARF3 function in ARF4-deleted cells is not critical to confer BFA resistance
A549 cells simultaneously depleted for ARF3 and ARF4 display the ARF4 single KD phenotype indicating a negligible role of ARF3 for BFA resistance upon loss of ARF4. Cells were treated for 3 days with 20 ng/mL BFA or left untreated, and surviving cells were counted in both conditions to calculate the survival ratios. Western blotting confirms KD of ARF3 and ARF4 in these cells.

KD cells re-infected with shLUC or shRFP hairpins were BFA-resistant, ARF1 ARF4 DKD cells displayed up to 60% lower survival comparable to cells that had been successively infected with two innocuous hairpins (i.e. vector control + shLUC or shRFP) (Figure A-7B). We also found that ARF4 ARF5 DKD cells had a significantly lower survival ratio compared with ARF4 KD cells re-infected with control hairpins (Figure A-7C). Unlike ARF1 ARF4 or ARF4 ARF5 co-depletion, survival of BFA-exposed ARF3 ARF4 DKD cells did not differ from ARF4 KD cells infected with control hairpins suggesting that BFA protection against BFA occurs at the early Golgi but not at the TGN where ARF3 localizes(31) (Figure A-6). GBF1 acts as a GEF for several ARF isoforms including ARF1, ARF4, and ARF5 and is the rate-limiting factor to control their activity at the ERGIC and early Golgi(32). Downregulation of GBF1 therefore inhibits ARF activity, and GBF1 depletion should be functionally equivalent to ARF1 and ARF5 loss. Cells infected with both a control and a GBF1 hairpin showed a similar survival ratio as cells
infected with control hairpins upon BFA treatment, unlike ARF4 LUC DKD cells that were largely resistant to BFA. Strikingly, ARF4 GBF1 DKD cells were BFA-sensitive and displayed the same survival as single GBF1 KD cells (Figure A-7D). In summary, resistance of ARF4-depleted cells is abrogated upon ARF1, ARF5, or GBF1, but not ARF3 co-depletion, demonstrating that BFA resistance following ARF4 loss depends on compensatory accumulation of other ARF isoforms or GBF1. When DKD protein lysates were analyzed for ARF4 expression, we found that loss of ARF1 or GBF1 entailed the re-emergence of ARF4 expression both in vector control and ARF4-haripin infected cells indicative of a coordinate regulation of their expression (Figure A-7).

Golgi stress causes ARF4 induction mediated through CREB3/Luman

During this study we made the observation that most of the analyzed cancer cell lines upregulated ARF4 levels upon BFA treatment (Figure A-9A). In addition, treatment with GCA, Exo1 or Monensin enhanced ARF4 expression independent of general ER stress induction since GRP78 or CHOP levels were unchanged in Exo1 treated cells, and Tunicamycin or

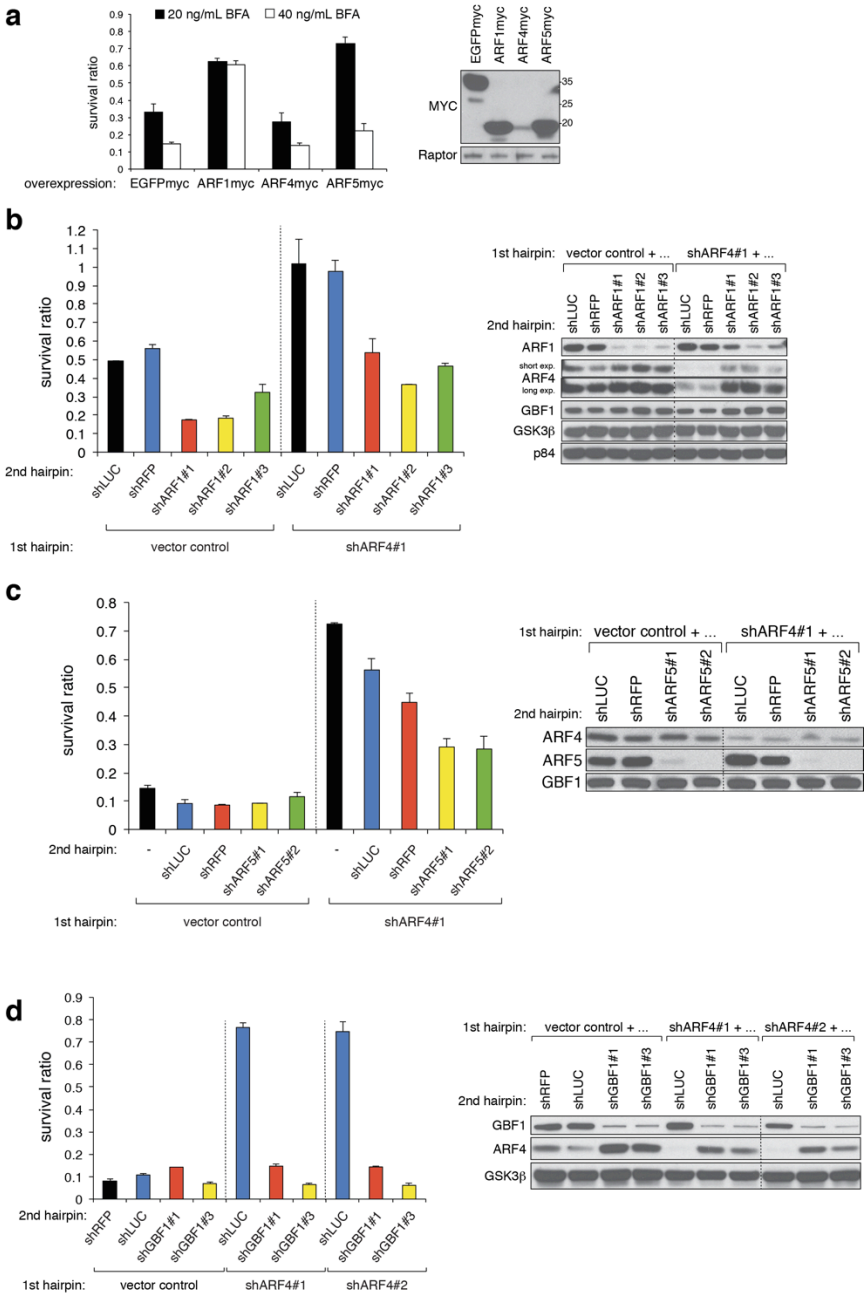

Figure A-7: BFA resistance of ARF4-depleted cells depends on ARF1, ARF5 and GBF1
(a) Stable overexpression of C-terminally tagged ARF1 or ARF5 but not ARF4 in A549 cells increases viability of BFA-treated cells. Treatment duration was 3 days, and cell viability was assessed by the CTG assay measuring 12 wells of each genotype and condition. At a concentration of 20 ng/mL but not 40 ng/mL BFA ARF4 overproduction slightly sensitized to the drug ($p=0.015$) despite its weak expression. P-values (for both BFA concentrations) are $p<1.8\times10^{-11}$ and $p<4\times10^{-5}$ for ARF1 and ARF5 overexpression, respectively.
(b) A reduction of ARF1 function in ARF4 KD A549 cells negates BFA resistance observed in ARF4 single KD cells as determined by coulter counter measurement (p-values of BFA-treated samples (compared with the mean of the two average survival ratios of shLUC shARF4 and

Figure A-7 (Continued) shRFP shARF4 DKD controls) are: shARF4 shARF1#1: p<0.046; shARF4 shARF1#2: p<0.017; shARF4 shARF1#3: p<0.005).
(c) ARF4 ARF5 co-depletion makes A549 cells significantly less resistant to BFA in comparison to DKD controls. P-values are (compared to the averaged cell number ratios of shLUC and shRFP under BFA-treated conditions): p<0.0066 (ARF5#1) and p<0.014 (ARF5#2).
(d) Removing GBF1 function makes ARF4 KD cells as sensitive to undergo apoptosis upon BFA treatment as GBF1 single KD cells. P-values for ARF4#1 DKD cells (BFA treatment): p<0.0066 (GBF1#1); p<0.0065 (GBF1#3). P-values for ARF4#2 DKD cells: p<0.03 (GBF1#1); p<0.02 (GBF1#3). Western blot analysis of co-depleted cells are presented to confirm KD of the indicated proteins. Note the upregulation of ARF4 levels in ARF1- or GBF1-deprived cells. Student's 2-tailed t-test was used for statistical analyses in (a-d).

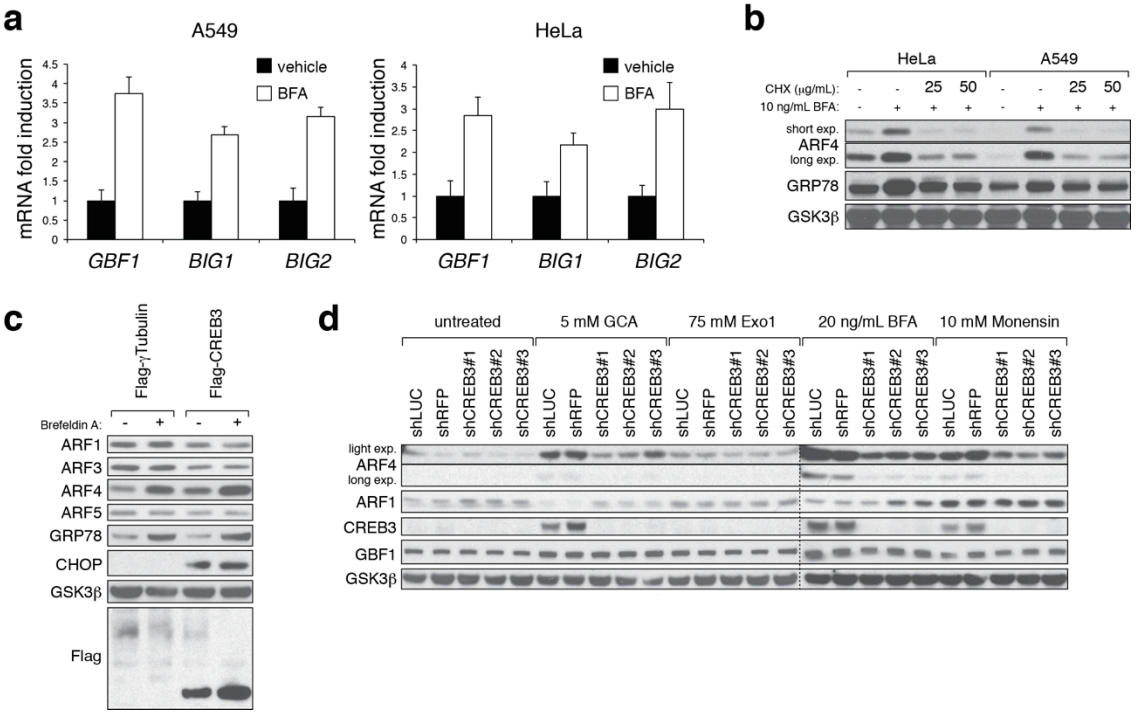

Figure A-8. Effect of Golgi stress treatments and CREB3 expression on ARFs and ARF-GEFs
(a) Shown are quantitative real-time PCR analyses of BFA treated and vehicle treated cells (treatment duration was 29 hours, and cells were either vehicle-treated or with 20 ng/mL BFA). P-values (student's 2-tailed t-test) are as follows: for GBF1, p<0.01 and p<0.004 (A549 and HeLa, respectively); BIG1, p<0.05 and p<0.009 (A549 and HeLa, respectively); BIG2, p<0.001 and p<0.004 (A549 and HeLa, respectively).
(b) HeLa and A549 cells were co-treated with BFA and two different doses of the protein synthesis inhibitor Cycloheximide (CHX) for 29 hours with the indicated concentrations.
(c) Stable Flag-CREB3 and control (Flag-γTubulin) protein-expressing HeLa cells were left untreated or treated for 24 hours with 10 ng/mL BFA before cell lysis, and the lysates tested for ARF isoforms and ER stress marker expression by immunoblotting.
(d) A549 cells infected with control or CREB3 hairpins were treated for 24 hours with several Golgi stressors and the lysates probed with the indicated antibodies after SDS-PAGE. Note ARF1 induction upon CREB3 downregulation.

Thapsigargin had minimal effects on ARF4 levels (Figure A-9B and 9C). Interestingly, Thapsigargin treatment was reported to induce Golgi fragmentation, which might explain the slightly increased ARF4 levels(33). To test if ARF4 upregulation could be prevented by antagonizing BFA-induced Golgi dispersal, cells were simultaneously treated with BFA and H-89 or Forskolin, respectively. H-89 is a non-selective, cell permeable protein kinase inhibitor that sustains Golgi morphology and ARF1-GTP levels in the presence of BFA, and Forskolin acts through a BFA-detoxification mechanism and accordingly renders cells less susceptible to BFA(2, 34, 35). Indeed, H-89 or Forskolin mitigated ARF4 upregulation in a dose-dependent manner when co-treated with BFA, which was paralleled by UPR marker expression (Figure A-9D and 9E). ARF4 levels therefore correlate with Golgi integrity with low ARF4 expression under basal conditions but increased levels following certain stress conditions impinging on Golgi homeostasis.

Quantitative real-time PCR analysis revealed that *ARF4* is transcriptionally induced upon BFA treatment (Figure A-11A). Although all other *ARFs* trended towards increased expression following BFA exposure, only *ARF1* reached significance, however, to a lower magnitude than ARF4. In addition to the *ARFs*, transcript levels of the three GEFs BIG1, BIG2, and GBF1 became upregulated in the presence of BFA (Figure A-8A). As shown earlier for GBF1, we also saw a concomitant increase in protein levels following BFA treatment. This increase was prevented by co-treatment of Cycloheximide and BFA (Figure A-8B). This indicates that ARF4 expression is controlled via new mRNA and protein production.

It was reported that phorbol 12-myristate 13-acetate (PMA) treatment induces ARF4 expression, in a manner dependent on sLZIP, a CREB3 (also called Luman or LZIP) isoform lacking the transmembrane domain(36). CREB3 is a basic leucine zipper (bLZIP) ER-bound transcription factor that is proteolytically cleaved following activation in the Golgi apparatus by site-1 protease (S1P) and site-2 protease (S2P), then enters the nucleus where it binds as a homodimer to canonical cAMP-response elements (CRE) to enhance transcription of its

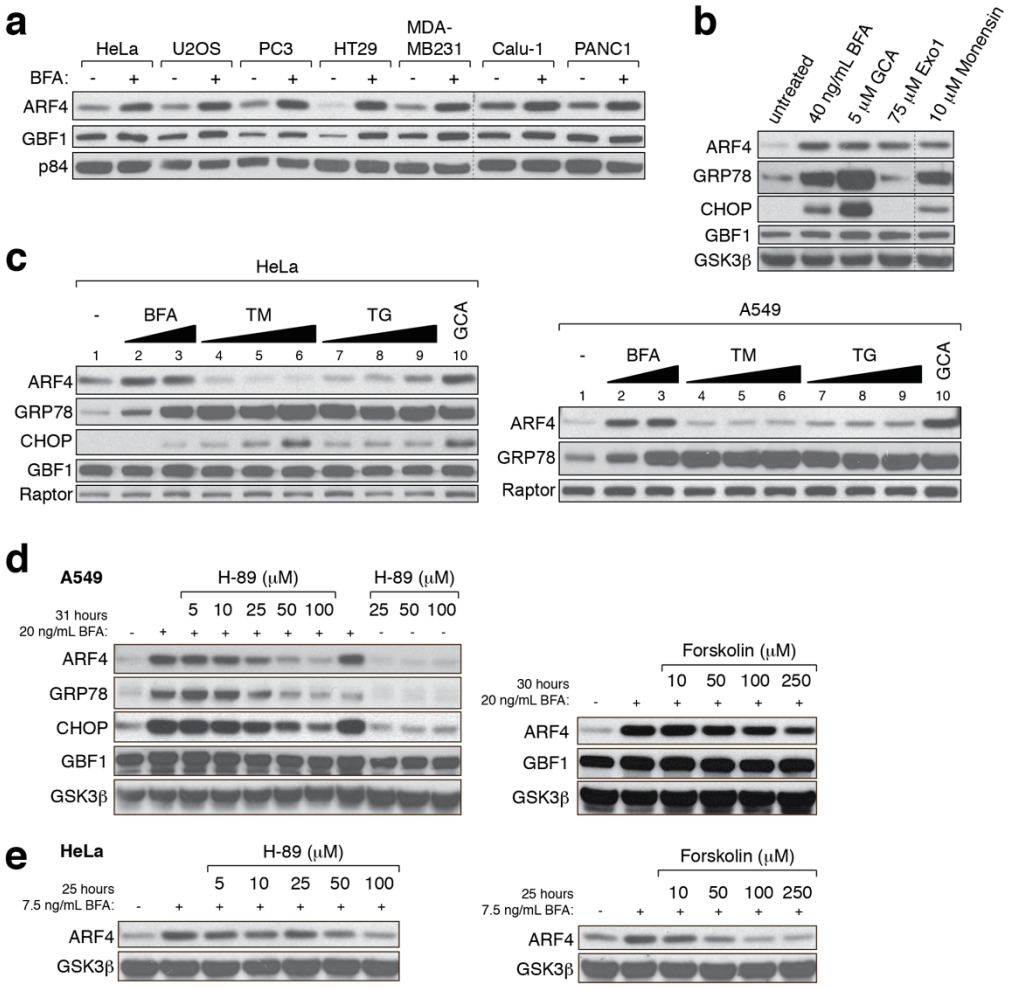

Figure A-9: Golgi stress causes ARF4 upregulation

(a) Several cancer cell lines were cultured with or without 20 ng/mL BFA for 29 hours before cell lysis, and protein extracts were analyzed with the indicated antibodies. Note the induction of ARF4 and GBF1 levels in the presence of BFA.

(b) A549 cells were left untreated or exposed to 40 ng/mL BFA, 5 μM GCA, 75 μM Exo1 or 10 μM Monensin for 29 hours revealing increased ARF4 expression.

(c) Immunoblots showing ARF4 and ER stress marker expression of HeLa and A549 cells treated for 29 hours with following compounds and concentrations: lane 1: untreated, lanes 2 and 3 Brefeldin A (BFA; used at 10 ng/mL= 36 nM and 50 ng/mL= 180 nM); lanes 4-6: Tunicamycin (TM; used at 100 ng/mL (119 nM), 500 ng/mL (597 nM) and 2 mg/mL (2.39 μM); lanes 7-9: Thapsigargin (TG; used at 10 nM, 100 nM and 500 nM); lane 10: Golgicide A (GCA; used at 5 μM).

(d, e) Co-treatment of A549 or HeLa cells with BFA and increasing amounts of H-89 or Forskolin, two compounds that antagonize BFA-induced Golgi dispersal, mitigates upregulation of ARF4 and UPR parameters.

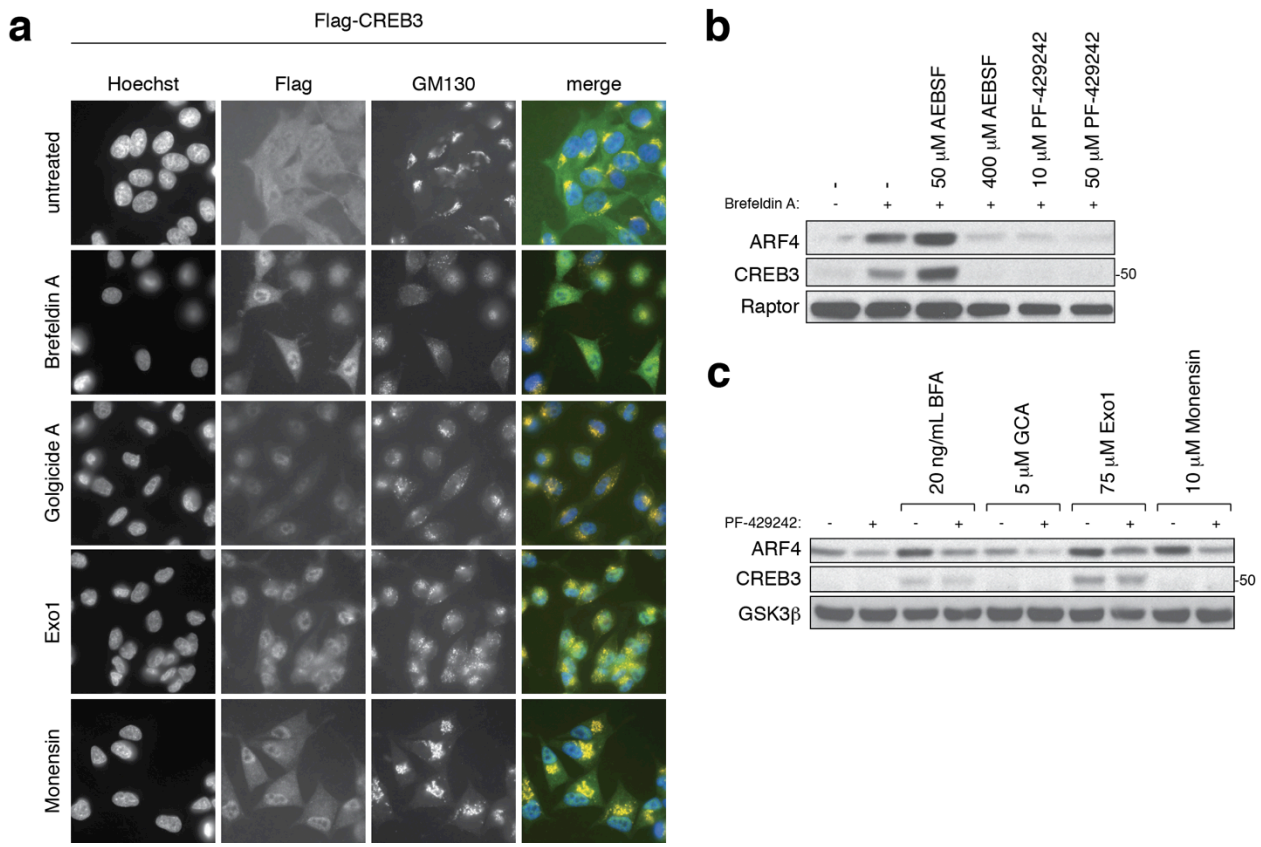

Figure A-10. Involvement and regulation of CREB3 and S1P in Golgi stress-induced ARF4 induction

(a) Lentivirally-transduced HeLa cells stably expressing Flag-CREB3 were left untreated or treated for 23 hours with 20 ng/mL BFA, 5 μM GCA, 75 μM Exo1 or 10 μM Monensin before fixation and immunofluorescent staining to assess CREB3 localization and Golgi morphology.
(b) Simultaneous treatment for 28 hours of A549 cells with 10 ng/mL BFA and either of two different serine protease inhibitors, AEBSF or PF-429242 mitigates ARF4 upregulation in a dose-dependent manner.
(c) Pharmacological inhibition of S1P in the presence of several Golgi stress agents decreases ARF4 expression compared with BFA only-treated HeLa cells. Treatment duration was 29 hours and PF-429242 was used at 10 μM.

targets(37). How ARF4 levels are regulated upon BFA treatment is unknown. To test if BFA-induced ARF4 expression requires CREB3, several cell lines were infected with CREB3 hairpins to deplete CREB3. Upon BFA treatment CREB3 KD A549 cells displayed substantially reduced ARF4 levels paralleled by GRP78 and CHOP downregulation compared to control cells (Figure A-11B). Similar results were obtained in PC3, PANC1, or MDA-MB231 cells demonstrating that CREB3 is a conserved mediator of the cellular response to BFA (Figure A-11C). Further strengthening this link, we found that CREB3 downregulation promoted ARF1 induction (Figure A-8D). Hence, CREB3 KD mirrors loss of ARF4 function. Akin to BFA treatment, CREB3 is also required for ARF4 induction in response to GCA, Exo1 and Monensin (Figure A-8D). These treatments also activated and redistributed ER-localized CREB3 into the nucleus (Figure A-10A). Moreover, proteolytic activation of CREB3 and ARF4 upregulation is dependent on S1P, because S1P inhibitors (AEBSF and PF-429242) lower CREB3 stabilization and ARF4 expression in response to BFA, GCA, Exo1 and Monensin (Figure A-10B and 10-C). Western blot analysis also revealed that in the presence of BFA CREB3 levels increase beyond the weakly detectable levels observed under basal conditions presumably due to inherent instability(38, 39) (Figure A-11B and 11C). To assess whether loss of CREB3 alters cellular BFA susceptibility, we cultured the KD cells in the absence or presence of the drug. Similar to ARF4-depletion, CREB3 KD cells showed enhanced resistance to BFA relative to control cells (Figure A-11D). Next, we monitored the effects of CREB3 overexpression on ARF4 levels and BFA sensitivity by establishing stable cell lines overexpressing epitope-tagged CREB3. Despite only modest CREB3 overexpression levels, ARF4 induction was readily discernable while other ARF isoforms were slightly but reproducibly downregulated (Figure A-11E). CREB3 overexpression sensitized cells to undergo apoptosis in response to BFA correlating with higher ARF4 levels and concomitant decrease in the amount of other ARFs (Figure A-11F).

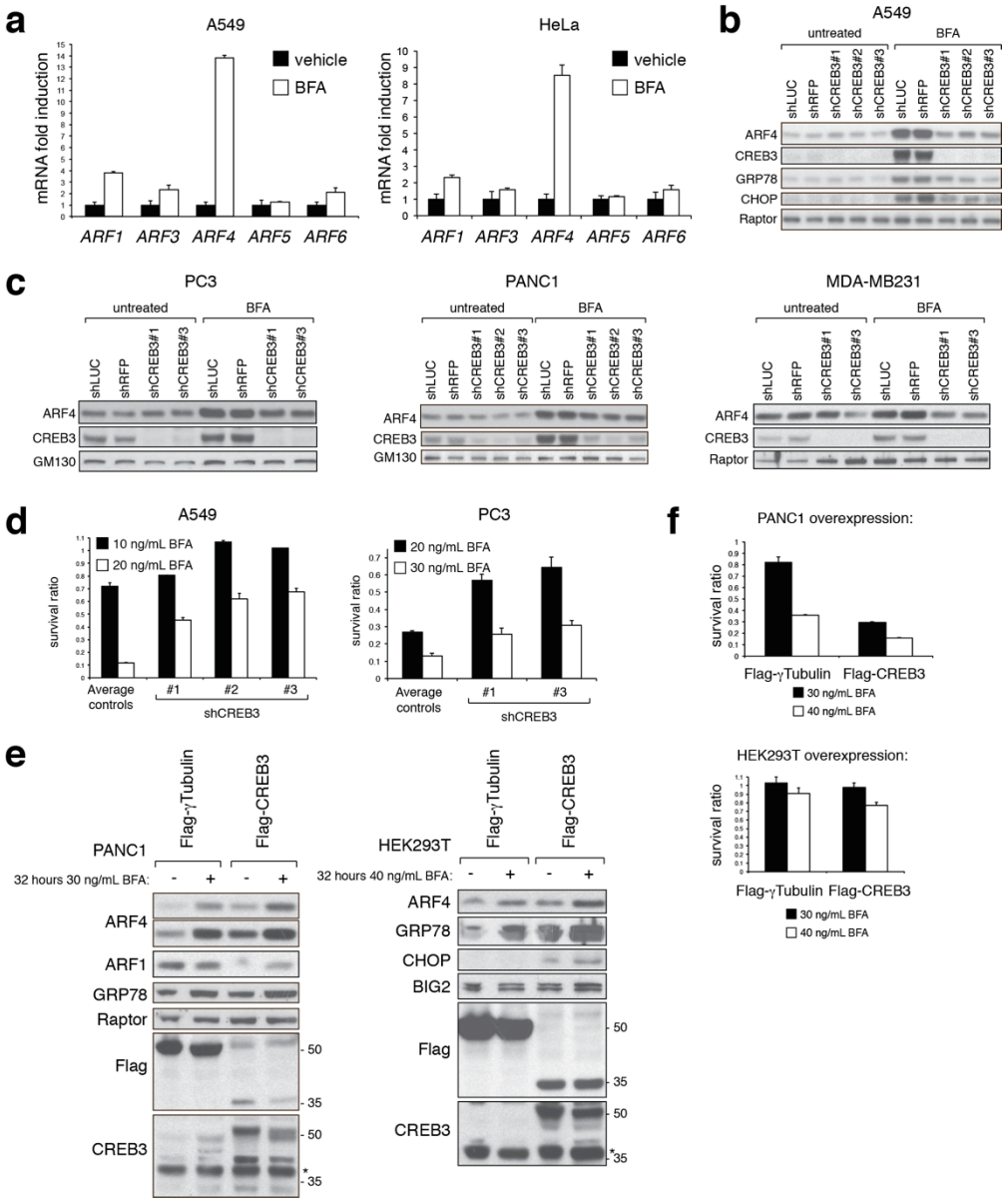

Figure A-11: CREB3/Luman mediates ARF4 induction upon Golgi stress
(a) A549 or HeLa cells were vehicle-treated (0.04% ethanol) or treated with 20 ng/mL BFA for 29 hours, and *ARF* mRNA levels were assessed by quantitative real-time PCR and normalized to *36B4* mRNA expression. Data points are represented as mRNA fold induction compared with vehicle-treated samples. Error bars denote S.D. values, and p-values are as follows (student's 2-tailed t-test): p=0.019 and 0.0003 for ARF4, and p=0.0015 and 0.01 for ARF1 (A549 and HeLa, respectively). All other p-values were not significant.
(b, c) Lentiviral-mediated KD of CREB3 in A549 (b), PC3, PANC1, or MDA-MB231 (c) in the presence of BFA reduces ARF4 expression relative to control hairpin-infected cells. BFA concentrations used were 20 ng/mL except for PANC1 (40 ng/mL), and treatment durations were 29 hours (A549 cells), 27 hours (PC3), 22 hours (PANC1), or 30 hours (MDA-MB231).

Figure A-11 (Continued) (d) shRNA-mediated CREB3 downregulation increases viability of BFA-treated A549 or PC3 cells in comparison to control cells. All p-values (n=2) for A549 and PC3 cells (20 ng/mL BFA) are < 0.05.
(e) Stable CREB3 overexpression is sufficient to elevate endogenous ARF4 levels in PANC1 or HEK293T cells. Upon overexpression, two bands could be detected by Western blotting when antibodies against the Flag-epitope or endogenous CREB3 were used. The predominant band detected in most cell lines when probed for endogenous CREB3 is the upper band (approximately 50 kDa, corresponding to the full length form), and a lower band (approximately 35-40 kDa) is occasionally discernable and might represent S1P/S2P-mediated cleavage products(40). * denotes unspecific band.
(f) Increased BFA susceptibility of stable cell lines overexpressing CREB3. P-values for PANC1 and HEK293T cells: p=0.04 for both (using 30 ng/mL BFA) and p=0.0005 or p=0.001, respectively (using 40 ng/mL BFA). * denotes unspecific band.

We wondered whether the increased BFA sensitivity of ARF1 or GBF1 KD cells and reemergence of ARF4 expression in these cells (Figure A-7) might be associated with altered CREB3 localization. To this end A549 GBF1 or ARF1 KD and control cells were transfected with a Flag-CREB3 overexpression vector and CREB3 localization tested by immunostaining. Similar to BFA treatment, ARF1 KD or GBF1 KD resulted in CREB3 accumulation in the nucleus presumably caused by partial Golgi fragmentation providing a possible explanation for enhanced ARF4 expression.

Loss of ARF4 protects against propagation of several pathogens

While BFA chemically induces Golgi dispersal, two intracellular bacterial pathogens, *Chlamydia trachomatis* and *Shigella flexneri,* naturally subvert host trafficking pathways to acquire lipids and disrupt cytokine secretion by inducing Golgi fragmentation(41). We hypothesized infection-mediated Golgi disruption was similar to BFA treatment, and therefore ARF4 KD cells may prevent efficient pathogen growth. When we tested the effects of Chlamydia infection on ARF4, no appreciable upregulation was detected in control cells. A slight boost in ARF4 expression was detected in ARF4 KD cells (Figure A-13). We wondered whether the life cycle of either *Chlamydia* or *Shigella* might be affected by ARF4 loss since its depletion protected against chemically-induced Golgi disruption. We infected control and ARF4 KD HeLa cells with *Chlamydia* or *Shigella*, and growth was assessed at various time points after infection. For both pathogens no significant replication level differences between control and ARF4-deprived cells were detected early, indicating that invasion of ARF4-depleted cells is not disrupted. However, we noted defects in persistence/growth for both pathogens late during infection. 48 hours post-infection *Chlamydia* replication was reduced by about 40-60% with two independent hairpins against ARF4 using a quantitative PCR assay (Figure A-12A). Because *Chlamydia* must complete a biphasic lifecycle to invade new host cells, we examined the production of infectious progeny in control or ARF4-deprived cells and found depletion inhibited the production of

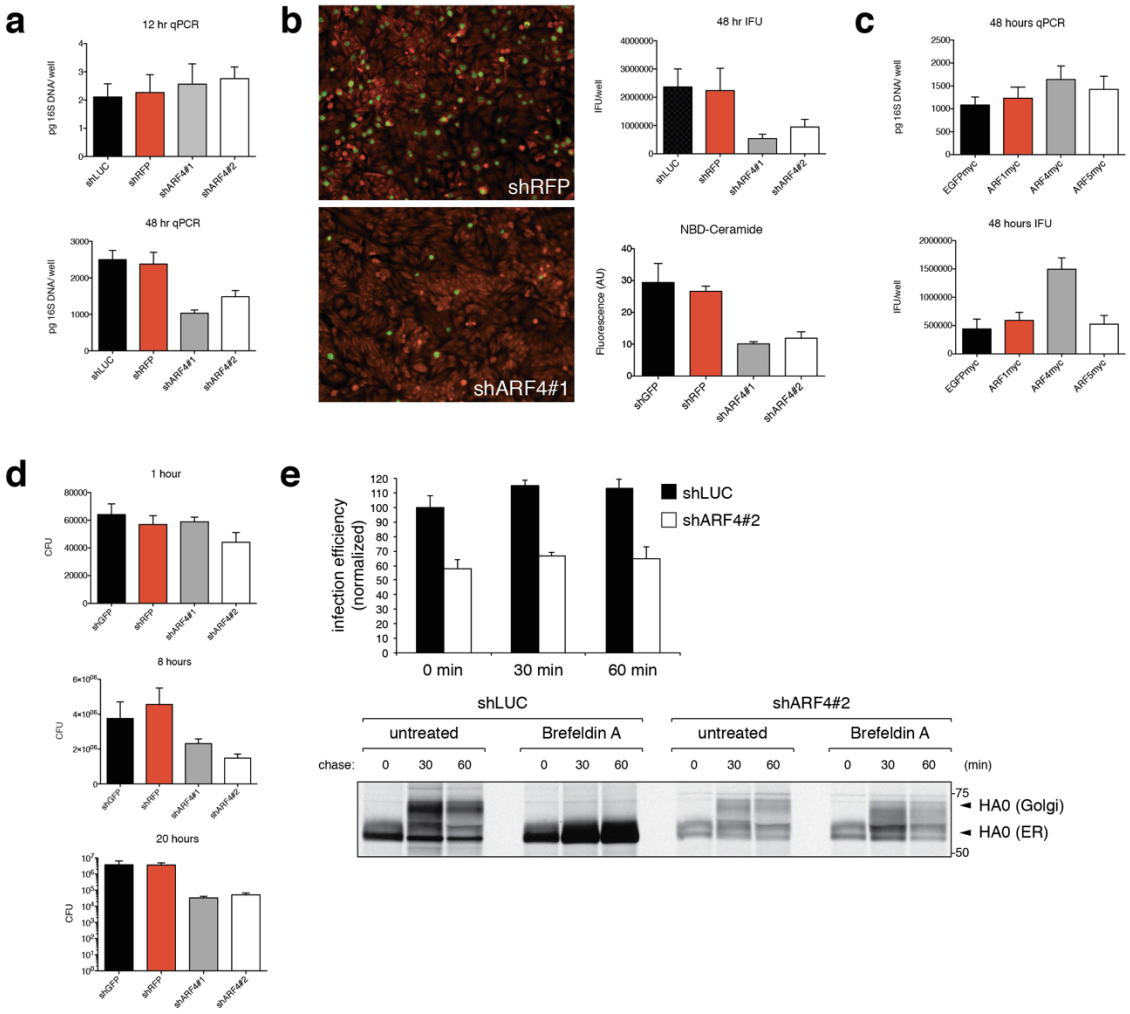

Figure A-12: ARF4 loss protects against several intracellular pathogens
(a, b) Intracellular replication and infectivity of *C. trachomatis* is inhibited upon loss of ARF4 in HeLa cells. (a) Quantitative PCR analysis of cells infected with *C. trachomatis* shows a significant decrease of bacterial genomes present after 48 hours but not after 12 hours in ARF4 KD cells relative to controls. (b) Representative IF images of wild type HeLa cells infected with *C. trachomatis* progeny produced from shRFP or ARF4 hairpin-infected cells reveal significant differences in infectivity. *C. trachomatis* inclusions are represented in green (stained for *C. trachomatis* major outer membrane protein (MOMP)), and cells were counter-stained with Evans Blue. The right upper panel shows inclusion forming unit (IFU) quantification. The lower right graph displays a quantification of cellular NBD-ceramide labeling demonstrating a lower fluorescent ceramide content in control cells relative to shARF4 cells (AU= arbitrary units). Cells were pulsed for one hour with NBD-ceramide. Six biological replicates were measured per genotype, $p<0.05$ (one-way ANOVA) and the experiment was performed twice. Bar graphs depict average values, and error bars correspond to S.D.
(c) Increased ARF4 expression enhances growth of *C. trachomatis*. HeLa cells were analyzed for inclusion formation 48 hours post-infection, $p<0.05$ using one-way ANOVA. Two independent experiments yielding qualitatively similar results have been performed using six biological replicates of each genotype.

Figure A-12 (Continued) (d) Decreased *S. flexneri* growth upon ARF depletion. Cells were infected with *S. flexneri* and treated with Gentamicin. The cells were then lysed at various time points after and dilution plating was used to count the number of bacterial colonies present (CFU=colony forming units). In (a-c) one-way ANOVA was used to calculate the p-values. All p-values comparing the individual controls and the two different shARF4 hairpins were $p<0.05$. Results are representative of at least two independent experiments with three to six biological replicates for each genotype and time point analyzed.

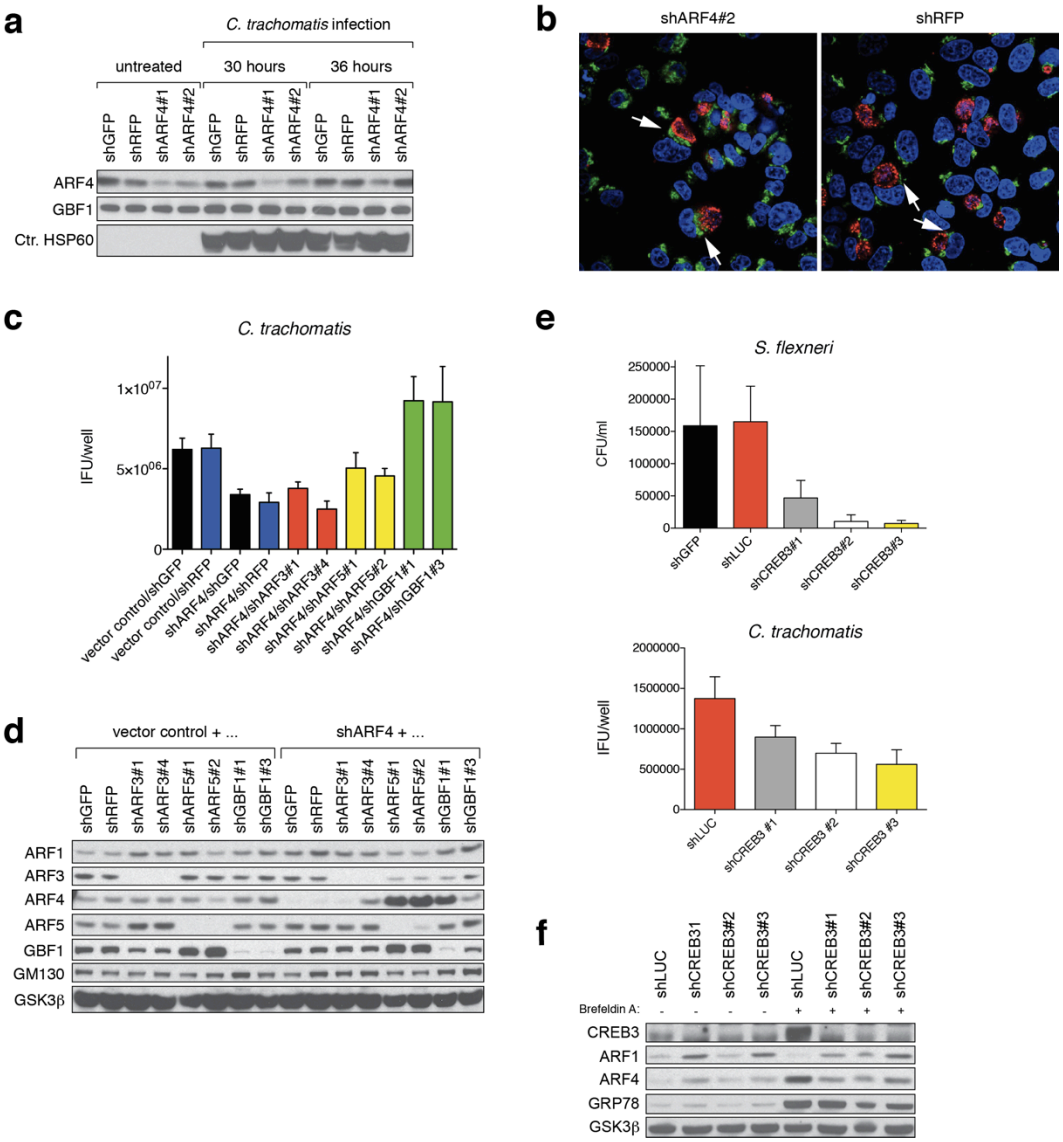

Figure A-13: Resistance of ARF4 KD cells to *C. trachomatis* and *S. flexneri* is mimicked by CREB3 loss of function and depends on ARF5 and GBF1
(a) HeLa cells transduced with lentiviral control or ARF4 hairpins were infected with *C. trachomatis*, and cells were lysed 30 or 36 hours after infection. Blots were probed with indicated antibodies. Ctr. HSP60 refers to *C. trachomatis* HSP60.

Figure A-13 (Continued) (b) HeLa ARF4 KD and control cells were infected with *Chlamydia*, and 30 hours post-infection cells were fixed and stained for *Chlamydia* HSP60 (red), GM130 (green) and DNA (blue). Arrows point to *Chlamydia*-infected cells and the effects on the Golgi apparatus.
(c) HeLa DKD cells were infected with *C. trachomatis* and bacterial progeny tested for their ability to form inclusions in wild type HeLa cells (48 hours post-infection). Statistically significant differences using one-way ANOVA, were observed between ARF4 DKD control cells and ARF4 GBF1; 4 biological replicates were measured per genotype. The graphs show the means ± SD.
(d) Immunoblots of cell lysates from HeLa DKD cells used in (c).
(e) Loss of CREB3 impairs *S. flexneri* growth (gentamicin protection assay was done 20 hours post-infection) and inhibits *C. trachomatis* reproduction (analysis done 40 hours post-infection). Both experiments have been repeated twice with n=3-4 and $p \leq 0.05$ using Student's t-test or one-way ANOVA test. Shown are the means ± SD.
(f) Western blot analysis of HeLa CREB3 KD cells used for *S. flexneri* and *C. trachomatis* infection as shown in (e). Cell lysates were derived from both untreated cells and cells treated with 10 ng/mL BFA for 27 hours.

inclusion-forming units (IFU) (Figure A-12B). We noted that 8 hours following *Shigella* infection there was a two-fold reduction in intracellular bacteria in shARF4 cells, a phenotype that became even stronger after 20 hours when intracellular persistence was reduced about 70-100-fold (Figure A-12D). Both *Shigella* and *Chlamydia* directly target ARF1-dependent pathways during infection(42). We also examined the growth of the pathogen *Salmonella enterica serovar typhimurium* that does not fragment the Golgi during intracellular replication. However, no survival defect was observed in ARF4-depleted cells compared to control cells (data not shown). This shows that restriction of both *Chlamydia* and *Shigella*, two pathogens with distinct intracellular lifestyles, may be due directly to defects in Golgi fragmentation and not pleiotropic effects of ARF4 depletion.

We further examined the mechanisms driving resistance to *Chlamydia* infection following a reduction in ARF4 levels. One requirement for *Chlamydia* propagation is sphingomyelin, which is synthesized from ceramide produced in the ER, and actively acquired by the bacteria(43). Blocking Golgi fragmentation in infected cells via chemical inhibition prevents efficient uptake of ceramide into the inclusion(41). We assessed the consequences of adding fluorescent NBD-C_6-ceramide to control and ARF4 hairpin-infected HeLa cells. The results show a significant reduction of intracellular ceramide accumulation upon loss of ARF4 (Figure A-12B) raising the possibility that sphingolipid transfer to the inclusion may be compromised. Using IF microscopy we assessed Golgi morphology of *Chlamydia*-infected cells. GM130 staining presented more discernable and pronounced in ARF4 KD cells with a more compact and dense appearance, whereas shRFP cells displayed a thinner structure and more dispersed Golgi elements (ministacks) (Figure A-13B). Complementary to the ARF4 loss of function phenotype, ARF4 but not ARF1 or ARF5 overexpression enhanced *Chlamydia* replication (Figure A-12C).

Previous work showed that loss of ARF1 or GBF1 enhances *Chlamydia* infection suggesting that enhanced ARF activity limits replication(44, 45). We hypothesized that the compensatory increase in ARF1 and/or ARF5 may underlie the resistance of ARF4 KD cells to

Chlamydia growth, similar to BFA resistance. To test this we established the corresponding DKD HeLa cells and examined whether increased resistance to *Chlamydia* is affected in cells co-depleted of ARF4 and other ARF isoforms or GBF1. Since we were not able to establish ARF1 ARF4 DKD HeLa cells due to lethality, our analysis was restricted to the remaining ARF4 DKD combinations. In line with our earlier results, the absence of both GBF1 and ARF4 enhanced the production of infectious *Chlamydia* compared with control ARF4 DKD cells (shARF4 shGFP and shARF4 shRFP). Combinatorial loss of both ARF4 and ARF5 led to a slight recovery of bacterial growth, but not to the levels of GBF1, suggesting an important role of ARF1 in bacterial growth. ARF3 depletion was without effect (Figure A-13C and 13D). These data show that bacterial restriction in ARF4 KD cells is driven by the compensatory upregulation of other ARFs similar to BFA treatment.

Since CREB3 regulates ARF4 expression and sensitivity to BFA (Figure A-12), we also assessed its effects on the survival of *Chlamydia* and *Shigella*. HeLa CREB3 KD cells were subjected to the same pathogen infection assays as described above. We found that these cells were several-fold more resistant to both pathogens relative to controls (Figure A-13E). Interestingly, under basal conditions we noted higher expression of ARF1 in CREB3 KD cells, consistent with the upregulation and pathogen restriction seen in ARF4 KD cells (Figure A-13F). Thus, these data suggest that a CREB3-ARF4 signaling pathway mediates the survival response to a number of pharmacological Golgi-perturbing agents and certain Golgi-fragmenting pathogens.

Discussion

We have identified ARF4, one of the five human members of the ARF family of small G proteins, in a loss of function viability screen in human cells for genes providing resistance to BFA. The ARF family members are regarded as providing overlapping functions such that depletion of any single ARF does not cause discernable secretory trafficking pathway alterations. Volpicelli-

Daley et al. (2005) used siRNA treatment of HeLa cells to deplete ARFs individually or in pairwise combinations, but no effects on the levels of other ARF isoforms were reported. We, however, found increased expression of other ARFs upon lentiviral-mediated downregulation of ARF4. A possible explanation could be differences in the ARF KD levels achieved in each respective study. Here, we have shown that ARF4 KD is sufficient to make cells resistant to BFA, GCA or Exo1, which is the opposite phenotype compared with ARF1- or ARF5-depleted cells. Cells lacking ARF4 preserve Golgi integrity and function even in the presence of BFA, and we found upregulated ARF1, ARF3 and ARF5 levels accompanied by increased pan-ARF activity in these cells. Furthermore we discovered that BFA exposure increased the levels of GBF1, BIG and BIG2. Altogether, these findings suggest that the combination of enhanced ARF and ARF-GEF levels in ARF4-depleted cells enables them to cope with toxic BFA concentrations allowing to sustain secretory pathway activity and hence survival in the presence of the drug. In agreement with this model, downregulation of ARF1, ARF5, and GBF1, but not ARF3, in ARF4 loss of function cells restored BFA sensitivity.

In addition to conferring resistance to several Golgi-disassembling agents, we found that ARF4 and CREB3 depletion protected against intracellular growth of two pathogenic bacteria, *C. trachomatis* and *S. flexneri* that cause Golgi fragmentation upon infection. It is likely that intracellular trafficking pathways important for bacterial nutrient supply or to escape host defense mechanisms are impaired in these cells(41, 46). For *Chlamydia,* transport of sphingolipids or cholesterol into the inclusion, which depends on Golgi fragmentation, could be inhibited upon loss of ARF4(41). *Chlamydia* and *Shigella* infect millions every year yet no effective vaccine is available(47-50). In light of the increased occurrence of antibiotic resistant *Chlamydia and Shigella* strains and the fact that cells without CREB3 or ARF4 restrict bacterial growth, inhibitors that target CREB3/ARF4 functions may become a new treatment option to combat a subset of intracellular infections. Altogether, these results suggest that inhibition of

ARF4 or CREB3 could prove beneficial in several disease settings to restrict the pathogenicity of intracellular pathogens.

A further unanticipated finding of this study was that incubation of cells with BFA induced ARF4 expression through CREB3. CREB3 belongs to a family of bZIP ER membrane-bound transcription factors that also includes OASIS (CREB3L1), BBF2H7 (CREB3L2), CREBH (CREB3L3) and CREB4 (CREB3L4/AIbZIP/Tisp40). This family is also related to ATF6α/β, one of the three major proximal ER stress transducers, and furthermore shares the same mechanism of activation. The functions of CREB3 are ill defined, and whereas several other of the five CREB3-like transcription factors are activated in response to ER stress and contribute to diversification of the UPR in a cell-type specific manner, there is some debate whether CREB3 is induced under ER stress conditions(40, 51-55). ARF1 or GBF1 depletion by RNAi caused ARF4 levels to rise indicating that their levels are coordinately regulated. GBF1 depletion causes relocation of S2P from the Golgi to the ER(56), and we demonstrate that inhibition of S1P alleviates CREB3 and ARF4 induction elicited by BFA treatment. Furthermore we found that exogenous CREB3 expression in GBF1 KD and ARF1 KD cells leads to its nuclear relocation. Presumably full length CREB3 is cleaved by S1P and S2P upon GBF1 or ARF1 KD thereby mimicking BFA treatment.

We extended the findings made with BFA to three other compounds compromising the Golgi – GCA, Exo1 and Monensin – which all increased ARF4 expression suggesting that its levels might parallel Golgi integrity or Golgi stress induction. Treatment with these chemicals leads to proteolytic CREB3 activation through S1P and S2P followed by its nuclear accumulation. What could be the specific Golgi stress stimulus leading to ARF4 induction? GCA has a mode of action comparable to BFA by inhibiting ARF1-GBF1 function and potentially other ARFs causing COPI vesicle coat dissociation from Golgi membranes(57, 58). The Golgi-fragmenting effects of Exo1 might be promoted by GTP hydrolysis on all Golgi-localized ARF members thereby mimicking reduced ARF activity(59). The cationic ionophore Monensin

promotes H^+/Na^+ exchange, which leads to alkalization of the Golgi lumen causing osmotic swelling mainly in late Golgi and post-Golgi/endosomal compartments and a block in anterograde and retrograde transport(60-62). Increased ARF4 expression therefore might be related to loss of ARF1 from Golgi membranes and/or decreased ARF1 activity leading to defects in Golgi integrity.

Another question is what the purpose of ARF4 upregulation during Golgi stress might be. Whether enhanced ARF4 expression as a result of Golgi stress treatments represents a cellular attempt to boost Golgi capacity and thereby to regain sufficient secretory pathway function in the presence of BFA, or conversely whether ARF4 induction initiates a so far uncharacterized apoptotic program to eliminate cells with irreparable Golgi damage, is not known. It could also be that increased ARF4 levels negatively regulate the activities of Golgi-protective ARFs such as ARF1. Notwithstanding the precise signaling mechanisms downstream of ARF4, we speculate that the Golgi apparatus might actively sense certain stress stimuli and relay a signal to the nucleus to induce factors critical for the re-establishment of Golgi homeostasis or to trigger pro-apoptotic events if the stress is insurmountable. The proposed signaling pathway could therefore be viewed as Golgi stress response comparable to the unfolded protein response that is initiated at the ER(63, 64). How Golgi stress might be sensed, and what the stress signals are, remains to be further investigated.

Golgi fragmentation is a pathological feature of several neurodegenerative diseases including amyotrophic lateral sclerosis (ALS), Alzheimer, Parkinson, spinocerebellar ataxia type 2 (SCA2)(33, 65-67) and is also observed in patients with Niemann-Pick type C (NPC) disease(68). In addition, several bacteria and viruses induce Golgi disassembly(69). It is therefore possible that these pathologies are associated with Golgi stress induction. Elucidating the components acting in this proposed Golgi stress signaling network might thus be valuable in identifying novel treatment options for neuronal disorders, cancer, or pathogen-induced disease states.

METHODS

General methods. A detailed description of common methods and protocols including extraction of DNA and determination of GT insertion sites, proliferation assays, immunofluoresecence (IF), and lentivirus production has been described previously(19, 21). Briefly, cell viability assays were performed either using a Z2 coulter counter apparatus (Beckman Coulter) for direct cell number counts (cells with diameters between 10 and 30 μm were counted), or using the CTG assay (Promega). IF pictures were generally acquired with an epifluorescence microscope (Zeiss Axiovert 200 M, 63x magnification) equipped with a Zeiss AxioCam camera. To acquire the images shown in Supplementary Fig. S6b a Zeiss LSM 710 NLO Laser Scanning confocal microscope was used. For Western blotting proteins were resolved on 4–12% NuPAGE Novex gradient Bis·Tris gels (Invitrogen) and transferred onto PVDF membranes (Immobilon). IgG-HRP–coupled secondary antibodies (Santa Cruz Biotechnology) for immunoblotting were used at 1:5000 in 5% milk/PBS-T for 1 hour incubation at room temperature. Proteins bands were visualized with Western Lightning chemiluminescence (ECL)/plus-ECL reagent (Perkin-Elmer).

Cell culture. All cell lines described with the exception of KBM7 cells were grown in standard Dulbecco's medium (DMEM) with 10% heat-inactivated fetal serum (IFS) in the presence of 250 units/mL penicillin and 250 μg/mL streptomycin. KBM7 cells were grown in Iscove's modified Dulbecco's medium (IMDM) supplemented with antibiotics.

Densitometric analyses. Quantification of Western blots presented in Fig. 3b to determine normalized ARF-GTP levels was done using ImageJ analysis software (densitometry measurement tool). In Fig. 3b, pan-ARF bands were normalized to PAR-4 protein lysate levels, which remain unchanged by BFA.

Bacterial strains and media. *Shigella flexneri* serovar 2a WT strain 2457T, *Salmonella enterica serovar typimurium* strain SL1344, and *Chlamydia trachomatis* serovar L2 434/Bu were used in this study and have been previously described(70-72).

***Chlamydia* quantitative PCR and Infectious forming unit assays.** To assess the levels of *C. trachomatis* present, we used a previously established qPCR method(73). Briefly, we isolated nucleic acid from infected cells using the DNeasy kit (Qiagen). *Chlamydia* 16S DNA was quantified by qPCR on an ABI Prism 7000 sequence detection system using primer pairs and dual-labeled probes. Using standard curves from known amounts of *Chlamydia* the levels of 16S DNA per well was calculated. For IFU experiments control cells or ARF4 KD cells were seeded at a density of $5x10^4$ into 24-well plates in triplicate. Cells were infected the following day with $5x10^4$ IFU of *C. trachomatis* for 48 hours. Cells were subsequently lysed and diluted 1:1000 or 1:10000 and re-seeded into 24- or 96-well plates containing 10^4 wild type HeLa cells. Twenty-four hours following infection, cells were fixed with ice-cold methanol for 30 minutes. Cells were washed two times with PBS containing 0.1% Tween. Cells were then stained using DAPI and an antibody to *C. trachomatis* MOMP. Cells were quantified by fluorescence microscopy and the mean number of IFU produced by control cells and ARF4 KD cells for each well was calculated.

Gentamicin protection assay. $5x10^4$ control or ARF4 KD cells were seeded in 24-wells plates in triplicate. Cells were infected with *S. flexneri* or *S. typhimurium* by centrifuging exponential phase bacteria diluted in PBS onto semi-confluent monolayers of cells at an MOI of 1:1 at 700×g for 10 minutes. The cells were subsequently incubated for 20 minutes at 37°C and 5% CO_2, washed 3 times with PBS, and replaced with media containing gentamicin (25 µg/mL) to kill extracellular bacteria. To assess intracellular bacterial number, the cells were then incubated for indicated amounts of time in media containing gentamicin, washed 3 times with PBS, and lysed in 0.1% sodium deoxycholate/PBS. Cell lysates were then plated on tryptic soy agar (TSA) or LB plates, and CFU were counted after overnight incubation at 37°C.

NBD C_6-ceramide pulse labeling . Control or shARF4 cells were infected with *C.trachomatis* at an MOI of 5 for 20 hours. The media was aspirated and replaced with PBS containing NBD-Ceramide (Invitrogen) and placed at 37° C for 1 hour. Cells were then washed with PBS and replaced with fresh media to allow back exchange of fluorescent ceramide. Five hours following pulse, the media was removed and replaced with PBS. Plates were then read using SpectraMax M2 plate reader with an excitation/emission of 466/536 nm.

Virus infections and pulse chase experiments. HeLa cells were grown in 10 cm culture dishes and infected with wild type WSN influenza A at an MOI of 0.5 for 4 hours in DMEM supplemented with BSA and 1 µg/mL TPCK-treated trypsin. Cells were harvested and resuspended in methionine- and cysteine-free DMEM and starved for 45 mins at 37ºC followed by a 10 min pulse labeling with [^{35}S]cysteine/methionine (Perkin Elmer) at 0.77mCi/mL and a chase with DMEM containing cold cysteine/methionine for 0, 30 and 60 min. For all experiments, 1 µg/mL trypsin was added to the chase media. At indicated time points during chase, cell pellets were collected, lysed in buffer containing NP-40 followed by immunoprecipitation with flu anti-HA serum.

Virus fusion with the plasma membrane at low pH. Influenza A in DMEM containing BSA and 20 mM MES (pH 5.5) was allowed to bind to HeLa cells (at an MOI of 0.5) for 1 hour at room temperature. The binding medium was removed and the cells were incubated for 4 hours at 37ºC in DMEM containing BSA and 1 µg/mL of TPCK-treated trypsin. Following infection cells were harvested and processed for pulse-chase as described above.

Trafficking of Class I MHC. HeLa cells infected with control or ARF4 lentiviral hairpins were grown in 10 cm dishes. Cells were either vehicle treated or treated with 50 ng/mL Brefeldin A for 2 hours at 37ºC. Cells (-/+BFA) were harvested and resuspended in methionine- and cysteine-free DMEM and starved for 45 minutes at 37ºC followed by a 15 min biosynthetic labeling with [^{35}S]cysteine/methionine (Perkin Elmer) at 0.77mCi/ml and chase for 0, 30 and 60 minutes either in the absence or presence of 50 ng/mL BFA. At indicated time points, cells were lysed in

buffer containing NP-40 and subjected to immunoprecipitation using mouse monoclonal W6/32 anti-HC antibodies, resolved by SDS-PAGE and visualized by autoradiography.

Assay for total protein secretion. HeLa cells infected with a shLUC control or ARF4 hairpins were grown in 10 cm dishes and biosynthetically labeled with [^{35}S]cysteine/methionine (Perkin Elmer) at 0.77mCi/ml for 4 hours in DMEM supplemented with inactivated calf serum. Cells were either vehicle (ethanol) treated or treated with 50 ng/mL Brefeldin A for 2 hours during the course of metabolic labeling. Following BFA treatment, labeling media was replaced with fresh media with or without 50 ng/mL BFA. At indicated time points, media was collected, total protein precipitated using trichloro acetic acid (TCA) and subjected to SDS-PAGE to resolve total secreted proteins.

Quantitative (Q) real-time PCR. Cells were grown in 6 cm dishes, and mRNA was isolated using the RNeasy Plus Mini kit (Qiagen). 1 μg total RNA was used for the reverse transcription (RT) reaction using Oligo dT primers and Superscript III (Invitrogen Life Sciences). cDNA was diluted 1:15 after RT for subsequent use for Q real-time PCR. SYBR Green PCR master mix (Applied Biosystems) was used and reaction volume was 10 μL per q real-time PCR reaction (384 well plate run on an ABI 7900 machine). Three biological replicates were analyzed per genotype and condition, and two technical replicates were run per biological replicate for calculating the mean Ct values.

VHS-GAT pull-down assay. ARF activity was measured using an ARF pull-down assay essentially as described earlier(74). GST-VHS-GAT (VHS-GAT from GGA3) was bacterially expressed, and the cell pellet spun down at 4000 rpm^{-1}. The cell pellet was lysed by sonication in 20 mL lysis buffer (40 mM Hepes pH 7.4, 150 mM NaCl, 2 mM EDTA, 1 μM DTT and protease inhibitor cocktail (Roche) added). The bacterial cell lysate was then centrifuged for 30 minutes at 20,000 rpm^{-1}, and Glutathione Agarose beads (Thermo Scientific) that had been washed two times with PBS and once with bacterial lysis buffer were added to the bacterial

supernatant for 1 hour to bind GST-VHS-GAT to the beads. Between 750 μg and 1.5 mg total human cell protein extracts (PC3 or HeLa lysed in 1% NP40 lysis buffer) were combined with 60 μL Glutathione Agarose-GST-VHS-GAT slurry and rotated for 2 hours at 4º C for ARF pull-down. Immunoprecipitates were washed three times in 1% NP40 lysis buffer before elution in 50-60 μL 2X sample buffer and boiling for 3 minutes. Eluates were resolved on a 4-12% gradient Bis-Tris gel and probed with anti-ARF1(1D9) antibody (pan-ARF).

Antibodies and reagents. Primary antibodies: mouse anti-GBF1 (BD Transduction Laboratories), rabbit anti-Giantin (Abcam), rabbit anti-CREB3 (Abcam), mouse anti-ARF1(1D9)/pan-ARF (Novus Biologicals), mouse anti-ARF3 (Santa Cruz Biotechnology), rabbit anti-ARF4 (Proteintech), mouse anti-ARF5 (Abnova), rabbit anti-ARF6 (Cell Signaling Technologies), rabbit anti-Rab1b (Proteintech), rabbit anti-GRP78 (Santa Cruz Biotechnology), mouse anti-CHOP (Cell Signaling Technologies), rabbit anti-Golgin-84 (GeneTex), goat anti-GM130 (Santa Cruz Biotechnology), mouse anti-Ctr. HSP60 (Santa Cruz Biotechnology), rabbit anti-GRASP65 (GeneTex), mouse anti-p84 (GeneTex), rabbit anti-GSK3β (Cell Signaling Technologies), rabbit anti-BIG1 (Bethyl Laboratories), rabbit anti-BIG2 (Bethyl Laboratories), mouse anti-*C. trachomatis*-MOMP (Fluorescein-conjugated; Biorad).

Compounds were obtained from following companies**:** Brefeldin A (Sigma-Aldrich), Golgicide A (Santa Cruz Biotechnology), Exo1 (Santa Cruz Biotechnology), H-89 (Santa Cruz Biotechnology), Forskolin (Santa Cruz Biotechnology), Monensin (Enzo Life Sciences), AEBSF (VWR), PF 429242 (AdooQ BioScience)

Cloning of CREB3 and ARFs *CREB3* was amplified from a HeLa cDNA pool using the primers LZIP/SalI and LZIP/NotI, sequence-verified and cloned into pLJM60 yielding N-terminally Flag-tagged CREB3. EGFPmyc was PCR-amplified using the primers oJR401 and oJR402myc/EcoRI and a vector containing *EGFP* sequence as DNA source. For *ARF1myc* cloning, we used primers oJR447/AgeI and oJR448myc/EcoRI in combination with *ARF1-HA*

cDNA (Addgene plasmid 10830, principal investigator: Thomas Roberts). *ARF4myc* cDNA was PCR-amplified from an A549 cDNA pool using primers oJR403/AgeI and oJR405myc/XbaI. *ARF5myc* cDNA construct was derived from two successive PCR steps: for the first PCR, ARF5 was amplified out of an A549 cDNA pool with primers oJR439/SalI and oJR440/NotI, for the second PCR primers ARF5/AgeI and ARF5myc/EcoRI were used. All PCR products were TOPO TA-subcloned and sequence-verified before digestion of the cDNAs and ligation into lentiviral expression vectors.

Transient transfection assays 70,000 GBF1 KD and ARF1 KD or control A549 cells were seeded into wells of 12 well cell culture plates and transfected with 100 ng *Flag-CREB3* cDNA expression vector 24 hours post cell seeding using X-tremeGene 9 transfection reagent (Roche). After additional 24 hours, cells were left untreated or treated with 20 ng/mL BFA for 24 hours before fixation in 4% paraformaldehyde, permeabilization in 0.05% Triton-X in PBS and further processing for immunofluorescent staining.

REFERENCES

1. Chiu VK, Bivona T, Hach A, Sajous JB, Silletti J, Wiener H, et al. Ras signalling on the endoplasmic reticulum and the Golgi. Nat Cell Biol. 2002;4(5):343-50. Epub 2002/05/04. doi: 10.1038/ncb783. PubMed PMID: 11988737.

2. Altan-Bonnet N, Phair RD, Polishchuk RS, Weigert R, Lippincott-Schwartz J. A role for Arf1 in mitotic Golgi disassembly, chromosome segregation, and cytokinesis. Proc Natl Acad Sci U S A. 2003;100(23):13314-9. Epub 2003/10/31. doi: 10.1073/pnas.2234055100. PubMed PMID: 14585930; PubMed Central PMCID: PMC263797.

3. Charest A, Kheifets V, Park J, Lane K, McMahon K, Nutt CL, et al. Oncogenic targeting of an activated tyrosine kinase to the Golgi apparatus in a glioblastoma. Proc Natl Acad Sci U S A. 2003;100(3):916-21. Epub 2003/01/23. doi: 10.1073/pnas.242741799. PubMed PMID: 12538861; PubMed Central PMCID: PMC298701.

4. Sutterlin C, Hsu P, Mallabiabarrena A, Malhotra V. Fragmentation and dispersal of the pericentriolar Golgi complex is required for entry into mitosis in mammalian cells. Cell. 2002;109(3):359-69. Epub 2002/05/23. PubMed PMID: 12015985.

5. Bisel B, Wang Y, Wei JH, Xiang Y, Tang D, Miron-Mendoza M, et al. ERK regulates Golgi and centrosome orientation towards the leading edge through GRASP65. J Cell Biol.

2008;182(5):837-43. Epub 2008/09/03. doi: 10.1083/jcb.200805045. PubMed PMID: 18762583; PubMed Central PMCID: PMC2528584.

6. Yadav S, Puri S, Linstedt AD. A primary role for Golgi positioning in directed secretion, cell polarity, and wound healing. Mol Biol Cell. 2009;20(6):1728-36. Epub 2009/01/23. doi: 10.1091/mbc.E08-10-1077. PubMed PMID: 19158377; PubMed Central PMCID: PMC2655245.

7. Kupfer A, Louvard D, Singer SJ. Polarization of the Golgi apparatus and the microtubule-organizing center in cultured fibroblasts at the edge of an experimental wound. Proc Natl Acad Sci U S A. 1982;79(8):2603-7. Epub 1982/04/01. PubMed PMID: 7045867; PubMed Central PMCID: PMC346248.

8. Singleton VL, Bohonos N, Ullstrup AJ. Decumbin, a new compound from a species of Penicillium. Nature. 1958;181(4615):1072-3. Epub 1958/04/12. PubMed PMID: 13541371.

9. Shao RG, Shimizu T, Pommier Y. Brefeldin A is a potent inducer of apoptosis in human cancer cells independently of p53. Experimental cell research. 1996;227(2):190-6. Epub 1996/09/15. doi: 10.1006/excr.1996.0266. PubMed PMID: 8831555.

10. Nojiri H, Manya H, Isono H, Yamana H, Nojima S. Induction of terminal differentiation and apoptosis in human colonic carcinoma cells by brefeldin A, a drug affecting ganglioside biosynthesis. FEBS letters. 1999;453(1-2):140-4. Epub 1999/07/14. PubMed PMID: 10403391.

11. Sausville EA, Duncan KL, Senderowicz A, Plowman J, Randazzo PA, Kahn R, et al. Antiproliferative effect in vitro and antitumor activity in vivo of brefeldin A. The cancer journal from Scientific American. 1996;2(1):52-8. Epub 1996/01/01. PubMed PMID: 9166499.

12. Anadu NO, Davisson VJ, Cushman M. Synthesis and anticancer activity of brefeldin A ester derivatives. Journal of medicinal chemistry. 2006;49(13):3897-905. Epub 2006/06/23. doi: 10.1021/jm0602817. PubMed PMID: 16789745.

13. Donaldson JG, Jackson CL. ARF family G proteins and their regulators: roles in membrane transport, development and disease. Nature reviews Molecular cell biology. 2011;12(6):362-75. Epub 2011/05/19. doi: 10.1038/nrm3117. PubMed PMID: 21587297; PubMed Central PMCID: PMC3245550.

14. D'Souza-Schorey C, Chavrier P. ARF proteins: roles in membrane traffic and beyond. Nature reviews Molecular cell biology. 2006;7(5):347-58. Epub 2006/04/25. doi: 10.1038/nrm1910. PubMed PMID: 16633337.

15. Peyroche A, Antonny B, Robineau S, Acker J, Cherfils J, Jackson CL. Brefeldin A acts to stabilize an abortive ARF-GDP-Sec7 domain protein complex: involvement of specific residues of the Sec7 domain. Molecular cell. 1999;3(3):275-85. Epub 1999/04/13. PubMed PMID: 10198630.

16. D'Souza-Schorey C, Li G, Colombo MI, Stahl PD. A regulatory role for ARF6 in receptor-mediated endocytosis. Science. 1995;267(5201):1175-8. Epub 1995/02/24. PubMed PMID: 7855600.

17. Peters PJ, Hsu VW, Ooi CE, Finazzi D, Teal SB, Oorschot V, et al. Overexpression of wild-type and mutant ARF1 and ARF6: distinct perturbations of nonoverlapping membrane

compartments. J Cell Biol. 1995;128(6):1003-17. Epub 1995/03/01. PubMed PMID: 7896867; PubMed Central PMCID: PMC2120412.

18. Cavenagh MM, Whitney JA, Carroll K, Zhang C, Boman AL, Rosenwald AG, et al. Intracellular distribution of Arf proteins in mammalian cells. Arf6 is uniquely localized to the plasma membrane. J Biol Chem. 1996;271(36):21767-74. Epub 1996/09/06. PubMed PMID: 8702973.

19. Reiling JH, Clish CB, Carette JE, Varadarajan M, Brummelkamp TR, Sabatini DM. A haploid genetic screen identifies the major facilitator domain containing 2A (MFSD2A) transporter as a key mediator in the response to tunicamycin. Proc Natl Acad Sci U S A. 2011;108(29):11756-65. Epub 2011/06/17. doi: 10.1073/pnas.1018098108. PubMed PMID: 21677192; PubMed Central PMCID: PMC3141996.

20. Carette JE, Guimaraes CP, Varadarajan M, Park AS, Wuethrich I, Godarova A, et al. Haploid genetic screens in human cells identify host factors used by pathogens. Science. 2009;326(5957):1231-5. Epub 2009/12/08. doi: 10.1126/science.1178955. PubMed PMID: 19965467.

21. Carette JE, Guimaraes CP, Wuethrich I, Blomen VA, Varadarajan M, Sun C, et al. Global gene disruption in human cells to assign genes to phenotypes by deep sequencing. Nature biotechnology. 2011;29(6):542-6. Epub 2011/05/31. doi: 10.1038/nbt.1857. PubMed PMID: 21623355; PubMed Central PMCID: PMC3111863.

22. Volpicelli-Daley LA, Li Y, Zhang CJ, Kahn RA. Isoform-selective effects of the depletion of ADP-ribosylation factors 1-5 on membrane traffic. Mol Biol Cell. 2005;16(10):4495-508. Epub 2005/07/21. doi: 10.1091/mbc.E04-12-1042. PubMed PMID: 16030262; PubMed Central PMCID: PMC1237059.

23. Nakai W, Kondo Y, Saitoh A, Naito T, Nakayama K, Shin HW. ARF1 and ARF4 regulate recycling endosomal morphology and retrograde transport from endosomes to the Golgi apparatus. Mol Biol Cell. 2013. Epub 2013/06/21. doi: 10.1091/mbc.E13-04-0197. PubMed PMID: 23783033.

24. Kondo Y, Hanai A, Nakai W, Katoh Y, Nakayama K, Shin HW. ARF1 and ARF3 are required for the integrity of recycling endosomes and the recycling pathway. Cell Struct Funct. 2012;37(2):141-54. Epub 2012/09/14. PubMed PMID: 22971977.

25. Claude A, Zhao BP, Kuziemsky CE, Dahan S, Berger SJ, Yan JP, et al. GBF1: A novel Golgi-associated BFA-resistant guanine nucleotide exchange factor that displays specificity for ADP-ribosylation factor 5. J Cell Biol. 1999;146(1):71-84. Epub 1999/07/14. PubMed PMID: 10402461; PubMed Central PMCID: PMC2199737.

26. Ooi CE, Dell'Angelica EC, Bonifacino JS. ADP-Ribosylation factor 1 (ARF1) regulates recruitment of the AP-3 adaptor complex to membranes. J Cell Biol. 1998;142(2):391-402. Epub 1998/07/29. PubMed PMID: 9679139; PubMed Central PMCID: PMC2133064.

27. Shinotsuka C, Yoshida Y, Kawamoto K, Takatsu H, Nakayama K. Overexpression of an ADP-ribosylation factor-guanine nucleotide exchange factor, BIG2, uncouples brefeldin A-induced adaptor protein-1 coat dissociation and membrane tubulation. J Biol Chem. 2002;277(11):9468-73. Epub 2002/01/05. doi: 10.1074/jbc.M112427200. PubMed PMID: 11777925.

28. Alvarez C, Garcia-Mata R, Brandon E, Sztul E. COPI recruitment is modulated by a Rab1b-dependent mechanism. Mol Biol Cell. 2003;14(5):2116-27. Epub 2003/06/13. doi: 10.1091/mbc.E02-09-0625. PubMed PMID: 12802079; PubMed Central PMCID: PMC165101.

29. Teal SB, Hsu VW, Peters PJ, Klausner RD, Donaldson JG. An activating mutation in ARF1 stabilizes coatomer binding to Golgi membranes. J Biol Chem. 1994;269(5):3135-8. Epub 1994/02/04. PubMed PMID: 8106346.

30. Santy LC, Casanova JE. Activation of ARF6 by ARNO stimulates epithelial cell migration through downstream activation of both Rac1 and phospholipase D. J Cell Biol. 2001;154(3):599-610. Epub 2001/08/02. doi: 10.1083/jcb.200104019. PubMed PMID: 11481345; PubMed Central PMCID: PMC2196419.

31. Manolea F, Chun J, Chen DW, Clarke I, Summerfeldt N, Dacks JB, et al. Arf3 is activated uniquely at the trans-Golgi network by brefeldin A-inhibited guanine nucleotide exchange factors. Mol Biol Cell. 2010;21(11):1836-49. Epub 2010/04/02. doi: 10.1091/mbc.E10-01-0016. PubMed PMID: 20357002; PubMed Central PMCID: PMC2877642.

32. Bui QT, Golinelli-Cohen MP, Jackson CL. Large Arf1 guanine nucleotide exchange factors: evolution, domain structure, and roles in membrane trafficking and human disease. Molecular genetics and genomics : MGG. 2009;282(4):329-50. Epub 2009/08/12. doi: 10.1007/s00438-009-0473-3. PubMed PMID: 19669794.

33. Nakagomi S, Barsoum MJ, Bossy-Wetzel E, Sutterlin C, Malhotra V, Lipton SA. A Golgi fragmentation pathway in neurodegeneration. Neurobiol Dis. 2008;29(2):221-31. Epub 2007/10/30. doi: 10.1016/j.nbd.2007.08.015. PubMed PMID: 17964175; PubMed Central PMCID: PMC2261378.

34. Lee TH, Linstedt AD. Potential role for protein kinases in regulation of bidirectional endoplasmic reticulum-to-Golgi transport revealed by protein kinase inhibitor H89. Mol Biol Cell. 2000;11(8):2577-90. Epub 2000/08/10. PubMed PMID: 10930455; PubMed Central PMCID: PMC14941.

35. Nickel W, Helms JB, Kneusel RE, Wieland FT. Forskolin stimulates detoxification of brefeldin A. J Biol Chem. 1996;271(27):15870-3. Epub 1996/07/05. PubMed PMID: 8663452.

36. Jang SY, Jang SW, Ko J. Regulation of ADP-ribosylation factor 4 expression by small leucine zipper protein and involvement in breast cancer cell migration. Cancer letters. 2012;314(2):185-97. Epub 2011/10/19. doi: 10.1016/j.canlet.2011.09.028. PubMed PMID: 22004728.

37. Asada R, Kanemoto S, Kondo S, Saito A, Imaizumi K. The signalling from endoplasmic reticulum-resident bZIP transcription factors involved in diverse cellular physiology. Journal of biochemistry. 2011;149(5):507-18. Epub 2011/04/02. doi: 10.1093/jb/mvr041. PubMed PMID: 21454302.

38. Kondo S, Hino SI, Saito A, Kanemoto S, Kawasaki N, Asada R, et al. Activation of OASIS family, ER stress transducers, is dependent on its stabilization. Cell death and differentiation. 2012. Epub 2012/06/19. doi: 10.1038/cdd.2012.77. PubMed PMID: 22705851.

39. Denboer LM, Iyer A, McCluggage AR, Li Y, Martyn AC, Lu R. JAB1/CSN5 inhibits the activity of Luman/CREB3 by promoting its degradation. Biochim Biophys Acta. 2013;1829(9):921-9. Epub 2013/04/16. doi: 10.1016/j.bbagrm.2013.04.001. PubMed PMID: 23583719.

40. Raggo C, Rapin N, Stirling J, Gobeil P, Smith-Windsor E, O'Hare P, et al. Luman, the cellular counterpart of herpes simplex virus VP16, is processed by regulated intramembrane proteolysis. Mol Cell Biol. 2002;22(16):5639-49. Epub 2002/07/26. PubMed PMID: 12138176; PubMed Central PMCID: PMC133973.

41. Heuer D, Rejman Lipinski A, Machuy N, Karlas A, Wehrens A, Siedler F, et al. Chlamydia causes fragmentation of the Golgi compartment to ensure reproduction. Nature. 2009;457(7230):731-5. Epub 2008/12/09. doi: 10.1038/nature07578. PubMed PMID: 19060882.

42. Burnaevskiy N, Fox TG, Plymire DA, Ertelt JM, Weigele BA, Selyunin AS, et al. Proteolytic elimination of N-myristoyl modifications by the Shigella virulence factor IpaJ. Nature. 2013;496(7443):106-9. Epub 2013/03/29. doi: 10.1038/nature12004. PubMed PMID: 23535599.

43. Hackstadt T, Scidmore MA, Rockey DD. Lipid metabolism in Chlamydia trachomatis-infected cells: directed trafficking of Golgi-derived sphingolipids to the chlamydial inclusion. Proc Natl Acad Sci U S A. 1995;92(11):4877-81. Epub 1995/05/23. PubMed PMID: 7761416; PubMed Central PMCID: PMC41810.

44. Elwell CA, Jiang S, Kim JH, Lee A, Wittmann T, Hanada K, et al. Chlamydia trachomatis co-opts GBF1 and CERT to acquire host sphingomyelin for distinct roles during intracellular development. PLoS pathogens. 2011;7(9):e1002198. Epub 2011/09/13. doi: 10.1371/journal.ppat.1002198. PubMed PMID: 21909260; PubMed Central PMCID: PMC3164637.

45. Gurumurthy RK, Maurer AP, Machuy N, Hess S, Pleissner KP, Schuchhardt J, et al. A loss-of-function screen reveals Ras- and Raf-independent MEK-ERK signaling during Chlamydia trachomatis infection. Science signaling. 2010;3(113):ra21. Epub 2010/03/18. doi: 10.1126/scisignal.2000651. PubMed PMID: 20234004.

46. Dong N, Zhu Y, Lu Q, Hu L, Zheng Y, Shao F. Structurally distinct bacterial TBC-like GAPs link Arf GTPase to Rab1 inactivation to counteract host defenses. Cell. 2012;150(5):1029-41. Epub 2012/09/04. doi: 10.1016/j.cell.2012.06.050. PubMed PMID: 22939626.

47. Brunham RC, Rey-Ladino J. Immunology of Chlamydia infection: implications for a Chlamydia trachomatis vaccine. Nature reviews Immunology. 2005;5(2):149-61. Epub 2005/02/03. doi: 10.1038/nri1551. PubMed PMID: 15688042.

48. Igietseme JU, Eko FO, Black CM. Chlamydia vaccines: recent developments and the role of adjuvants in future formulations. Expert review of vaccines. 2011;10(11):1585-96. Epub 2011/11/03. doi: 10.1586/erv.11.139. PubMed PMID: 22043957.

49. Scidmore MA. Recent advances in Chlamydia subversion of host cytoskeletal and membrane trafficking pathways. Microbes and infection / Institut Pasteur. 2011;13(6):527-35. Epub 2011/02/22. doi: 10.1016/j.micinf.2011.02.001. PubMed PMID: 21334451; PubMed Central PMCID: PMC3092832.

50. Kotloff KL, Winickoff JP, Ivanoff B, Clemens JD, Swerdlow DL, Sansonetti PJ, et al. Global burden of Shigella infections: implications for vaccine development and implementation of control strategies. Bull World Health Organ. 1999;77(8):651-66. Epub 1999/10/12. PubMed PMID: 10516787; PubMed Central PMCID: PMC2557719 1997 on Shigella infection.

51. DenBoer LM, Hardy-Smith PW, Hogan MR, Cockram GP, Audas TE, Lu R. Luman is capable of binding and activating transcription from the unfolded protein response element. Biochemical and biophysical research communications. 2005;331(1):113-9. Epub 2005/04/23. doi: 10.1016/j.bbrc.2005.03.141. PubMed PMID: 15845366.

52. Liang G, Audas TE, Li Y, Cockram GP, Dean JD, Martyn AC, et al. Luman/CREB3 induces transcription of the endoplasmic reticulum (ER) stress response protein Herp through an ER stress response element. Mol Cell Biol. 2006;26(21):7999-8010. Epub 2006/08/31. doi: 10.1128/MCB.01046-06. PubMed PMID: 16940180; PubMed Central PMCID: PMC1636730.

53. Chen X, Shen J, Prywes R. The luminal domain of ATF6 senses endoplasmic reticulum (ER) stress and causes translocation of ATF6 from the ER to the Golgi. J Biol Chem. 2002;277(15):13045-52. Epub 2002/02/01. doi: 10.1074/jbc.M110636200. PubMed PMID: 11821395.

54. Nadanaka S, Okada T, Yoshida H, Mori K. Role of disulfide bridges formed in the luminal domain of ATF6 in sensing endoplasmic reticulum stress. Mol Cell Biol. 2007;27(3):1027-43. Epub 2006/11/15. doi: 10.1128/MCB.00408-06. PubMed PMID: 17101776; PubMed Central PMCID: PMC1800683.

55. Zhang K, Shen X, Wu J, Sakaki K, Saunders T, Rutkowski DT, et al. Endoplasmic reticulum stress activates cleavage of CREBH to induce a systemic inflammatory response. Cell. 2006;124(3):587-99. Epub 2006/02/14. doi: 10.1016/j.cell.2005.11.040. PubMed PMID: 16469704.

56. Citterio C, Vichi A, Pacheco-Rodriguez G, Aponte AM, Moss J, Vaughan M. Unfolded protein response and cell death after depletion of brefeldin A-inhibited guanine nucleotide-exchange protein GBF1. Proc Natl Acad Sci U S A. 2008;105(8):2877-82. Epub 2008/02/22. doi: 10.1073/pnas.0712224105. PubMed PMID: 18287014; PubMed Central PMCID: PMC2268553.

57. Saenz JB, Sun WJ, Chang JW, Li J, Bursulaya B, Gray NS, et al. Golgicide A reveals essential roles for GBF1 in Golgi assembly and function. Nature chemical biology. 2009;5(3):157-65. Epub 2009/02/03. doi: 10.1038/nchembio.144. PubMed PMID: 19182783.

58. Chun J, Shapovalova Z, Dejgaard SY, Presley JF, Melancon P. Characterization of class I and II ADP-ribosylation factors (Arfs) in live cells: GDP-bound class II Arfs associate with the ER-Golgi intermediate compartment independently of GBF1. Mol Biol Cell. 2008;19(8):3488-500. Epub 2008/06/06. doi: 10.1091/mbc.E08-04-0373. PubMed PMID: 18524849; PubMed Central PMCID: PMC2488303.

59. Feng Y, Yu S, Lasell TK, Jadhav AP, Macia E, Chardin P, et al. Exo1: a new chemical inhibitor of the exocytic pathway. Proc Natl Acad Sci U S A. 2003;100(11):6469-74. Epub 2003/05/10. doi: 10.1073/pnas.0631766100. PubMed PMID: 12738886; PubMed Central PMCID: PMC164470.

60. Barzilay E, Ben-Califa N, Hirschberg K, Neumann D. Uncoupling of brefeldin a-mediated coatomer protein complex-I dissociation from Golgi redistribution. Traffic. 2005;6(9):794-802. Epub 2005/08/17. doi: 10.1111/j.1600-0854.2005.00317.x. PubMed PMID: 16101682.

61. Dinter A, Berger EG. Golgi-disturbing agents. Histochemistry and cell biology. 1998;109(5-6):571-90. Epub 1998/07/29. PubMed PMID: 9681636.

62. Zhang GF, Driouich A, Staehelin LA. Effect of monensin on plant Golgi: re-examination of the monensin-induced changes in cisternal architecture and functional activities of the Golgi apparatus of sycamore suspension-cultured cells. Journal of cell science. 1993;104 (Pt 3):819-31. Epub 1993/03/01. PubMed PMID: 8314876.

63. Hicks SW, Machamer CE. Golgi structure in stress sensing and apoptosis. Biochim Biophys Acta. 2005;1744(3):406-14. Epub 2005/06/28. doi: 10.1016/j.bbamcr.2005.03.002. PubMed PMID: 15979510.

64. Oku M, Tanakura S, Uemura A, Sohda M, Misumi Y, Taniguchi M, et al. Novel cis-acting element GASE regulates transcriptional induction by the Golgi stress response. Cell Struct Funct. 2011;36(1):1-12. Epub 2010/12/15. PubMed PMID: 21150128.

65. Huynh DP, Yang HT, Vakharia H, Nguyen D, Pulst SM. Expansion of the polyQ repeat in ataxin-2 alters its Golgi localization, disrupts the Golgi complex and causes cell death. Human molecular genetics. 2003;12(13):1485-96. Epub 2003/06/19. PubMed PMID: 12812977.

66. Winslow AR, Chen CW, Corrochano S, Acevedo-Arozena A, Gordon DE, Peden AA, et al. alpha-Synuclein impairs macroautophagy: implications for Parkinson's disease. J Cell Biol. 2010;190(6):1023-37. Epub 2010/09/22. doi: 10.1083/jcb.201003122. PubMed PMID: 20855506; PubMed Central PMCID: PMC3101586.

67. Cooper AA, Gitler AD, Cashikar A, Haynes CM, Hill KJ, Bhullar B, et al. Alpha-synuclein blocks ER-Golgi traffic and Rab1 rescues neuron loss in Parkinson's models. Science. 2006;313(5785):324-8. Epub 2006/06/24. doi: 10.1126/science.1129462. PubMed PMID: 16794039; PubMed Central PMCID: PMC1983366.

68. Walkley SU, Suzuki K. Consequences of NPC1 and NPC2 loss of function in mammalian neurons. Biochim Biophys Acta. 2004;1685(1-3):48-62. Epub 2004/10/07. doi: 10.1016/j.bbalip.2004.08.011. PubMed PMID: 15465426.

69. Gonatas NK, Stieber A, Gonatas JO. Fragmentation of the Golgi apparatus in neurodegenerative diseases and cell death. Journal of the neurological sciences. 2006;246(1-2):21-30. Epub 2006/03/21. doi: 10.1016/j.jns.2006.01.019. PubMed PMID: 16545397.

70. Jehl SP, Nogueira CV, Zhang X, Starnbach MN. IFNgamma inhibits the cytosolic replication of Shigella flexneri via the cytoplasmic RNA sensor RIG-I. PLoS pathogens. 2012;8(8):e1002809. Epub 2012/08/23. doi: 10.1371/journal.ppat.1002809. PubMed PMID: 22912573; PubMed Central PMCID: PMC3415441.

71. Gondek DC, Olive AJ, Stary G, Starnbach MN. CD4+ T cells are necessary and sufficient to confer protection against Chlamydia trachomatis infection in the murine upper genital tract. J Immunol. 2012;189(5):2441-9. Epub 2012/08/03. doi: 10.4049/jimmunol.1103032. PubMed PMID: 22855710.

72. van der Velden AW, Dougherty JT, Starnbach MN. Down-modulation of TCR expression by Salmonella enterica serovar Typhimurium. J Immunol. 2008;180(8):5569-

74. Epub 2008/04/09. PubMed PMID: 18390741.

73. Coers J, Gondek DC, Olive AJ, Rohlfing A, Taylor GA, Starnbach MN. Compensatory T cell responses in IRG-deficient mice prevent sustained Chlamydia trachomatis infections. PLoS pathogens. 2011;7(6):e1001346. Epub 2011/07/07. doi: 10.1371/journal.ppat.1001346. PubMed PMID: 21731484; PubMed Central PMCID: PMC3121881.

74. Cohen LA, Donaldson JG. Analysis of Arf GTP-binding protein function in cells. Current protocols in cell biology / editorial board, Juan S Bonifacino [et al]. 2010;Chapter 3:Unit 14 2 1-7. Epub 2010/09/21. doi: 10.1002/0471143030.cb1412s48. PubMed PMID: 20853342; PubMed Central PMCID: PMC2969170.

Appendix B: Characterization of host interactions with the *Chlamydia* effector CrpA

Contributions

Madeleine Haff and Zarine Balsara conducted the immunoblots for Figure B-1E and B-1F.

Zarine Balsara made the stable the CrpA cell lines used throughout

Introduction

Chlamydia trachomatis is predicted to secrete over 100 virulence determinants directly into the host cell cytosol where they manipulate host cell functions and promote bacterial survival. In Chapters 5 and 6 of this dissertation, I have characterized how the host proteome is changed directly throughout infection with *C. trachomatis*. Using both quantitative mass spectrometry in conjunction with gain-of-function screening approaches, I identified hundreds of host proteins that are altered in their levels or stability during infection. One question that remains to be answered however, is whether any of these changes are directly mediated by individual *C. trachomatis* effectors.

As discussed previously, genetic manipulation of *C. trachomatis* has remained limited, with investigators now resorting to EMS-induced mutatgenesis to create loss-of-function strains of *C. trachomatis*. This approach is time consuming and does not guarentee successful generation of loss-of-function alleles. An alternative approach to characterize the function of unknown effector proteins is to use gain-of-function analyses and individually express *Chlamydia* effector proteins in host cells. This allows investigators to then examine the impact of specific virulence proteins on particular host phenotypes. We hypothesized that we could adapt the GPS reporter cell lines, that shift in EGFP:DsRed ratio following *C. trachomatis* infection, to identify effector proteins responsible for the underlying host protein alterations. If a particular bacterial effector targets a host protein or family of host proteins in the GPS validation screen, then the EGFP:DsRed should shift when the effector is expresed independently of infection. This approach would allow rapid screening by flow cytometry, to identify the function of effectors with unknown function.

As a proof-of-principle of this concept, we used this approach to identify host targets of two *Chlamydia* proteins known to have access to the cytosol, CrpA and Cap1. Previous work in our lab has described that both of these *Chlamydia* derived proteins are secreted into the host cytosol where they can stimulate CD8+ T cell responses. Unfortunately, while we have

characterized the immune response to these effector proteins in great detail, the molecular function of each bacterial protein remains entirely uncharacterized. The Experiments that follow serve as preliminary data suggesting further use of the GPS screening platform to identify individual host protein/bacterial effector interactions, allowing us to better understand mechanisms used by *Chlamydia* to infect and alter host cells for intracellular survival.

Results

The *Chlamydia* effector CrpA destabilizes the host protein BNIP3L

Both SILAC and GPS identified host proteins that are altered during infection and are necessary for normal replication. One shortcoming of these analyses is the lack of insight into which, if any, *C. trachomatis* proteins directly alter host proteins. We speculated that a single *Chlamydia* virulence factor might be able to recapitulate some of the changes in host protein stability identified by SILAC and GPS. Previously, our lab has identified two *Chlamydia* proteins, Cap1 and CrpA, that gain access to the host cytosol and stimulate $CD8^+$ T cell responses, but their functions remain undescribed (1, 2). Since we created individual reporter constructs for over 100 host proteins that are altered following infection (such as those in Chapter 6), we then used those constructs to examine whether the expression of either Cap1 or CrpA alone was sufficient to recapitulate the EGFP:DsRed ratio shift of individual host-protein reporter lines observed when the cells were infected with *C. trachomatis*. We transfected vector alone, Cap1, or CrpA into host reporter cell lines and 24 hours later examined the EGFP:DsRed ratio by high-throughput 96 well-plate flow cytometry. We then overlayed the plots and saw a distinct destabilization with one host protein, BNIP3L, only in the presence of CrpA (Figure B-1A). Unfortunately, we did not see any host proteins shift under any circumstances in the presence of Cap1 (Figure B-1B).

To examine *C. trachomatis*-induced degradation of BNIP3L we first confirmed that BNIP3L is destabilized following infection with *C. trachomatis* (Figure B-1C). We then tested

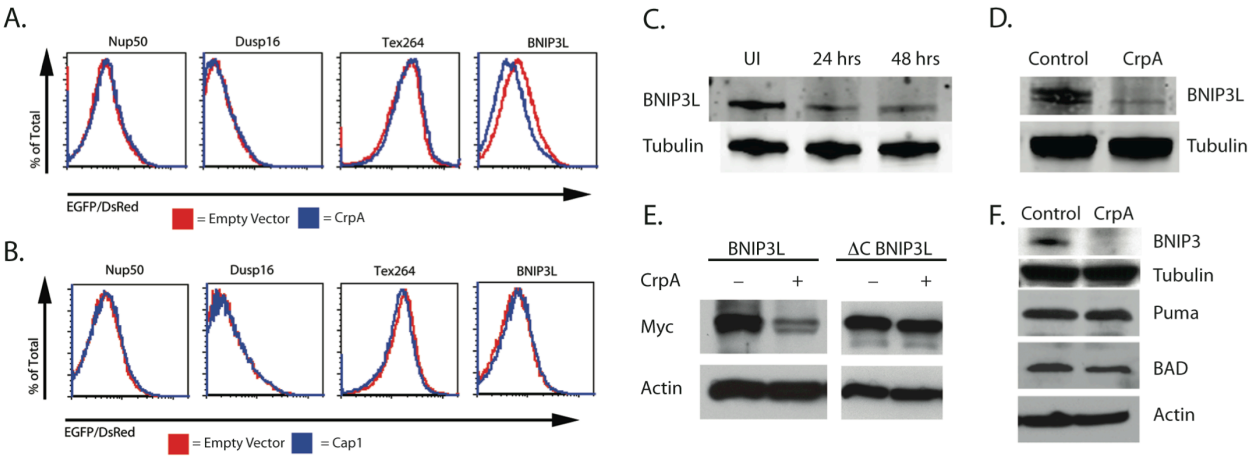

Figure B-1. Gain-of-function screen identifies BNIP3L and BNIP3 as targets of the secreted *Chlamydia* virulence factor CrpA.
A) A subset GPS hits were tested in 293T cells using flow cytometry. Cells were mock-transfected (red line) or transfected with CrpA (blue line) for 24 hours.
B) A subset GPS hits were tested in 293T cells using flow cytometry. Cells were mock-transfected (red line) or transfected with Cap1 (blue line) for 24 hours.
C) HeLa cells were mock-infected or infected with *C. trachomatis* for the indicated timepoints. Cells were analyzed by immunoblot for levels of BNIP3L and Tubulin (loading control).
D) HeLa cells expressing EGFP or CrpA-EGFP were analyzed by immunoblot for levels of BNIP3L and Tubulin (loading control).
E) HeLa cells were mock-infected or infected and transfected with a BNIP3L or DC-BNIP3L. Twenty-four hours after infection cells were analyzed by immunoblot for levels of BNIP3L (myc-tag) and Actin (loading control).
F) HeLa cells expressing EGFP or CrpA-EGFP were analyzed by immunoblot for levels of BNIP3, Puma, BAD and Actin (loading control).

whether cells stably expressing the fusion protein, CrpA-EGFP or EGFP alone would alter levels of BNIP3L in host cells. We first examined the levels of endogenous BNIP3L. As shown in Figure B-1D, cells expressing CrpA-EGFP had lower levels of monomeric BNIP3L and no detectable levels of dimeric BNIP3L when compared to EGFP alone. These data confirm our gain-of-function screen, suggesting that CrpA decreases the levels of BNIP3L in host cells.

BNIP3L contains a putative BH3 domain similar to other pro-apoptotic proteins such as BAD and PUMA (3). To determine whether CrpA-induced degradation of BNIP3L depends upon an intact BH3 domain, we deleted the C-terminus of BNIP3L (up to and including the BH3 domain) and examined the ability of CrpA to specifically degrade the truncated construct. First, we confirmed that expression of a myc-tagged version of full-length BNIP3L in the presence or absence of CrpA recapitulated our results seen at the endogenous levels of expression. Similar to our previous results we observed a significant degradation for full-length BNIP3L-myc in the presence of CrpA-EGFP (Figure B-1E). In contrast levels of BNIP3LΔC-myc were similar regardless of coexpression with CrpA-EGFP or EGFP in the cells (Figure B-1E). These results suggest that CrpA induces the degradation of BNIP3L in a manner that requires the presence of the BH3 domain.

The observation that CrpA-induced degradation of BNIP3L is sensitive to the presence of the BH3 domain led us to speculate that CrpA may also alter the closely related protein BNIP3, or more generally alter BH3-containing factors, such as Puma and BAD. We tested whether cells stably expressing CrpA-EGFP exhibited lower levels of BNIP3, Puma and Bad compared to control cells stably expressing EGFP alone. Interestingly, levels of Puma and BAD were indistinguishable in these cell lines (Figure B-1F) yet the levels of BNIP3 were decreased in the presence of CrpA. This observation, that CrpA does not universally degrade members of the BH3 family of proteins, suggests that this virulence factor does not be globally alter host proteins during infection but may specifically target a host cell process.

CrpA alters the cellular response to hypoxia

Recent work has elucidated a role for BNIP3 and BNIP3L in controlling the balance between autophagy and apoptosis under hypoxic conditions (4, 5). These studies showed that loss of both BNIP3 and BNIP3L leads to the prevention of autophagy under hypoxia while increasing cellular apoptosis. Hypoxia has recently become of interest to those studying *C. trachomatis*, as it now appears that hypoxia has a beneficial effect on *C. trachomatis* growth (6).

We next examined whether CrpA was able to alter the cellular response to hypoxia. Several studies have shown that the basal levels of BNIP3 and BNIP3L in host cells are low under normoxic conditions (4, 5). However, shortly after cells sense hypoxia, BNIP3 and BNIP3L are strongly induced in a HIF1α-dependent manner. A recent study showed that *C. trachomatis* induces a hypoxic-like response during infection that relies on the transcription factor HIF1α and is critical for *C. trachomatis* induced apoptosis resistance (7). We hypothesized that the effect of CrpA on BNIP3 and BNIP3L would be exacerbated under simulated hypoxic conditions that occur normally during infection. We treated stable cell lines expressing CrpA-EGFP or EGFP alone with cobalt chloride to mimic the hypoxic response and examined the cells 6 hours later. We found the levels of both monomeric BNIP3 and BNIP3L were strikingly higher in EGFP control cells (Figure B-2A). We also detected a strong dimer of BNIP3L following treatment, but never reliably detected BNIP3 dimers. This suggested that under hypoxia, as in normoxia, the level of BNIP3 was dramatically lower in the presence of CrpA. Surprisingly, the levels of monomeric BNIP3L were elevated following treatment, albeit consistently lower than EGFP controls. However, we never identified the dimeric BNIP3L in cells expressing CrpA. Twelve hours post-treatment the results were more robust and consistent with our previous findings. These data suggest that under simulated hypoxic conditions, CrpA efficiently removes BNIP3 and BNIP3L from host cells and prevents

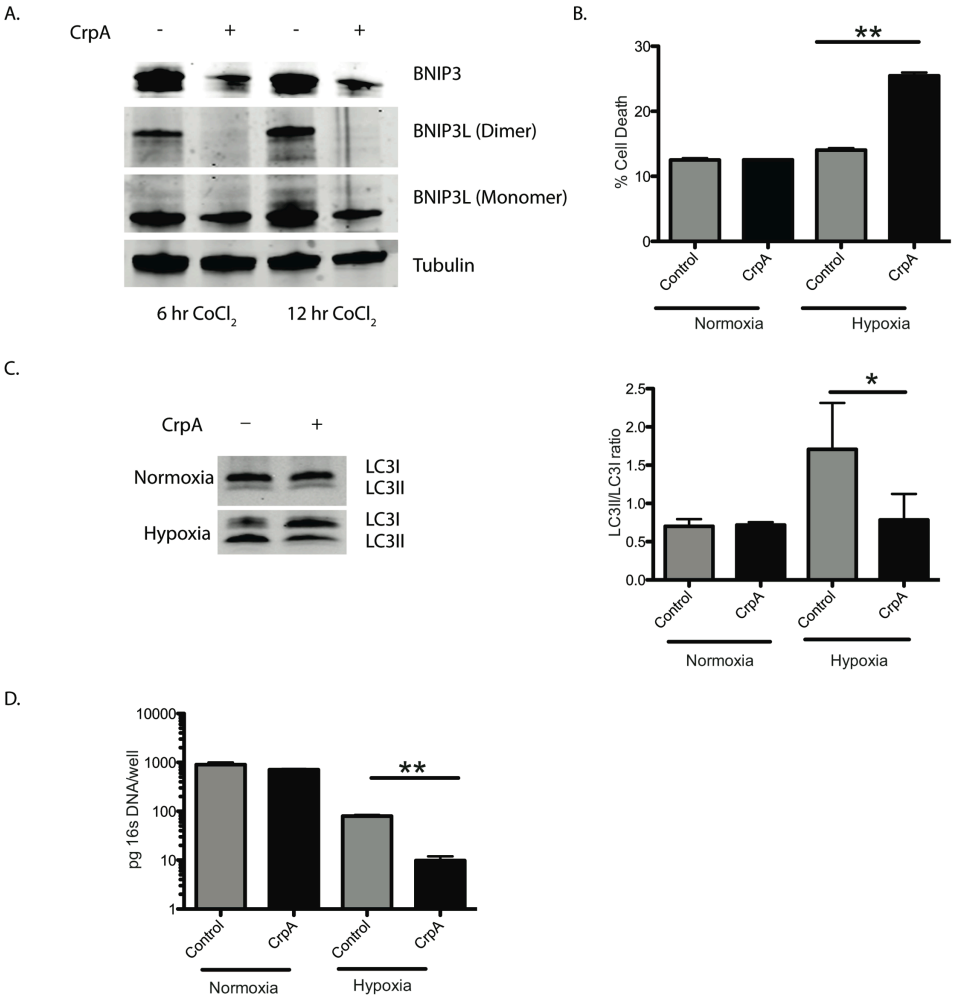

Figure B-2. CrpA alters the hypoxic response in cells.
A) HeLa cells expressing EGFP or CrpA-EGFP were subjected to conditions mimicking hypoxia using $CoCl_2$ for the indicated amount of time time. Cells were then analyzed by immunoblot for BNIP3, BNIP3L and Tubulin (loading control).
B) HeLa cells expressing EGFP or CrpA-EGFP were placed under normoxia or hypoxia-like conditions for 12 hours. Cells were stained with Live/Dead dye (Aqua fixable Dead Cell stain kit) and examined by flow cytometry. The graph shows the percent cell death for triplicate samples +/- the standard deviation (**p<.01) (n=3).
C) Left: HeLa cells expressing EGFP or CrpA-EGFP were subjected to normoxia or hypoxia-like conditions for 12 hours. Bafilomycin A was then added to the cultures and 20 minutes later the cells were analyzed by immunoblot for LC3I and LC3II. Right: Semi-quantitative determination of the LC3II/LC3I ratio. The graph shows the mean LC3II/LC3I ratio from triplicate samples +/- the standard deviation (*P<.05) (n=2).
D) HeLa cells expressing EGFP or CrpA-EGFP were infected with *C. trachomatis*, and 2 hours later cells were placed under normoxia or hypoxia-like conditions. Thirty-six hours post-infection the levels of *C. trachomatis* were examined using qPCR of the 16s gene. The graph shows the mean levels of *C. trachomatis* for triplicate samples +/- the standard deviation (**P<.01) (n=3).

dimerization of these host proteins.

A recent study has shown that loss of BNIP3 and BNIP3L simultaneously leads to higher levels of cell death. We reasoned that since CrpA removed BNIP3 and BNIP3L following hypoxia induction, cells expressing CrpA should also have higher levels of cell death under hypoxic conditions. To test this we examined the levels of cell death under normoxic and hypoxic conditions in cells expressing CrpA or Control cells. Under normoxic conditions, levels of cell death were similar between control cells and cells expressing CrpA (Figure B-2B). However following the addition of $CoCl_2$, cells expressing CrpA had two-fold higher levels of cell death, while control cells remained relatively unchanged. These data suggest that the removal of BNIP3 and BNIP3L by CrpA under hypoxic conditions may serve to inhibit the induction of autophagy, but at a cost of higher levels of cell death. To confirm that cells expressing CrpA are unable to induce autophagy under hypoxic conditions we examined the levels of the autophagy-activated protein LC3II. We compared the levels of LC3II in control cells and cells expressing CrpA following hypoxia induction. As shown in Figure B-2C control cells had elevated levels of LC3II following hypoxia induction while cells expressing CrpA had lower levels of LC3II under hypoxic conditions. These data confirm the hypothesis that CrpA prevents the efficient induction of autophagy under hypoxia, and biases the cells towards cell death.

To date it has not been easy to create targeted mutations in *C. trachomatis*. Therefore it is extremely difficult to examine how loss-of-function mutants alter *C. trachomatis* growth. Because of this limitation we examined whether the overexpression of CrpA would alter the growth of *C. trachomatis* under normoxic or hypoxic conditions. We hypothesized that under hypoxic conditions, since the overexpression of CrpA pushes the host cell strongly towards cell death, *C. trachomatis* growth may be inhibited due to the loss of its essential intracellular niche. We infected cells overexpressing CrpA or control cells with *C. trachomatis*. 2 hours following infection, we induced hypoxic-like conditions by adding media containing $CoCl_2$. Thirty-six hours post-infection we examined the levels of *C. trachomatis* by qPCR. When we compared levels of

C. trachomatis in control cells or cells expressing CrpA, we found they were almost identical (Figure B-2D). Surprisingly, we found that the presence of CrpA inhibited *C. trachomatis* growth over ten times more than control cells under hypoxic-like conditions. These data confirm that CrpA alters the cellular hypoxic response. Furthermore, when CrpA is overexpressed during infection, it can significantly inhibit the ability of *C. trachomatis* to grow under hypoxic-like conditions.

Discussion

One question that our screens alone do not answer is which host protein alterations are directly caused by *C. trachomatis* effectors and which are induced indirectly. Here we found that the *C. trachomatis* effector CrpA destabilizes the host proteins BNIP3L and BNIP3. CrpA did not alter any other BH3 domain proteins we examined, suggesting that CrpA directly targets BNIP3 and BNIP3L.

Recent work has characterized BNIP3 and BNIP3L as critical mediators of the balance between autophagy and cell death under hypoxic conditions (5). Loss of BNIP3 and BNIP3L prevents hypoxia-induced autophagy in cells and promotes apoptosis. Genital strains of *C. trachomatis* infect the upper genital tract where oxygen levels are less than 5%. One group recently showed that hypoxia protects *C. trachomatis* from IFNγ-mediated growth restriction that would occur under normoxia (6). Furthermore, a recent study examining host factors required for *C. trachomatis*-induced prevention of apoptosis showed that HIF1α is activated in cells as early as 12 hours post-infection (7). Two proteins that are strongly upregulated in response to HIF1α activity are BNIP3 and BNIP3L. Here we show that the *C. trachomatis* effector CrpA alters the protein levels of both BNIP3 and BNIP3L, and that this effect is exacerbated under hypoxia-like conditions. The loss of BNIP3 and BNIP3L in hypoxic conditions prevents the efficient induction of autophagy, where autophagy is a factor restricting *C. trachomatis* growth (8). By preventing autophagy during hypoxia, cells would be

pushed towards death by apoptosis. However, it has been clearly demonstrated that *C. trachomatis* has factors which prevent apoptosis and necrosis during infection (9). Our data here show that overexpression of CrpA during infection leads to significantly reduced *C. trachomatis* growth under hypoxia-like conditions. We speculate that the overexpression of CrpA overwhelms the *C. trachomatis* effectors that normally prevent cell death. Unfortunately, we are not currently able to examine how the loss of CrpA would alter the growth of *C. trachomatis* during hypoxia. While several recent advances have been made in the genetic manipulation of *C. trachomatis*, it is still unclear whether a mutant *C. trachomatis* lacking CrpA can be constructed (10-12).

In the absence of loss-of-function mutants, our current study highlights the potential use of gain-of-function analyses to identify effector-host substrate pairs and to identify specific host pathways manipulated during infection. With the function of the majority of *C. trachomatis* effectors unknown, the catalog of altered proteins we have generated now allows for testing individual effectors for their ability to recapitulate an alteration we found occurring during infection. While this study has identified a large number of protein alterations, it is almost certainly incomplete. Here we have examined the stability of individual proteins and identified changes in host protein levels following infection. Many effectors however, may not directly alter host protein stability. In these cases our current list of altered proteins would not include the host substrate. Our study must also be refined to identify host protein alterations that are directly caused by *C. trachomatis* and those that are a result of indirect causes. There is also a need to develop screens able to identify other post-translational modifications induced by *C. trachomatis*. Major advances in proteomics have allowed systems-level understanding of changes in phosphorylation, ubiquitination, and lysine acetylation, and similar screens could be used to identify the individual *C. trachomatis* effectors driving those changes (13-15).

References

1. Starnbach MN, Loomis WP, Ovendale P, Regan D, Hess B, Alderson MR, et al. An inclusion membrane protein from Chlamydia trachomatis enters the MHC class I pathway and stimulates a CD8+ T cell response. J Immunol. 2003;171(9):4742-9. Epub 2003/10/22. PubMed PMID: 14568950.

2. Fling SP, Sutherland RA, Steele LN, Hess B, D'Orazio SE, Maisonneuve J, et al. CD8+ T cells recognize an inclusion membrane-associated protein from the vacuolar pathogen Chlamydia trachomatis. Proceedings of the National Academy of Sciences of the United States of America. 2001;98(3):1160-5. Epub 2001/02/07. doi: 10.1073/pnas.98.3.1160. PubMed PMID: 11158611; PubMed Central PMCID: PMC14725.

3. Mellor HR, Harris AL. The role of the hypoxia-inducible BH3-only proteins BNIP3 and BNIP3L in cancer. Cancer metastasis reviews. 2007;26(3-4):553-66. Epub 2007/09/07. doi: 10.1007/s10555-007-9080-0. PubMed PMID: 17805942.

4. Mazure NM, Pouyssegur J. Atypical BH3-domains of BNIP3 and BNIP3L lead to autophagy in hypoxia. Autophagy. 2009;5(6):868-9. Epub 2009/07/10. PubMed PMID: 19587545.

5. Bellot G, Garcia-Medina R, Gounon P, Chiche J, Roux D, Pouyssegur J, et al. Hypoxia-induced autophagy is mediated through hypoxia-inducible factor induction of BNIP3 and BNIP3L via their BH3 domains. Molecular and cellular biology. 2009;29(10):2570-81. Epub 2009/03/11. doi: 10.1128/MCB.00166-09. PubMed PMID: 19273585; PubMed Central PMCID: PMC2682037.

6. Roth A, Konig P, van Zandbergen G, Klinger M, Hellwig-Burgel T, Daubener W, et al. Hypoxia abrogates antichlamydial properties of IFN-gamma in human fallopian tube cells in vitro and ex vivo. Proceedings of the National Academy of Sciences of the United States of America. 2010;107(45):19502-7. Epub 2010/10/27. doi: 10.1073/pnas.1008178107. PubMed PMID: 20974954; PubMed Central PMCID: PMC2984208.

7. Sharma M, Machuy N, Bohme L, Karunakaran K, Maurer AP, Meyer TF, et al. HIF-1alpha is involved in mediating apoptosis resistance to Chlamydia trachomatis-infected cells. Cellular microbiology. 2011;13(10):1573-85. Epub 2011/08/10. doi: 10.1111/j.1462-5822.2011.01642.x. PubMed PMID: 21824245.

8. Al-Younes HM, Al-Zeer MA, Khalil H, Gussmann J, Karlas A, Machuy N, et al. Autophagy-independent function of MAP-LC3 during intracellular propagation of Chlamydia trachomatis. Autophagy. 2011;7(8):814-28. Epub 2011/04/06. PubMed PMID: 21464618.

9. Sharma M, Rudel T. Apoptosis resistance in Chlamydia-infected cells: a fate worse than death? FEMS immunology and medical microbiology. 2009;55(2):154-61. Epub 2009/03/14. doi: 10.1111/j.1574-695X.2008.00515.x. PubMed PMID: 19281566.

10. Nguyen BD, Valdivia RH. Virulence determinants in the obligate intracellular pathogen Chlamydia trachomatis revealed by forward genetic approaches. Proceedings of the National Academy of Sciences of the United States of America. 2012;109(4):1263-8. Epub 2012/01/11. doi: 10.1073/pnas.1117884109. PubMed PMID: 22232666; PubMed Central PMCID: PMC3268281.

11. Kari L, Goheen MM, Randall LB, Taylor LD, Carlson JH, Whitmire WM, et al. Generation of targeted Chlamydia trachomatis null mutants. Proceedings of the National Academy of Sciences of the United States of America. 2011;108(17):7189-93. Epub 2011/04/13. doi: 10.1073/pnas.1102229108. PubMed PMID: 21482792; PubMed Central PMCID: PMC3084044.

12. Wang Y, Kahane S, Cutcliffe LT, Skilton RJ, Lambden PR, Clarke IN. Development of a transformation system for Chlamydia trachomatis: restoration of glycogen biosynthesis by acquisition of a plasmid shuttle vector. PLoS pathogens. 2011;7(9):e1002258. Epub 2011/10/04. doi: 10.1371/journal.ppat.1002258. PubMed PMID: 21966270; PubMed Central PMCID: PMC3178582.

13. Huttlin EL, Jedrychowski MP, Elias JE, Goswami T, Rad R, Beausoleil SA, et al. A tissue-specific atlas of mouse protein phosphorylation and expression. Cell. 2010;143(7):1174-89. Epub 2010/12/25. doi: 10.1016/j.cell.2010.12.001. PubMed PMID: 21183079; PubMed Central PMCID: PMC3035969.

14. Kim W, Bennett EJ, Huttlin EL, Guo A, Li J, Possemato A, et al. Systematic and quantitative assessment of the ubiquitin-modified proteome. Molecular cell. 2011;44(2):325-40. Epub 2011/09/13. doi: 10.1016/j.molcel.2011.08.025. PubMed PMID: 21906983; PubMed Central PMCID: PMC3200427.

15. Choudhary C, Kumar C, Gnad F, Nielsen ML, Rehman M, Walther TC, et al. Lysine acetylation targets protein complexes and co-regulates major cellular functions. Science. 2009;325(5942):834-40. Epub 2009/07/18. doi: 10.1126/science.1175371. PubMed PMID: 19608861.

Appendix C: Supplementary Tables Associated with Chapters 5 and 6

Table S5-1	**SILAC Dataset**
Worksheet 1	SILAC data 4 hours post-infection
Worksheet 2	SILAC data 14 hours post-infection
Worksheet 3	SILAC data 24 hours post-infection (Replicate #1)
Worksheet 4	SILAC data 24 hours post-infection (Replicate #2)
Worksheet 5	24 hour SILAC Replicate overlap analysis
Worksheet 6	Transcriptional microarray data
Table S5-2	**DAVID analysis of enriched host protein networks from SILAC data**
Table S5-3	**Gain-of-Function Screen dataset**
Worksheet 1	Gain-of-function screen data for experimental proteins.
Worksheet 2	Gain-of-function screen data for control proteins
Table S6-1	**GPS validation summary, Screen data, and Probe info**
Worksheet1	GPS screen Validation summary
Worksheet 2	Merged GPS data for each probe to positive hits in GPS screen
Worksheet 3	Raw GPS Screen Data
Worksheet 4	Sequence information for each probe present in the library/microarrays**.**
Table S6-2	**Bioinformatics analysis summary.**
Worksheet 1	DAVID analysis of stabilized proteins in the GPS screen
Worksheet 2	DAVID analysis of destabilized proteins in the GPS screen.
Table S6-3	**Log_2 Ratios for growth in Loss-of-Function screen (Experimentals and Controls)**
Worksheet 1	siRNA screen full data (experimentals)
Worksheet 2	siRNA Controls
Table S6-4	**Customized Macro for plotting GPS histograms**